



저작자표시-비영리-변경금지 2.0 대한민국

이용자는 아래의 조건을 따르는 경우에 한하여 자유롭게

- 이 저작물을 복제, 배포, 전송, 전시, 공연 및 방송할 수 있습니다.

다음과 같은 조건을 따라야 합니다:



저작자표시. 귀하는 원저작자를 표시하여야 합니다.



비영리. 귀하는 이 저작물을 영리 목적으로 이용할 수 없습니다.



변경금지. 귀하는 이 저작물을 개작, 변형 또는 가공할 수 없습니다.

- 귀하는, 이 저작물의 재이용이나 배포의 경우, 이 저작물에 적용된 이용허락조건을 명확하게 나타내어야 합니다.
- 저작권자로부터 별도의 허가를 받으면 이러한 조건들은 적용되지 않습니다.

저작권법에 따른 이용자의 권리는 위의 내용에 의하여 영향을 받지 않습니다.

이것은 [이용허락규약\(Legal Code\)](#)을 이해하기 쉽게 요약한 것입니다.

[Disclaimer](#)

A THESIS FOR THE DEGREE OF DOCTOR OF
PHILOSOPHY

**Structural and Functional Dissects of the JAK/STAT Signaling
Pathway in Teleosts Through Molecular Delineation of STAT
Family Members from Rock Bream (*Oplegnathus fasciatus*)
Revealing Their Roles During Infection and Injury**

S.D.N.K. Bathige

Department of Marine Life Sciences

GRADUATE SCHOOL

JEJU NATIONAL UNIVERSITY

REPUBLIC OF KOREA

February 2016

**Structural and Functional Dissects of the JAK/STAT Signaling Pathway
in Teleosts Through Molecular Delineation of STAT Family Members
from Rock Bream (*Oplegnathus fasciatus*) Revealing Their Roles During
Infection and Injury**

S.D.N.K. Bathige

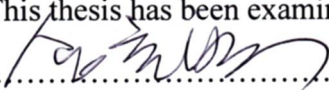
(Supervised by Professor Jehee Lee)

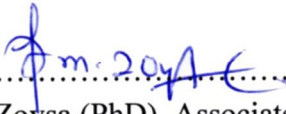
A thesis submitted in partial fulfilment of the requirement for the degree of

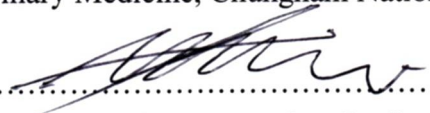
DOCTOR OF PHILOSOPHY

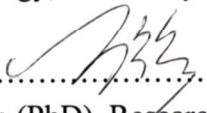
February, 2016


This thesis has been examined and approved by


.....
Thesis Director, Choon Bok Song (PhD), Professor of Marine Life Sciences
School of Bio Medical Sciences, Jeju National University


.....
Mahanama De Zoysa (PhD), Associate Professor of Aquatic Life Medicine
College of Veterinary Medicine, Chungnam National University


.....
Chulhong Oh (PhD), Associate Professor
Department of Marine Biology, University of Science and Technology


.....
Qiang Wan (PhD), Research Professor
Fish Vaccine Research Center, Jeju National University


.....
Jehee Lee (PhD), Professor of Marine Life Sciences
School of Bio Medical Sciences, Jeju National University

19.02.2016

Date

**Department of Marine Life Sciences
GRADUATE SCHOOL
JEJU NATIONAL UNIVERSITY
REPUBLIC OF KOREA**

*Dedicated to beloved parents,
my ever loving wife and son*

Acknowledgments

I would like to thank all the people who made this thesis possible and unforgettable experience for me.

Apart from the efforts of mine, the success of any project depends largely on the encouragement and guidelines of many others. I would like to take this opportunity to express my sincere gratitude to the people who have been instrumental in the successful completion of this thesis.

First of all, I would like to express my special and sincere gratitude to my academic supervisor Professor Jehoo Lee for giving me the opportunity to pursue my doctoral studies and conduct the thesis research in his Marine Molecular Genetic Laboratory (MMGL). I acknowledge him for the constant encouragement, systematic guidance, personal care and great effort he put into training me in the scientific research field.

I would also like to express my sincere gratitude to the thesis Director Prof. Choon Bok Song, and members of the thesis committee Ass.Prof. Mahanama De Zoysa, Ass.Prof. Chulhong Oh and Dr. Qiang Wan, who spent time in reading my thesis, and provided valuable suggestions for shaping the study. Also, I acknowledge with great thanks to all the professors of my department; especially, Kwang-Sik Choi and Gi-Young Kim for their inspiring and encouraging guidance for a deeper understanding of knowledge and conductive comments during my course work.

I extend my sincere thanks to Dr. Navaneethaiyer Umasuthan for introducing me to Prof. Lee and, his guidance and ideas to improve my research work during laboratory experiments. In addition, I am especially thankful to Dr. Ilson Whang and Dr. Qiang Wan for their valuable guidance and intellectual ideas to improve my laboratory experiments and writings. I acknowledge Dr. Bong-Soo Lim and Dr. Hyung-Bok Jung, along with the team members, those who work in Fish Vaccine Research Centre, Jeju National University for their immense help during the field and laboratory experiments.

I am grateful to Dr. Youngduk Lee, Dr. S. R. Kasthuri and Dr. W.D. Niroshana Wickramaarachchi, who were senior members of the MMGL, for their valuable ideas for my academic as well as personal life. I also extendedly acknowledge my MMGL's Korean companions of both past and present including Mr. Yucheol Kim, Ms. Sukkyoung Lee,

Ms. Minyoung Oh, Ms. Hyowon Kim, Mr. Seongdo Lee, Mr. Taesoo Kim, Ms. Ko Jiyeon, Ms. Eunyong Jo, Ms. Eunju Yang, Ms. Jeong-in Ma, Ms. Sunhye Kang, Ms. Gabin Kim and Ms. Jeongeun Kim.

In addition, I would like to thank my past and current friends in the MMGL, Mr. Anushka Sandaruwan, Mr. Ajith Premachandra, Mrs. Thulasitha William, Ms. Mothishri Seran, Mr. Gelshan Imarshana, Mr. Thiunuwan Piyathilaka, Mr. Viraj Udayantha, Mr. Handun Eranga, Mr. Lalinka Herath, Mr. Sachitch Udara, Mrs. Chaturika Nadeeshani and Mr. R. Kugapreethan for their valuable support during my academic research work and personal life in Jeju. I extend my sincere thanks to Dr. Janaka, Dr. Kalpa, Mr. Prasad, Mrs. Dilshara, Mr. Lakmal, Mr. Shanura, Mr. Asanka and Korean friends who attached to the other laboratories for their support during my laboratory works and their kind co-operation to the completion of my project work. I am also thankful to my Sri Lankan friends who attached to the other laboratories for providing a joyful togetherness in Jeju.

I thank all the members of Jeju National University International Student Organization (JISO) for their strength and encouragement especially to Prof. Young-Hoon Kang, the Dean Center of International affairs and his team members for their help and hospitality. I am always thankful for the Department of Marine Life Sciences at Jeju National University for providing me an excellent work environment during my study and I appreciate the department's administrative officers, who were always willing to help.

I thank Brain Korea (BK) 21, BK 21-plus scholarship programs, National Fisheries Research and Development Institute (NFRDI), National Research Foundation of Korea (NRF), the Golden Seed Project, Ministry of Agriculture, Food and Rural Affairs (MAFRA), the Ministry of Oceans and Fisheries (MOF), the Rural Development Administration (RDA), and the Korea Forest Service (KFS), which provided the funding for my entire doctoral research and presenting my findings in Korea and abroad.

I thank all Korean and international students who support me during my stay at student dormitory, and the staff members of student dormitory office for their kind help and hospitality.

I would like to thank all those whom I have not mentioned above but helped me in numerous ways to my success.

My deepest gratitude is for my loving parents and parents-in-law for their unflagging love and support. Besides my parents, I appreciate my brothers, brother-in-law and sisters-in-law for their excellent support and love during my studies.

Finally I would like to express my eternal appreciation to my ever loving wife, Nilusha Perera for her invaluable encouragements and moral supports gave me at every time with looking after my dearest son Hiruja Nimtharu during my graduate career.



Table of Contents

Table of Contents	IV
List of Figures	IX
List of Tables	XIII
Summary	XIV
CHAPTER 1	1
An introduction to JAK/STAT signaling cascade in teleost	1
1.1 General introduction	2
1.2. Immune system.....	2
1.2.1. Innate immune system	3
1.2.2. Adaptive immune system.....	3
1.3. Fish immune system	5
1.3.1. Innate immunity of fish.....	5
1.3.2 Adaptive immunity of fish	6
1.4. The JAK/STAT signal transduction pathway	8
1.4.1. Components of JAK/STAT signaling pathway	8
1.4.1.1. Ligands and receptors.....	8
1.4.1.2. Janus kinases (JAKs).....	9
1.4.1.3. Signal transducer and activator of transcription (STAT)	10
1.4.2. Mechanism of JAK/STAT signaling.....	11
1.5. STATs in teleosts	16
1.6. Biological species of this study.....	16
1.6.1. Rock bream aquaculture and diseases.....	17
1.7. Main objectives of this study	18
CHAPTER 2	19
Materials and Methods	19
2.1 The rock bream cDNA library construction and identification of genes.....	20
2.2 Construction of bacterial artificial chromosome (BAC) library for rock bream.....	21
2.3 <i>In silico</i> characterization of CDS, amino acid sequence, genome structural arrangement and phylogenetic analysis	22
2.4 Experimental animals and <i>in vivo</i> challenge experiments	23

2.4.1 Bacterial challenge.....	24
2.4.2 Viral challenge.....	24
2.4.3 Immune stimulant challenge	26
2.4.4 Control challenge.....	26
2.4.5 Tissue injury experiment.....	26
2.5 Tissue collection.....	26
2.6 RNA isolation and cDNA synthesis	27
2.7 Quantification of transcripts level	27
2.9 <i>In vitro</i> challenge.....	29
2.10. Antiviral potential assay.....	30
2.10.1. Isolation of RBIV.....	30
2.10.2. Assay.....	30
2.11. Sub cellular localization.....	31
2.12. Statistical analysis.....	31
CHAPTER 3	33
Two isoforms of Signal transducer and activator of transcription 1 (STAT1): Genomic organization, transcriptional modulation and subcellular localization.....	33
Abstract.....	34
3.1. Introduction	35
3.2. Results.....	37
3.2.1. Bioinformatics of RbSTAT1 and RbSTAT1L cDNA sequences	37
3.2.1.1 Primary sequence characterization.....	37
3.2.1.2. Homology analysis.....	39
3.2.1.3. Phylogenetic analysis	42
3.2.2. Genomic sequence characterization of <i>RbSTAT1</i> and <i>RbSTAT1L</i>	45
3.2.2.1. Comparative genomic structural organization	45
3.2.2.2. Putative TFBS analysis at 5'-proximal region	46
3.2.3. Quantification of <i>RbSTAT1</i> and <i>RbSTAT1L</i> transcripts	47
3.2.3.1. Expressional changes in different tissues of healthy fish	47
3.2.3.2. Expressional patterns upon <i>in vivo</i> immune challenges	48
3.2.3.3. Expressional patterns in response to injury	50
3.2.3.4. Expressional patterns upon <i>in vitro</i> challenge	51
3.2.4. Antiviral activity assay.....	52
3.2.5. Subcellular localization of RbSTAT1 and RbSTAT1L	53
3.3. Discussion	54

3.4. Conclusion.....	58
CHAPTER 4	59
Molecular cloning, transcriptional profiling and subcellular localization of signal transducer and activator of transcription 2 (STAT2) ortholog from rock bream, <i>Oplegnathus fasciatus</i>	59
Abstract.....	60
4.1. Introduction.....	61
4.2. Results and discussion	63
4.2.1. cDNA and genomic sequence characteristics.....	63
3.2. Putative promoter region.....	65
4.2.3. Comparative studies and phylogenetic analysis	67
4.2.4. Spatial expression of <i>RbSTAT2</i> mRNA	71
4.2.5. Temporal expression of <i>RbSTAT2</i> mRNA upon pathogenic and PAMP challenges, and antiviral effect	72
4.2.6. Temporal expression of <i>RbSTAT2</i> mRNA against tissue injury.....	75
4.2.7. Temporal expression of <i>RbSTAT2</i> in response to the rRbIL-10.....	76
4.2.8. Subcellular localization.....	77
4.3. Conclusion.....	78
CHAPTER 5	79
A homolog of teleostean signal transducer and activator of transcription 3 (STAT3) from rock bream, <i>Oplegnathus fasciatus</i>: structural insights, transcriptional modulation and subcellular localization.....	79
Abstract.....	80
5.1. Introduction.....	81
5.2. Results.....	83
5.2.1 <i>In silico</i> analysis of RbSTAT3	83
5.2.1.1. cDNA sequence characterization	83
5.2.1.2. Homology analysis.....	85
5.2.1.3 Phylogenetic analysis	88
5.2.1.4 Genomic sequence analysis	89
5.2.1.5 Putative promoter characterization	90
5.2.2 Expression patterns of <i>RbSTAT3</i> mRNA	92
5.2.2.1 Tissue specific expression pattern.....	92
5.2.2.2 Expression patterns after <i>in vivo</i> immune challenges.....	93
5.2.2.3 Expression patterns after injury challenges	95
5.2.2.4 Expression patterns after <i>in vitro</i> challenges	96

5.2.3. Subcellular localization.....	96
5.3. Discussion	97
5.4. Conclusion.....	101
CHAPTER 6	102
Genomic structure and immunological response of STAT4 family member from Rock bream (<i>Oplegnathus fasciatus</i>)	102
Abstract.....	103
6.1. Introduction	104
6.2. Results and Discussion	105
6.2.1. Genomic and cDNA sequence identification	105
6.2.2. Sequence characterization	109
6.2.3. Tissue specific gene expression.....	112
6.2.4. Regulated gene expression after immune stimulation	113
6.2.5. Regulated gene expression after tissue injury	117
6.2.6. Regulated gene expression after <i>in vitro</i> challenges	117
6.3. Conclusion.....	119
CHAPTER 7	121
Two teleostean signal transducer and activator of transcription 5 (STAT5) orthologs from rock bream <i>Oplegnathus fasciatus</i>: Genomic structure, transcriptional modulation and subcellular localization.....	121
Abstract.....	122
7.1. Introduction	123
7.2. Results.....	125
7.2.1. Characteristics of RbSTAT5-1 and RbSTAT5-2 cDNA sequences	125
7.2.1.1. Primary sequence characterization.....	125
7.2.1.2. Homology analysis of RbSTAT5s.....	127
7.2.1.3. Phylogenetic analysis of RbSTAT5s.....	132
7.2.2. Characteristics of RbSTAT5-1 genomic sequence	133
7.2.2.1. Comparative organization of RbSTAT5-1 genomic structure.....	133
7.2.2.2. Putative promoter of RbSTAT5s at 5'-proximal region	134
7.2.3. Transcriptional profile of <i>RbSTAT5-1</i> and <i>RbSTAT5-2</i>	136
7.2.3.1. Expression of RbSTAT5s mRNA in tissues of healthy juvenile fish.....	136
7.2.3.2. Expression of RbSTAT5s mRNA in immune challenged fish	137
7.2.3.3. Expression of RbSTAT5s mRNA in injured fish	141
7.2.3.3. Expression of RbSTAT5s mRNA in injured fish	141

7.3. Discussion	142
7.4. Conclusion.....	145
CHAPTER 8	146
Structural insights and transcriptional modulation of signal transducer and activator of transcription 6 (STAT6) from rock bream, <i>Oplegnathus fasciatus</i>	146
Abstract.....	147
8.1. Introduction	148
8.2. Results.....	150
8.2.1. cDNA sequence characterization of RbSTAT6.....	150
8.2.2. Amino acid sequence comparison and tertiary structure of RbSTAT6.....	152
8.2.3. Phylogenetic analysis	154
8.2.4. Expression profiles of RbSTAT6 mRNA	155
8.2.4.1. Expression profile in different tissues of healthy fish	155
8.2.4.2. Expression profile after <i>in vivo</i> immune challenge	156
8.2.4.3. Expression profile after tissue injury.....	158
8.2.4.4. Expression profile after rRbIL-10 challenge	158
8.3. Discussion	159
8.4. Conclusion.....	162
9. Concluding remarks.....	163
10. References	164

List of Figures

Fig. 1.1. The main components of the innate and adaptive immune system.....	4
Fig. 1.2. Schematic representation of domain organization in STAT protein. Model of.....	10
Fig. 1.3. Outline of the JAK/STAT3 Pathway.....	12
Fig. 1.4. Comprehensive details of JAK/STAT mammalian signaling pathway.....	13
Fig. 1.5. JAK usage by cytokines.....	14
Fig. 1.6. Structure of the STAT1 core dimer on a GAS element.....	15
Fig. 1.7. Rock bream fish.....	17
Fig. 2.1. TaKaRa TP800 -Thermal Cycler Dice™ Real Time System	28
Fig. 3.1. The full length cDNA and deduced amino acid sequences of RbSTAT1 (a) and RbSTAT1L (b).....	38
Fig. 3.2. Multiple sequence alignment analysis of RbSTAT1 and RbSTAT1L amino acid sequences with known orthologs from different species.....	41
Fig. 3.3. Surface representations of RbSTAT1 (a), RbSTAT1L (b) and human STAT1 3D homology models.	42
Fig. 3.4. Unrooted phylogenetic tree of STAT family	43
Fig. 3.5. Phylogeny of RbSTAT1 and RbSTAT1L.....	44
Fig. 3.6. Schematic representation of genomic structure comparison of RbSTAT1 and RbSTAT1L with fish (a), bird (b) and mammalian (c) counterparts	45
Fig. 3.7. Putative promoter proximal region of RbSTAT1 (a) and RbSTAT1L (b).....	47
Fig. 3.8. Tissue-specific expression of rock bream STAT1 and STAT1L transcripts in healthy fish.....	48
Fig. 3.9. The expressional patterns of RbSTAT1 in (a) blood and (b) liver tissues after in vivo immune challenges	49
Fig. 3.10. The expressional patterns of RbSTAT1L in (a) blood and (b) liver tissues after in vivo immune challenges	50
Fig. 3.11. The expressional patterns of RbSTAT1 (a) and RbSTAT1L (b) in blood cells and liver tissues after injury	51
Fig. 3.12. The expressional patterns of RbSTAT1 and RbSTAT1L in heart cells after in vitro immune challenge with rRbIL-10	52
Fig. 3.13. Effect of RbSTAT1 and RbSTAT1L for cell viability after RBIV infection	53
Fig. 3.14. Subcellular localization of RbSTAT1 and RbSTAT1L in rock bream heart cells..	54
Fig. 4.1. Nucleotide and deduced amino acid sequence of RbSTAT2.....	64

Fig. 4.2. Schematic illustration of rock bream STAT2 at genomic (a), mRNA (b), protein (c) and 3D homology model	65
Fig. 4.3. Putative promoter proximal region of RbSTAT2.....	66
Fig. 4.4. Multiple amino acid sequence alignment of RbSTAT2 with other counterparts from various taxonomical origins.....	69
Fig. 4.5. Comparison of genomic structure organization of RbSTAT2 with other vertebrate orthologs.	69
Fig. 4.6. Rooted molecular phylogenetic tree of STAT2 genes.....	70
Fig. 4.7. Tissue distribution profiling of RbSTAT2 in rock bream.	71
Fig. 4.8. Temporal mRNA expression profiling of RbSTAT2 in blood (a) and liver tissue (b) after pathogens and PAMPs challenges.....	73
Fig. 4.9. Effect of RbSTAT2 for cell viability after RBIV infection.....	74
Fig. 4.10. Temporal mRNA expression profiling of RbSTAT2 in blood cells and liver tissue after tissue injury.....	76
Fig. 4.11. Temporal expression profiling of RbSTAT2 in heart cells after in vitro challenge with rRbIL-10	77
Fig. 4.12. Subcellular localization of RbSTAT2 in rock bream heart cells.....	78
Fig. 5.1. Nucleotide and deduced amino acid sequence of RbSTAT3.....	84
Fig. 5.2. Multiple sequence alignment of RbSTAT3 amino acid sequence with other orthologs from different taxonomical origins	86
Fig. 5.3. Domain structure of RbSTAT3 and multiple alignments with biologically important binding/active sites in SH2 domain.....	87
Fig. 5.4. Homology model of RbSTAT3 (a) and mouse STAT3 (b).	87
Fig. 5.5. Phylogenetic tree based on the STAT3 amino acid sequences from various taxonomical origins	88
Fig. 5.6. Comparison of genomic organization of RbSTAT3 with other counterparts.....	89
Fig. 5.7. Putative promoter proximal region at the 5' flanking region of RbSTAT3 gene.....	91
Fig. 5.8. Tissue specific expression of RbSTAT3 in healthy fish under normal physiological condition.	92
Fig. 5.9. Expressional patterns of RbSTAT3 in blood (a) and liver (b) after in vivo immune challenge experiments	94
Fig. 5.10. The expressional patterns of RbSTAT3 in blood cells and liver tissue in response to the injury.	95

Fig. 5.11. The expressional patterns of RbSTAT3 in heart cells upon in vitro challenge with rRbIL-10.	96
Fig. 5.12. Subcellular localization of RbSTAT3 in rock bream heart cells.....	97
Fig. 6.1. Schematic representation of the STAT4 genomic structures.....	106
Fig. 6.2. Putative promoter region and transcription factor binding sites of the RbSTAT4 .	108
Fig. 6.3. Multiple sequence alignment and pairwise comparison of RbSTAT4 with other STAT4 members	112
Fig. 6.4. Evolutionary relationship analysis of the RbSTAT4 with other members in the STAT4 family proteins.....	112
Fig. 6.5. Tissue-specific mRNA expression of the RbSTAT4 in healthy rock breams.	113
Fig. 6.6. Relative mRNA expression of RbSTAT4 in response to LPS, poly I:C, E. tarda and RBIV infections in (A) gill, (B) head kidney and (C) spleen tissues.	116
Fig. 6.7. Relative mRNA expression of RbSTAT4 in blood cells and liver tissue in response to the injury.....	117
Fig. 6.8. Relative mRNA expression of RbSTAT4 in heart cells upon in vitro challenge with rRbIL-10	118
Fig. 7.1. Nucleotide and deduced amino acid sequence of RbSTAT5-1 (a) and RbSTAT5-2 (b).	127
Fig. 7.2. Multiple amino acid sequence alignment of RbSTAT5-1 and RbSTAT5-2 with other counterparts from various taxonomical origins	131
Fig. 7.3. Surface representations of RbSTAT5-1 (a), RbSTAT5-2 (b) and Mouse STAT5 3D homology models.	131
Fig. 7.4. Phylogeny of RbSTAT5-1 and RbSTAT5-2.....	132
Fig. 7.5. Schematic representation of genomic structure comparison of RbSTAT5-1 and RbSTAT5-2 with fish (a), bird (b) and mammalian (c) counterparts	134
Fig. 7.6. Putative promoter proximal region of RbSTAT5-1	135
Fig. 7.7. Tissue-specific expression of rock bream STAT5-1 and STAT5-2 transcripts in healthy fish.....	136
Fig. 7.8. The expressional patterns of RbSTAT5-1 in (a) liver and (b) blood tissues after in vivo immune challenges	138
Fig. 7.9. The expressional patterns of RbSTAT5-2 in (a) liver and (b) blood tissues after in vivo immune challenges	140
Fig. 7.10. The expressional patterns of RbSTAT5-1 (a) and RbSTAT5-2 (b) in liver tissues and blood cells after injury	141

Fig. 7.11. The expressional patterns of RbSTAT5-1 (a) and RbSTAT5-2 in heart cells after in vitro immune challenge with rRbIL-10.....	142
Fig. 8.1. Nucleotide and deduced amino acid sequence of RbSTAT6.....	151
Fig. 8.2. Multiple sequence alignment and pairwise comparison of RbSTAT4 with other STAT6 members	153
Fig. 8.3. Surface representation of RbSTAT6 3D homology model.....	154
Fig. 8.4. Phylogeny of RbSTAT6	155
Fig. 8.5. Tissue-specific expression of rock bream STAT6 transcripts in healthy fish	156
Fig. 8.6. The expressional patterns of RbSTAT6 in blood cells (a) liver (b) after in vivo immune challenges	157
Fig. 8.7. The expressional patterns of RbSTAT6 in blood cells and liver tissue after injury	158
Fig. 8.8. The expressional patterns of RbSTAT6 in heart cells after in vitro immune challenge with rRbIL-10	159

List of Tables

Table 1.1 Key features of innate and adaptive immunity.....	4
Table 1.2. Differences between immunity of fish and mammals	8
Table 1.3. Summary of STAT genes identified from fish species.....	16
Table 2.1. Description of experimental challenges conducted in this study	25
Table 3.1. Primers used in this study.....	37
Table 3.2. Percentage of identity (I%) and similarity (S%) of interspecies amino acid sequences in comparison with RbSTAT1 and RbSTAT1L sequences.	40
Table 4.1. Primers used in this study.....	63
Table 5.1. Description of primers used in this study.....	83
Table 5.2. Exon organization in genomic structure of fish and higher vertebrates.	90
Table 6.1. Primers used in this study.....	105
Table 7.1. Primers used in this study.....	124
Table 7.2. Percentage of identity (I%) and similarity (S%) of interspecies amino acid sequences in comparison with RbSTAT5-1 and RbSTAT5-2 sequences	128
Table 8.1. Primers used in this study.....	149

Summary

The rock bream, *Oplegnathus fasciatus* is a commercially important mariculture aquacrop widely cultured in Eastern and Southeastern Asian countries. The production of rock bream fish in the aquaculture farm was unable to fulfill the high demand due to the loss of production caused by various issues. The high vulnerability of rock bream towards bacterial and viral diseases was led to the mass mortality of rock bream accounting great losses to the aquaculture farmers. The infectious disease outbreaks are very common in fish farms due to high stocking density and intensive culture techniques. It has been identified that number of diseases such as edwardsiellosis caused by *Edwardsiella tarda* and streptococcosis caused by *Streptococcus iniae* are mostly infected bacterial diseases have affected the rock bream fish. In addition, most serious virus disease caused by rock bream irido virus (RBIV) has led great loss of rock bream production. In order to battle against enormous pathological threatens, sustainable disease management strategies are required to be introduced. Therefore, deeper understanding of the molecular and cellular mechanisms of host immunity will be greatly effect for the rock bream aquaculture farm. The immune system is a complex network of organs containing cells that recognize foreign substances in the body and eliminate them. Numbers of components or signaling molecules such as antibacterial and/or antiviral peptides, signaling molecules that can initiate the antibacterial and/or antiviral pathways have been widely studied particularly in mammals. Janus kinase/signal transducers and activators of transcription (JAK/STAT) signaling pathway is a key signaling pathway that essentially work on various immune responses.

In mammals, the JAK/STAT signaling pathway has been well studied and showed its relation to the wide array of functional roles including cell differentiation, migration, proliferation, embryo development, brain development, initiation of gene expression, apoptosis, dendritic cell development, myogenic differentiation, tissue injury and other essential immune responses. Seven STATs including STAT1, STAT2, STAT3, STAT4, STAT5a, STAT5b and STAT6 have been identified and well characterized in mammals. All these STATs share common structural features with six conserved domains with different functions: N-terminal domain regulates the nuclear translocation, coiled coil domain interacts with various proteins, DNA binding domain interacts with DNA, Src homology 2 (SH2) domain plays a vital role in signal transduction via phosphotyrosins, linker domain connects both DNA binding domain and SH2 domain, and transcriptional activation domain located at the C-terminal and regulates the transcriptional responses. However, the signaling components and their

associated elements of the teleostean JAK/STAT signaling cascade are poorly understood or haphazardly studied in some fish species. The study of complete JAK/STAT signaling pathway with its associated modules in teleost is a challenging task for the researchers.

The major effort of this study was to characterize all the STAT members that have been already identified in mammals. Eight STAT members including two STAT1 isoforms, STAT2, STAT3, STAT4, two isoforms of STAT5 and STAT6 have identified and characterize structurally and functionally. The cDNA sequence and its corresponding amino acid sequence of all the STAT members were well characterized and compared with other counterparts from various taxonomical lineages. In addition, the genomic organization of all the STAT members except one of STAT5 isoform and STAT6 were investigated and compared with other vertebrate lineages in order to determine the evolutionary aspects. Moreover, 5'-proximal regions of each gene were analyzed to predict the putative sites for transcriptional factor binding elements. Tissue specific expression of each STAT in healthy rock bream was examined using the quantitative real time PCR technique. Transcriptional modulations were kinetically assessed after bacterial (*E. tarda* and *S. iniae*), viral (RBIV) and PAMP (LPS and poly I:C) injections. In addition, transcriptional changes were monitored after tissue injury in order to understand the wound healing ability of STATs. The STAT genes transcriptions were also evaluated after rock bream interleukin-10 (RbIL-10) stimulation in rock bream heart cells. To further understand the antiviral potential of STAT proteins, STAT genes were cloned into pcDNA3.1(+) vector, transfected into heart cells and measured the cell viability by WST-1 assay, after introducing RBIV. Finally, subcellular localization and nuclear translocation upon poly I:C stimulation was determined. These comprehensive studies provide substantial understanding of the structural and functional role of STAT members in rock bream JAK/STAT signaling pathway.

This dissertation was divided into eight chapters; two of them were for general introduction and, materials and methods, while other six chapters were separated based on the different STAT families (STAT1, 2, 3, 4, 5 and 6) and presented the results and discussion for each rock bream STATs. Identification and characterization of rock bream STAT1 genes was discussed in the third chapter. Using the combined transcriptomic and genomic sequence obtained from bacterial artificial chromosome (BAC) library, two isoforms homologous to the STAT1 were identified and designated as RbSTAT1 and RbSTAT1L. The complete cDNA sequences of RbSTAT1 (2741 bp) and RbSTAT1L (3014 bp) comprised full length coding sequences encoding poly peptides with 750 aa and 755 aa, respectively. Pairwise

sequence analysis revealed that RbSTAT1 (96.5%) and RbSTAT1L (65.1%) shared highest percent of identity with mandarin fish and Burton's mouthbrooder, respectively. In comparison of RbSTAT1 with RbSTAT1L showed 42.4% identity. Characteristic STAT domains were identified in both RbSTAT1 genes. Phylogenetic studies revealed that RbSTAT1 belongs to the canonical STAT1 group, while RbSTAT1L was clustered in a separate group indicating as a novel STAT group. Genomic organization of both RbSTAT1 and RbSTAT1L revealed that both comprised with 23 exons disrupted by 22 introns. Several transcription factor binding sites (TFBSs) were recognized in the putative promoter proximal regions of the RbSTAT1 and RbSTAT1L. The qPCR analysis depicted the highest expression of RbSTAT1 and RbSTAT1L in blood cells, while exhibiting universal expression in other tissues with varied amount. Significantly elevated expression of RbSTAT1 and RbSTAT1L was examined in blood cells and liver tissues in response to the microbial and mitogen administrations, although some time points detected suppressed expressions. Transcriptional modulations were also detected in response to the tissue injury. In addition, significantly up-regulated expressions of both RbSTAT1s were observed in rock bream heart cells upon stimulation with rock bream IL-10. Further we have analyzed the antiviral potential *in vitro*, and revealed the significant effect of both RbSTAT1s against RBIV. Subcellular localization study revealed that both RbSTAT1s protein localized in cytoplasm as mammals under normal conditions. Based on the results, we can suggest that both RbSTAT1s play crucial roles in immune defense against invading microbes and wound healing process.

Next chapter described about the molecular characteristics and functional insight of rock bream STAT2 (RbSTAT2) gene. A single sequence contig homologous to the STAT2 was identified from rock bream transcriptome database and revealed with 804 aa. Bioinformatic analysis revealed the presence of characteristic STAT domains in peptide sequence of RbSTAT2. The BAC screening identified a complete genomic sequence of RbSTAT2 with 24 exons. In addition, essential TFBSs were identified at the 5'-proximal region of RbSTAT2 gene. Based on the phylogenetic studies and comparative analysis of genomic organization of RbSTAT2 with other vertebrate origins revealed that STAT2 gene from fish and other vertebrates were distinctly evolved. The SYBR Green qPCR analysis revealed that the ubiquitous expression of RbSTAT2 transcripts in all tissues analyzed, while depicting highest expression in blood cells. Significantly modulated expressions of *RbSTAT2* mRNA were detected upon viral (rock bream irido virus; RBIV), bacterial (*E. tarda* and *S. iniae*) and immune stimulants (poly I:C and LPS) challenge. Antiviral potential was further confirmed

by WST-1 assay by measuring the cell viability using rock bream heart cells with RBIV. In addition possible role of RbSTAT2 on wound healing process was affirmed by analyzing the transcriptional changes after tissue injury. *In vitro* challenge experiment with RbIL-10 revealed the significant impact on transcription of RbSTAT2. Subcellular localization studies revealed that RbSTAT2 protein was localized in cytoplasm as others and further confirmed the signal transduction ability by adding poly I:C. Altogether, these results provide the information about the involvement of RbSTAT2 on various biologically important mechanisms.

The fifth chapter describes the molecular insights and various functional roles of rock bream STAT3 (RbSTAT3). The STAT3 is one of the key transcription factors in JAK/STAT signaling pathway involved in various biologically essential events such as pleiotropic activities including immune responses, cell proliferation, inflammation, embryo development, brain development, initiation of gene expression, and apoptosis. In the present study, an ortholog of STAT3 (RbSTAT3) was identified from rock bream transcriptome database and characterized structurally and functionally. The full length sequence of RbSTAT3 was encoded a polypeptide with 764 aa, and identified characteristic STAT domains with highly conserved aa residues except in TA domain region. Sequence comparison revealed that RbSTAT3 shared relatively higher identity of percentage (> 90%) with fish counterparts. Genomic sequence of *RbSTAT3* was obtained from BAC sequencing, and identified as a multi-exonic (24 exons) gene as other vertebrates. Genomic structural comparison and phylogenetic studies evidently showed that the different evolutionary route for teleostean and non-teleostean vertebrates. The qPCR analysis revealed that the spatial distribution of *RbSTAT3* mRNA expression was ubiquitous and highly detected in blood, heart and liver tissues. Transcriptional modulation of *RbSTAT3* was examined in blood and liver tissues upon challenges with bacteria (*E. tarda* and *S. iniae*), rock bream irido virus (RBIV) and immune stimulants (LPS and poly I:C). Significant changes in *RbSTAT3* transcription were also noticed, in response to the tissue injury. Significant impact of RbIL-10 on RbSTAT3 transcription was recognized after analyzing the expression level of RbSTAT3 mRNA in heart cell stimulated with RbIL-10 protein. Subcellular localization and nuclear translocation of rock bream STAT3 following poly I:C treatment were also demonstrated. Taken together, the results of the current study provide important evidences for potential roles for rock bream STAT3 in immune system and wound healing process.

Bioinformatic analysis and functional evidences of rock bream STAT4 gene are described in chapter 6. A member of STAT4 was identified from rock bream and designated as RbSTAT4. The cDNA sequence of RbSTAT4 was comprised with a 2205 bp ORF encoding 735 amino acids. As typical features, conserved 6 domains were identified. Phylogenetic study revealed the closest relationship with mandarinfish, and distinct evolution between fish and other vertebrates. Genomic sequence obtained from BAC screening was comprised with 24 exons interrupted by 23 exons. Immunologically crucial TFBSs were predicted at the putative promoter region of *RbSTAT4*. The SYBR Green qPCR analysis revealed that the expression of *RbSTAT4* transcripts was highly detected in gill tissues followed by spleen and liver. Upon stimulations with LPS, poly I:C, *E. tarda* and RBIV, significant elevations were examined in gill, head kidney and spleen particularly in middle phase of the experiment. According to the results of this study, the expression of RbSTAT4 in healthy fish showed in gill tissues. However, the expressions of other STAT members were highly detected in blood cells. Therefore, these results suggest that RbSTAT4 is mainly functioned in gill tissues. Based on these evidences, we can hypothesize that RbSTAT4 might play possible immune roles against bacterial and viral stresses in rock bream.

The next chapter describes the structural and functional characterization of rock bream STAT5 genes. Here, two different isoforms homologous to the STAT5 were identified from rock bream transcriptome database and designated as RbSTAT5-1 and RbSTAT5-2. Sequence analysis of these sequences revealed that both RbSTAT5-1 and RbSTAT5-2 were comprised with 786 amino acids in their protein sequence. In comparison of these protein sequences with other counterparts revealed the conserved residues important for functions and, typical domain regions including N-terminal domain, coiled coil domain, DNA binding domain, linker domain, Src homology 2 (SH2) domain and trans activation domain (TAD) as mammalian counterparts. As other STAT genes, a distinct evolutionary path for fish and other vertebrates was observed based on the phylogenetic tree constructed by NJ method. BAC sequence analysis was able to identify the complete genomic sequence only for RbSTAT5-1, even though the genomic sequence of RbSTAT5-2 needed to be established. According to the genomic structure of *RbSTAT5-1*, the coding sequence was distributed into eighteen exons with seventeen introns. Further, the 5'-proximal region of RbSTAT5-1 was analyzed to predict the possible TFBSs, and detected number of sites which were corresponding to bind the immunologically essential transcription factors such as ICSBP, ISGF-3, GATA-1, HNF-3, SP1, C/EBP, Oct-1, AP1, c-Jun, IRF-1 and NF- κ B. tissue specific expression analysis

performed by qPCR revealed the highest expression of both RbSTAT5-1 and RbSTAT5-2 in blood cells. Transcriptional modulations of RbSTAT5s were examined upon challenge with live bacterial, viral and PAMPs. In addition, significant changes of RbSTAT5s were observed in response to the tissue injury. These results provide important information for the capability of RbSTAT5s in immune responses against microbes and wound healing process.

Last chapter of this dissertation describes the discovery of structural and functional features of rock bream STAT6 genes. In this study a full length sequence of STAT6 gene was identified from rock bream sequence database and designated as RbSTAT6. The cDNA sequence of RbSTAT6 (4683 bp) comprised an ORF of 2313 bp that encodes 771 amino acids. Bioinformatics analysis of RbSTAT6 revealed its structural conservation as other STAT6 counterparts. Mainly, six different domain regions including N-terminal domain, coiled coil domain, DNA binding domain, linker domain, Src homology 2 (SH2) domain and transactivation domain (TAD), and some residues important for function were conserved well. In comparison of RbSTAT6 with other counterparts revealed that the percentage of identity was relatively low. As other STATs, the teleostean and non-teleostean STAT6 members evolved distinctly according to the molecular phylogenetic tree. Quantification of transcription level of *RbSTAT6* in different tissues of healthy fish showed highest expression in blood cells followed by liver tissue as other STAT members of rock bream except RbSTAT4. Transcriptional modulations of RbSTAT6 were detected in blood cells and liver tissues upon viral, bacterial and PAMP injections. In addition, significantly altered transcription of RbSTAT6 was detected in blood cells and liver tissue in response to injury. Meanwhile, transcriptional changes were kinetically analyzed in rock bream heart cells after treatment with rock bream IL-10, and results revealed the significantly elevated expression of *RbSTAT6* at middle phase experiment. Taken together these results implied the potential role of RbSTAT6 in host immune responses and wound healing in rock bream.

As concluding remarks, the present study describes the all STAT members for the first time in a single fish species. This approach in comprehensive study of STAT family members in JAK/STAT signaling cascade of rock bream will provide the enormous information about the structural features and functional roles specifically in response to the host immunity and tissue injury. Further, this information regarding all STAT genes may contribute to establish the teleostean JAK/STAT signaling pathway.

CHAPTER 1

An introduction to JAK/STAT signaling cascade in teleost

1.1 General introduction

The overall objective of this dissertation was to explore the molecular insights, functional role and cellular localization of selected genes involved in JAK/STAT signaling pathway in rock bream, *Oplegnathus fasciatus*. JAK/STAT pathway is one of the handfuls of pleiotropic cascades used to transduce a multitude of signals for development and homeostasis in animals from human to amoeba. The structural and functional insights of this mechanism in mammals have been extensively investigated. However, the corresponding effort to demonstrate the existence of these components is very limited, and detailed profiling of their molecular profiles, expression and functional evidence has been reported haphazardly in several fish species. Exploring the existence and functional characterization of the elements of this signaling cascade in a single teleost fish species is a potential challenging task for molecular immunologists, and to the best of my knowledge, no such study has been reported so far. In this dissertation, all the STAT genes involved in JAK/STAT signaling pathway were identified using an integrated transcriptomic and genomic-approach, and characterized at genomic and/or transcriptional levels. The details of each STAT member are presented in each chapter. I believe that the study presented in this dissertation is not only advances the knowledge of rock bream immunology in a broader perspective, but also provides an understanding about genomic evolution of the JAK/STAT signaling cascade.

1.2. Immune system

The immune system is a complex network of cells and proteins that defends the body against infection. It has a great ability to identify the wide variety of external agents such as microbial pathogens from viruses to parasites, and distinguish them from own tissues of the organism. There two main immune systems particularly in vertebrates have been classified based on their functional features.

- (a) Innate immune system
- (b) Adaptive immune system

The macrophages and neutrophils of the innate immune system provide a first line of defense against many common microorganisms and are essential for the control of common bacterial infections. However, they cannot always eliminate infectious organisms, and there are some pathogens that they cannot recognize. The lymphocytes of the adaptive immune system have evolved to provide a more versatile means of defense which, in addition, provides increased

protection against subsequent reinfection with the same pathogen. The cells of the innate immune system, however, play a crucial part in the initiation and subsequent direction of adaptive immune responses, as well as participating in the removal of pathogens that have been targeted by an adaptive immune response. Moreover, because there is a delay of 4–7 days before the initial adaptive immune response takes effect, the innate immune response has a critical role in controlling infections during this period.

1.2.1. Innate immune system

Innate immunity refers to nonspecific defense mechanisms that come into play immediately or within hours of an antigen's appearance in the body. It consists of cells and proteins that are always present and ready to mobilize and fight microbes at the site of infection. The main components of the innate immune system are 1) physical epithelial barriers, 2) phagocytic leukocytes, 3) dendritic cells, 4) a special type of lymphocyte called a natural killer (NK) cell, and 5) circulating plasma proteins (**Fig. 1.1**).

1.2.2. Adaptive immune system

Adaptive immunity refers to antigen-specific immune response. The adaptive immune response is more complex than the innate. The antigen first must be processed and recognized. Once an antigen has been recognized, the adaptive immune system creates an army of immune cells specifically designed to attack that antigen (**Table 1.1**). Components of the adaptive immune system are normally silent; however, when activated, these components “adapt” to the presence of infectious agents by activating, proliferating, and creating potent mechanisms for neutralizing or eliminating the microbes. There are two types of adaptive immune responses: humoral immunity, mediated by antibodies produced by B lymphocytes, and cell-mediated immunity, mediated by T lymphocytes (**Fig. 1.1**).

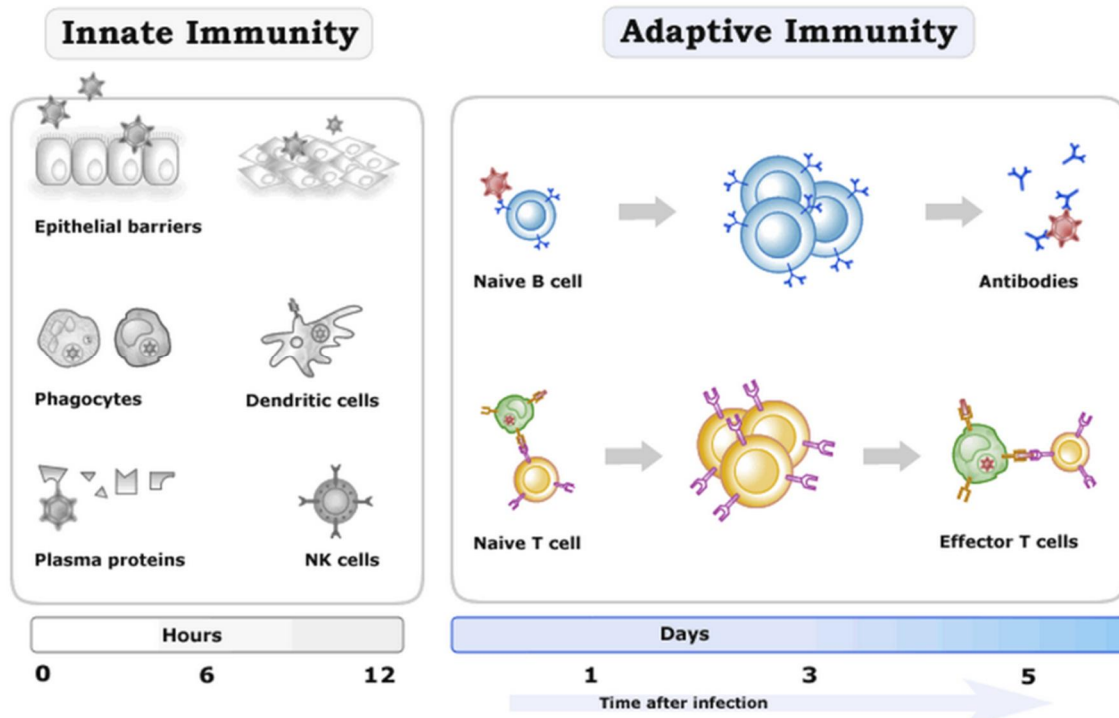


Fig. 1.1. The main components of the innate and adaptive immune system

Table 1.1 Key features of innate and adaptive immunity

[adopted from (Hansson et al., 2002)]

	Innate	Adaptive
<i>Appearance in evolution</i>	<ul style="list-style-type: none"> • Primitive organisms 	<ul style="list-style-type: none"> • Vertebrates
<i>Induction time</i>	<ul style="list-style-type: none"> • Fast (hours to days) 	<ul style="list-style-type: none"> • Slow (days to decades)
<i>Recognizes</i>	<ul style="list-style-type: none"> • Common “pathogen-associated microbial patterns” (PAMPs) 	<ul style="list-style-type: none"> • Unique epitopes on each pathogen/antigen
<i>Cellular components</i>	<ul style="list-style-type: none"> • Macrophages; NK cells; mast cells 	<ul style="list-style-type: none"> • T and B cells
<i>Generation of specificity</i>	<ul style="list-style-type: none"> • Encoded in germ-line 	<ul style="list-style-type: none"> • Somatic rearrangement
<i>Distribution</i>	<ul style="list-style-type: none"> • Non-clonal and all cells of a class identical 	<ul style="list-style-type: none"> • Clonal and all cells of a class distinct
<i>Effector mechanisms</i>	<ul style="list-style-type: none"> • Complement (alternative pathway); cytokines; chemokines; cell-mediated cytotoxicity 	<ul style="list-style-type: none"> • Antibodies; cytotoxic T cells (CTL); classical complement activation; antibody-dependent cell-mediated cytotoxicity; cytokines, chemokines
<i>Characteristic transcription factors</i>	<ul style="list-style-type: none"> • NF-κB (+JNK/AP1) 	<ul style="list-style-type: none"> • Jak/STAT, NF-κB, etc.

1.3. Fish immune system

The immune system of fish is physiologically similar to that of higher vertebrates, despite certain differences. In contrast to higher vertebrates, fish are free-living organisms from early embryonic stages of life and depend on their innate immune system for survival (Bowden et al., 2005). Nonspecific immunity is a fundamental defense mechanism in fish. In addition, it plays a key role in the acquired immune response and homeostasis through a system of receptor proteins. These receptor proteins identify molecular patterns that are typical of pathogenic microorganisms, including polysaccharides, lipopolysaccharide (LPS), peptidoglycan bacterial DNA, viral RNA and other molecules that are not normally on the surface of multicellular organisms. This response is divided into physical barriers and cellular and humoral immune response. These immunological parameters include growth inhibitors, lytic enzymes, the classic complement pathways, the alternative and lectin pathway, agglutinins and precipitins (opsonins and primary lectins), antibodies, cytokines, chemokines and antibacterial peptides. Various internal and external factors can influence innate immune response parameters. Temperature changes, stress management and density may have suppressive effects on this type of response, while several food additives and immunostimulants can enhance their efficiency (Magnadottir, 2006; Magnadottir, 2010). Fish possess both innate immunity as well as adaptive immunity. However, the innate immunity is stronger than adaptive immunity.

1.3.1. Innate immunity of fish

Fish are constantly in intimate contact with aquatic environment surrounded by various pathogens, and therefore a strong first line of defense is imperative to their survival. In fish, the innate response is considered an essential component in battling pathogens due to limitations of the adaptive immune system, their limited repertoire of antibodies and the slow proliferation, maturation and memory of their lymphocytes (Whyte, 2007). The innate immune system is a very efficient immune arm in fish, and acts as the fundamental mechanism in fighting infections against both bacteria and virus (reviewed in (Ellis, 2001; Uribe et al., 2011)). Fish innate immunity constitutes physical parameters, specific cells and humoral parameters (Magnadottir, 2006). Fish mucus act as first defense line and it contains substances like lectins, pentraxins, lysozyme, complement proteins, antibacterial peptides and IgM (Alexander and Ingram, 1992; Aranishi and Nakane, 1997). There are number of cells act in cell-mediated innate immunity, which includes phagocytic cells (granulocytes (neutrophils) and monocytes/macrophages) and the non-specific cytotoxic cells (Nakanishi et

al., 1999; Neumann et al., 2001). As humoral parameters, they possess a wide spectrum of antiviral and antibacterial components and mechanisms. Interferons, Mx proteins, viral sensing receptors, antiviral cytotoxic cells and some complement components act as the mediators of antiviral mechanisms in fish. On the other hand, antibacterial innate defense measures of fish include broad-spectrum antimicrobial substances and acute phase proteins, non-classical complement activation, release of cytokines, inflammation and phagocytosis. Antimicrobial substances are generally peptides (antimicrobial peptides; AMPs) with function against not only bacteria, but also combat fungi, parasites and viruses (Hancock and Diamond, 2000). They are responsible for a range of biological activities including inflammatory responses, decreasing cytokine production, neutralizing bacterial lipopolysaccharide (LPS) and preventing endotoxin-induced damage (Plouffe et al., 2005). Numerous AMPs, including LEAP, Salmonicidin, defensin, Hecpudin, CRP/Pentraxin, Parasin, Moronecidin and Epinecidin have been identified from a number of fish species (Desriac et al., 2013). Various growth inhibitors such as transferrin retard the bacterial growth in vivo. Lytic enzymes, such as lysozymes and chitinase have been identified and characterized from several species (Whang et al., 2011b). Diverse numbers of cytokines and chemokines that control and coordinate the innate and acquired immune response have been reported from fish (Secombes et al., 2001). Complement, an important component of the fish innate immune system, is comprised of about 35 individual proteins and actively functions against many microbial pathogens (Holland and Lambris, 2002). In addition to all of these measures, PRRs, which recognize the non-self from self, are one of the important role-players of innate immunity. Since, the aim of study is mainly focused on a PRR; a detailed introduction is presented in following chapters.

1.3.2 Adaptive immunity of fish

Fish are the first vertebrate group with the appearance of the adaptive immunity. However, due to the lack of structural complexity, the capability of generating functional adaptive immune responses against pathogen invasion is relatively limited. This is because; fish adaptive immune responses are primitive, inefficient and depend on temperature, result in a limited antibody repertoire, affinity maturation and memory and a slow lymphocyte proliferation.

The Igs/ Abs are crucial components of humoral adaptive responses elicited by fish, and mainly consisted of IgM class with 8 antigen-liganding sites. IgD has also been identified in catfish and shown to have similar sequence attributes to that of mammals (Wilson et al.,

1997). Recently, IgT has been discovered and its unique structure and functions related to mucosal immunity has been documented (Hansen et al., 2005; Zhang et al., 2010). The relative concentrations of Abs in serum of fish have been determined in different species. Teleost Abs are found to be distributed in skin, intestine, gill mucus, bile and plasma (Uribe et al., 2011). Furthermore, several studies have also demonstrated the ability of numerous fish species to mount a robust and specific antibody response in response to various foreign-antigens, vaccine and bacterial challenges (Killie and Jørgensen, 1994; Eggset et al., 1997).

As a part of their cell-mediated immunity, fish possess lymphocyte populations analogous to B and T cells, nonspecific cytotoxic cells (similar to NK cells), macrophages and granulocytes. They also have MHC/T cell receptor system. MHC genes including class IA, B2m, class IIA and class IIB have been reported from many fish. However, compared to humoral immunity, the cell-mediated immunity of acquired arm in fish is poorly understood (Stet et al., 1996; Nakanishi et al., 1999; Secombes et al., 2005; Nakanishi et al., 2011).

There are a number of resemblances between the mammalian and fish adaptive immune systems with most of the fundamental features present in fish. However, the immune system of fish lacks bone marrow, lymph nodes and Peyer's patches. In summary, fish possess an immunity system which is highly relied on its innate arm, when compared to that of highly sophisticated mammalian immunity, based on basic physiological, structural and functional aspects summarized in **Table 1.2**.

Table 1.2. Differences between immunity of fish and mammals

[adopted from (Tort et al., 2003)]

	Jawed Fishes	Mammals
Biotic constrictions		
<i>Temperature range</i>	-2 to 35°C	36.5 to 37.5°C
<i>Primary environment</i>	Water	Air
<i>Metabolism</i>	Poikilothermia	Homeothermia
<i>External interfaces</i>	Mucous skin, gills	Respiratory tree
Humoral diversity		
<i>Ig isotypes</i>	IgM, IgD? (Teleostei) IgM, IgX/IgR, IgW, NAR(C) (Chondrichthyes) IgM redox forms	IgM, IgA, IgD, IgE, IgG
<i>Ig gene rearrangement</i>	Multicluster	Translocon
<i>Non-specific diversity</i>	Several C3 isoforms	No C3 isoforms
Overall performance		
<i>Antibody affinity</i>	Low	High
<i>Antibody response</i>	Slow	Fast
<i>Memory response</i>	Weak	Strong
<i>Affinity maturation</i>	Low or absent	High
<i>Low temperatures</i>	High dependence, immunosuppressive response	Low dependence
Lymphoid organs		
<i>Haematopoietic tissue</i>	Head kidney	Bone marrow
<i>Lymphoid nodes</i>	Absent	Present
<i>Gut-lymphoid tissues</i>	Not organized, lymphoid aggregates	Organized, Peyer patches

1.4. The JAK/STAT signal transduction pathway

The JAK/STAT pathway is an evolutionary conserved signaling network involved in a wide range of distinct cellular process, including inflammation, apoptosis, cell cycle control and development. JAKs are cytosolic tyrosine kinases which are associated with the intracellular domain of membrane bound receptors, whose function is to transduce signals from extracellular ligands such as cytokines, growth factors and hormones to the nucleus in order to orchestrate the appropriate cellular response (O'Shea et al., 2002). There are four family members; JAK1, 2, 3 and Tyk2, all of which show different receptor affinities, they all however transduce their signal through recruitment of STAT transcription factors (Levy and Darnell, 2002).

1.4.1. Components of JAK/STAT signaling pathway

1.4.1.1. Ligands and receptors

Mechanistically, JAK/STAT signaling is relatively simple, with only a few principal components. A variety of ligands including Cytokines, Hormones and Growth factors, and their receptors stimulate the JAK/STAT pathway. Intracellular activation occurs when ligand binding induces the multimerization of receptor subunits. For some ligands, such as Epo

(Erythropoietin) and GH (Growth Hormone), the receptor subunits are bound as homodimers while, for others, such as Ifns (Interferons) and ILs (Interleukins), the receptor subunits are heteromultimers. For signal propagation, the cytoplasmic domains of two receptor subunits must be associated with JAK tyrosine kinases. JAK activation occurs upon ligand-mediated receptor multimerization because two JAKs are brought into close proximity, allowing trans-phosphorylation. The activated JAKs subsequently phosphorylate additional targets, including both the receptors and the major substrates, STATs. The seven mammalian STATs bear a conserved tyrosine residue near the C-terminus that is phosphorylated by JAKs. This phosphotyrosine permits the dimerization of STATs through interaction with a conserved SH2 domain. Different JAKs and STATs are activated by different ligands. For example, Hormones such as GH, Epo and Tpo (Thrombopoietin) generally stimulates the activation of JAK2 as well as STAT3 and 5. Phosphorylated STATs then enter the nucleus by a mechanism that is dependent on Importin Alpha-5 (also called nucleoprotein interactor 1) and the Ran nuclear import pathway. Once in the nucleus, dimerized STATs bind specific regulatory sequences to activate or repress transcription of target genes. Thus the JAK/STAT cascade provides a direct mechanism to translate an extracellular signal into a transcriptional response. RTKs (Receptor Tyrosine kinases) commonly activate Ras/Raf/MEK/ERK signaling but when overactivated can also induce the JAK/STAT pathway, originally identified as the signaling cascade downstream of cytokine receptors (Gao, 2005; Marrero, 2005).

1.4.1.2. Janus kinases (JAKs)

Janus kinases (JAKs) were identified through sequence comparisons as a unique class of tyrosine kinases that contain both a catalytic domain and a second kinase-like domain that serves an auto-regulatory function, hence the homage to the two-faced Roman god. They were functionally linked to STATs and interferon signaling in powerful somatic cell genetic screens (Darnell et al. 1994; Schindler and Plumlee 2008). The JAK/STAT cascade is among the simplest of the conserved metazoan signaling pathways. The binding of extracellular ligand leads to pathway activation via changes to the receptors that permit the intracellular JAKs associated with them to phosphorylate one another. Trans-phosphorylated JAKs then phosphorylate downstream substrates, including both the receptor and the STATs. Activated STATs enter the nucleus and bind as dimers or as more complex oligomers to specific enhancer sequences in target genes, thus regulating their transcription.

1.4.1.3. Signal transducer and activator of transcription (STAT)

STAT proteins were identified more than a decade ago, as being latent cytoplasmic transcription factors that upon activation regulate cell growth, proliferation and differentiation (Schindler et al., 1992). The events leading to STAT activation follow directly after cytokine induction and JAK mediated phosphorylation of STATs, which then dimerize, translocate to the nucleus and bind to consensus DNA-binding sites also known as GAS sites (gamma interferon-activated sites). These sites are present in the promoters of cytokine inducible pathway target genes, and require STAT binding for their active transcription (Bromberg et al., 1998; Darnell et al., 1994; Song and Grandis, 2000). Much research to characterize the activation of STATs has been carried out and has demonstrated that STAT proteins are activated in response to ligand binding to many cytokine receptors, including growth hormone (GH), prolactin (Prl), erythropoietin (Epo), as well as several other growth factor receptors (Davy et.al., 1999; Ihle, 2001; Leaman et al., 1996).

To date, seven STAT proteins have been identified in mammals ranging in size from 750 to 850 aa. The chromosomal distribution of these STATs, as well as the identification of STATs in more primitive eukaryotes suggests that this family arose from a single primordial gene. The locus seems to have duplicated over years, possibly reflecting an increasing need for cell to cell communication as complexity within eukaryotes evolved (reviewed in Kisselva et al., 2002). The STAT family consists of seven members; STAT1, 2, 3, 4, 5a, 5b and 6, and although they are structurally similar proteins, they are functionally heterogeneous (Levy and Daenell, 2002). STATs possess a series of conserved structural domains; the N-terminal domain (NTD) is involved in reciprocal STAT interactions and is loosely tethered to the rest of the STAT protein, the coiled coil (CC) domain contains consensus sites for nuclear transport, the DNA binding domain (DBD) binds to conserved regulatory sequences in the promoters of target genes, the src homology 2 (SH2) domain controls receptor binding and the C-terminal transactivation domain (TAD) contains the phosphorylation sites necessary for STAT activation (**Fig. 1.2**).

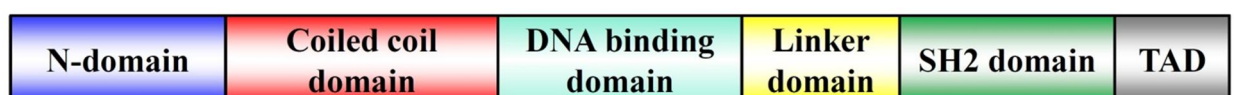


Fig. 1.2. Schematic representation of domain organization in STAT protein. Model of STAT protein structure consisting of an N-terminal domain (NTD), a coiled coil domain (CC), a DNA binding domain (DBD), a linker domain, a Src homology 2 domain (SH2) and a C-terminal transactivation domain (TAD).

1.4.2. Mechanism of JAK/STAT signaling

A large array of cytokines and growth factors utilize the JAK/STAT network to transduce their cognate signal to the nucleus, for example IL-6, IL-10, cardiotrophin 1 (CT-1) and G-CSF induce STAT3 activity, while interferons (IFN) utilize predominantly STAT1 and STAT2. Ligand binding to the extracellular domain of JAK associated cytokine receptors induces receptor dimerisation and JAK autophosphorylation. JAKs then transphosphorylate the cytoplasmic domain of the cytokine receptor and create a docking site for the SH2 domain of STATs (Levy and Darnell, 2002). Once STATs bind to the intracellular receptor chain, they are phosphorylated by JAKs at distinct tyrosine residues, causing the bound STATs to be released from the receptor and translocate to the nucleus where they bind specific sequences such as the IFN γ activated sequence (GAS) in the promoters of target genes (**Fig. 1.3**) (Levy and Darnell, 2002). Once bound to DNA, the NTD is responsible for recruiting RNA Pol II and co-factors such as the histone acetyl transferase p300 (Hou et al., 2008). Thus, the STAT members and their functional roles are known to be varied. As shown in Fig. 1.4, signals from various cytokines pass through their cognate receptors associated with JKAs and then via STAT members to the nucleus to show the respective functions.

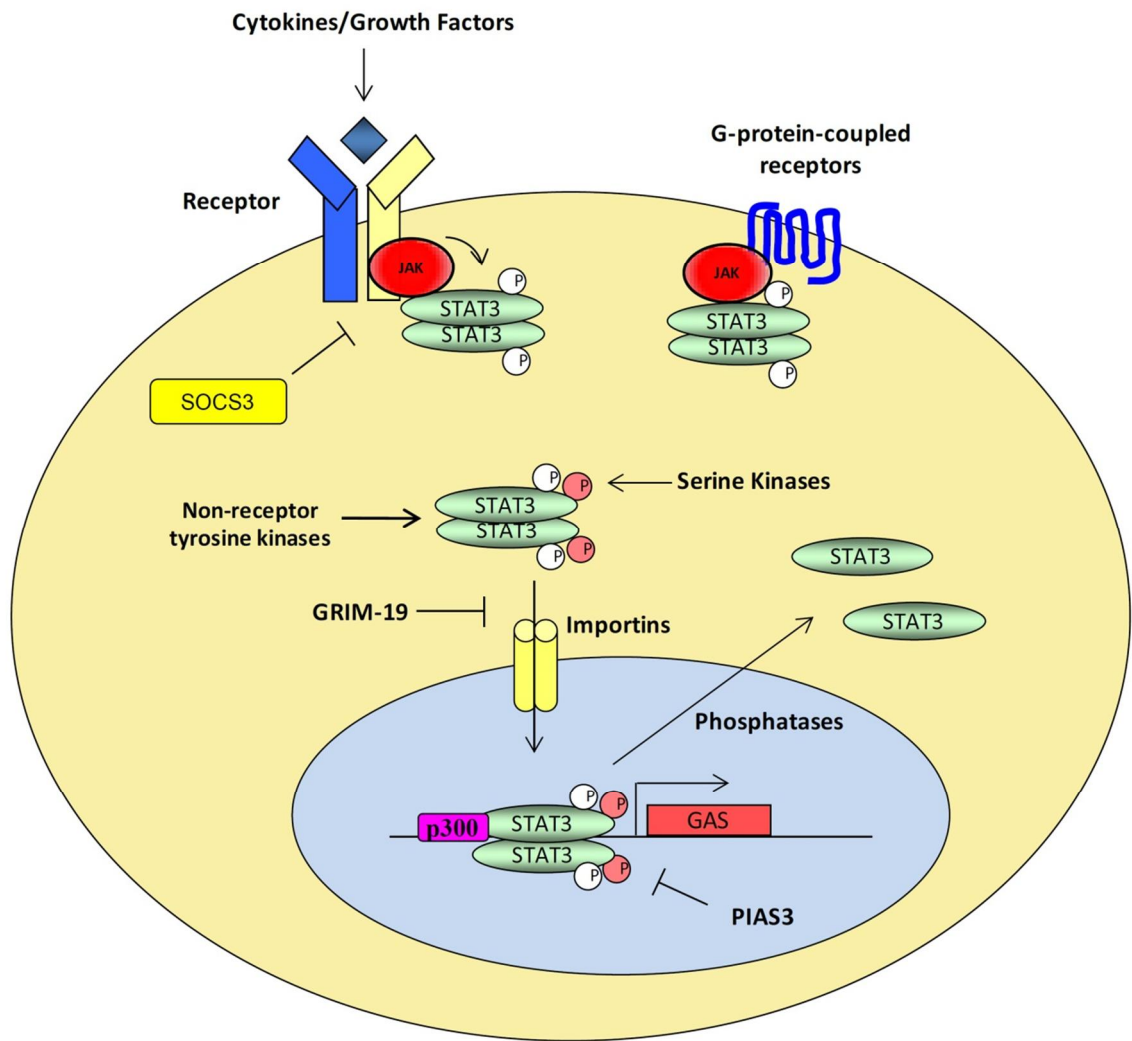


Fig. 1.3. Outline of the JAK/STAT3 Pathway. Members of the JAK tyrosine kinases are recruited to cytokine receptors, growth factor receptors or G-protein coupled receptors. They induce tyrosine phosphorylation of STAT3 which causes it to translocate to the nucleus. In addition, STAT3 can be phosphorylated by non-receptor tyrosine kinases and serine kinases. Transport into the nucleus is controlled by importins and once in the nucleus, active STAT3 binds to target sequences such as the IFN γ activated sequence (GAS), this is aided by histone acetyl transferases such as p300. Dephosphorylation allows STAT3 to dissociate from DNA and return to the cytosol. Activation of STAT3 is antagonized SOCS3 and nuclear translocation is blocked by GRIM-19. In the nucleus PIAS blocks STAT3 binding to DNA.

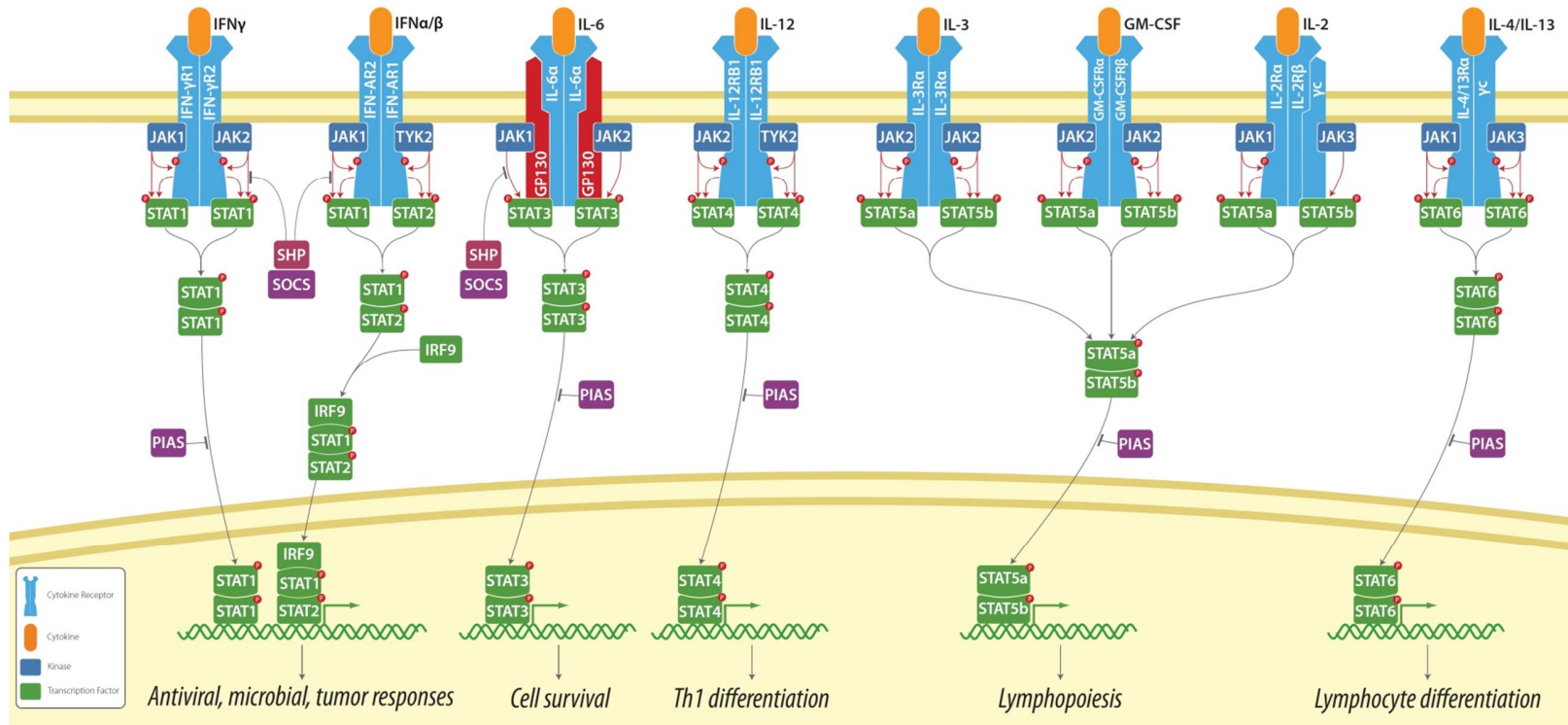


Fig. 1.4. Comprehensive details of JAK/STAT mammalian signaling pathway.

Adopted from: <http://www.jablonskidiagram.com/illust.html>

There are currently around 36 known cytokine receptor combinations that respond to 38 cytokines which utilize distinct combinations of JAKs and STATs (Murray, 2007). The selective use of receptor combinations outlined in **Fig 1.5** allow a certain specificity for signaling but it is currently unknown precisely how cytokines exert differing responses utilizing the same JAK and STAT combinations. The JAK/STAT pathway can also be stimulated by G-protein coupled receptors such as the angiotensin II receptor and this may be mediated through Rho family GTPases (Marrero et al., 1995, Pelletier et al., 2003). Another mode of JAK/STAT activation is via non-receptor tyrosine kinases such as Src, Fer, Abl, Etk and Lck which all induce STAT3 activity (Yu et al., 1995, 1997, Nelson et al., 1998, Lund et al., 1999, Wen et al., 1999, Priel-Halachami et al., 2000). The IL-6 family of cytokines comprises IL-6, IL-11, leukaemia inhibitory factor (LIF), oncostatin M (OSM), ciliary neurotrophic factor (CNTF), cardiotrophin-1 (CT-1) and cardiotrophin-like cytokine (CLC). IL-6 cytokine receptors are comprised of the signal transducer gp130 in combination with IL-6R, IL-11R, LIF-R or OSM-R. All IL-6 cytokines potently activate STAT3 and this is followed by internalization and degradation of gp130 (Fischer and Hilfiker-Kleiner, 2007). Serum levels of IL-6, soluble gp130, LIF and CT-1 have all been shown to be elevated in patients suffering from heart failure and these levels correlate with the severity of left ventricular dysfunction, suggesting that the IL-6/STAT3 axis may have a role to play in myocardial cell death (Roig et al., 1998, Hirota et al., 2004, Torea-Aminone et al., 1996, Khan et al., 2006).

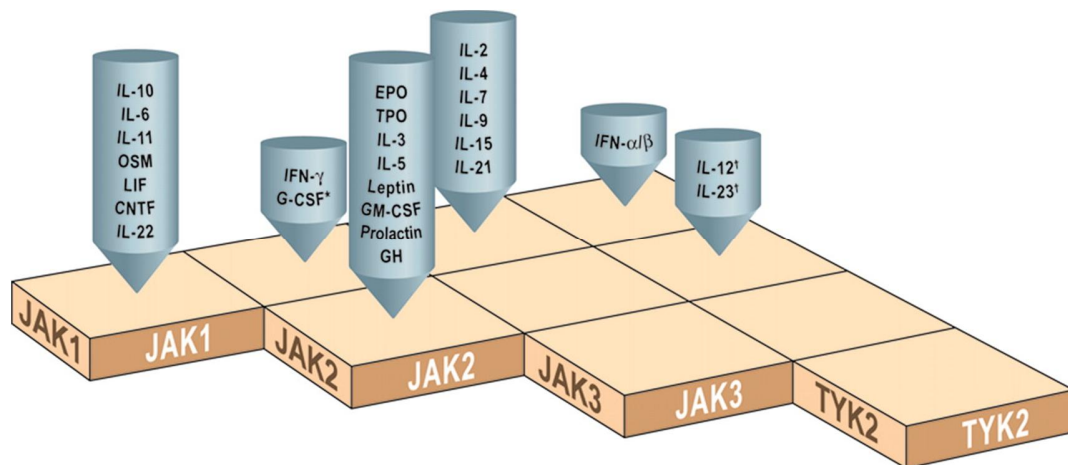


Fig. 1.5. JAK usage by cytokines. Shown are cytokines and the JAK combinations which they utilize. Taken from (Murray, 2007).

Dimerization of STATs appears to be essential for DNA binding and retention in the nucleus. Traditionally it was thought that inactive STATs were present as monomers and only undergoes dimerization after phosphorylation; however accumulating evidence suggests that unphosphorylated STATs are present in the cytosol as dimers or higher order multimers (Ndubuisi et al., 1999). Unphosphorylated STAT1 dimers are formed by reciprocal interactions of their N-terminal domains, coiled-coil and DNA binding domains in an anti-parallel conformation (**Fig. 1.6**) (Chen et al., 1998). Phosphorylation promotes dimerization through the SH2 domains in a parallel confirmation which is essential for DNA binding and nuclear retention and these parallel and anti-parallel conformations appear to be mutually exclusive (**Fig 1.6**) (Mao et al., 2005, Wenta et al., 2008). Recently it has been shown that tyrosine phosphorylation of STAT1 is dispensable for DNA binding per se, however phosphorylation promotes the parallel conformation which increases DNA binding activity by more than 200 fold (Wenta et al., 2008).

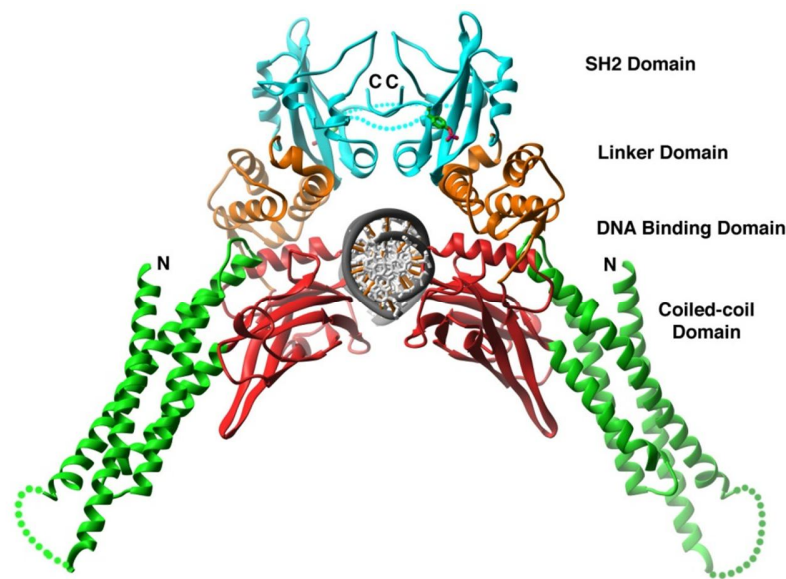


Fig. 1.6. Structure of the STAT1 core dimer on a GAS element. The component domains are colored green (coiled-coil domain), red (DNA-binding domain), orange (linker domain), blue (SH2 domain). Disordered loops (one in the coiled-coil domain and one connecting the SH2 domain to the tail segment) are shown as interrupted lines. The phosphotyrosine residue is shown in a stick representation. The N and C termini of the STAT-1 core are indicated. The DNA backbone is shown in gray. Adopted from (Chen et al., 1998).

1.5. STATs in teleosts

The complete JAK/STAT signaling pathway from fish species is still under investigating level. Number of studies has reported the identification of STAT members from various species, and studied their functional roles, and the identified STAT members summarized in **Table 1.3**. Up to now there are no all STAT members that have been identified from single species. However, all STAT members except STAT2 have been identified and characterized from mandarin fish and zebrafish. In the present thesis we have described the structural features and functional roles of all STAT members which were homologous to the mammalian STAT members.

Table 1.3. Summary of STAT genes identified from fish species

Scientific name	Common name	STAT1	STAT2	STAT3	STAT4	STAT5	STAT6
<i>Oplegnathus fasciatus</i>	Rock bream	STAT1	STAT2	STAT3	STAT4	STAT5-1	STAT6
		STAT1L				STAT5-2	
<i>Siniperca chuatsi</i>	Mandarin fish	STAT1	-	STAT3	STAT4	STAT5	STAT6
<i>Danio rerio</i>	Zebrafish	STAT1a	-	STAT3	STAT4	STAT5	STAT6
		STAT1b					
<i>Samo salar</i>	Atlantic salmon	STAT1	STAT2	STAT3	STAT4	-	-
<i>Channa argus</i>	Snakehead	STAT1	-	-	-	-	-
<i>Paralichthys olivaceus</i>	Olive flounder	STAT1	-	-	-	-	-
<i>Carassius auratus</i>	Crucian carp	STAT1	STAT2	-	-	-	-
<i>Scophthalmus maximus</i>	Turbot	STAT1	STAT2	STAT3	-	STAT5	-
<i>Tetraodon nigroviridis</i>	Pufferfish	STAT1	STAT2	-	-	STAT5	STAT6
<i>Ctenopharyngodon idellus</i>	Grass carp	-	-	STAT3	-	-	-
<i>Epinephelus spp</i>	Grouper	-	-	STAT3	-	-	-
<i>Epinephelus malabaricus</i>	Malabar grouper	STAT1	-	-	-	-	-

Gray color shaded boxes indicate the available STAT genes in Genbank but not studied.

1.6. Biological species of this study

In an attempt to investigate the STAT members in teleostean JAK/STAT signaling pathway at molecular level and functional roles, rock bream, *Oplegnathus fasciatus* (Temminck & Schlegel, 1844), was chosen as the biological animal model. Rock bream also known as the barred knifejaw or striped beakfish, is a species of knifejaw native to the northwestern Pacific Ocean though the area a smattering of records from other localities in the eastern Pacific such as Hawaii and Chile. It is an inhabitant of rocky reefs and occurs at depths of from 1 to 10 metres (3.3 to

32.8 ft). Juvenile members of this species can be found with patches of drifting seaweed. This species can reach a length of 80 cm (31 in) total length with the greatest recorded weight for this species of 6.4 kilograms (14 lb). The color pattern consists of light and dark vertical bars from which it derives its name (**Fig. 1.7**). It has been recorded as feeding on hard-shelled invertebrates such as crustaceans and molluscs. It is a commercially important species and is also farmed. It is also sought after as a game fish. Rock bream belongs to the class Actinopterygii (Ray-fin fishes) and order Perciformes (perch-like). It is one of the most commercially important fish species of Eastern Asian aquaculture (Lipton and Kim, 2010). However, production losses have also increased in recent years with the growing and intensified mariculture industry owing to the occurrence of many infectious diseases (Park Ii, 2009). Therefore, researchers have directed their focus towards understanding the underlying pathogenic mechanisms and immune responses to establish a healthier and sustainable industry.



Fig. 1.7. Rock bream fish

1.6.1. Rock bream aquaculture and diseases

The rock bream is very popular for Sashimi and thus is very expensive in both Korea and Japan. In Korea, most fish farmers want to culture rock bream. However, since there is a shortage in the supply of fry, mortality is very high. The Vibriosis was dominant disease of all cultured fish. And also, Edwardsiellosis, Streptococcosis, Flavobacterial disease and Scuticociellosis disease are sometimes found as well. In the case of the Rock bream, iridovirus was identified as a predominant pathogen. Therefore in order to prevent these crucial effects from various microbial pathogens, it is essential to study the immune system of fish.

1.7. Main objectives of this study

The principal goal of this study was to establish the molecular evidences for the existences of JAK/STAT signaling pathway in rock bream. Seven numbers of cytosolic elements which are important to transduce the signals from cell membrane to nucleus in order to initiate the relevant functions are identified from the sequence data bases. The main objectives of this study are as follows;

- To characterize the genes involved in JAK/STAT signaling pathway at nucleic acid (cDNA and genomic DNA) and amino acid levels.
- To conduct the comprehensive and comparative analyses of the genomic arrangement of the genes, and their relationship with evolutionary differences between fish and other vertebrates
- To predict the possible transcription factor binding sites those are important for the transcription initiation of each gene.
- To examine the transcriptional profiles of STAT genes
 - In different tissues of healthy fish to show the spatial distribution of each gene
 - In fish injected with microbial pathogens (*Edwardsiella tarda* , *Streptococcus iniae*, rock bream irido virus) and mitogens [lipopolysaccharides (LPS) and Polyinosinic:polycytidylic acid (poly I:C)]
 - In fish after injured at dorsal side of the fish
 - In rock bream heart cells treated with rock bream recombinant IL-10 protein
- Subcellular localization of STAT proteins and nuclear translocation after poly I:C stimulation.

CHAPTER 2

Materials and Methods

2.1 The rock bream cDNA library construction and identification of genes

A rock bream cDNA sequence database was established by using the Roche 454 Genome sequencer (GS-FLX™), a next generation DNA sequencing technology (Droege and Hill, 2008). Healthy rock bream fish with an average weight of ~50 g, obtained from the Jeju Special Self-Governing Province Ocean and Fisheries Research Institute (Jeju, Republic of Korea) were adapted to the laboratory conditions (salinity $34 \pm 1\%$, pH 7.6 ± 0.5 at 24 ± 1 °C) in 400 L tanks. Whole blood samples were withdrawn from the caudal fin of three healthy fish using a 22 gauge needle and centrifuged immediately for 10 min at $3000 \times g$ at 4 °C, to collect the hematic cells. Subsequently, fish were killed and various tissues were excised and immediately flash-frozen in liquid nitrogen and stored in -80 °C, until RNA extraction. The total RNA was isolated from individual tissues (pituitary gland, brain, gill, blood, liver, spleen, head kidney, and kidney) pooled from three fish using the Tri Reagent™ (Sigma, USA) following the manufacturer's instructions. The concentration and purity of RNA was determined by absorbance at 260 and 280 nm using a UV-spectrophotometer (BioRad, USA). Then, the purification of polyadenylated mRNA from the isolated total RNA was carried out by means of an mRNA isolation kit (FastTrack® 2.0; Invitrogen, USA). First strand cDNA was synthesized from 1.5 µg of mRNA using Creator™ SMART™ cDNA library construction kit (Clontech, USA). Amplification was performed with Advantage 2 polymerase mix (Clontech) under conditions of 95 °C for 7 s, 66 °C for 30 min and 72 °C for 6 min. Over-representation of the most commonly expressed transcripts was excluded by normalizing the synthesized cDNA using Trimmer-Direct cDNA normalization kit (Evrogen, Russia). Thereafter, the sequencing of rock bream cDNA was performed on a Roche 454 pyrosequencing platform with GS-FLX Titanium instrument and related reagents (DNA Link Inc., Republic of Korea). A single full-plate run was performed using the above normalized cDNAs and the reads obtained were processed and assembled with Arachne assembly program (Batzoglou et al., 2002). Finally, a cDNA GS-FLX shotgun library was created based on this sequencing data. The cDNA contigs demonstrating significant homology to the known genes in JAK/STAT signaling pathway were identified using BLAST-X and BLAST-P searching tools (Altschul et al., 1990).

2.2 Construction of bacterial artificial chromosome (BAC) library for rock bream

Rock bream obtained from the Jeju Special Self-Governing Province Ocean and Fisheries Research Institute (Jeju, Republic of Korea) were acclimated to the laboratory conditions. Whole blood was aseptically harvested from the caudal fin using a sterile 1 mL syringe with 22 gauge needles, and a BAC library was constructed from the isolated blood cells (Lucigen® Corp., Middleton, WI, USA). Briefly, genomic DNA obtained from peripheral blood cells was randomly sheared, and the blunt ends of large inserts (>100 kb) were cloned into pSMART® BAC vector to obtain an unbiased, full coverage library. The corresponding constructs were then transformed to *E. coli* and around 92160 clones, possessing an average insert size of 110 kb (100-120 kb), were arrayed in 240 microtiter plates with 384 wells. The BAC library was stored in -80 °C (Quiniou et al., 2003). Aliquots of the grown cultures were pooled with other clones from the same plate, row or column pools for DNA preparation. Then, they were further combined to form Super Pools (n = 20). For the screening purpose, the DNA was extracted from each clone separately and arranged by super pooling and pooling system, comprising 20 super pools, 16 row pools and 24 column pools, spanning the entire rock bream genome.

Primers for BAC library screening were designed based on the cDNA sequence identified from the rock bream cDNA database (Details of primers are given in separate tables in each chapters of results part). A two-step PCR-based screening of the BAC library was used to identify the super pools and the individual plate, row, and columns through which the location of the clone of interest bearing the respective candidate genes could be located. Each Super Pool had a corresponding 96-well plate containing its Plate-pools, Row-pools, and Column pools (P-R-C pools). The Super Pools were screened during the first round of PCR, and plates, rows, and columns were screened during the second round of PCR to determine the exact well containing the clone of interest. Finally, the identified clone was isolated from the corresponding well, and confirmed by a colony PCR with gene-specific primers. The positive BAC clones were cultured and purified with a Qiagen Plasmid Midi Kit (Hilden, Germany). Finally, 15 positive clones were pooled and subjected to Pyro-sequencing (GS-FLX 454, Macrogen, Republic of Korea). Once the genomic sequence was obtained by sequencing, the exon and intron structures were derived by comparing cDNA sequences of each gene. Genomic sequences were identified by

cDNA alignment using the Spidey (<http://www.ncbi.nlm.nih.gov/IEB/Research/Ostell/Spidey/>) mRNA to genomic alignment program on NCBI or based on the prediction data offered by the sequencing company (Macrogen, Republic of Korea) or based on the comparison with the genomic arrangement of known orthologous sequences.

2.3 *In silico* characterization of CDS, amino acid sequence, genome structural arrangement and phylogenetic analysis

The cDNA sequence(s) exhibiting significant similarity with known orthologs a gene of interest available in NCBI, was identified by BLAST and subjected to DNAssist (version 2.2) to predict the CDS, and translated to corresponding amino acid sequence(s). Each amino acid sequence was analyzed by BLAST-P at the NCBI and Ensembl databases (Altschul et al., 1990), and the orthologous sequences were retrieved. The deduced amino acid sequence and its architecture were analyzed using the ExPASy Resource Portal (<http://www.expasy.org/>). The conserved domains were identified using SMART server (<http://smart.embl-heidelberg.de/>) (Letunic et al., 2009) and conserved domain database (CDD) search (<http://www.ncbi.nlm.nih.gov/Structure/cdd/cdd.shtml>). Prediction of motifs, specific signature and family characteristics of protein(s) was carried out using the PROSITE profile database (Bairoch et al., 1997), SMART platform (<http://smart.embl-heidelberg.de/>) and MyHits (<http://myhits.isb-sib.ch/>). Pairwise alignment and multiple sequence alignment were executed using ClustalW (Thompson et al., 1994). Identity, similarity, and gap percentages were calculated by the EMBOSS pairwise alignment algorithms (http://www.ebi.ac.uk/Tools/psa/emboss_needle/) or MatGAT program using default parameters (Campanella et al., 2003). The phylogenetic trees were constructed with the molecular evolutionary genetic analysis (MEGA) software package (version 6.06) using an appropriate method (either NJ or ML) (Tamura et al., 2011) with bootstrap values calculated with 5000 replications to estimate the robustness of internal branches.

The tertiary structure analysis of certain proteins was demonstrated by web-based computer simulation models generated by either SWISS-MODEL (Arnold et al., 2006; Whang et al., 2011a). For the visualization of three dimensional (3D) structures and annotation of sub-

components PyMOL molecular graphic system (version 1.3) and POV-ray for windows (version 3.62) were used.

Genomic DNA sequences of the respective BAC clones were used to determine the exon-intron structures and the putative promoter regions of each gene. The exon-intron structures were derived by aligning the cDNA sequence with genomic sequence using Spidey program (<http://www.ncbi.nlm.nih.gov/IEB/Research/Ostell/Spidey/>). The genomic structures used for inter-lineage comparison were obtained from the exon view of Ensembl genome database or the GENE database at NCBI. The genomic structures were constructed using Gene Mapper v2.5 (<http://genemapper.googlepages.com>) and decorated with Adobe® Photoshop CS2.

In certain circumstances, BAC DNA from the positive clone was extracted by using QIAGEN Plasmid Midi Kit, and was subjected to sequencing by primer walking with gene-specific primer(s) to obtain the 5'-flanking sequence upstream of the untranslated region (UTR). The putative transcriptional factor binding sites (TFBS) in the 5'-flanking regions were identified using TFSEARCH v1.3 according to the highest threshold score (90%) (Heinemeyer et al., 1998), Alibaba v2.1 (<http://www.gene-regulation.com/pub/programs/alibaba2/index.html>), TESS and TRANSFAC tools. The putative transcription initiation site(s) (TIS) was inferred using the Neural Network Promoter Prediction in Berkeley Drosophila Genome Project (BDGP) (Hoskins et al., 2011).

2.4 Experimental animals and *in vivo* challenge experiments

The healthy rock bream (~50 g) were obtained from the Jeju Special Self-governing Province Ocean and Fisheries Research Institute (Jeju, Republic of Korea). They were acclimatized for one week prior to the experiments under laboratory conditions (salinity: $34 \pm 1\text{‰}$, pH 7.6 ± 0.5 at $24 \pm 1\text{ °C}$) in 400 L tanks filled with aerated and sand-filtered sea water in Fish Vaccine Research Centre, Jeju National University (Jeju, Republic of Korea). After adaptation, to minimize stress factors, a maximum of 40 animals per 40 L were housed in each tank. Fish were fed with a commercial feed with the daily ration equaling 3% (w/w) of body weight. The laboratory environmental settings such as aeration, temperature and circulation were uniformly maintained during all the experiment.

In order to determine the immune responses of the genes of interest at mRNA level and to examine their transcriptional regulation upon pathological conditions, two pathogenic bacterial strains *Edwardsiella tarda* (Gram negative) and *Streptococcus iniae* (Gram positive), and a live virus (rock bream iridovirus; RBIV) were used in time-course experiments, as described in **Table 2.1**. In addition, purified LPS (055:B5 from *Escherichia coli*; Sigma), polyinosinic-polycytidylic acid (Poly I:C; double stranded RNA mimicking the viral nucleic acid material) were used as immunostimulants. In addition, all the pathogen/stimulant challenge experiments were conducted in accordance with The Code of Ethics of the EU Directive 2010/63/EU.

2.4.1 Bacterial challenge

The bacterial strains, *E. tarda* and *S. iniae* were kindly provided by the Department of Aquaculture Medicine at Chonnam National University (Republic of Korea). These strains were grown in brain heart infusion (BHI) agar (Eiken Chemical Co., Japan) + 1.5% NaCl plates at 30 °C for overnight. A single colony was picked into incubated at BHI broth supplemented with 1.5% NaCl and allowed to grow at 30 °C with 200 rpm shaking incubator until the OD₆₀₀ reached the absorbance of 1.0-1.5. Then, the bacterial suspension was briefly spun down at 3500 rpm for 20 min. Finally, bacterial pellet(s) was re-suspended in PBS and cell numbers were adjusted to 5×10^3 CFU/mL (*E. tarda*), and 1×10^5 CFU/mL (*S. iniae*) by serial dilution, and used as stock for experimental injection. Then, each fish was intraperitoneally injected with *E. tarda* (5×10^3 CFU/mL). In the other group, fish were intraperitoneally injected with *S. iniae* (1×10^5 CFU/mL) suspended in 1× phosphate-buffered saline (PBS; 100 µL/animal).

2.4.2 Viral challenge

RBIV was obtained from the kidney of an RBIV-infected moribund rock bream. The viral specimen was prepared by homogenizing the kidney of RBIV-infected rock bream with approximately 20 volumes of 1 × PBS (1 mL PBS/100 mg tissue). The homogenate was centrifuged at $3000 \times g$ for 10 min, and the supernatant containing the virus was filtered through a 0.45 µm syringe filter, and stored at -80 °C until use. For the RBIV challenge experiment, the supernatant was thawed and diluted to obtain 10^2 TCID₅₀ (tissue culture infective dose; that amount of a pathogenic agent that will produce pathological change in 50% of cell cultures inoculated) of RBIV per 100 µL, and intramuscularly injected at a dosage of 100 µL per 50 g fish (**Table 2.1**).

Table 2.1. Description of experimental challenges conducted in this study

Group No.	Pathogen/mitogen	Source	Dose (per fish)	Stock concentration	Route of administration	Volume	Resuspension
1	<i>Edwardsiella tarda</i>	CNU*	5×10^5 CFU	5×10^3 CFU/ μ L	Intraperitoneal (i.p.)	100 μ L	In 1 \times PBS
2	<i>Streptococcus iniae</i>	CNU*	1×10^7 CFU	1×10^5 CFU/ μ L	Intraperitoneal (i.p.)	100 μ L	In 1 \times PBS
3	RBIV	Infected kidney	10^2 TCID ₅₀ /fish	10^3 TCID ₅₀ /mL	Intramuscular (i.m.)	100 μ L	In 1 \times PBS
4	LPS	<i>E. coli</i> 055:B5, Sigma	125 μ g	1.25 mg/mL	Intraperitoneal (i.p.)	100 μ L	In 1 \times PBS
5	Poly I:C	Sigma	150 μ g	1.5 mg/mL	Intraperitoneal (i.p.)	100 μ L	In 1 \times PBS
6	PBS				Intraperitoneal (i.p.)	100 μ L	
7	Un-challenged						

* Obtained from Department of Aqualife Medicine at Chonnam National University (Republic of Korea); CFU, colony forming unit.

2.4.3 Immune stimulant challenge

A sterile LPS stock was prepared by dissolving LPS in PBS at the rate of 1.25 $\mu\text{g}/\mu\text{L}$, and filtered through a 0.2 μm filter. For the LPS challenge, fish ($n=15$) were injected with 100 μL LPS in PBS suspension (1.25 $\mu\text{g}/\mu\text{L}$). In order to examine the transcriptional changes of certain genes post-dsRNA injection in vivo, poly I:C was employed as an immunostimulant. A sterile poly I:C stock was prepared by dissolving poly I:C at the rate of 1.5 $\mu\text{g}/\mu\text{L}$ in PBS, and filtered through a 0.2 μm filter. A time course experiment was performed by intraperitoneally injecting the animals with 100 μL suspension of poly I:C stock.

2.4.4 Control challenge

Similar volume (100 μL) of sterile PBS which used to resuspend/dissolve the pathogens or immunostimulants, was injected intraperitoneally as a negative control group. The last group was kept as unchallenged and used as a blank for the whole experiment.

2.4.5 Tissue injury experiment

A fish group was injured with two incisions (one on each side) on the dorsal surface (2 cm \times 0.5 cm in length and depth, respectively), using sterile surgical blades, and transferred into individual experimental tanks just after injury. A group of uninjured intact fish served as negative control. At different time periods (3, 6, 12, 24, 48 h), blood and liver tissue were collected.

2.5 Tissue collection

In order to profile the tissue distribution of transcripts, whole blood was withdrawn from the caudal fin of three healthy, unchallenged juvenile rock breams (~ 1 mL/fish) and centrifuged immediately for 10 min at $3000 \times g$ at 4 $^{\circ}\text{C}$, to separate the peripheral blood cells (PBCs) from plasma. Subsequently, fish were killed and various tissues (muscle, intestine, brain, skin, gill, liver, spleen, heart, kidney, and head kidney) were dissected.

From challenged animals, whole blood was withdrawn to harvest the PBCs, and subsequently, liver, gills, spleen and head kidney tissue specimens were collected from three randomly selected fish ($n = 3$) at different time points of 3, 6, 12, 24 and 48 h post-injection (p.i.), from each of

immune-challenged and PBS-injected groups. All the tissues and PBCs were flash-frozen in liquid nitrogen, and stored at -80 °C before being processed.

2.6 RNA isolation and cDNA synthesis

Total RNA was extracted from isolated tissues using Tri Reagent™ (Sigma-Aldrich), according to the manufacturer's protocol. The RNA concentration and purity was determined spectrophotometrically, by measuring the absorbance at 260 nm and 280 nm on a UV spectrophotometer (Bio-Rad, USA). Purified RNA was diluted and the concentration was adjusted to 1 µg/µL after spectrometric assessment. The aliquot of 2.5 µg RNA from each tissue was used to synthesize the cDNA with the PrimeScript™ First-Strand cDNA Synthesis Kit (TaKaRa, Japan). Briefly, the diluted RNA, 1 µL of 50 mM oligo (dT)₂₀ and 1 µL of 10 mM dNTPs were incubated at 65 °C for 5 min, and combined with 4 µL of 5 × PrimeScript™ buffer, 0.5 µL of RNase inhibitor (40 U/µL), and 1 µL of PrimeScript™ reverse transcriptase (200 U/µL). The solution mixture was incubated at 42 °C for 1 h and the reaction was terminated by heating at 70 °C for 15 min. The synthesized cDNA was diluted 40 times and stored at -20 °C until use for quantitative real-time PCR (qPCR).

2.7 Quantification of transcripts level

The SYBR Green quantitative real-time PCR was performed to determine the level of transcripts in healthy and challenged animal tissues at different time points. The Thermal Cycler Dice™ (TP800 or TP850) Real-Time System (TaKaRa, Japan) (**Fig. 2.1**) was used to perform the qPCR following guidelines for “Minimum Information for Publication of Quantitative Real-Time PCR experiments” (MIQE)(Bustin et al., 2009). The rock bream *β-actin* (GenBank accession no. FJ975145) was selected as an internal reference gene for standardization and a fragment of 108 bp of *β-actin* was amplified with primer pair (forward, 5'-TCATCACCATCGGCAATGAGAGGT-3' and reverse, 5'-TGATGCTGTTGTAGGTGGTCT CGT-3'). The specific primers for genes used in this study and were designed according to the following guidelines: amplicon size 100-200 bp, GC content 50% and T_m 60 ± 1 °C, listed in separate tables in each chapters of results part. All qPCRs were carried out in triplicate using a 10 µL reaction mixture comprising 3 µL of diluted cDNA, 5 µL of 2 × SYBR® *Premix Ex Taq*™ (Takara, Japan), 0.4 µL of each

primer (10 pmol/ μ L) and 1.2 μ L of PCR-graded water. The thermal cycling conditions included one cycle of 95 °C for 10 s, followed by 40 cycles of 95 °C for 5 s, 58 °C for 20 s and 72 °C for 20 s. To evaluate the specificity of the target amplification by dissociation curve, a single cycle of 95 °C for 15 s, 60 °C for 30 s and 95 °C for 15 s was executed at the end of each reaction. The baseline was set automatically by the TaKaRa Thermal Cycler Dice TP800 Real Time System software (2.01) in order to maintain the uniformity of the Ct values. The amplification efficiencies of two primers were between 95% and 105%, examined by using the Ct slope method.

Triplicate Ct values for each assay were subjected to Livak-comparative Ct ($2^{-\Delta\Delta C_t}$) method to calculate the mRNA levels (Livak and Schmittgen, 2001), using the *β -actin* as the reference gene. In spatial mRNA expression profiling, the relative transcript levels calculated in each tissue was compared with respective expression in muscle (or any other tissue). In temporal transcriptional profiling, the relative-fold change in mRNA levels after the immune challenges was computed with respect to the expression in corresponding PBS-injected controls, and then compared with that of untreated (0 h) control. The expression normalized to PBS-injected controls to eliminate possible bias from the injection medium is represented in the figures.



Fig. 2.1. TaKaRa TP800 -Thermal Cycler Dice™ Real Time System

2.8 Cloning, over-expression and purification of recombinant IL-10 (rRbIL-10)

The CDS for mature peptide of rock bream interleukin-10 was amplified using *Ex Taq*TM DNA polymerase (TaKaRa) and specific primers for the 5'- and 3'-end of the sequence tagged with EcoRI and HindIII restriction sites. The PCR product was ligated into pMAL-c5X expression vector (New England BioLabs[®] Inc. USA) after digesting with corresponding endonucleases. Subsequently, the pMAL-c5X/RbIL-10 recombinant plasmid was transformed into *E. coli* DH5 α competent cells, and confirmed the correct in-frame insertion by sequencing. In order to express the recombinant protein, the recombinant pMAL-c5X/RbIL-10 construct was transformed into *E. coli* ER2523 (New England BioLabs[®] Inc. USA) competent cells. The recombinant RbIL-10 (rRbIL-10) protein was over-expressed and purified as per a protocol in our previous report (Bathige et al., 2014) with some modifications. Briefly, the bacterial culture was grown in LB rich medium supplemented with 100 μ g/mL ampicillin and 0.2% glucose, and incubated at 37 °C. Once the OD₆₀₀ of bacterial culture reached ~0.6, isopropyl-b-thiogalactopyranoside (IPTG) was added to the medium at a concentration of 0.5 mM. Subsequently, the culture medium was incubated for 10 h at 20 °C to induce the protein expression. Finally, the rRbIL-10 protein was purified using pMALTM protein fusion and purification system (New England BioLabs[®] Inc. USA) according to the instructions in the manual. The MBP protein was also over expressed and purified using the same protocol. The size and concentration of recombinant proteins were assessed by 12% SDS-PAGE along with molecular standards (EnzyomicsTM, Korea) and Bradford assay (Bradford, 1976), respectively.

2.9 *In vitro* challenge

To understand the function of RbSTAT genes in response to IL-10, the rock bream heart cells were treated with rRbIL-10, and analyzed the transcription level at different time points. The rock bream heart cell lines were established according to the protocol described in previous report(Wan et al., 2012). Briefly, heart tissues were aseptically isolated from four rock bream fish, minced into small pieces, and washed thrice with Hanks' Balanced Salt solution (HBSS; Sigma, USA) containing antibiotics (400 IU/mL penicillin and 400 g/mL streptomycin). Subsequently, tissue pieces were digested in collagenase II solution (0.2%) for 2 h at 20 °C. The

digested cells were filtered through a sterile cell strainer (70 μm mesh size), and centrifuged at 1000 rpm for 10 min to collect the cells. The isolated cells were resuspended in Leibovitz's L-15 (L-15; Sigma) medium supplemented 20% FBS (fetal bovine serum), 100 IU/mL penicillin and 100 g/mL streptomycin, and transferred into 75 cm^2 cell culture flask. In order to adapt, the cells were sub-cultured more than three times in L-15 medium with 10% FBS.

The heart cells were seeded in 12-well plates, and allowed to grow up to $\sim 100\%$ confluence at 25 $^{\circ}\text{C}$. Cells were treated with 10 $\text{ng}/\mu\text{L}$ of rRbIL-10, and harvested at 0 (untreated control), 3, 6, 12, 24 and 48 h post stimulation. As a mock control group, another set of cells were treated with rMBP at a similar concentration. The SpinCleanTM RNA Mini purification kit (Mbiotech, Korea) was used to extract the total RNA. The cDNA was synthesized as described in section 2.6.

2.10. Antiviral potential assay

2.10.1. Isolation of RBIV

RBIV was isolated from the infected rock bream spleen and confirmed by PCR using specific primers as described earlier (Kasthuri et al., 2013). The spleen was homogenized in 1 \times PBS, and centrifuged at 3000 \times g for 10 min. Supernatant was filtered through 0.45 μm filter and stored at -80°C until use. The virus titer was determined on monolayers of rock bream heart cells grown in 96-well plates supplemented with L-15, 5% FBS. Viral suspensions were diluted from 10^{-1} to 10^{-6} , and 50 μL from each dilution was added to the wells seeded with cells. Cultures were incubated at 18 $^{\circ}\text{C}$ for 5-7 days and the susceptibility of rock bream heart cells to RBIV-infection was confirmed by observing the CPE. The maximal non-cytotoxic concentration was identified and used in subsequent antiviral activity assays.

2.10.2. Assay

To understand the antiviral potential of RbSTAT genes against viral attack, cell viability was assessed in response to viral (RBIV) stimulation. In brief, the complete CDS of RbSTAT1s were cloned into pcDNA3.1(+) vector (Clontech, BD Biosciences) using pre-designed primers (listed in each chapter), and the correct insertion was affirmed by sequencing. Rock bream heart cell line which was previously established in our laboratory (Wan et al., 2012), were subcultured in 96-well plate with the cell density at 1×10^6 cells/well. The plasmid containing RbSTAT gene (0.4 $\mu\text{g}/\text{well}$; RbSTAT/pcDNA3.1(+)) was transfected into rock bream heart cells using X-

tremeGENE™ 9 DNA transfection reagent (Roche, Germany) according to the manufacturer's instructions. Similarly, empty vector pcDNA3.1(+) (0.4 µg/well) was transfected into rock bream cells and used as mock control group. After 48 h, 2 µL of RBIV (maximal non-cytotoxic concentration) was introduced to the cells and kept in 18 °C incubator for another 72 h to observe the considerable cytotoxicity in control wells. The cell morphology was examined through light microscope. Ten microliter of WST-1 reagent (Premix WST-1 cell-proliferation assay kit, TaKaRa) was added to the each well after 72 h post stimulation and incubated in room temperature (25 °C). The absorbance at 450 nm was monitored spectrophotometrically (Thermo Scientific Mutiscan) at the 1 h intervals and the reference wavelength was set at 670 nm. The measured absorbance after 3 h of incubation was used for the final calculation, and the cell viability was assessed.

2.11. Sub cellular localization

The CDS of RbSTAT was amplified using pre-designed primers (listed in each chapters), and cloned into the eukaryotic expression pEGFP-N1 vector (Clontech, BD Biosciences) at the corresponding restriction sites indicated in primer sets. The correct insertion was confirmed by PCR amplification and sequencing. Subsequently, the rock bream heart cells were seeded in 12 well plate and grown in LB-15 medium supplemented with 5% FBS 24 h prior to transfection. When the cell confluence reached ~80%, the old media was changed by fresh L-15 without FBS or antibiotics, and 2µg of recombinant vector (RbSTAT/pEGFP-N1) was transfected into rock bream heart cells using X-tremeGENE™ 9 DNA transfection reagent (Roche, Germany) following vendors instructions. After six hours, the media was changed with fresh L-15 supplemented with 2% FBS, and 200 µg of poly I:C was introduced as a stimulant to identify the nuclear translocation. Simultaneously, empty vector (2 µg) was transfected in a similar way, in order to use as a mock control. After 48 h of transfection, cells were observed by fluorescence confocal microscopy (Leica, Germany).

2.12. Statistical analysis

All experiments were performed in triplicate. All data are presented as the amount of particular mRNA relative to that of *β-actin* mRNA, and are expressed as mean ± standard deviation (SD).

The data were further subjected to either unpaired, two-tailed t-test to calculate the p -value using GraphPad program (GraphPad Software, Inc.) or one-way analysis of variance (ANOVA) followed by Duncan's or Tukey's multiple comparison tests as a post hoc comparison using the SPSS 16.0 program (USA). The p values less than 0.05 was considered as statistically significant.

CHAPTER 3

**Two isoforms of Signal transducer and activator of transcription 1 (STAT1):
Genomic organization, transcriptional modulation and subcellular
localization.**

Abstract

The JAK/STAT signal transduction pathway plays a critical role in host defense against viral and bacterial infections. Herein, we describe the structural insights at cDNA and genomic level and functional roles of two STAT1 orthologs identified from rock bream (RbSTAT1 and RbSTAT1L). The bioinformatics analysis revealed that RbSTAT1 shared comparatively higher identity than RbSTAT1L. RbSTAT1 shared highest identity with mandarinfish (96.5%), while RbSTAT1L showing highest identity with burton's mouthbrooder (65.1%). In comparison of RbSTAT1 and RbSTAT1L presented a lower identity between them (42.4%). Comparative studies revealed the higher conservation among other species and identified the characteristic domains, functional residues important for the phosphotyrosine binding pockets and homodimer interface. Phylogenetic studies revealed that RbSTAT1L belongs to the separate group of STAT1. In addition, comparative studies of genomic organization along with the phylogenetic tree suggest the evolutionary differences between fish and other vertebrates. Genomic organization of both RbSTAT1 and RbSTAT1L revealed that both comprised with 23 exons disrupted by 22 introns. Immunologically important transcription factor binding sites were recognized in putative promoter regions of both RbSTAT1s. Spatial distribution analysis by qPCR indicated the highest expression of both *RbSTAT1s* in blood cells while depicting a ubiquitous expression in other tissues. Upon microbial and mitogen injections, the expression of both RbSTAT1 and RbSTAT1L were elevated at varied time points in blood cells and liver tissue, even though some time points observed suppression of *RbSTAT1s* transcription. Meanwhile, transcriptional modulations were observed after tissue injury in blood cells and liver tissue. *In vitro* challenge experiment with rock bream IL-10 demonstrated the significant up-regulations of *RbSTAT1s* mRNA at middle phase experiment, whilst showing significant down-regulations at 3 h and 48 h post treatment. Further, we have studied the cellular localization of RbSTAT1 proteins under normal physiological conditions, and observed them in cytoplasm as mammalian counterparts. Finally, the results of the present study explored the structural conservations and functional impacts on microbial attack and wound healing process.

3.1. Introduction

Signal transducers and activators of transcription (STATs), a family of transcription factors comprising seven distinct representatives in mammals including STAT1, STAT2, STAT3, STAT4, STAT5a, STAT5b and STAT6, play a momentous role in Janus kinase (JAK)/STAT signaling pathway (O'Shea et al., 2002). Signals received from various cytokines and growth factors are transduced to the nucleus by activating of STATs via JAKs phosphorylation. The activated STATs bind to the respective binding sites in promoters and initiate the transcription of related genes in order to mediate the cellular functions such as cell differentiation, migration, proliferation and immune responses (Rawlings et al., 2004; Harrison, 2012; Richard and Stephens, 2014). Structurally all the STATs are shared with similar conservative domains including N-terminal, coiled-coil, DNA binding, linker, Src homology 2(SH2) and transcriptional activation domains, those were distinguished based on the functional properties (O'Shea et al., 2002).

STAT1 is an essential cellular component mediates number of biological activities in response to the various signaling molecules such as interferons (IFN), growth factors and number of cytokines (Ramana et al., 2000). The type I and type II IFNs lead to activate the transcription of immune responsive genes by interacting with IFN stimulated response element (ISRE) and IFN γ activated site (GAS), respectively in relevant gene promoters via association with STAT1/STAT2 transcription factors (Platanias, 2005). Broad spectrum of studies has been conducted to understand the possible functions of STAT1 basically in mammalians. The STAT1 is involved in various biological mechanisms such as host immune defense under pathological conditions (Durbin et al., 1996; Meraz et al., 1996), apoptosis (Tanabe et al., 2005), cell death via caspase independent pathway (Kim and Lee, 2005), regulation of macrophage hepcidin expression (Sow et al., 2009), internal tissue injury (Takagi et al., 2002; Stephanou, 2004; Kim et al., 2009), toll like receptor (TLR) induced inflammation (Luu et al., 2014), etc.

As in mammals, the role of STAT1 in response to the IFN γ has been shown in teleost origin (Zou et al., 2005). In addition, host immune responses by STAT1 against viral incursion have been reported in various fish species (Zhang and Gui, 2004; Collet et al., 2008; Yu et al., 2010; Tso et al., 2013). Even though number of studies reported on STAT1 counterpart from fish lineage, few studies have focused on its functional aspects. The basic components involved in the

JAK/STAT signaling pathway and their diverse functions are still not fully understood in teleosts. Hence, the investigation of members associated with multiple functions in the JAK/STAT pathway will be beneficial to enhance the immune system by developing novel strategies, and thereby improve the growth and survival rate in aquaculture industry.

The rock bream, *Oplegnathus fasciatus* is a commercially important mariculture aquacrop widely cultured in Eastern and Southeastern Asian countries. The high vulnerability of rock bream towards bacterial and viral diseases was led to the mass mortality of rock bream accounting great losses to the aquaculture farmers (Jung and Oh, 2000; Park, 2009). In order to battle against enormous pathological threats, sustainable disease management strategies are required to be introduced. Therefore, deeper understanding of the molecular and cellular mechanisms of host immunity will be greatly effect for the rock bream aquaculture farm.

In the current study we describe the molecular characteristics and functional aspects of two orthologs of STAT1 gene from rock bream (RbSTAT1 and RbSTAT1L). The molecular features were studied at complementary DNA (cDNA) and genomic level. In addition, evolutionary directions of each gene were deliberated by phylogenetic studies based on the ClustalW alignments with known counterparts. The insights into the functional role of rock bream STAT1 orthologs in response to the viral and bacterial pathogens, and pathogen associated molecular patterns (PAMPs) were investigated by expressional analysis by mean of *in vivo* challenges. The *in vitro* challenges were performed interleukin-10 (IL-10) in rock bream heart cells, and examined the possible roles. Further, we investigated the mediation of rock bream STAT1 genes on wound healing process by introducing an external tissue injury.

Table 3.1. Primers used in this study

Primer	Purpose	Sequence, 5'-3'
<i>RbSTAT1-F</i>	qPCR amplification, BAC screening	AGCTCAACATGCTGGCTGACAAAC
<i>RbSTAT1-R</i>	qPCR amplification, BAC screening	AAAGCTTTCTCGTTGGCGCTCTTG
<i>RbSTAT1L-F</i>	qPCR amplification, BAC screening	ACAGCACATTGCACCACATGACAG
<i>RbSTAT1L-R</i>	qPCR amplification, BAC screening	TGGGAGTCACTGAAGAACTGCACA
<i>Rb β-actin-F</i>	qPCR internal reference	TCATCACCATCGGCAATGAGAGGT
<i>Rb β-actin-R</i>	qPCR internal reference	TGATGCTGTTGTAGGTGGTCTCGT
<i>RbSTAT1/pcDNA-F</i>	Clone into pcDNA3.1(+)	(GA) ₃ <u>gaattc</u> ATGGCGCAGTGGTGCCAA - EcoRI
<i>RbSTAT1/pcDNA-R</i>	Clone into pcDNA3.1(+)	(GA) ₃ <u>ctcgag</u> TCAGTTTTGGTCCATCGTAGCGTGAC - XhoI
<i>RbSTAT1L/pcDNA-F</i>	Clone into pcDNA3.1(+)	(GA) ₃ <u>gataac</u> ATGGCCCAGTGGCAGGAAC - EcoRV
<i>RbSTAT1L/pcDNA-R</i>	Clone into pcDNA3.1(+)	(GA) ₃ <u>ctcgag</u> TCAGAGGGAGCTAACAGGATCGGCATAG - XhoI
<i>RbIL-10/pMAL-F</i>	Clone into pMAL-c5x	(GA) ₃ <u>gaattc</u> AGTCCCATGTGCAACAACCACTG - EcoRI
<i>RbIL-10/pMAL-R</i>	Clone into pMAL-c5x	(GA) ₃ <u>aaagctt</u> TCAATTAGAGGCCACTTGTTCGGAC - HindIII
<i>RbSTAT1/GFP-F</i>	Clone into pEGFP-N1	(GA) ₃ <u>ctcgag</u> ATGGCGCAGTGGTGCCAA - XhoI
<i>RbSTAT1/GFP-R</i>	Clone into pEGFP-N1	(GA) ₃ <u>ccgctg</u> GTTTTGGTCCATCGTAGCGTGACTCAC - SacII
<i>RbSTAT1L/GFP-F</i>	Clone into pEGFP-N1	(GA) ₃ <u>ctcgag</u> ATGGCCCAGTGGCAGGAAC - XhoI
<i>RbSTAT1L/GFP-R</i>	Clone into pEGFP-N1	(GA) ₃ <u>ccgctg</u> GAGGGAGCTAACAGGATCGGCATAG - SacII

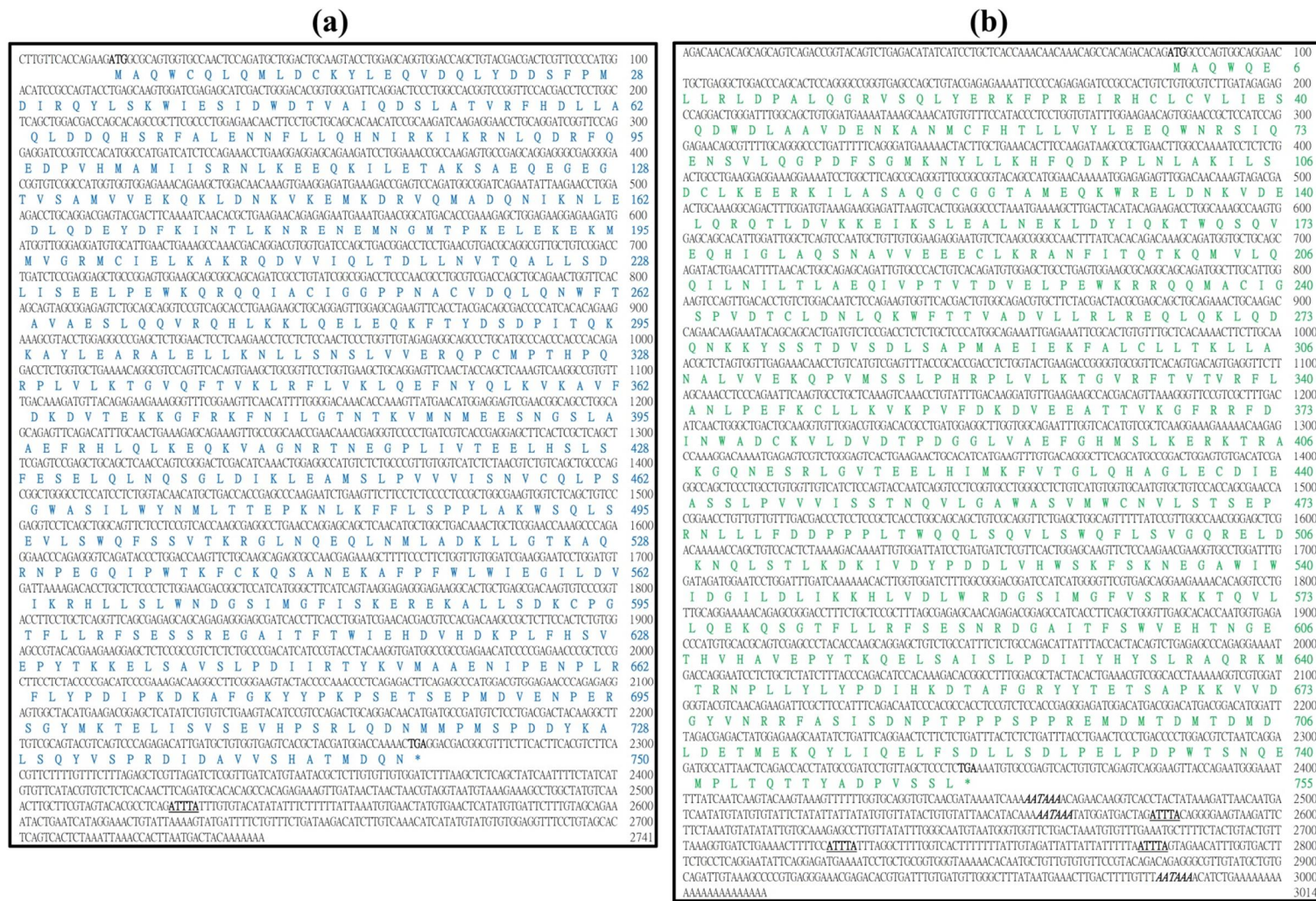
Restriction sites in the cloning primers are shown with small case letters and indicated at the end of each primer sequence.

3.2. Results

3.2.1. Bioinformatics of RbSTAT1 and RbSTAT1L cDNA sequences

3.2.1.1 Primary sequence characterization

The full length cDNA sequences of *RbSTAT1* and *RbSTAT1L* were retrieved after BAC clone sequencing and, they were further confirmed by sequencing after cloning into pMD20-T vector. The cDNA sequence of *RbSTAT1* (2741 bp) was comprised a 2253 bp of CDS that coded a polypeptide with 750 aa residues. As basic features, the theoretical molecular mass and isoelectric point (*pI*) of RbSTAT1 were predicted with 86.7 kDa and 5.79, respectively. There were untranslated regions (UTR) at the 5' (5'-UTR) and 3' (3'-UTR) with 15 bp and 473 bp, respectively. A single RNA instability motif (ATTTA) was predicted at the 3'-UTR of *RbSTAT1* cDNA (**Fig. 3.1a**). The *RbSTAT1L* cDNA sequence (3014 bp) was consisted with 2268 of CDS encoding a 755 aa poly peptide with molecular mass of 86.6 kDa and *pI* of 5.47. The 5'- and 3'-UTRs were composed of 81 bp and 665 bp, respectively. Three polyadenylation signals (AATAAA) and three RNA instability motifs were identified at the 3'-UTR in addition to the poly A tail (**Fig. 3.1b**).



3.2.1.2. Homology analysis

The predicted polypeptide sequences of RbSTAT1 and RbSTAT1L were compared with homologous counterparts, and revealed the broad range of identities and similarities (**Table 3.2**). The RbSTAT1 (96.5%) and RbSTAT1L (65.1%) shared highest percent of identity with mandarin fish and Burton's mouthbrooder. Remarkably, the percent of identity was high when compare the RbSTAT1 with fish counterparts, and it was ranged above 57% except few fish species those comprising STAT1-like orthologs. Meanwhile, a narrow range of identity percentage (66% – 70%) was observed for comparison between RbSTAT1 and higher vertebrates. In the case of RbSTAT1L, comparatively low identity percentage was observed, where it shared less than 43 % with all STAT1 counterparts. However, RbSTAT1L showed higher identity (> 60%) with orthologs those belong to the STAT1L group. On the other hand, RbSTAT1 and RbSTAT1L also shared moderately low percentage of identity (42.4%) and similarity (63.3%). Multiple sequence alignment also depicted a clear discrepancy of conservation between RbSTAT1 and RbSTAT1L (**Fig. 3.2**). Characteristic STAT domains including N-terminal domain, coiled coil domain, DNA binding domain, linker domain, SH3 domain and TAD domain at the C-terminal were predicted based on the previous sequences and NCBI CDD results. Remarkably, N-terminal domain, DNA binding domain, linker domain and SH2 domain were well conserved in RbSTAT1. In addition, residues important for phosphotyrosine binding pockets are completely conserved in RbSTAT1. Residues in dimer interface were completely conserved in RbSTAT1 but not in RbSTAT1L. The tyrosine residue of RbSTAT1 (Y⁶⁹⁸) which is phosphorylated upon activation was conserved among other STAT1 members, while RbSTAT1L was not. The 3D models of RbSTAT1s revealed their high conservation of structural topology and position of functional sites when compare with human 3D structure (**Fig. 3.3**).

Table 3.2. Percentage of identity (I%) and similarity (S%) of interspecies amino acid sequences in comparison with RbSTAT1 and RbSTAT1L sequences.

Scientific name	Common name	Gene name	Accession number	RbSTAT1		RbSTAT1L	
				I%	S%	I%	S%
<i>Oplegnathus fasciatus</i>	Rock bream	STAT1		100.0	100.0	42.4	63.3
<i>Oplegnathus fasciatus</i>	Rock bream	STAT1-like		42.4	63.3	100.0	100.0
<i>Siniperca chuatsi</i>	Mandarinfish	STAT1	ACU12484	96.5	98.1	42.4	63.6
<i>Channa argus</i>	Northern snakehead	STAT1	ABK60089	93.7	96.3	42.2	62.5
<i>Oreochromis niloticus</i>	Nile tilapia	STAT1	XP_003446584	91.9	95.7	41.2	62.4
<i>Oreochromis niloticus</i>	Nile tilapia	STAT1-like	XP_005463411	41.3	63.1	63.7	80.0
<i>Paralichthys olivaceus</i>	Japanese flounder	STAT1	ABS19629	90.1	95.1	42.0	62.5
<i>Salmo salar</i>	Atlantic salmon	STAT1	ACI33829	79.7	89.0	41.9	62.2
<i>Carassius auratus</i>	Goldfish	STAT1	AAO88245	60.3	76.1	40.8	63.2
<i>Takifugu rubripes</i>	Pufferfish	STAT1-like	XP_003962244	39.1	62.3	61.5	76.6
<i>Haplochromis burtoni</i>	Burton's mouthbrooder	STAT1-like	XP_005939894	42.0	63.8	65.1	79.6
<i>Danio rerio</i>	Zebrafish	STAT1a	NP_571555	64.0	79.2	40.6	61.2
<i>Danio rerio</i>	Zebrafish	STAT1b	NP_956385	57.4	75.5	41.8	62.7
<i>Gallus gallus</i>	Chicken	STAT1	NP_001012932	68.8	83.0	40.0	63.8
<i>Xenopus laevis</i>	Frog	STAT1	NP_001082256	66.8	81.8	39.8	62.0
<i>Rattus norvegicus</i>	Norway rat	STAT1a	NP_116001	67.5	83.1	41.3	62.4
<i>Rattus norvegicus</i>	Norway rat	STAT1b	NP_001029336	65.7	79.5	41.7	61.0
<i>Mus musculus</i>	House mouse	STAT1	AAH04808	67.5	83.1	41.4	62.8
<i>Sus scrofa</i>	Pig	STAT1	AER08620	67.9	83.6	41.3	63.6
<i>Bos taurus</i>	Cattle	STAT1	XP_005202630	67.6	83.2	40.7	62.9
<i>Homo sapiens</i>	Human	STAT1	NP_009330	67.9	83.9	41.4	63.2

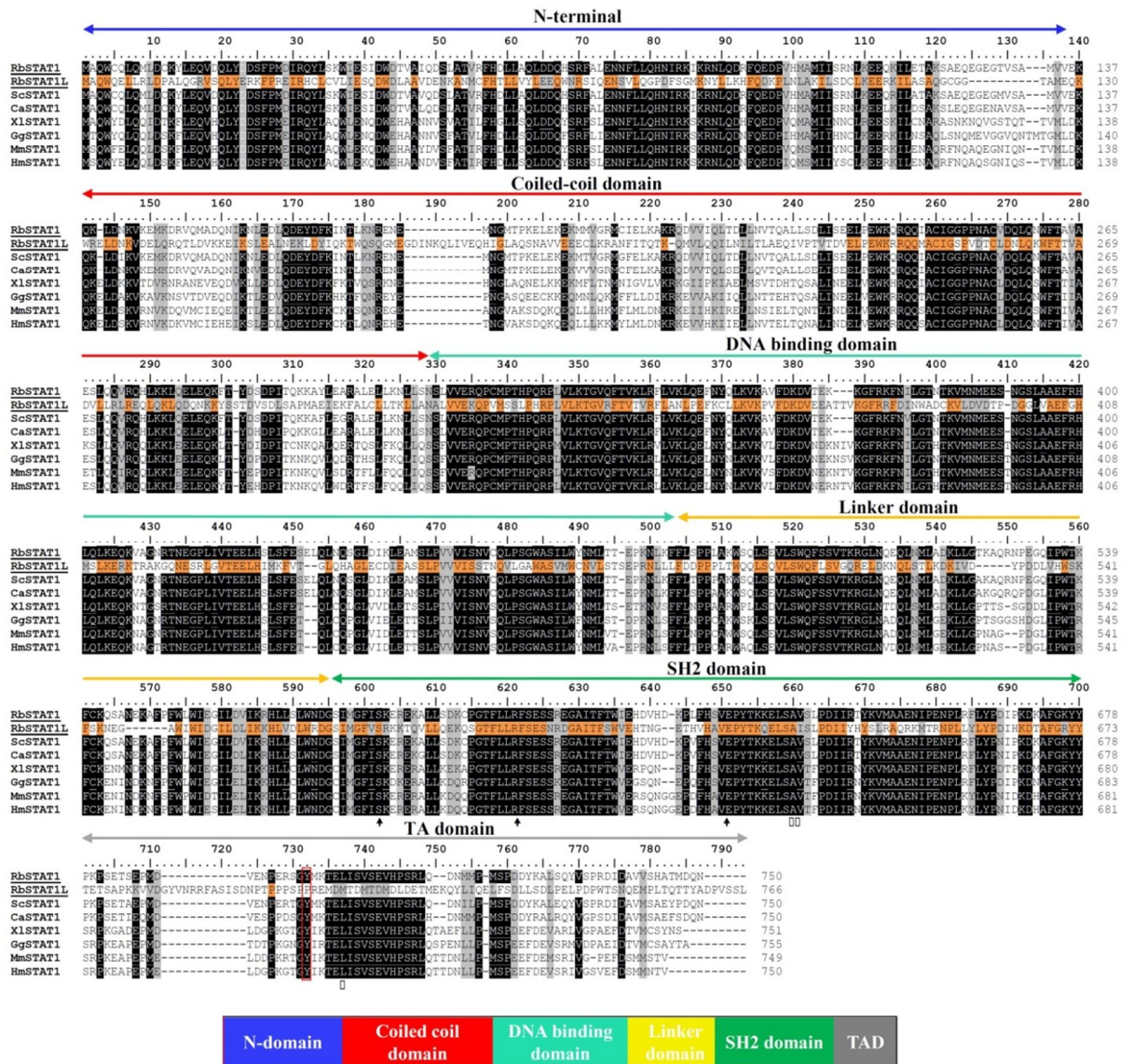


Fig. 3.2. Multiple sequence alignment analysis of RbSTAT1 and RbSTAT1L amino acid sequences with known orthologs from different species. Identical and similar residues in all sequences are shaded with black and gray colors, respectively. The amino acid residues identical with RbSTAT1L were highlighted in orange color. Characteristic domain regions were marked in the top of the alignment with different colors. The conserved amino acids important for the phosphotyrosine binding pockets and homodimer interface are marked with \blacktriangle and \square , respectively. Conserved tyrosine residue (Y⁶⁹⁸ in RbSTAT1, but not conserved in RbSTAT1L) essential for the activation via phosphorylation is marked with red colored box. Consecutive domain regions are summarized with different colored boxes and showed in below the alignment.

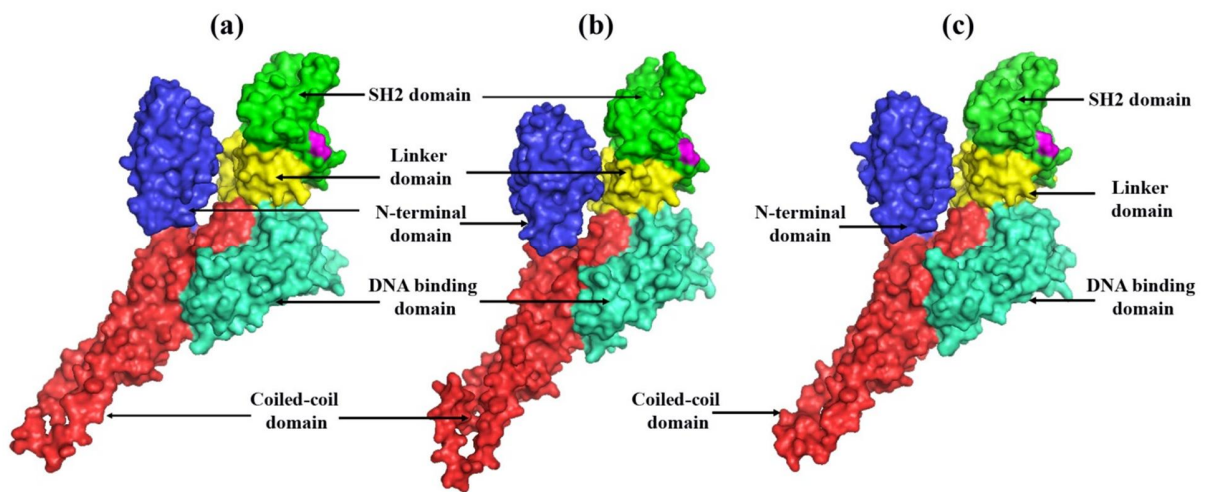


Fig. 3.3. Surface representations of RbSTAT1 (a), RbSTAT1L (b) and human STAT1 3D homology models. The domain regions were highlighted with different surface colors and residues important for the homodimer interface are marked with pink color. The images were generated from SWISS-MODEL and visualized by PyMOL molecular graphic software version 1.3.

3.2.1.3. Phylogenetic analysis

To understand the evolutionary position of RbSTAT1 and RbSTAT1L genes among STAT family, two individual phylogenetic trees were constructed based on ClustalW alignment. As shown **Fig. 3.4**, STAT family members were clustered into seven different groups sorting into corresponding STAT sub groups. Meanwhile, STAT1L together with other fish STAT1-like orthologs was clustered into separate group. In the case of evolutionary tree with STAT1 members, distinct evolution was observed for fish and other vertebrates, while showing separate cluster for STAT-like members as expected and located as a basal group for other all STAT1 members (**Fig. 3.5**).

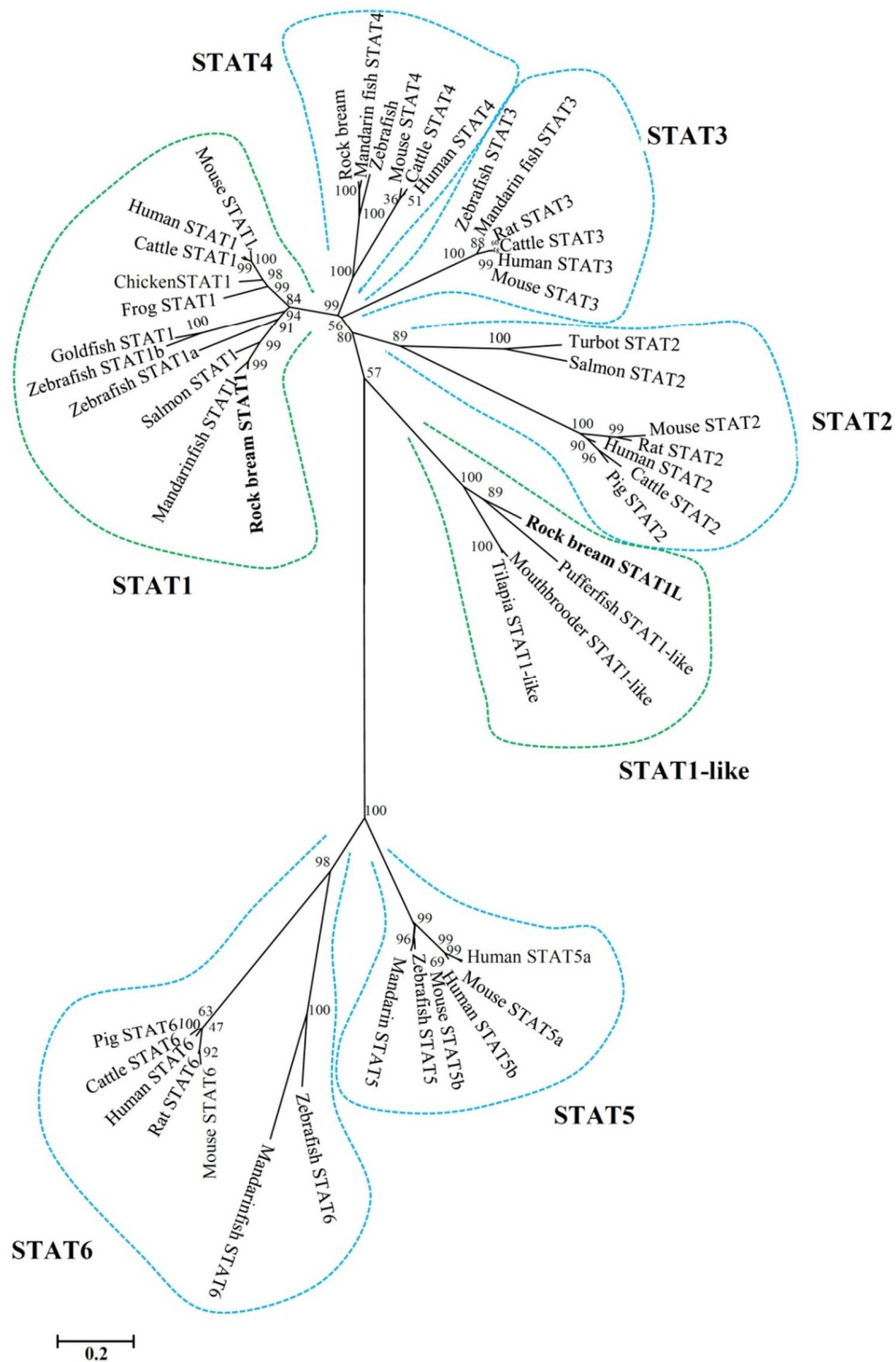


Fig. 3.4. Unrooted phylogenetic tree of STAT family. It was constructed by ML method with the MEGA 6.0 program based on the core sequences from all STAT family members. The bootstrap confidence values (%) according to the 5000 bootstrap replications are indicated at the nodes of the tree.

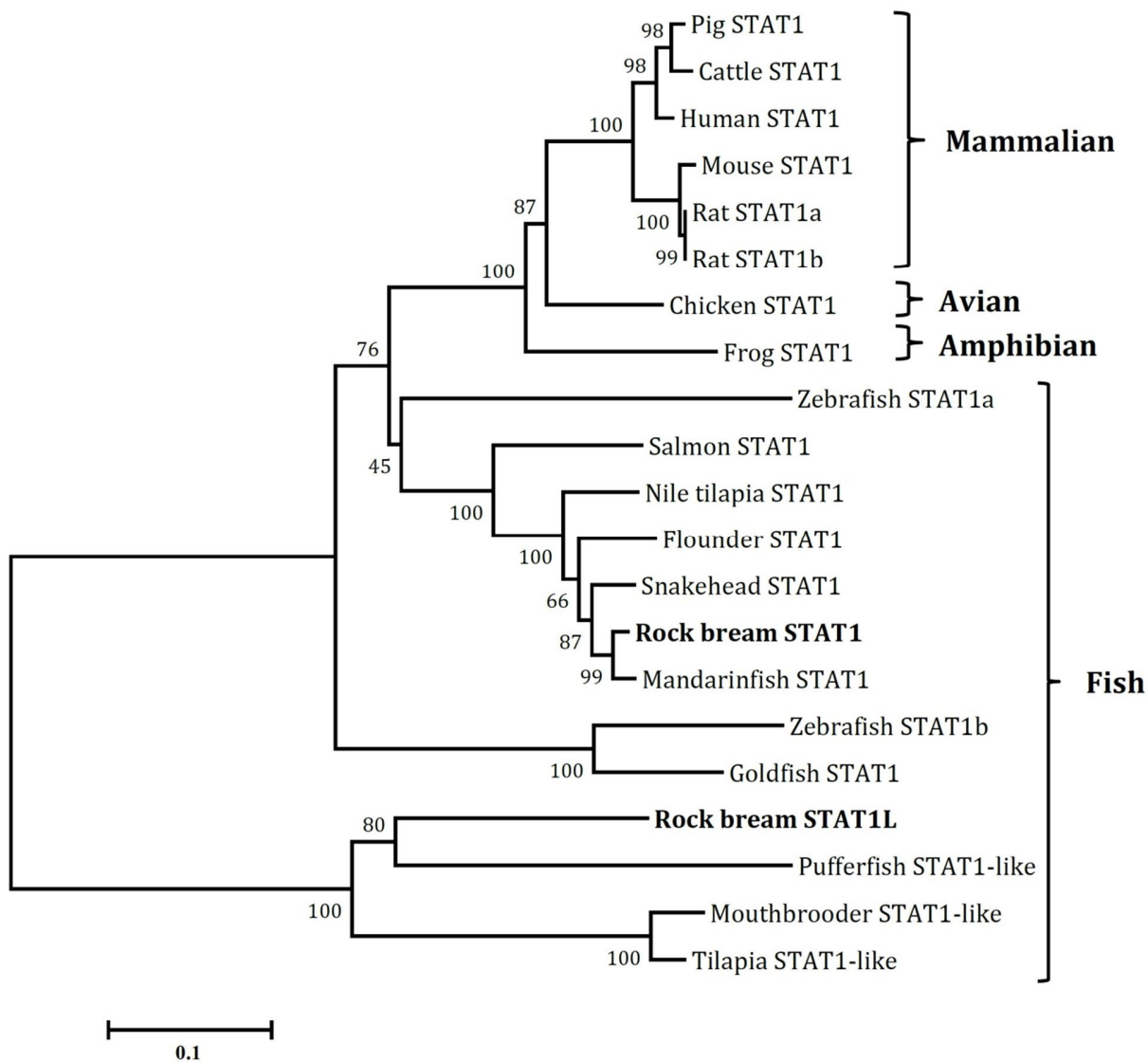


Fig. 3.5. Phylogeny of RbSTAT1 and RbSTAT1L. The rooted phylogenetic tree was constructed using ML method based on the ClustalW alignment of core sequences of STAT1 family members from various taxonomical origins. The numbers at the each nodes are represented the bootstrap confidence values (%) according to the 5000 bootstrap replications.

3.2.2. Genomic sequence characterization of *RbSTAT1* and *RbSTAT1L*

3.2.2.1. Comparative genomic structural organization

Genomic sequences of both *RbSTAT1* and *RbSTAT1L* obtained from BAC library screening, was organized into 23 exons disrupting by 22 introns for CDS regions. Each genomic structure was compared with other species from different taxonomical origins and revealed the considerable conservation (Fig. 3.6). The exon numbers in CDS among fish species were 22 to 24 numbers (Fig. 3.6a), while in other vertebrates (Fig. 3.6b and 3.6c) restricted to 23 exons. According to the genomic structural organization, five exons of *RbSTAT1* (exon 1, 2, 7, 10 and 16) were identical amongst all the species analyzed. In mammalians, all the exons in CDS were identical.

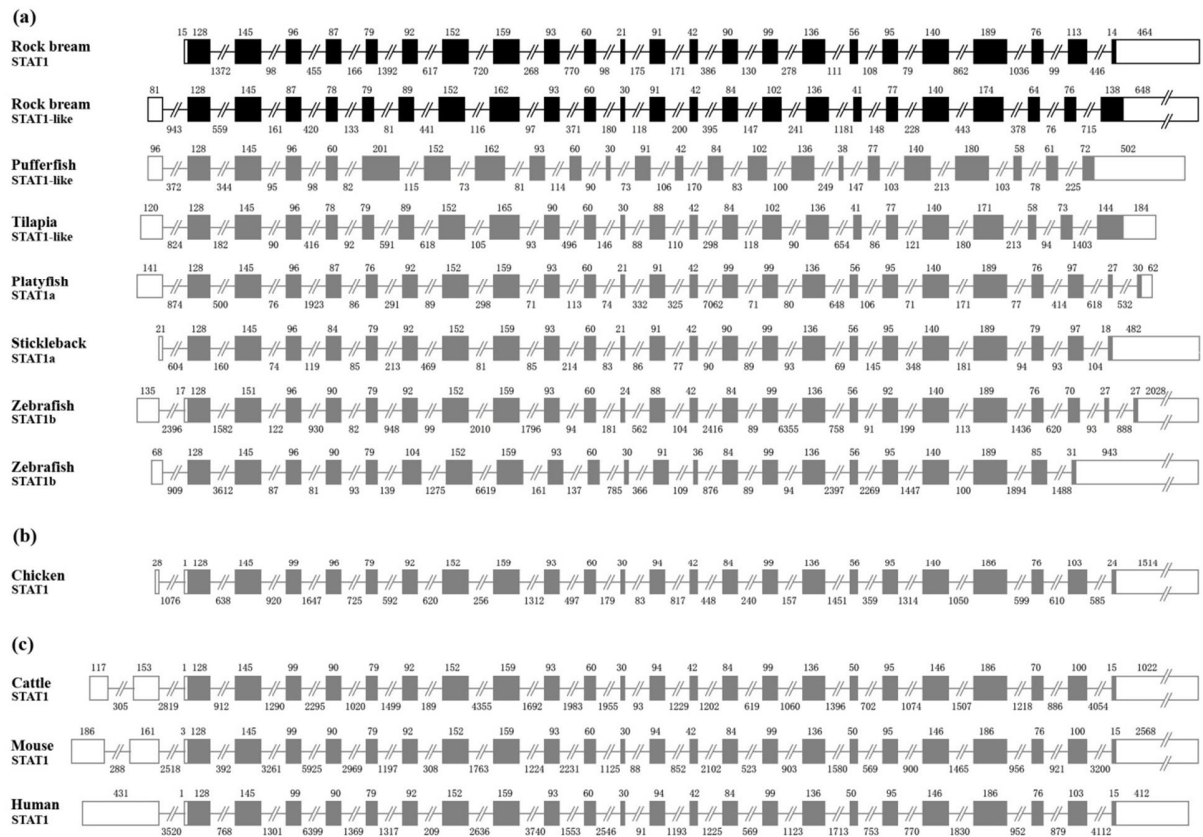


Fig. 3.6. Schematic representation of genomic structure comparison of *RbSTAT1* and *RbSTAT1L* with fish (a), bird (b) and mammalian (c) counterparts. The exons and UTRs are represented by solid and empty boxes, respectively. The introns are shown by lines connecting each box. Numbers indicated in the top and bottom of the genomic structures are denoted for size of the exon and intron, respectively.

3.2.2.2. Putative TFBS analysis at 5'-proximal region

Based on the AliBaba2.1 prediction with 85% threshold conservation, various TFBSs were predicted at the 5'-proximal regions of each gene. A canonical TATA box was located at the 27 bp upstream region from 5'-UTR of RbSTAT1L (Supplementary fig. 2b), while it was not recognized in the RbSTAT1 (Supplementary fig. 2a) gene. TFBSs including CCAAT enhancer binding protein alpha (C/EBP α), C/EBP β , octamer transcription factor-1 (Oct-1) and specificity protein 1 (SP1) were identified in both putative promoter regions of RbSTAT1 and RbSTAT1L genes. In addition, binding sites for nuclear factor kappa-light-chain-enhancer of activated B cells (NF- κ B), GATA-binding factor-1 (GATA-1), interferon consensus sequence-binding protein (ICSBP), cAMP response element-binding protein (CREB), hepatocyte nuclear factor 3 (HNF-3) were predicted in the RbSTAT1 promoter. Whereas, TFBSs such as interferon-stimulated gene factor 3 (ISGF3), c-Jun (a member of AP-1), nuclear factor of activated T-cells, cytoplasmic 3 (NF-ATc3), cAMP response element-binding protein 1 (CRE-BP1) was recognized at the putative promoter region of RbSTAT1L.

(a)

```

ATTGATGCAACAATTC AATTCAGTTCCTTCAATTTTCAGGTTTAGCTGAAGTTTATGATAGTTACTGTGTGTAATAATCTTCAGCCTT 90
TCAGATGCAAGAATGAGTCAAAATCTTCTTTTATGATGACCATTATTATTAATAAGTCTTCCTTTTTGGGGATTTTCATCAAAAAAGT 180
                                     NF- $\kappa$ B
ACAAAATGTTTAAACACAGACTCTAAAGCTTCAAATGTTGGACTTTCCTGATGACAGTGAATGCATCTTAAAAATTTTTTAACCTCTAAC 270
                                     NF- $\kappa$ B
TTTTTTAACCTGATTTAATCCTCCAGATTATAAGACCTCTTGATTTAAGTTTCTAATTTAATTGTTTTCTCTGAGCAGAATTGAGGA 360
AGAGGAGGAGGAGGAGGAGGGGAGGGCCACAGTCCATAATAATTATGGAGTCTAGCAGTATGATTTCCCATTTCTTGCTCTGCAAAACAAGCA 450
                                     SP1                                     C/EBPalpha                                     Oct-1
GCTGGGTTGGTGTAGCGAGTGAAGAGAGGATTCAAACCTTTCACCTCTGCCCTGACCTTTGACCTCTCACCACCCTGAGGGACACAGATT 540
                                     SP1
AGATGGTCAAATTAATGCACTATTCTTATATTTAAGATGACTTCAGGGATTAGATGAAACAGTGGGAGACTGCAGAGGCCAAAACGTTGCA 630
GAATACAATAAAGCAGAAGTAAATAGAGGAAGAAAACATGTCAGTAGGGAGTTGCAACACCAGGATTTTGAATACAACAGTAGTATTG 720
CAGATCATAATTTGAATAAGAAAATTAATTAATAAACAAGTAAAATTATAATTTTGTCTGACTTTATATGTTTTAATAAAGGGATT 810
                                     Oct-1
GTTGTTTTTACTAGACCCCACTGATTAGGGCTGCACTAACGATTAATTTTCATTATCGATTAATCTGTGCGATCATTTTCTCGATTAAAT 900
                                     GATA-1
CGATTAGTTGTTTGGTCCATGAAATGTCAGAAAACGGTGAAAAATGTTGATCACTGTTTCCCAAAGCCCAGGGTGACGTCCTCAAATGTC 990
                                     CREB
TTGTTTTGTCCACAGCCCAAAGATATTTCAGTTTACTGTCCAGACGAGTAAAGAAACCAGAAAAATATTCACATCTGAGAAGCTGAAATCA 1080
                                     C/EBPbeta                                     ICSBP
GAGAATTTTCTTTAAAAAAAATGAATCAAAACGATTAATCGATTATCAAAATAGTATGCGATTAATTTAATCGTTGACAGCTAATCGA 1170
TTAATCGACTAATCATTGCAGCTCTACAACGATAAATCTGTGTTAGGGTGCATATTGGCTGATAATCACAGATATATTGGTGCAGCAT 1260
GTATGCTGTGTGCTCTGAATTTGCAGTTCATATTGAATCAGAAATGTTTGTGTTTAAAAATAAATATTGGATCATTATCAGTTTT 1350
                                     ICSBP                                     HNF-3                                     C/EBPalpha
TTTTAACTACAGTCTGGTCAAGGCTGTAGTTTTTGCCTGAACAGCCCTCATGAAGCTGCT 1410

```

(b)

```

GCCATCTGTTAGAAACAAGTTGTAGATCGTTTATGATTGATTATTAGTCCTAGGGGATAATTCATTATTAATTTTATGTGTGAACCACT 90
GGCTACATCCAGGATATTGCATAAAGCCCTCTTTTCACATATTTGGCAGACACTGTGCAGAACCTGTCAATACGATTTATTTCAATACA 180
      C/EBPbeta      Oct-1
ACGGCCCTGCAATCAGAGCCACCCACCTTGTGCACCCTACCTGTCTCACATGGCCTGACACCCATCTTTGAAGGATGGTGGGGAGGGGG 270
CTTCCGTCAACAAAATGCTGCCAGTCCTCGTGAGGTCAGGGGCGGGTCTAAAAAAGAAATGCAGATTAGAAAAAGTAGAAGGAATTCAGC 360
      CRE-BP1      C/EBPalpha
TTTTAAGATGATATAGGATATTACTGTGATAATACAATATTCAGTCAATCATAGTACAAAGCTGGGTTAAAGGAGTAGTCAGACATTTT 450
      NF-ATc3      c-Jun
GGGAAGCGTATTCACTTACTGGTATGTTTATTTGTTAAACTTTGGACAGAGCCGGGCTAGCTGTGTCCCCCTGCCTCCATTCTTTATGCT 540
      SP1
AAGCTAAACTGACCTTCTGCTGGCTCTAGCTTCATGCAGCATACAGACATAAAAAGTGGTTCACCTTCTCATTTAACTCAAGAAAGCGA 630
GTTCCCAAATGTCTCACTATTCTTTAAAAAGTAGTCAAAGTCGAGTTCTGGCTCTATAAAAAATAAAGACGAAATTATACTTCTCCAT 720
GTTTAGTTGTTGTGCCAGTGTTCATTCAAGTAAATAATGTTAAAGCTATTCAATTTTTGGCCACTTGGGGGCAGCAGAACAAGCAGAAA 810
      C/EBPalpha
ACACAACAGTGACATATTATTACCTTATAATGTAGTTATACATGCAAAATCATCTGCATACTACACGTCAGCAGACAGAGCAACACTA 900
      Oct-1
GTATTCATTTGGGATCATGTCTGTGCACCTGATGAAACTAAATATTCACCTACTTTTAACTCTGTTTTGGTCTCCACCACCTCCTCGAA 990
      SP1
GGAAACATCAAGCTCTTTAGCTGCTACATGCTCCACTGTGTTACCAGAGTCTCTAACTGTGTGTGTCGGTCTTGTCTGGGTATAT 1080
ACTGTAGTGTAGGTGGGTTTATCAGAGCTTTTTCACCTCAAACAGCCATCTGCTGCTGCCAGGAACAAGGCTGATGAAGAGCTGAGGT 1170
      C/EBPalpha
GCAGCGGGCCACAAGACCAAAACCATGTGCTAAAAGAGGGCTAAAAAATCATCTGAGCTGAGAAACTACAGAGTTGGTGATAAAGCAGGA 1260
      ISGF-3
AAAGCACAGGTGTTACTGGTAATTTAAGTGTCCAGTGCACCAGGACAGTGAAGCCAGCATAATGATACCATTATAATTAATAAATGT 1350
CTGCCATGAAAAAGGACAATGGAGCAGTCATATTCAACACCACCCGAAAAAGCCGGATGTAGAAAGCAACCATTGTCATAGCAACA 1440
      C/EBPalpha
CACAAACAGCTTACTTTTAGTATTGTGAAAGCGGAAATGAATAGCGGTAGCCACCGGTTGACTTGACGCCGCTCAGCAGAACCATTT 1530
CTCGAGAATCAGTGGTTTGTGGGCGTACCCGGTGAATATAAAGAACCCTCCTCCCTCACATTACATTC 1600
      TATA box

```

Fig. 3.7. Putative promoter proximal region of RbSTAT1 (a) and RbSTAT1L (b). Predicted transcription factor binding sites are shown by underlined green color letters and indicated below the sequence. The canonical TATA box is marked with box and light blue colored letters.

3.2.3. Quantification of *RbSTAT1* and *RbSTAT1L* transcripts

The transcription levels of *RbSTAT1s* were quantified using SYBR Green qPCR technique and rock bream β -actin was used as an internal reference. According to the last step of PCR program (mentioned in chapter 2 section 2.6), a single peak was observed for each *RbSTAT1s* and rock bream β -actin representing a specific of amplifications.

3.2.3.1. Expressional changes in different tissues of healthy fish

The qPCR results revealed that the transcription of *RbSTAT1* was predominantly observed in blood cells, heart and liver tissues of healthy rock bream. Meanwhile, muscle and skin tissues expressed lower amount of *RbSTAT1* mRNA, while showing moderate expression in other

tissues. In the sense of *RbSTAT1L*, the transcripts were highly expressed in blood cells, gills and heart tissues, although showing lower expression in muscle and skin tissues (**Fig. 3.8**).

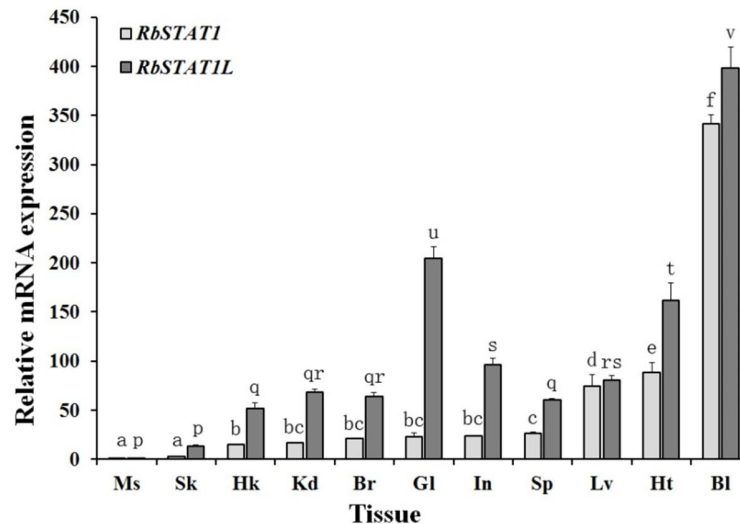


Fig. 3.8. Tissue-specific expression of rock bream STAT1 and STAT1L transcripts in healthy fish. The level expression was examined by SYBR Green qPCR and, rock bream β -actin was used as an internal reference gene to calculate the relative mRNA expression. Based on the results, the calculation was performed using Livak method and values were compared relative to muscle which showed lowest expression. Eleven different tissues including muscle (Ms), skin (Sk), head kidney (Hk), kidney (Kd), brain (Br), gill (Gl), intestine (In), spleen (Sp), liver (Lv), heart (Ht) and blood cells (Bl) were used. The results are reported as mean \pm standard deviation (SD) of triplicates. Statistical analysis was performed by one-way ANOVA followed by Duncan's Multiple Range Test. Data with small case letters are indicated the significant differences at $P < 0.05$ among different tissues.

3.2.3.2. Expressional patterns upon *in vivo* immune challenges

The results of the expressional studies in *RbSTAT1* exhibited as middle phase responses, where mostly in between 6 - 24 h post injection of pathogens and PAMPs in blood and liver tissues (**Fig. 7**). Upon poly I:C injection, the highest expression of *RbSTAT1* transcripts was detected at 12 h in both blood cells (3.9-fold) and liver tissue (2.5-fold) compare to the un-injected control (0 h). In the meantime, RBIV significantly ($P < 0.05$) triggered the expression of *RbSTAT1* at 12 h in blood, and 12 h and 48 h in liver tissue, while presenting down regulations at 48 h in blood and 3 h in liver. According to the LPS stimulation, the highest expression was detected at 12 h in blood cells and 6 h in liver tissue. Gram-negative *E. tarda* bacterial infection led to peak the expression at 24 h in blood and 12 h in liver tissue. Meanwhile, the highest expression was detected at 12 h in blood and 48 h in liver in response to the Gram-positive *S. iniae* bacterial infection.

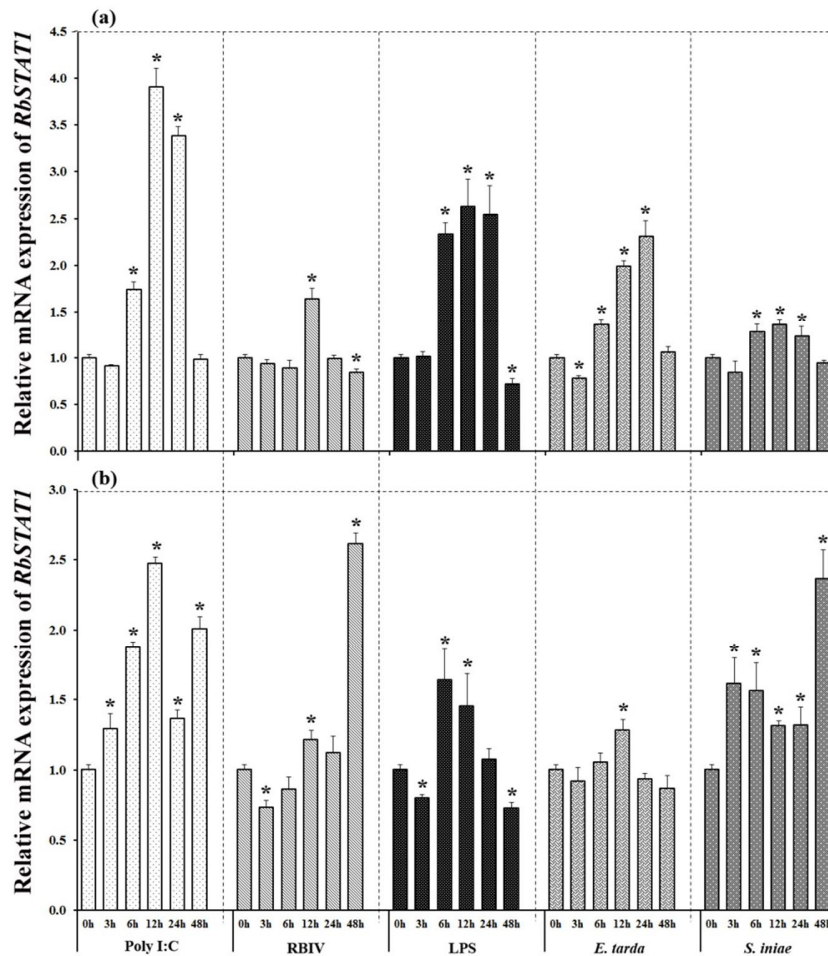


Fig. 3.9. The expressional patterns of RbSTAT1in (a) blood and (b) liver tissues after in vivo immune challenges. The rock bream β -actin was used as an internal reference gene to calculate the relative mRNA expression. The fold change of mRNA expression at each time point was compared with the PBS-injected control at corresponding time points and, represented as relative fold changes. The results are reported as mean \pm standard deviation (SD) of triplicates, and results were statistically compared relative to the un-injected control (0 h) using t-test. Data with statistically difference at $P < 0.05$ are indicated by asterisks.

Comparatively, low inductions of *RbSTAT1L* transcripts were observed in blood cells, while showing down-regulations at 6 h and 24 h post injection of pathogens and PAMPs (Fig. 8). The up-regulation of *RbSTAT1L* mRNA expression was only observed in blood cells upon poly I:C (at 12 h), RBIV (48 h) and LPS (12 h) stimulation. In contrast, the expression in liver tissue was mostly triggered at every time points towards all pathogen and PAMPs stimulations.

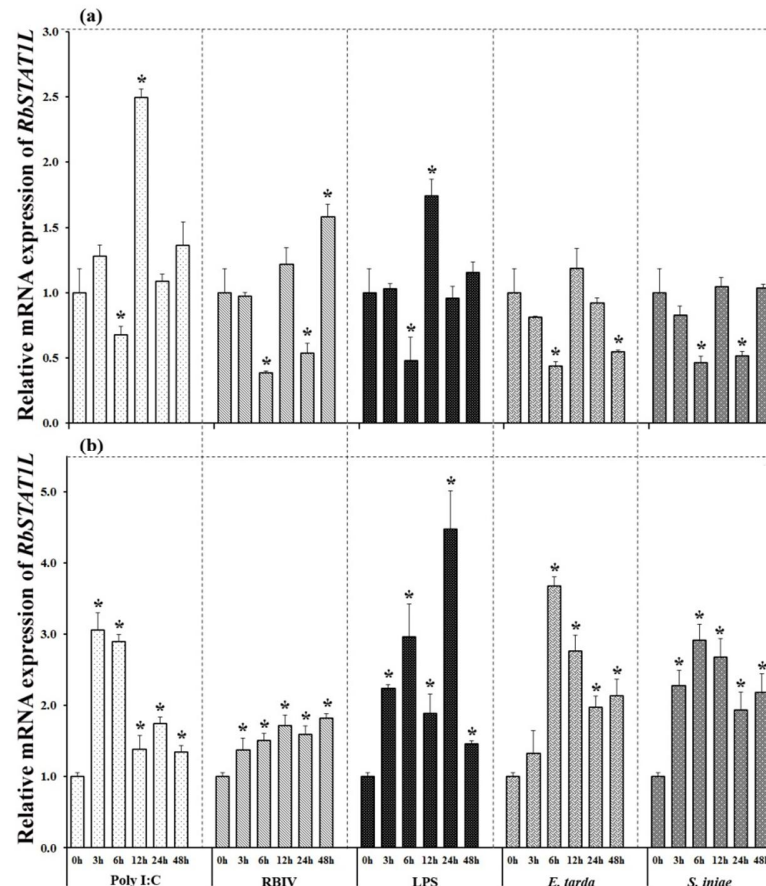


Fig. 3.10. The expressional patterns of RbSTAT1L in (a) blood and (b) liver tissues after in vivo immune challenges. The rock bream β -actin was used as an internal reference gene to calculate the relative mRNA expression. The fold change of mRNA expression at each time point was compared with the PBS-injected control at corresponding time points and, represented as relative fold changes. The results are reported as mean \pm standard deviation (SD) of triplicates, and results were statistically compared relative to the un-injected control (0 h) using t-test. Data with statistically difference at $P < 0.05$ are indicated by asterisks.

3.2.3.3. Expressional patterns in response to injury

The responsiveness of RbSTAT1 and RbSTAT1L on wound healing was evaluated by measuring the level of transcripts in blood cells and liver tissue. Results demonstrated that significant ($P < 0.05$) elevation of both *RbSTAT1*s mRNA at 6 h in blood cells, while at 24 h in liver tissue compare to the un-injured control (**Fig. 3.11**). In addition, significantly up-related *RbSTAT1* mRNA expression in blood cells was observed at 48 h post injury although it showed down-regulation at 3h. Meanwhile, significantly suppressed expression of *RbSTAT1L* was detected at 3 h, 24 h and 48 h in blood cells. A down-regulated transcription of *RbSTAT1L* in liver tissue also observed at 48 h post injury.

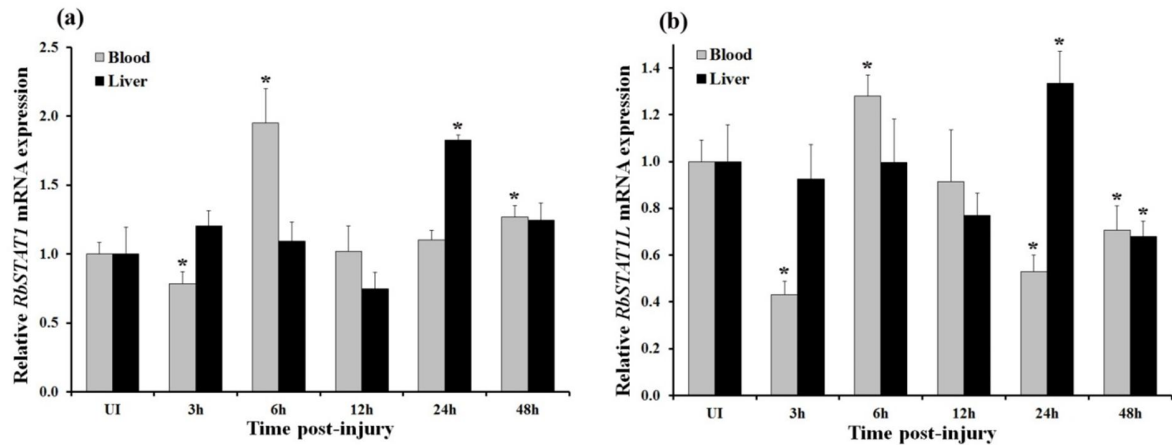


Fig. 3.11. The expressional patterns of RbSTAT1 (a) and RbSTAT1L (b) in blood cells and liver tissues after injury. The fold change of mRNA expression at each time point was compared with the un-injured control (UI) and, represented as relative fold changes. The results are reported as mean \pm standard deviation (SD) of triplicates, and results were statistically compared relative to the un-injured control (UI) using t-test. Data with statistically difference at $P < 0.05$ are indicated by asterisks.

3.2.3.4. Expressional patterns upon *in vitro* challenge

To understand the effect of rock bream IL-10 on RbSTAT1s activation, rRbIL-10 protein was used for the *in vitro* challenge experiment. According to the qPCR results, the transcription of both *RbSTAT1* and *RbSTAT1L* significantly modulated by RbIL-10. Interestingly, similar expression patterns were observed for both *RbSTAT1* and *RbSTAT1L*. Significantly induced expression was detected at 6 h and 12 h, while showing significant down-regulations at 3 h and 48 h, post stimulation of rRBIL-10 (**Fig. 3.12**).

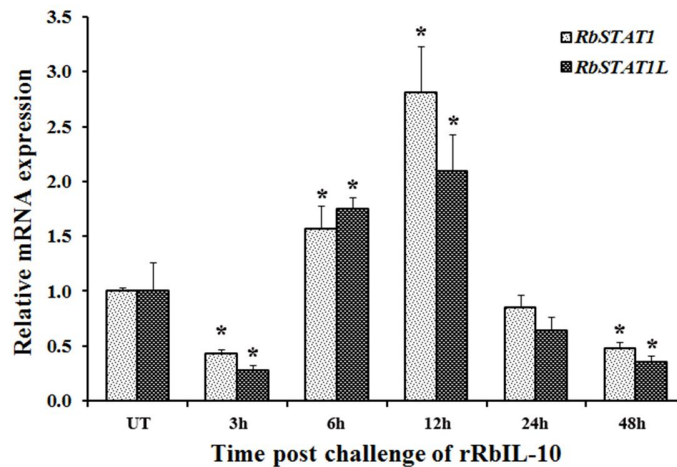


Fig. 3.12. The expressional patterns of RbSTAT1 and RbSTAT1L in heart cells after in vitro immune challenge with rRbIL-10. The fold change of mRNA expression at each time point was compared with the un-treated (UT) control at corresponding time points and, represented as relative fold changes. The results are reported as mean \pm standard deviation (SD) of triplicates, and results were statistically compared relative to the un-treated control (UT) using t-test. Data with statistically difference at $P < 0.05$ are indicated by asterisks

3.2.4. Antiviral activity assay

The antiviral effect was assessed by analyzing the cell viability by WST-1 reagent after adding RBIV. As shown in **Fig. 3.13**, cells containing RbSTAT1 and RbSTAT1L plasmids have more viability compare to the mock control (pcDNA3.1 empty vector transfected) as well as to cell control (only cells) implying its potential antiviral effect. These evidences strongly indicate the potential mediation of STAT1s on antiviral responses. However, the real mechanism behind antiviral activity of RbSTAT1s is required to be explored.

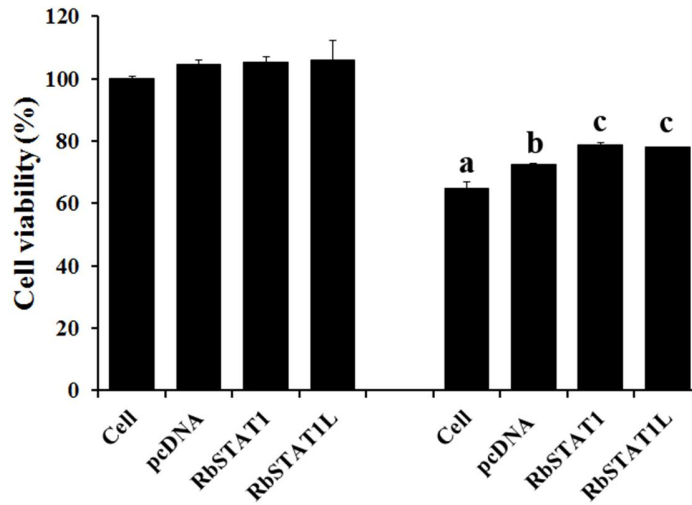


Fig. 3.13. Effect of RbSTAT1 and RbSTAT1L for cell viability after RBIV infection. Cell viability was assessed by WST-1 assay. Triplicate wells containing cells only (cell), pcDNA3.1(+) transfected cells (pcDNA) or RbSTAT1/pcDNA3.1(+) or RbSTAT1L/pcDNA3.1(+) transfected cells were grown 48 h at 25 °C. One set of cells were treated with RBIV and evaluated the cell viability after 3 days by measuring absorbance at 450 nm. Percentage of viable cells was calculated with comparison of normal cells those not treated with RBIV. Data was represented as mean \pm SD of triplicates and significant difference ($P < 0.05$) was analyzed by comparing with respective cell control.

3.2.5. Subcellular localization of RbSTAT1 and RbSTAT1L

Subcellular localization of RbSTAT1 and RbSTAT1L proteins was examined in rock bream heart cells using GFP containing vector system. As mammalian STATs, both RbSTAT1 and RbSTAT1L were localized in the cytoplasm under normal conditions (**Fig. 3.14**).

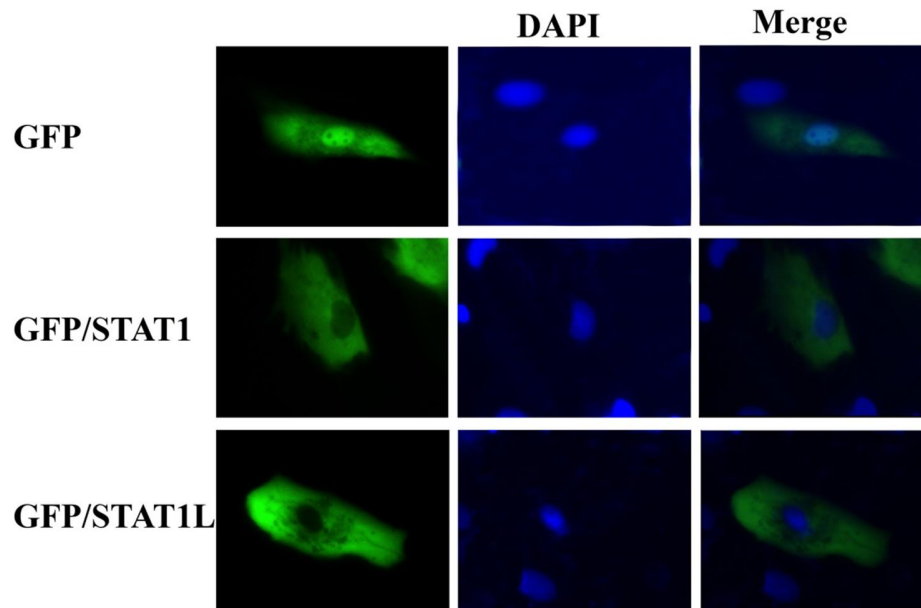


Fig. 3.14. Subcellular localization of RbSTAT1 and RbSTAT1L in rock bream heart cells. Nucleus stained by DAPI. Cells in the first row indicate the localization of GFP protein, where pEGFP-N1 empty vector was transfected. Cells in the second row indicate the localization of RbSTAT1 protein, where pEGFP-N1/RbSTAT1 vector was transfected. Cells in the third row indicate the localization of RbSTAT1 protein, where pEGFP-N1/RbSTAT1L vector was transfected.

3.3. Discussion

Enormous studies have been focused on JAK/STAT signaling cascade with their associates, in response to the multiple functions such as immune responses against microbial pathogens, inflammatory responses, hematopoiesis, mammary gland development and so on (Rawlings et al., 2004). However, the complete signaling cascade and diverse functional aspects in teleosts were poorly studied. In the current study, two sequences homologous to STAT1 were identified from rock bream and functionally characterized. Bioinformatics analysis revealed that both RbSTAT1 counterparts were remarkably differed and shared 42.4% identity. The amino acid sequence of both RbSTAT1s were compared with respective equivalents from different taxonomical lineages and affirmed that RbSTAT1 showed substantial similarity with others, while showing poor conservation of RbSTAT1L with others. The characteristic domain regions including N-terminal domain, coiled coil domain, DNA binding domain, linker domain, SH2

domain and TA domain were noticed as other STAT members. The 3D structural illustrations of each RbSTAT1s also revealed the distinct domain regions as human STAT1 indicating their functional conservations. However, the tyrosine residue of RbSTAT1 which is phosphorylated upon activation of JAK/STAT signaling pathway was well conserved among other counterparts, while tyrosine residue displaced in RbSTAT1L. Hence, broad spectrum of study needs to be attended to determine the functional tyrosine residue in RbSTAT1s, particularly in RbSTAT1L.

To establish the molecular evolution of STAT genes, unrooted phylogenetic tree was constructed based on the ClustalW alignment with different STAT members. Fascinatingly, the tree was clustered into seven different groups separating respective six different STAT members and RbSTAT1L which was grouped with fish STAT1-like members. The results clearly displayed that RbSTAT1-like genes were evolved in different path indicating them as novel group of STAT members. As shown in **Fig. 3.5**, the STAT1 members from fish and other vertebrates were distinctly evolved, and it was consistent with the previous reports (Park et al., 2008; Guo et al., 2009). The genomic structural analysis also further supported the notion of distinct evolution between fish and other vertebrates. According the genomic organization of *RbSTAT1* and *RbSTAT1L*, the sizes of the exons were not conserved, although they shared same number of exons in the CDS region. The outcomes of the sequence analysis of RbSTAT1L, pointed out that it might be a novel STAT family member which restricted to fish counterparts. Further analysis in this regard is recommended to conduct, in order to affirm as a novel member.

Furthermore, TFBSs those were known to be involved in various immune functions, were predicted at the 5'-proximal region of each RbSTAT1 genes. Several transcription factors such as NF- κ B, C/EBP, ICSBP, SP1 and CREB are known to be involved in essential roles of immune functions (Nerlov, 2007; Oeckinghaus and Ghosh, 2009; Tan and Khachigian, 2009; Huang et al., 2010; Wen et al., 2010). In addition, HNF3, GATA1 and Oct-1 play a vital role in metabolism (Kaestner, 2000), hematopoiesis (Ferreira et al., 2005), and cellular stress responses (Tantin et al., 2005), respectively. In the presence of many TFBSs in putative promoter region of RbSTAT1 and RbSTAT1L genes suggesting that the transcription of these genes might be regulated according to the diverse functional aspects.

The transcription of a gene in different tissues under normal physiological condition is presented its biological importance to the living organisms. The levels of *RbSTAT1*s mRNA expression

were measured as tissue specific manner by SYBR Green qPCR technique to understand the functional distribution in different tissues. Most of the immune related tissues depicted the higher expression of *RbSTAT1* and *RbSTAT1L* transcripts indicating their diverse functions in rock bream. Limited studies have been described on the subject of expressional analysis in fish origin under normal physiological conditions. A study on mandarin fish has observed the expression of *STAT1* predominantly in spleen, heart and liver tissues of healthy fish (Guo et al., 2009). Park *et al* (Park et al., 2008) confirmed that the expression of olive flounder *STAT1* transcripts was highly detected in gill, spleen and kidney tissues, while lower expression in liver, skin and muscles. Evenly distributed expression of *STAT1* mRNA in different tissues was reported in Atlantic salmon (Skjesol et al., 2010). Tso C.H and coworkers (2013) reported the highest transcription of Malabar grouper *STAT1* in liver tissue (Tso et al., 2013). Meanwhile, the transcription of *STAT1* was highly detected in liver tissue of fruit bat (Fujii et al., 2010). According to the results described in the past studies, it is apparent that the expression of *STAT1* mRNA might be species specific.

The activation of *STAT1* in JAK/STAT signaling pathway in response to the various signaling elements associated with several receptors, and its mediation on several biological operations were broadly studied in mammals (Ramana et al., 2000). However, the complete JAK/STAT pathway with its associated constituents and functional features were poorly understood in fish lineage. The immune responses of *STAT1* against viral pathogens have been fairly reported in few fish species. Significantly elevated *STAT1* mRNA expression was recorded in crucian carp against grass carp hemorrhagic virus (Zhang and Gui, 2004), Atlantic salmon against orthomyxovirus ISAV and birnavirus IPNV (Collet et al., 2008), and Malabar grouper against nervous necrosis virus (Tso et al., 2013). In addition, mandarin fish (Guo et al., 2009) and Malabar grouper (Tso et al., 2013) showed the significant induction of *STAT1* transcripts in response to the poly I:C stimulation. In the present study, significantly induced as well as suppressed expression of *RbSTAT1* and *RbSTAT1L* mRNA were examined upon RBIV and poly I:C injection. Furthermore, we have measured the expression level of each *RbSTAT1*s on bacterial (*E. tarda* and *S. iniae*) and LPS (a major component of bacteria cell wall) stimulations, and revealed the potential responses. Previous study in Malabar grouper demonstrated that there is no significant change upon LPS stimulation (Tso et al., 2013). However, the studies showing responses against bacterial infections were scarce in fish species. A study conducted using mouse

model confirmed that STAT1 is a crucial transcription factor for the elimination of bacterial infection with *Listeria monocytogenes* (Varinou et al., 2003). On the other hand, the differential expression patterns of *RbSTAT1* and *RbSTAT1L* highlighted the functional discrepancy. Consequently, the results of the present study manifested that both orthologs of *RbSTAT1* and *RbSTAT1L* possibly be involved in eradication of bacterial and viral attack in rock bream.

Inflammation is one of the vital processes that can protect the cells or tissues from various injurious causes. A number of studies have been focused on the involvement of members of the JAK/STAT signaling pathway towards tissue injuries. The great contribution of STAT1 on brain injury (Takagi et al., 2002), and spinal cord injury in mice (Osuka et al., 2011) has been reported in previous studies. Meanwhile, another study described the possible role of STAT1 and STAT3 in ischaemia/reperfusion injury, and suggested them as therapeutic targets against the myocardial damage (Stephanou, 2004). In the sense of fish species, there are no reports describing the involvement of STAT on wound healing process. Here we attempted to understand the responsiveness of rock bream STAT1 and STAT1L on tissue injury by analyzing the level of expression following execution of two incisions (one on each side) on the dorsal surface near to the caudal fin of rock bream. The results revealed the significant changes of transcription of each *RbSTAT1s* suggesting their potential role in wound healing process of rock bream. Nonetheless, the mechanism behind complete wound healing process and association of JAK/STAT signaling pathway is remained to be perceived.

Interleukins are vital signal components pass the signal via various signaling cascades by association with their receptors located in cell membrane. The IL-10 is one of the important cytokine that pass the signals through JAK/STAT signaling pathway. Many studies have been reported the relationship between STAT proteins and IL-10. The STAT proteins including STAT1, STAT3 and STAT5 activation upon IL-10 treatment have been reported by Wehinger *et al* (Wehinger et al., 1996). Another study reported the involvement of IL-10 for inhibition of STAT1 in the live which is activated by IFN- α (Shen et al., 2000). In this study, we measured the level of expression of *RbSTAT1s* mRNA in heart cells after IL-10 treatment. Results showed the significant modulation of *RbSTAT1s* transcription. These results suggesting that the expression of *RbSTAT1s* might be governed by IL-10.

3.4. Conclusion

Herein, we reported the molecular features and functional aspects of two STAT1 orthologs identified from rock bream. It was revealed that RbSTAT1 was highly conserved among vertebrate species based on the *in silico* analysis. The other RbSTAT1L ortholog comparatively shared lower percentage of identity with other vertebrates. However, the 3D structural topology showed similar structural pattern indicating functional similarities. Phylogenetic studies revealed the separated evolution of fish and other vertebrates. Further it depicted the distinct evolution of RbSTAT1 and RbSTAT1L. Upon immune challenge experiments and tissue injury, both RbSTAT1s were significantly modulated. In addition, transcriptional changes were observed after RbIL-10 treatment. Finally, all the results implied essential roles of RbSTAT1s in host immunity and wound healing process.

CHAPTER 4

Molecular cloning, transcriptional profiling and subcellular localization of signal transducer and activator of transcription 2 (STAT2) ortholog from rock bream, *Oplegnathus fasciatus*

Abstract

Signal transducer and activator of transcription 2 (STAT2) is a key element that transduce signals from cell membrane to the nucleus via type I interferon signaling pathway. Although structural and functional aspects of STAT proteins well studies in mammals, information available for teleostean STATs are very limited. In this study, a STAT paralog which is highly homologous to the STAT2 members was identified from commercially important rock bream and designated as RbSTAT2. The *RbSTAT2* gene was characterized at cDNA and genomic sequence level, and revealed the common structural features as mammals. The complete cDNA sequence was distributed into 24 exons in the genomic sequence. Putative promoter proximal region was analyzed and found to be presence of various immunologically crucial transcription factor binding sites. Phylogenetic studies and comparative genomic structure organization revealed the distinguishable evolution for fish and other vertebrate STAT2 orthologs. Transcriptional quantification was performed by SYBR Green quantitative real time PCR (qPCR) and observed the ubiquitous expression of *RbSTAT2* transcripts in all tissues analyzed from healthy fish, while detecting a remarkably high expression in blood cells. Significantly ($P < 0.05$) changed transcription of *RbSTAT2* was detected after immune challenged experiments with viral (rock bream irido virus; RBIV), bacterial (*Edwardsiella tarda* and *Streptococcus iniae*) and immune stimulants (poly I:C and LPS). Antiviral potential was further confirmed by WST-1 assay by measuring the cell viability using rock bream heart cells with RBIV. Possible role of RbSTAT2 in wound healing process was affirmed by measuring the transcripts level following tissue injury. In addition, *in vitro* challenge experiment signified the great influence of rock bream interleukin-10 (RbIL-10) on transcription of *RbSTAT2*. Finally, subcellular localization was examined, and confirmed that RbSTAT2 protein was located usually in the cytoplasm under normal physiological condition and translocation near to the nucleus under poly I:C stress indicating its signal transduction ability. Altogether, these findings implicate that RbSTAT2 possibly be involved in various biologically crucial mechanisms and provide great protection for rock bream.

4.1. Introduction

Many cytokines and growth factors activate the functional aspects via various proteins in Janus kinase (JAK)/ Signal transducer and activator of transcription (STAT) signaling pathway. Basically, the STAT proteins in the cytoplasm activate by JAK activation when ligands bind to the respective receptors existed in the cell wall. The activated STATs transduce signals as homo- or heterodimers by translocating to the nucleus and thereby induce the transcription of specific gene after binding to the corresponding transcription factor binding sites (Rawlings et al., 2004). The STAT family composed of seven different members (STAT1, 2, 3, 4, 5a, 5b and 6) and shared common domain architecture with six different domains including N-terminal domain, coiled coil domain, DNA-binding domain, linker domain, Src homology 2 (SH2) domain, and a transactivation domain (TAD) (O'Shea et al., 2002).

The STAT2 is an essential co-factor that response to the type I interferon (IFN) mediated signaling. Type I IFN interacts with its cognate receptor which is pre-associated with tyrosine kinase 2 (TYK2) and JAK1, and activates the STAT1 and STAT2 by phosphorylation. The phosphorylated STAT1 and STAT2 assemble together, and form a complex referred as IFN stimulated gene factor 3 (ISGF3) with interferon regulatory factor 9 (IRF9). The ISGF3 complex interacts with IFN stimulated response element (ISRE) located in the promoters of IFN stimulated genes (ISGs), and initiate the gene expression (Steen and Gamero, 2013). In addition, STAT2 shown to be interact with various mediators such as DRIP150, a subunit of the multimeric mediator coactivator complex (Lau et al., 2003), CREB-binding protein (Bhattacharya et al., 1996), Brahma related gene 1 (BRG1) (Huang et al., 2002), IFN alpha/beta receptor alpha chain (IFNAR1) (Li et al., 1997), IFN alpha/beta receptor beta chain (IFNAR2) (Nguyen et al., 2002b), regulator of calcineurin 1 (RCAN1) (Lee et al., 2012). By association with those co-factors, STAT2 plays essential roles in immune responses, dendritic cell development, myogenic differentiation, tissue injury (O'Shea et al., 2002; Khorrooshi et al., 2008; Wang et al., 2008; Chen et al., 2009). Number of studies have been reported the involvement of STAT2 on host immune responses particularly against viral attack with the association of type I IFN (Hahm et al., 2005; Chen et al., 2009; Ashour et al., 2010; Kadeppagari et al., 2012; Blaszczyk et al., 2015).

Structural and functional characteristics of STAT2 gene from teleostean origins have been reported by few research groups. Collet *et al*, 2009 (Collet et al., 2009) demonstrated the transcriptional modulation of Atlantic salmon (*Salmo salar*) STAT2 upon Infectious Salmon Anaemia Virus (ISAV), Infectious Pancreatic Necrosis Virus (IPNV) and Salmon Alphavirus (SAV). Another group of research reported the significant role of salmon STAT2 and IRF9 for the expression of specific genes containing IFN γ stimulated gene response element (GAS) at their promoters (Sobhkhez et al., 2014). Meanwhile, Shi jun and coworkers (Shi et al., 2012) reported the involvement of crucian carp (*Carassius auratus*) STAT2 and IRF9 on activation of ISRE containing promoters and ISGs. In recent study on turbot (*Scophthalmus maximus*) described the immune responses of STAT2 against bacterial and viral stimulations (Wang et al., 2013).

Rock bream, *Oplegnathus fasciatus* is an economical crucial aquacrop in South Korea due to its high demand as delicacy. The environment rich with pathogens and other stress factors, and mass scale culturing practices will be immensely caused for the mass mortality of rock bream (Park, 2009; Sun et al., 2011; Park et al., 2012). Investigation of immune related genes and their functional aspects might be beneficial to improve the quality of fish life and sustainable development of rock bream aquaculture.

The JAK/STAT signaling pathway is essential machinery for the activation of wide array of functional elements in the biological system and it has not yet been completely studied in fish lineages. In the present study, our main goal was to characterize a STAT member structurally and functionally from rock bream. Herein, we presented the structural insights of STAT2 ortholog at complementary DNA (cDNA) and genomic DNA (gDNA) level. As functional aspects, transcriptional modulations upon bacterial (*Edwardsiella tarda* and *Streptococcus iniae*), viral (Rock bream iridovirus; RBIV) and pathogen-associated molecular patterns (PAMPs; LPS and poly I:C) and, tissue injury were investigated. Furthermore, transcriptional changes upon rock bream interleukin-10 (RbIL-10), and antiviral effect of STAT2 were analyzed.

Table 4.1. Primers used in this study

Primer name	Application	Sequence (5' -3')
<i>RbSTAT2/BAC-F</i>	BAC screening	TGACAGGGATGCTTTGCCTATGGA
<i>RbSTAT2/BAC-R</i>	BAC screening	CCAAATTCTCCAACAGGACCTGGA
<i>RbIL-10/pMAL-F</i>	Clone into pMAL-c5x	(GA) ₃ gaattcAGTCCCATGTGCAACAACCACTG - EcoRI
<i>RbIL-10/pMAL-R</i>	Clone into pMAL-c5x	(GA) ₃ aagcttTCAATTAGAGGCCACTTGTTTTTCGGAC - HindIII
<i>RbSTAT2/qPCR-F</i>	qPCR amplification	ACCTTGAAGACCTGTGGAGGGATG
<i>RbSTAT2/qPCR-R</i>	qPCR amplification	GGTGAAGGGCTGGACTGTCTTTATGT
<i>RbSTAT2/pcDNA-F</i>	Clone into pcDNA3.1(+)	(GA) ₃ aagcttATGGCTCAGTGGGACAGACTGAG - HindIII
<i>RbSTAT2/pcDNA-R</i>	Clone into pcDNA3.1(+)	(GA) ₃ ctcgagTTATTGGAAAAGGCTTCCACAGGATTGC - XhoI
<i>RbSTAT2/GFP-F</i>	Clone into pEGFP-N1	(GA) ₃ ctcgagATGGCTCAGTGGGACAGACTGAG - XhoI
<i>RbSTAT2/GFP-R</i>	Clone into pEGFP-N1	(GA) ₃ ccgctgTTGGAAAAGGCTTCCACAGGATTGC - SacII
<i>β-actin</i>	qPCR of internal reference	TCATCACCATCGGCAATGAGAGGT
<i>β-actin</i>	qPCR of internal reference	TGATGCTGTTGTAGGTGGTCTCGT

Restriction sites in the cloning primers are shown with small case letters and indicated at the end of each primer sequence.

4.2. Results and discussion

4.2.1. cDNA and genomic sequence characteristics

The cDNA contig (3309 bp, including poly A tail) identified from transcriptome database was composed of an open reading frame (ORF) of 2412 bp excluding stop codon, and it was coded for poly peptide sequence with 804 aa. The molecular mass and theoretical isoelectric point (*pI*) of RbSTAT2 protein, were predicted to be as 92.17 kDa and 5.43, respectively. Two polyadenylation signals (AATAAA) and six RNA instability motifs (ATTTA) were identified at the 3'-untranslated region (UTR) (**Fig. 4.1** and **4.2**).

```

GAAGCGAAGAAGCAAGGAATAATACACACGCGCTGCTGTTGTTGGAAAGTGTGTTGTTGTACCAACGCCCTAACAGCTAGCTACT 90
ACTCGGAGAAAAGTGTGTTAGCTAAGTACCTGCTGTTGTTAAATTAAGCTAGTTGCTAGTTAGTAGAAGCAATTTCTAGTGGACTCGGAC 180
TGACCGCACAAAAGCAAGATGCGCTCAGTGGGACAGACTGAGGCGAGCTTCTGCTGTGTACAGACAGCAGTTTACATGAGCTCTATGACAGG 270
M A Q W D R L R Q L P A V Y R Q Q L H E L Y D R
GATGCTTTGCTTATGGATGTCCTGCTCACTACCTGTCGCTGGATAGAGAAAACAAGAGTGGCAAAGACAGCGCGGACCATGATTTGGCT 360
D A L P M D V R H Y L S V W I E K Q E W O R A A R D H D L A
GTGGCTCTGTCCAGGCTGTTGGAGAATTTGGATATCCAACACAGCCGCTTTGTCAGGAGGAGTGTCTTACTGACAGCAACAATT 450
V V L F Q V L L E N L D I Q H S R F V Q E E S F L L Q H N I
AGACCTACAAAAGAACTTTCAGAGGTACCTGGATGACCCGCTGTCCTTGGCACACACTATCCTGTGTGTTTGGAAAAAGAGAAGAA 540
R R Y K Q N F Q R Y L D D P C A L A H T I L W F L E K E K E
ATCCTGACAGGCTGATGCTGGCTGAGCAGGTCAGTATTGCTGTAGAGCCAGAAACCATGGAGACAAGCAGCCAGGACCTTGAA 630
I L Q S A D L A E Q V Q L L R V E P E A M E T S S Q Q D L E
CGTAAATGGCTGGCTCAGGAATGAAGTGCAGTGCATGGAACATACAATGTTATGCTGGAGGAGCAGCAAGATGATTTGATTTAA 720
R K M A G L R N E V Q C M E H T M L C L E E Q Q D E F D F K
TACCAACTTCAAGATGGAAGCTGTGTAGATGAGGCTGTGAAGAAAACAATGAAACATTTTCAGTTCTTATCAACAGACTGAAT 810
Y Q T F K M E A V V D E A V K K E Q M K H F Q F L I N R L N
GAAGGTAGAAAAGCAGCACTGTGACCTCAGTAGTCTCTGGACAGACTGAGGACCTGATGTCATATTTGGTGAACAGGAATGCTGT 900
E G R K S T L S D L S S L L D R T E D L I V I L V N K E L V
GAGTGGCAGAGGAGTCAAGCAGAAAAGCTGCATTTGGCTCCAGACATGTTGCTGGATCAGATAGAGAAGTGGTTCACCTGTGTGGCA 990
E W Q R S Q Q K A C I G A P D N V C L D O I E K W F T C V A
GTGTGCTGTCCAGCTGGGAGTTCTTGTGTAAGCTGGAGGAGCTGGTGGAAAAGTGTCTTATGAAAACGACCCCGTGAAGGCCAA 1080
V C L F Q V R E F L G K L E E L V G K V S Y E N D P V K A Q
AAAGCTGCGCTGGACAGGAGCAGACTACTTCTGAAAACCTTACTCAAGAGTCTTCTTGTGTTGAGACTCAGCCATCATGCTCAG 1170
K P A L Q T R A D T L L K N L L K S S F V V E T Q P S M P Q
GGGAAAGACCCCTGGCTCCCGACAAAGTACAGTCTCTGTGAAGACAGACTCTGTTAAGTTTCTGAGCTGAACCTCCTCATG 1260
G K G P L V L R T N V Q F S V K T R L L V K F P E L N H S M
AAAGTGAATGTCATGACAGGAGGCTCTCAGATCAAGGATATCGGCGTTTAAATGCTGGGACCAAAACCAAGGCTTGAAC 1350
K V N V S M D R E A P Q I K G Y R R F N V L G T K T K A L N
ATGGCAGAGGCCAGACTGGAGCAGTGGGACACTCAGACATCTGACTGAAAGGAGCAGAGTCTGGAGGTGGTGGCAAGGAGTCA 1440
M A E S Q T G G M V A D F R H L T L K E Q K S G G G K G V
AGTGAATTTCTCAGTGTACAGAGGAGTGCACATCTTCTTCAACACTGATTTGAGCTGAAAGGCGTGTGATGATGATGATG 1530
S D I S L S V T E E L H I I F F N T V F E L K G V S V E L Q
GCCTCCCTCCCGGTGTCATCTTCCAACTCAGCCAGCAGAGCCGCTGGCATCTGTCTCTGTTCACATGATGATGATGATG 1620
A S S L P V V I I S N S S Q Q Q S A W A S V L W F N M I S H
GACACCAGGAGCTCATGTTCTTCCCAACTCTCTGACGCCACTTGGCCGAGTTTGGAGAGATGTTGAGCTGGCAGTTTCTCTCTGCC 1710
D T K D V M F F A N S P A A T W P Q F G E M L S W Q F L S A
ACTAAAGCTGGTCTGATGATGCTCAGCTGGAGATGATGACACAGACTCTTTGGAAACAGCCGAACTATGACACTGCAAAAGTAC 1800
T K R G L N D A Q L E M I A H R L F G N Q R N Y D N C K V A
TGTCAAAGTTTACCAAGAAAATACCCGACACTTCTGGGTGTGTTGATGATGATGATGATGATGATGATGATGATGATGATGATG 1890
W S K F S K E N T P D T F W V W F D G I L V M V K T Y L E D
CTGTGAGGGATGCCACATCATGGGTTTTGTGAACAAAGGCAAGAGAGGTCCTCTGAAAGAAAACAGAGAGGCGCTTCTTTGTTG 1980
L W R D G H I M G F V N K G K E R S L L K K K Q R G T F L L
CGCTCAGTGAAGTGTCAATTGGAGAAATCACCTTCTTGGGTGGAAACAGCATAACCGGTGACCTGACATAAAGCAGTCCAGCCC 2070
R F S E S V I G G I T F S W V E T S I T G D P D I K T V Q P
TTACCAAAGTTGACCTTTCCAGATGCCCTTCCATGAAATCATCAGGAATACAGATCTTAGAAGCTGAAAATGTTCCAGAAAATGCT 2160
F T K V D L S Q I P F H E I I R N Y Q I L E A E N V P E N P
CTACTGTACTTTATCCCAACCCCTAAAGAGGAGGCTTTCCGAAAATATTACTCCGAAAGGACTGGAAGTGACAGCCCTTACATAAG 2250
L L Y L Y P N T P K D E A F G K Y Y S E R T G S D S P Y I K
TACATCAAAACCAAGCTGATGTTTGTGCAAAAGGAGACACACTGAGGCTAGGCCCCCAATGCCCCCTGACATGCTCAGGTTGAAGG 2340
Y I K T K L M F V S K E N T L E A R P P M P P D M A Q G E G
CTGGAGCCAATGAATGGCTGTCTGGAGAGGAGCTGAAACAAACGGGAATCCCTCCTCTGAAATTCACCTTGGAACTTATCACTCT 2430
L E P M N G L S G E A A E Q N G N P H P L N S P L E T Y H S
GATCCATGCTGTGCTGCTGTGCAAGCCAGAGGAGGATTTACTGCTGTATCTCAACAACCCCAACCTCTATGCTGACTGTGACATC 2520
D P M L S G S V A A P E D D L L Y L N N P N L Y A D S D I
TTGCAAGTAGAGCGGGCTGGCTGATTTCAAGTAAATTTTCAAGGATTTAATGGCTGCCCGCAATCCTGTGAAAGCCTTTTCCAA 2610
L Q D E P G L P D F S L N F Q G F N G L P P Q S C G S L F Q
TAAGCCCTCTTGTGATATTTAACCACCAACCACTGATCACTCATGTCAGCTTTACTTTTACTTTTACTTTTACTTTTACTTTTACTTT 2700
AAAATTTAGCTTACGTAGCAAAATCCAGGTGCAACATAATAGTTTGTCTTGAATACGTGTTTATTACTGACAGCGGCTCTGCTAATCT 2790
GACAGTCAGTATTTAAGAATGCTTTTGAATCAGCAATTTGAATGCTGCTGCTTTGAAATCAITAAAATAAACCTTTATAATAT 2880
CTTTTATCATGTTGATATTTGTAACAATGATTTAAGACAATCTGAAAGACAAAAGAGACCTCTTAGACCTCAACTATCATC 2970
ATCATAAATCCTTTTATTTTATTTTGTGATTTTAGGACCTGTTATTTTAAAGATAAGACATCAAGGAATACAAATTAATC 3060
GAGGATGCAAGCTGCTGTTAAAGTTTCTATGAGGATTTGAGAATATGTTGCCAGACTACACATAATTTAATTTTAAATGTTGTT 3150
GTGAGTCCCTTTGTGTTTATAATGTTGCCACATGAAAGCTTTGACAAAACACTGAAACATGCGACTCTCCCTTTAAAGTACATGC 3240
TTTTATTAACCTGCTCATTGAAATCAAATTTGACCAAAATTAAGGAAATGACTGTAAAAA 3309

```

Fig. 4.1. Nucleotide and deduced amino acid sequence of RbSTAT2. RNA instability motifs (ATTTA) are marked with bolded and underlined letters. Polyadenylation signals (AATAAA) are shown by italic bolded letters.

The full length genomic sequence obtained from BAC library was found to be comprised with 24 exons interrupted by 23 exons, and it was deposited in NCBI GenBank. The CDS of *RbSTAT2* was restricted to 23 exons, while having an additional exon for 5'-UTR (Fig. 4.2a).

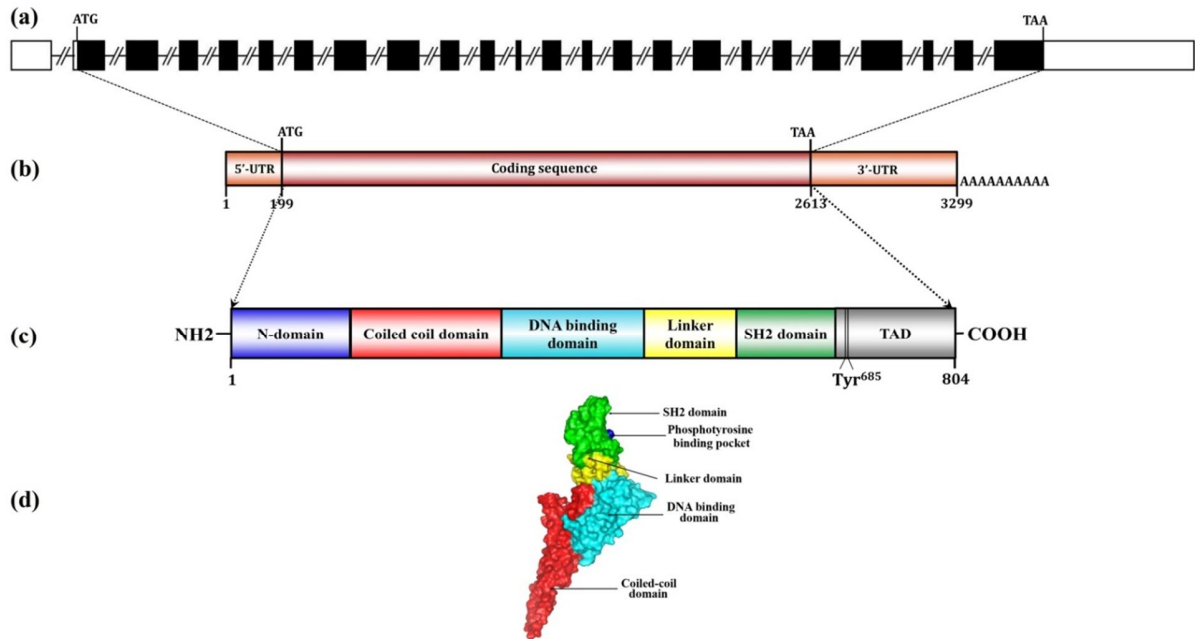


Fig. 4.2. Schematic illustration of rock bream STAT2 at genomic (a), mRNA (b), protein (c) and 3D homology model. Exons and introns in the genomic structure are indicated by boxes and lines, respectively. Black and white color boxes are represented for CDS and UTR, respectively. The position of the start codon (ATG), stop codon (TAA) and polyA tail are marked in the mRNA, respective nucleotide numbers are shown at the bottom line of the figure. In protein structure, characteristic domains are shown by different colors, and tyrosine residue (Tyr⁶⁸⁵) which is phosphorylated upon activation is depicted at the TAD domain. Different colors in the 3D protein structure are highlighted for each domain.

3.2. Putative promoter region

The 5'-flanking region of *RbSTAT2* gene was analyzed by AliBaba online TFBS prediction tool, and found to be existence of number of TFBSs which are mostly involved in immune regulations. The potential binding sites for interferon-stimulated gene factor 3 (ISGF3), CCAAT/enhancer-binding protein family members (C/EBP α or β), interferon consensus sequence binding protein (ICSBP), octamer transcription factor-1 (Oct-1), homeobox domain containing protein (Hb), GATA-binding factor 1 (GATA-1), activator protein (AP-1), specificity protein 1 (SP1), c-Jun, nuclear factor -1 (NF-1) and glucocorticoid receptor (GR) were identified from putative promoter of *RbSTAT2* (Fig. 4.3). Some of the TFBSs including GATA-1, ISGF3 and SP1 were also identified in the promoter region of human *STAT2* (SABiosciences DECODE database), and implied that their functional conservation. In addition, various studies have been reported that

some of the transcription factors such as NF-1, AP-1, C/EBP, GATA-1, Oct-1, ICSBP and ISGF3 were potentially involved in host immune and/or stress related responses (Wedel and Ziegler-Heitbrock, 1995; Foletta et al., 1998; Lekstrom-Himes and Xanthopoulos, 1998; Ferreira et al., 2005; Tantin et al., 2005; Xu et al., 2005; Horiuchi et al., 2012; Sung et al., 2015). Based on these evidences, we can hypothesize that TFBSs identified in the promoter proximal region might be involved in regulation of RbSTAT2 expression.

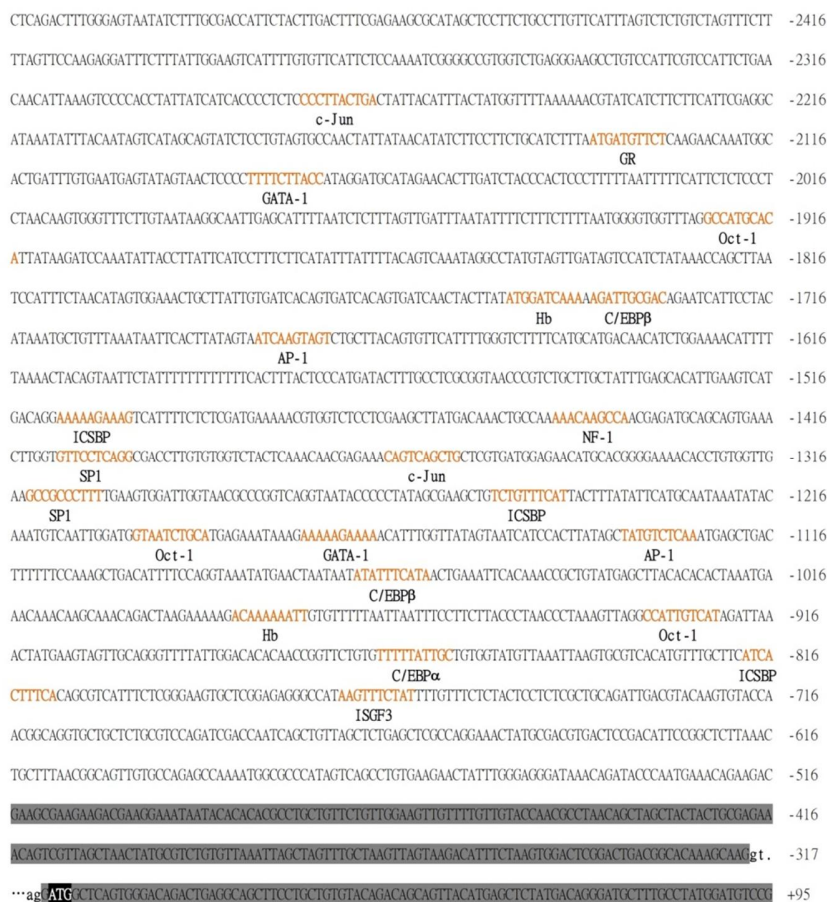


Fig. 4.3. Putative promoter proximal region of RbSTAT2. First exon and second exon initial part are shaded with dark gray color. The first intron region is marked with dotted line, and 5' and 3' splicing sites are marked with gt and ag, respectively. Numbers in the sequence are marked relative to the start codon shown by white color letters in the second exon. Possible transcription factor binding sites predicted by AliBaba 2.1 program are shown by brownish orange color letters and names are indicated at the bottom of sequence.

4.2.3. Comparative studies and phylogenetic analysis

To understand the structural conservation, number of STAT2 amino acid sequences from different taxonomical lineages and RbSTAT2 were aligned using ClustalW algorithm. Characteristic domains including N-terminal domain, coiled coil domain, DNA binding domain, linker domain, SH2 domain and TAD domain were identified based on the alignment and previous report (Collet et al., 2009). As shown in **Fig. 4.4**, the aa residues of mammalian counterparts were highly conserved. Comparatively the aa residues in DNA binding domain, linker domain and SH2 domain were conserved well in all species analyzed. In contrast, the aa residues in TAD domain were poorly conserved among fish species. Completely or partially conserved aa residues important for phosphotyrosine binding pocket (Lys⁵⁷⁷, Arg⁵⁹⁵, Thr⁶²¹ and Gln⁶²³) and hydrophobic binding pocket (Val⁶²² and Ile⁶³⁸) were identified in SH2 domain of RbSTAT2. In addition, a tyrosine residue (Tyr⁶⁸⁵) which is phosphorylated via activation was completely conserved among all species analyzed, and it was comparable with human Tyr⁶⁹⁰ (Improta et al., 1994; Shuai, 1999). Pairwise sequence alignment revealed that RbSTAT2 shared highest identity (81.9%) with turbot, while showing low identity (< 42%) with mammals (**Fig. 4.4**).

N-terminal domain

Rock beam MAQWDRQLPAAVYRQQLHELDYDRALPDRHYLSVHLEKQWRAAR--DHDVAVLFVLLFNLDIQHSRFVQVE-ESEFLQNHRRYKQNFQR--LDDRCALHTLWHEKKEKELQSDLEWQLRVPEPAM 136
 Salmon MAQWDRQLPAAVYRQQLHELDYDRALPDRHYLSVHLEKQWRAAR--DHDVAVLFVLLFNLDIQHSRFVQVE-ESEFLQNHRRYKQNFQR--LDDRCALHTLWHEKKEKELQSDLEWQLRVPEPAM 137
 Pufferfish MAQWDRQLPAAVYRQQLHELDYDRALPDRHYLSVHLEKQWRAAR--DHDVAVLFVLLFNLDIQHSRFVQVE-ESEFLQNHRRYKQNFQR--LDDRCALHTLWHEKKEKELQSDLEWQLRVPEPAM 136
 Goldfish MTQWERLQDVTYSQRADLYNGDEPPEVRYLAWHLEQDWERASR--DSSQAFVFLVLLFNLDIQHSRFVQVE-ESEFLQNHRRYKQNFQR--LDDRCALHTLWHEKKEKELQSDLEWQLRVPEPAM 137
 Zebrafish MTQWERLQDVTYSQRADLYNGDEPPEVRYLAWHLEQDWERASR--DSSQAFVFLVLLFNLDIQHSRFVQVE-ESEFLQNHRRYKQNFQR--LDDRCALHTLWHEKKEKELQSDLEWQLRVPEPAM 137
 Turbot MAQWDRQLPAAVYRQQLHELDYDRALPDRHYLSVHLEKQWRAAR--DHDVAVLFVLLFNLDIQHSRFVQVE-ESEFLQNHRRYKQNFQR--LDDRCALHTLWHEKKEKELQSDLEWQLRVPEPAM 136
 Frog MSQWAAITLKLSTEFQKVMALYSQELFPEVRYLAWHLEQDWERASR--DSSQAFVFLVLLFNLDIQHSRFVQVE-ESEFLQNHRRYKQNFQR--LDDRCALHTLWHEKKEKELQSDLEWQLRVPEPAM 137
 Rat MAQWDRQLPAAVYRQQLHELDYDRALPDRHYLSVHLEKQWRAAR--DHDVAVLFVLLFNLDIQHSRFVQVE-ESEFLQNHRRYKQNFQR--LDDRCALHTLWHEKKEKELQSDLEWQLRVPEPAM 138
 Pig MAQWDRQLPAAVYRQQLHELDYDRALPDRHYLSVHLEKQWRAAR--DHDVAVLFVLLFNLDIQHSRFVQVE-ESEFLQNHRRYKQNFQR--LDDRCALHTLWHEKKEKELQSDLEWQLRVPEPAM 139
 Cattle MAQWDRQLPAAVYRQQLHELDYDRALPDRHYLSVHLEKQWRAAR--DHDVAVLFVLLFNLDIQHSRFVQVE-ESEFLQNHRRYKQNFQR--LDDRCALHTLWHEKKEKELQSDLEWQLRVPEPAM 139
 Human MAQWDRQLPAAVYRQQLHELDYDRALPDRHYLSVHLEKQWRAAR--DHDVAVLFVLLFNLDIQHSRFVQVE-ESEFLQNHRRYKQNFQR--LDDRCALHTLWHEKKEKELQSDLEWQLRVPEPAM 139

Coiled coil domain

Rock beam TSSQDLERKMAGLRNEVQCHETDMLCLEEQDEFDFVYOTFRMEAVVD--EAVKQEMQHFQFLNRLNEGRKSTSDLSLDRKTELDLIVLVNKLVEVQRSSQKACIGAP-DVACDQ1EWFVTCVAVCLFVRE 273
 Salmon TDSQRMS--ADGRRRISQCHTSECLR-----HKMVLVHTDSYMRD--HHKRETEQMSAAGSTQDTRFRMSLQMSVLLT-LRDLCLVVRGELVQVQRQKACIGAP-DSTCDQLEKWFTEAECLFVRE 265
 Pufferfish TSSQDLERKMAGLRNEVQCHETDMLCLEEQDEFDFVYOTFRMEAVVD--EAVKQEMQHFQFLNRLNEGRKSTSDLSLDRKTELDLIVLVNKLVEVQRSSQKACIGAP-DVACDQ1EWFVTCVAVCLFVRE 273
 Goldfish MESQRMEKLLKDLKIVVEVHEHTRCLEEQDEFDFVYOTFRMEAVVD--EENKM-ORGLQKMLNLDKCRDFSDISTDADTCLSSVLEIDELVDRKROOKACIGAP-DTSLDQLEKWFVTO1EIMCFLOK 273
 Zebrafish LESHQIKERKDKFKTRIEVHEHTRCLEEQDEFDFVYOTFRMEAVVD--EENKM-ORGLQKMLNLDKCRDFSDISTDADTCLSSVLEIDELVDRKROOKACIGAP-DTSLDQLEKWFVTO1EIMCFLOK 273
 Turbot TSSQDLERKMAGLRNEVQCHETDMLCLEEQDEFDFVYOTFRMEAVVD--EAKNDQIKVLOGLVNRLEDECRKSTSDLNKLDKTELDLIVLVNKLVEVQRSSQKACIGAP-DVACDQ1EWFVTCVAVCLFVRE 273
 Frog GRO-QEIEKRVNLEAERVQSDCEKLFLELDQETDFKYKNNFEIMARSHPKDKLKKRDELOSLNLDKRRKVELDQIKGLLGLCELTVEFLQO-ELDEWLLKQLECGAP-TETSLKQLOWVTKTAEFCFLHRI 274
 Rat SYQLEIEHRLITAVAVLAVSISLQKQDQDFRYFRYVLANHRSISLDFHOSOROLVYVVELDARKEVLDLQKALGTLTITLLELLEKFWVQKQKACIGAP-PMGDFLEWVTPAKKALFHHLR 276
 Pig NQO-HFESRLHFRAMBELAVSISLQKQDQDFRYFRYVLANHRSISLDFHOSOROLVYVVELDARKEVLDLQKALGTLTITLLELLEKFWVQKQKACIGAP-PMGDFLEWVTPAKKALFHHLR 275
 Cattle NQO-HFESRLHFRAMBELAVSISLQKQDQDFRYFRYVLANHRSISLDFHOSOROLVYVVELDARKEVLDLQKALGTLTITLLELLEKFWVQKQKACIGAP-PMGDFLEWVTPAKKALFHHLR 275
 Human NQO-HFESRLHFRAMBELAVSISLQKQDQDFRYFRYVLANHRSISLDFHOSOROLVYVVELDARKEVLDLQKALGTLTITLLELLEKFWVQKQKACIGAP-PMGDFLEWVTPAKKALFHHLR 275

DNA binding domain

Rock beam LKGLDEELKGVSTENDEPKAKPQALQTRADITLNLKSSPVVETQPSMPO--GRGPLVLRITNDFSVKTRLVKIPFELNISMKNVSMIDREAPQIKGYRRFNVLGKTKALNMAESQJGKAVDPRHLLTAEKRS--GG 409
 Salmon LKGLDEELKGVSTENDEPKAKPQALQTRADITLNLKSSPVVETQPSMPO--GRGPLVLRITNDFSVKTRLVKIPFELNISMKNVSMIDREAPQIKGYRRFNVLGKTKALNMAESQJGKAVDPRHLLTAEKRS--GG 401
 Pufferfish LKGLDEELKGVSTENDEPKAKPQALQTRADITLNLKSSPVVETQPSMPO--GRGPLVLRITNDFSVKTRLVKIPFELNISMKNVSMIDREAPQIKGYRRFNVLGKTKALNMAESQJGKAVDPRHLLTAEKRS--GG 409
 Goldfish LKGLDEELKGVSTENDEPKAKPQALQTRADITLNLKSSPVVETQPSMPO--GRGPLVLRITNDFSVKTRLVKIPFELNISMKNVSMIDREAPQIKGYRRFNVLGKTKALNMAESQJGKAVDPRHLLTAEKRS--GG 409
 Zebrafish LKGLDEELKGVSTENDEPKAKPQALQTRADITLNLKSSPVVETQPSMPO--GRGPLVLRITNDFSVKTRLVKIPFELNISMKNVSMIDREAPQIKGYRRFNVLGKTKALNMAESQJGKAVDPRHLLTAEKRS--GG 406
 Turbot LKGLDEELKGVSTENDEPKAKPQALQTRADITLNLKSSPVVETQPSMPO--GRGPLVLRITNDFSVKTRLVKIPFELNISMKNVSMIDREAPQIKGYRRFNVLGKTKALNMAESQJGKAVDPRHLLTAEKRS--GG 409
 Frog FKNLAELEPSRISYDQPLKIDPPNQLORNLKSLLOSEFVDRQPIMAFPCKPLVKTSTOFVSRVRLNPKLKNLVKSFVCKDKNPNSIKGYRKNLGLTQKQAMELOGE--GLVDFKHLKAEKAGTKG 412
 Rat LKGLDEELKGVSTENDEPKAKPQALQTRADITLNLKSSPVVETQPSMPO--GRGPLVLRITNDFSVKTRLVKIPFELNISMKNVSMIDREAPQIKGYRRFNVLGKTKALNMAESQJGKAVDPRHLLTAEKRS--GG 412
 Pig LKGLDEELKGVSTENDEPKAKPQALQTRADITLNLKSSPVVETQPSMPO--GRGPLVLRITNDFSVKTRLVKIPFELNISMKNVSMIDREAPQIKGYRRFNVLGKTKALNMAESQJGKAVDPRHLLTAEKRS--GG 412
 Cattle LKGLDEELKGVSTENDEPKAKPQALQTRADITLNLKSSPVVETQPSMPO--GRGPLVLRITNDFSVKTRLVKIPFELNISMKNVSMIDREAPQIKGYRRFNVLGKTKALNMAESQJGKAVDPRHLLTAEKRS--GG 412
 Human LKGLDEELKGVSTENDEPKAKPQALQTRADITLNLKSSPVVETQPSMPO--GRGPLVLRITNDFSVKTRLVKIPFELNISMKNVSMIDREAPQIKGYRRFNVLGKTKALNMAESQJGKAVDPRHLLTAEKRS--GG 412

Linker domain

Rock beam GKGVSDISLVSVEELHIFHTVTEELKGVSVELQASSLPVVIISNSSQOQSAWASLWFNMLSHDTDMVFANSPTATWQFGEILSWOFLSATKRLNDAGLEMIHRLFRQNRNDKXVASKFSKENTPOT--- 546
 Salmon GKGVSDISLVSVEELHIFHTVTEELKGVSVELQASSLPVVIISNSSQOQSAWASLWFNMLSHDTDMVFANSPTATWQFGEILSWOFLSATKRLNDAGLEMIHRLFRQNRNDKXVASKFSKENTPOT--- 541
 Pufferfish GKGVSDISLVSVEELHIFHTVTEELKGVSVELQASSLPVVIISNSSQOQSAWASLWFNMLSHDTDMVFANSPTATWQFGEILSWOFLSATKRLNDAGLEMIHRLFRQNRNDKXVASKFSKENTPOT--- 545
 Goldfish GKGVSDISLVSVEELHIFHTVTEELKGVSVELQASSLPVVIISNSSQOQSAWASLWFNMLSHDTDMVFANSPTATWQFGEILSWOFLSATKRLNDAGLEMIHRLFRQNRNDKXVASKFSKENTPOT--- 549
 Zebrafish GKGVSDISLVSVEELHIFHTVTEELKGVSVELQASSLPVVIISNSSQOQSAWASLWFNMLSHDTDMVFANSPTATWQFGEILSWOFLSATKRLNDAGLEMIHRLFRQNRNDKXVASKFSKENTPOT--- 546
 Turbot GKGVSDISLVSVEELHIFHTVTEELKGVSVELQASSLPVVIISNSSQOQSAWASLWFNMLSHDTDMVFANSPTATWQFGEILSWOFLSATKRLNDAGLEMIHRLFRQNRNDKXVASKFSKENTPOT--- 546
 Frog GKGVSDISLVSVEELHIFHTVTEELKGVSVELQASSLPVVIISNSSQOQSAWASLWFNMLSHDTDMVFANSPTATWQFGEILSWOFLSATKRLNDAGLEMIHRLFRQNRNDKXVASKFSKENTPOT--- 551
 Rat AKGVNKGGLVTEELHIFHTVTEELKGVSVELQASSLPVVIISNMQLSIAWASLWFNMLSDQDFSSPKAPWNLGPAWQSSVAVGQUNSDQMLRKLFGQSSSTGLSWMDFHRESPPGQF 552
 Pig AKGVNKGGLVTEELHIFHTVTEELKGVSVELQASSLPVVIISNMQLSIAWASLWFNMLSDQDFSSPKAPWNLGPAWQSSVAVGQUNSDQMLRKLFGQSSSTGLSWMDFHRESPPGQF 552
 Cattle AKGVNKGGLVTEELHIFHTVTEELKGVSVELQASSLPVVIISNMQLSIAWASLWFNMLSDQDFSSPKAPWNLGPAWQSSVAVGQUNSDQMLRKLFGQSSSTGLSWMDFHRESPPGQF 552
 Human AKGVNKGGLVTEELHIFHTVTEELKGVSVELQASSLPVVIISNMQLSIAWASLWFNMLSDQDFSSPKAPWNLGPAWQSSVAVGQUNSDQMLRKLFGQSSSTGLSWMDFHRESPPGQF 552

SH2 domain

Rock beam FVWFDGILVAVVITEDLWRDHLKGFVNSGKERSLAKKQRTITLLRFSSEVIGG--ITSSVETSITDFDIPKIQPTKVDLSQTPHHEIRNYQLAEENIENPNLILYNTPRDEAFKQYYSERTOSDSDPYIK 685
 Salmon FVWFDGILVAVVITEDLWRDHLKGFVNSGKERSLAKKQRTITLLRFSSEVIGG--ITSSVETSITDFDIPKIQPTKVDLSQTPHHEIRNYQLAEENIENPNLILYNTPRDEAFKQYYSERTOSDSDPYIK 679
 Pufferfish FVWFDGILVAVVITEDLWRDHLKGFVNSGKERSLAKKQRTITLLRFSSEVIGG--ITSSVETSITDFDIPKIQPTKVDLSQTPHHEIRNYQLAEENIENPNLILYNTPRDEAFKQYYSERTOSDSDPYIK 684
 Goldfish LWVWLDGILVAVVITEDLWRDHLKGFVNSGKERSLAKKQRTITLLRFSSEVIGG--ITSSVETSITDFDIPKIQPTKVDLSQTPHHEIRNYQLAEENIENPNLILYNTPRDEAFKQYYSERTOSDSDPYIK 689
 Zebrafish LWVWLDGILVAVVITEDLWRDHLKGFVNSGKERSLAKKQRTITLLRFSSEVIGG--ITSSVETSITDFDIPKIQPTKVDLSQTPHHEIRNYQLAEENIENPNLILYNTPRDEAFKQYYSERTOSDSDPYIK 686
 Turbot FVWFDGILVAVVITEDLWRDHLKGFVNSGKERSLAKKQRTITLLRFSSEVIGG--ITSSVETSITDFDIPKIQPTKVDLSQTPHHEIRNYQLAEENIENPNLILYNTPRDEAFKQYYSERTOSDSDPYIK 685
 Frog FVWFDGILVAVVITEDLWRDHLKGFVNSGKERSLAKKQRTITLLRFSSEVIGG--ITSSVETSITDFDIPKIQPTKVDLSQTPHHEIRNYQLAEENIENPNLILYNTPRDEAFKQYYSERTOSDSDPYIK 690
 Rat FVWFDGILVAVVITEDLWRDHLKGFVNSGKERSLAKKQRTITLLRFSSEVIGG--ITSSVETSITDFDIPKIQPTKVDLSQTPHHEIRNYQLAEENIENPNLILYNTPRDEAFKQYYSERTOSDSDPYIK 690
 Pig FVWFDGILVAVVITEDLWRDHLKGFVNSGKERSLAKKQRTITLLRFSSEVIGG--ITSSVETSITDFDIPKIQPTKVDLSQTPHHEIRNYQLAEENIENPNLILYNTPRDEAFKQYYSERTOSDSDPYIK 690
 Cattle FVWFDGILVAVVITEDLWRDHLKGFVNSGKERSLAKKQRTITLLRFSSEVIGG--ITSSVETSITDFDIPKIQPTKVDLSQTPHHEIRNYQLAEENIENPNLILYNTPRDEAFKQYYSERTOSDSDPYIK 690
 Human FVWFDGILVAVVITEDLWRDHLKGFVNSGKERSLAKKQRTITLLRFSSEVIGG--ITSSVETSITDFDIPKIQPTKVDLSQTPHHEIRNYQLAEENIENPNLILYNTPRDEAFKQYYSERTOSDSDPYIK 690

TAD domain

Rock beam IKTKLAVFVSKENTLEARPPMPDQAQ-----GEGLEPIN---GLS---GEAAEQNG-----NPHPLNSPLETHSDPMLSGSVAAPEDQLL---YLNPNVYADS-----DILQDEQFLPDFSLNF 788
 Salmon IKTKLAVFVSKENTLEARPPMPDQAQ-----GEGLEPIN---GLS---GEAAEQNG-----NPHPLNSPLETHSDPMLSGSVAAPEDQLL---YLNPNVYADS-----DILQDEQFLPDFSLNF 786
 Pufferfish IKTKLAVFVSKENTLEARPPMPDQAQ-----GEGLEPIN---GLS---GEAAEQNG-----NPHPLNSPLETHSDPMLSGSVAAPEDQLL---YLNPNVYADS-----DILQDEQFLPDFSLNF 783
 Goldfish IKTKLAVFVSKENTLEARPPMPDQAQ-----GEGLEPIN---GLS---GEAAEQNG-----NPHPLNSPLETHSDPMLSGSVAAPEDQLL---YLNPNVYADS-----DILQDEQFLPDFSLNF 817
 Zebrafish IKTKLAVFVSKENTLEARPPMPDQAQ-----GEGLEPIN---GLS---GEAAEQNG-----NPHPLNSPLETHSDPMLSGSVAAPEDQLL---YLNPNVYADS-----DILQDEQFLPDFSLNF 797
 Turbot IKTKLAVFVSKENTLEARPPMPDQAQ-----GEGLEPIN---GLS---GEAAEQNG-----NPHPLNSPLETHSDPMLSGSVAAPEDQLL---YLNPNVYADS-----DILQDEQFLPDFSLNF 785
 Frog LQKRLIVSTRQVDELESN-----FSPRTSENNDMEW-----NYTDDGLAGIAMNI 739
 Rat LKHLRIVSNRQDELQDFELKLEPPESELEDAELMSVGEARDHLSQSNVQGLD-----VAKPKPDLSPAPKILLHEDPAR-----ALVQHPPEPDLQDQ-----QNTNHEHFRNSMIR 803
 Pig LKHLRIVSNRQDELQDFELKLEPPESELEDAELMSVGEARDHLSQSNVQGLD-----VAKPKPDLSPAPKILLHEDPAR-----ALVQHPPEPDLQDQ-----QNTNHEHFRNSMIR 824
 Cattle LKHLRIVSNRQDELQDFELKLEPPESELEDAELMSVGEARDHLSQSNVQGLD-----VAKPKPDLSPAPKILLHEDPAR-----ALVQHPPEPDLQDQ-----QNTNHEHFRNSMIR 818
 Human LKHLRIVSNRQDELQDFELKLEPPESELEDAELMSVGEARDHLSQSNVQGLD-----VAKPKPDLSPAPKILLHEDPAR-----ALVQHPPEPDLQDQ-----QNTNHEHFRNSMIR 812

	%	%
Rock beam	804	100.0 100.0
Salmon	802	63.1 78.2
Pufferfish	798	72.6 84.7
Goldfish	849	56.6 71.8
Zebrafish	835	54.5 72.8
Turbot	793	81.9 89.1
Frog	765	42.6 60.9
Rat	842	39.0 57.2
Pig	864	39.4 57.2
Cattle	857	40.1 57.3
Human	851	41.1 59.6



Fig. 4.4. Multiple amino acid sequence alignment of RbSTAT2 with other counterparts from various taxonomical origins. Completely conserved aa residues among all the species analyzed are marked with asterisks at the bottom of the alignment. Completely conserved residues among fish species and mammals are shaded with gray and black color, respectively. The regions characteristic for domains are shown by different colored lines on top of the alignment. Amino acid residues important for phosphotyrosine binding pocket and hydrophobic binding pocket are shaded with blue and green color, respectively. Tyrosine residue (Tyr⁶⁸⁵) that phosphorylates during activation was shaded by red color. Percent of identity (I%) and similarity (S%) of RbSTAT2 with other orthologs are shown at the end of each sequence.

Genomic structure organization of *RbSTAT2* also compared with the available counterparts and revealed that number of exons in CDS region of all species were conserved with 23 exons. Seven numbers of exons in CDS (1st, 3rd, 8th, 10th, 14th, 15th and 16th) were identical in size. Meanwhile, sixteen numbers of exons among fish species were completely identical, while showing same number identical exons in mammals (**Fig. 4.5**).

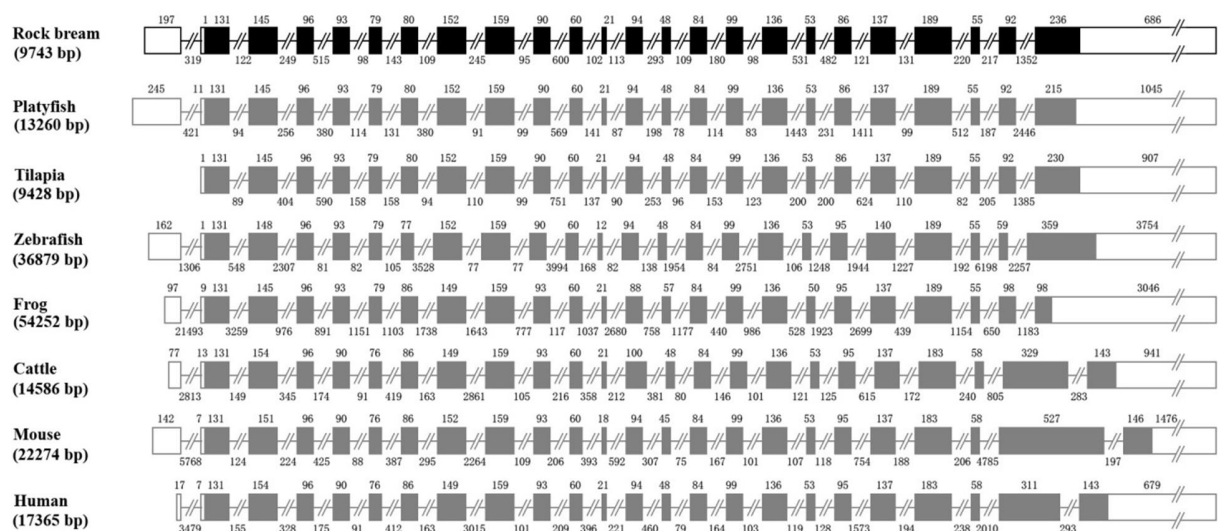


Fig. 4.5. Comparison of genomic structure organization of RbSTAT2 with other vertebrate orthologs. CDS and UTRs are indicated by filled and empty boxes, respectively. Size annotations for the exons and introns are indicated on top of the exons and below the intron lines, respectively. Accession numbers for genomic structures obtained from Ensembl genomic database are as follows; platyfish: ENSXMAT00000002070, tilapia: ENSONIT000000024057, zebrafish: ENSDART00000148661, frog: ENSXETT00000047227, cattle: ENSBTAT00000005749, mouse: ENSMUST00000085708 and human: ENST00000314128.

A phylogenetic tree was constructed based on the NJ method in order to determine the evolutionary path of *STAT2* genes. *STAT2* ortholog from fresh water snail (*Biomphalaria glabrata*) was used as an out group for this analysis. According to the results, it was clearly demonstrated that fish and other vertebrates were distinctly evolved (**Fig. 4.6**). As expected, rock bream and turbot was closely clustered in fish clade, while showing separate cluster for amphibians and mammals. The result observed in phylogeny of present study was consistent with the previous reports (Collet et al., 2009; Wang et al., 2013; Sobhkhez et al., 2014). The comprehensive bioinformatics analysis indicated that the RbSTAT2 indeed a *STAT2* ortholog and it showed higher homologous features as other fish orthologs. Further, genomic structure organization and phylogenetic study affirmed their separate evolutionary path for fish and other vertebrates.

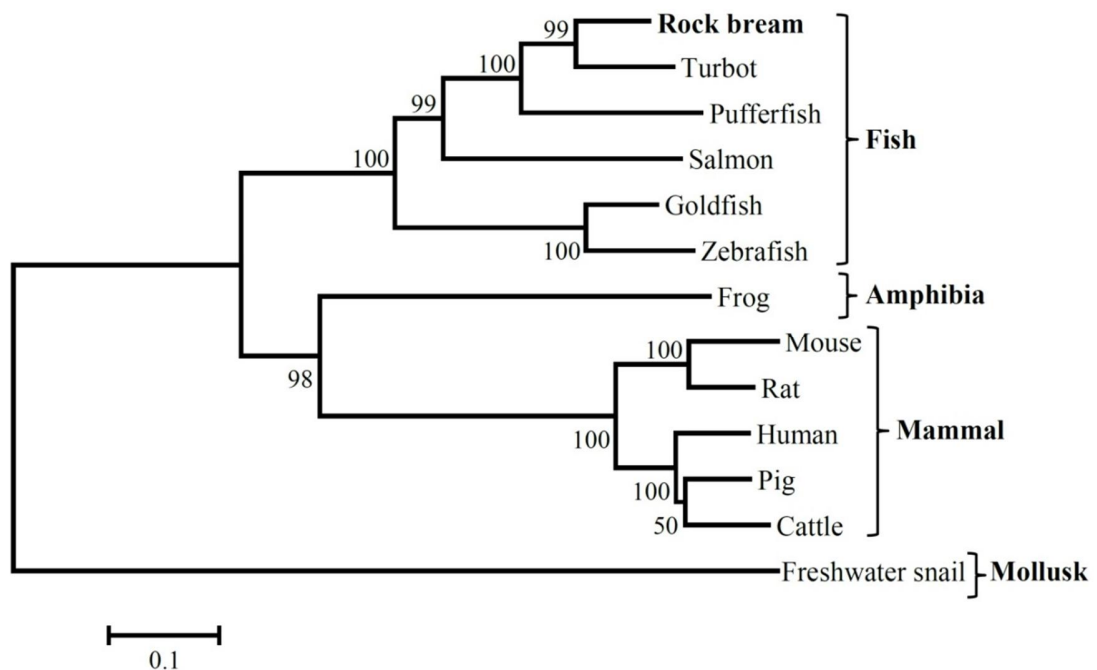


Fig. 4.6. Rooted molecular phylogenetic tree of *STAT2* genes. Phylogenetic tree was constructed using MEGA6 software based on Neighbor-joining algorithm. Bootstrapping was performed 5000 times to confirm the topological stability of the tree and percentage of bootstrap values are indicated at the nodes of the tree. The accession numbers of each orthologs obtained from GenBank at NCBI are as follows; turbot: ACX69848, pufferfish: AFQ98274, salmon: NP_001138896, goldfish: AFL69829, zebrafish: NP_001258730, frog: AAI67467, mouse: NP_064347, rat: NP_001011905, human: AAA98760, pig: ADU03225, cattle: NP_001192618 and fresh water snail: ACZ25562.

4.2.4. Spatial expression of *RbSTAT2* mRNA

Tissue-wise expression of *RbSTAT2* transcripts might be helpful to understand the association of various functional aspects under normal physiological conditions. In the present study, a robust expression of *RbSTAT2* mRNA was observed in blood cells and it was 1916-fold highest compare to the lowest expressed muscle tissue which was set as a 1. Muscle and skin tissue displayed lower expression of *RbSTAT2*, while showing moderate expression in other tissues (Fig. 4.7). Previous study in turbot reported that the expression of *STAT2* mRNA was highly detected in liver and spleen tissues (Wang et al., 2013), while in salmon demonstrated highly in heart, gill, intestine, head kidney, muscle and liver (Sobhkhez et al., 2014). By taking these evidences, we can suggest that *RbSTAT2* might be associated with the wide range of biological functions in different tissues. However, the studies on teleostean *STAT2* have been limitedly reported and proper functional aspects are under investigation.

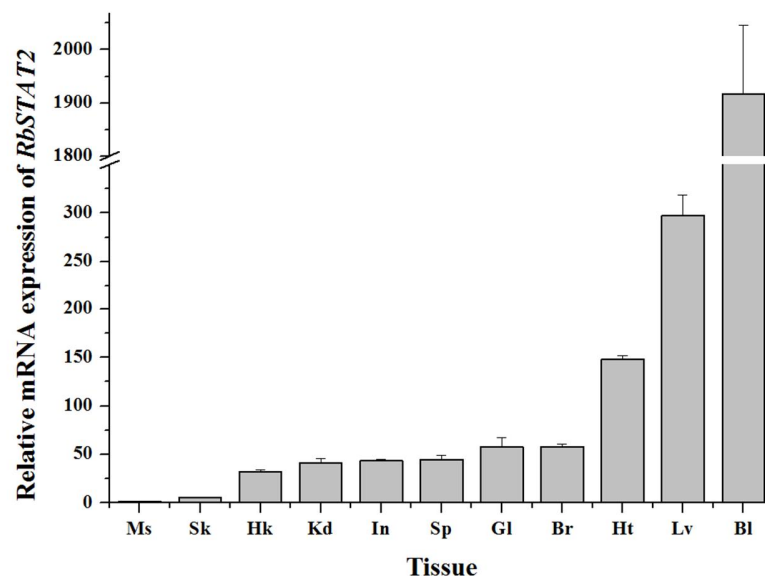


Fig. 4.7. Tissue distribution profiling of *RbSTAT2* in rock bream. Tissue specific expression was analyzed in different tissues including muscle (Ms), skin (Sk), head kidney (Hk), kidney (Kd), intestine (In), spleen (Sp), gill (Gl), brain (Br), heart (Ht), liver (Lv) and blood cells (Bl) by SYBR Green qPCR. Rock bream β -actin was used as an internal reference gene and relative mRNA expression was calculated by Livak method. The results are represented as mean \pm standard deviation (SD) of triplicates.

4.2.5. Temporal expression of *RbSTAT2* mRNA upon pathogenic and PAMP challenges, and antiviral effect

To examine the potential role of *RbSTAT2* upon microbial invasion, the expression profile was assessed upon viral, bacterial and PAMPs stimulation. Results revealed that the expression of *RbSTAT2* mRNA was significantly ($P < 0.05$) altered by those stimuli with irregular manner (Fig. 4.8). After RBIV challenge, the expression of *RbSTAT2* was significantly suppressed in blood cells at 3 h, 24 h and 48 h post injection (p.i), whilst detecting a significantly induced expression in liver tissue at 48 h p.i. In the case of poly I:C (a double stranded RNA viral mimic) challenge, significantly triggered expression was detected at 12 – 24 h p.i in blood cells, while showing down-regulated expression at 3 h and 48 h p.i. Whereas, the expression of *RbSTAT2* was up-regulated throughout the experiment upon poly I:C injection. Previous report in turbot demonstrated that the up-regulated expression of *STAT2* mRNA in different tissues at several time points after lymphocystis disease virus (LCDV) infection (Wang et al., 2013). Meanwhile, Collet B. and co-workers detected the significant elevations of *STAT2* mRNA upon stimulation with Infectious Pancreatic Necrosis Virus (IPNV), Salmon Alphavirus (SAV) and/or Infectious Salmon Anemia virus (IPNV) (Collet et al., 2009). In mammals, vast numbers of studies have been conducted to explore the essential role of *STAT2* in response to viral attack (Gotoh et al., 2003; Chen et al., 2009; Perry et al., 2011; Kadeppagari et al., 2012; Hambleton et al., 2013). Lu J. and coworkers described that enterovirus 71 (EV71) which was highly threatened particularly for children, could block the interferon mediated phosphorylation of *STAT1*, *STAT2* and *TYK2* (Lu et al., 2012). Another study in respiratory syncytial virus (RSV), reported the ability of degradation of *STAT2* by nonstructural protein NS1 from RSV (Elliott et al., 2007). As those studies, the down-regulated expressions might be caused by some of the protein secreted from virus or any other mechanism. However, these results implied that the expressional responses of *RbSTAT2* might be depends on the types of viruses (DNA or RNA).

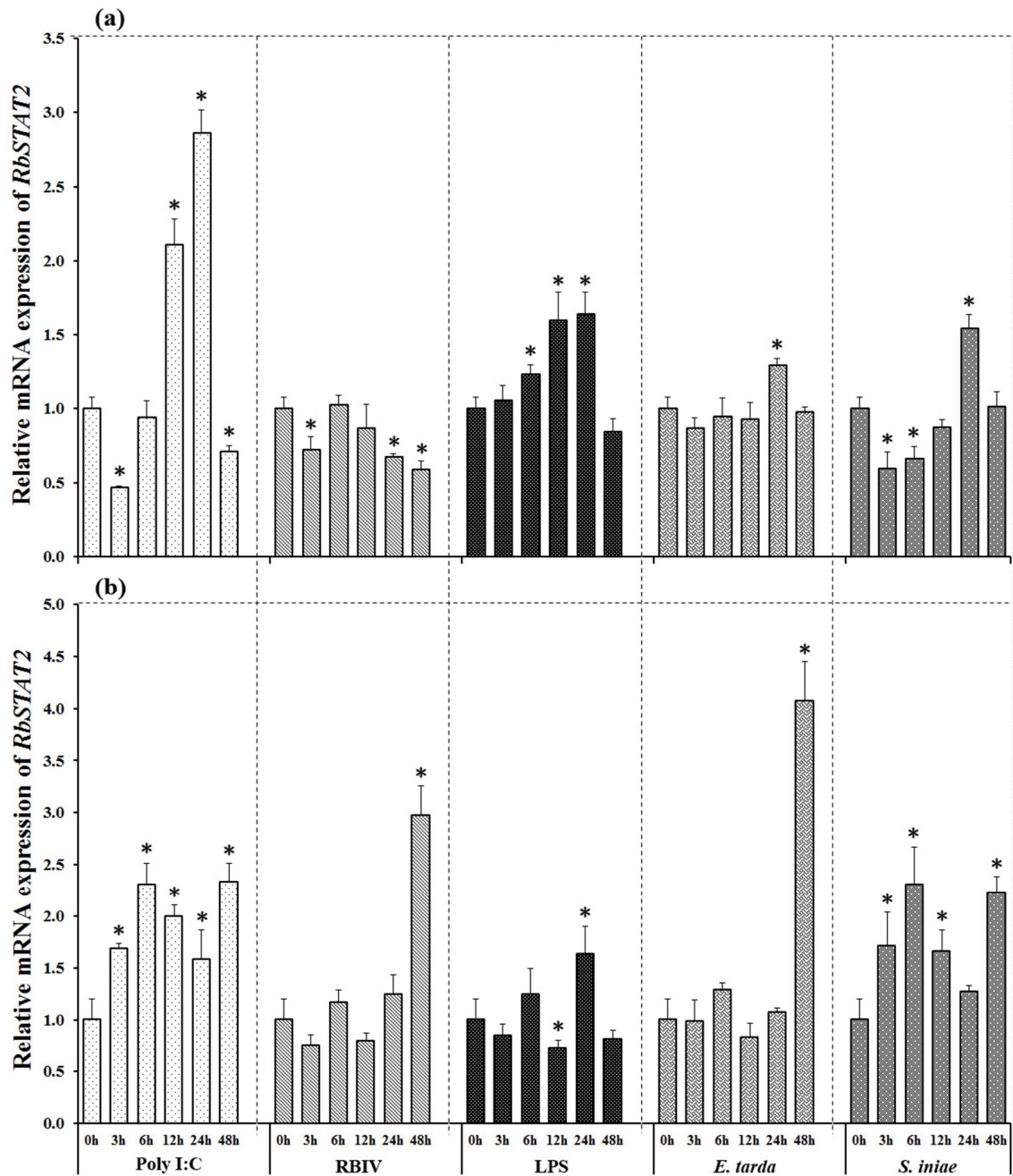


Fig. 4.8. Temporal mRNA expression profiling of RbSTAT2 in blood (a) and liver tissue (b) after pathogens and PAMPs challenges. The mRNA expression was calculated by Livak method with β -actin as an internal reference gene. The data was represented as relative mRNA expression which was normalized to the expression in PBS-injected control at each time points. The results are represented as mean \pm SD of triplicates and asterisks are indicated for statistically different data at $P < 0.05$.

As an additional experiment, antiviral effect was assessed by analyzing the cell viability by WST-1 reagent after adding RBIV. As shown in **Fig. 4.9**, cells containing RbSTAT2 has more viability compare to the mock control (pcDNA3.1 empty vector transfected) as well as to cell control (only cells) implying its potential antiviral effect. These evidences strongly indicate the potential mediation of STAT2 on antiviral responses. However, the real mechanism behind antiviral activity of RbSTAT2 is required to be explored.

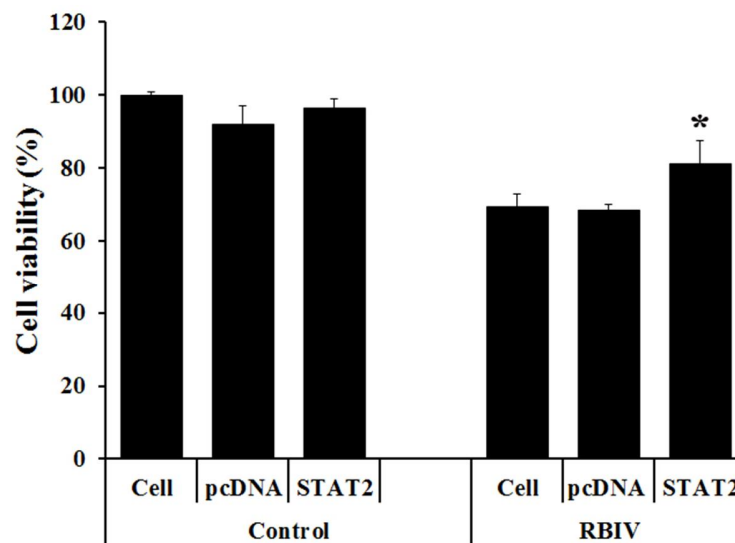


Fig. 4.9. Effect of RbSTAT2 for cell viability after RBIV infection. Cell viability was assessed by WST-1 assay. Triplicate wells containing cells only (cell), pcDNA3.1(+) transfected cells (pcDNA) or RbSTAT2/pcDNA3.1(+) transfected cells were grown 48 h at 25 °C. One set of cells were treated with RBIV and evaluated the cell viability after 3 days by measuring absorbance at 450 nm. Percentage of viable cells was calculated with comparison of normal cells those not treated with RBIV. Data was represented as mean \pm SD of triplicates and significant difference ($P < 0.05$) was analyzed by comparing with respective cell control.

Upon bacterial challenge, Gram-negative *E. tarda* was caused to induce the expression of *RbSTAT2* transcripts at late phase in both blood cells (24 h p.i) and liver tissue (48 h p.i). Gram-positive *S. iniae* initially (3 - 6 h p.i) suppressed the expression of *RbSTAT2* mRNA in blood cells, while showing significantly induced expression at 24 h p.i. Meanwhile, significantly up-regulated expression was observed at 6 – 12 h and 48 h p.i of *S. iniae*. In addition, significant up-regulations were detected at 6 – 24 h p.i of LPS in blood cells. However, the expression of *RbSTAT2* in liver tissue was down-regulated at 12 h, while detecting an up-regulation at 24 p.i of

LPS (**Fig. 4.8**). Studies describing expression analysis of *STAT2* in response to the bacterial and bacterial related PAMPs were rarely reported. A single study reported the significant effect of *Vibrio anguillarum* on transcription of teleostean *STAT2* (Wang et al., 2013). Other STAT members also demonstrated the transcriptional changes upon bacterial infections. For an instance; turbot *STAT3* transcription was significantly induced at early phase by *V. anguillarum* (Wang et al., 2011c). In contrast, several studies have been described about the great impact of bacterial and viral infection on type I interferon transcription (Perry et al., 2005; Monroe et al., 2010; Eshleman and Lenz, 2014). These observations implied that the responses driven by *STAT2* against bacterial and viral attack might be mediated via activation of interferons. However, the JAK/STAT signal cascade and its association with interferons in teleost are still not completely understood as mammals. Further studies are recommended to execute, in order to understand the complete JAK/STAT signaling pathway and its connections with cytokines.

4.2.6. Temporal expression of *RbSTAT2* mRNA against tissue injury

External or internal tissue damage is a common process in living organism and it can be caused by various factors. However, the repairing of damaged tissues is an essential part of the biological system. Number of studies has been conducted to understand the real healing mechanisms, and revealed that involvement of the STAT members in the JAK/STAT signaling pathway, particularly in mammals. Some of the STAT proteins play a major role in response to the brain injury, lung injury, liver injury and ischaemia/reperfusion injury (Takagi et al., 2002; Gao et al., 2004; Stephanou, 2004; Wang et al., 2011a). However, the involvement of *STAT2* against injury has not yet been studied even in mammals. In the present study, we have analyzed the transcription profile of *RbSTAT2* upon tissue injury. Results revealed a controversial expression profile for blood and liver tissue. The expression of *RbSTAT2* mRNA in blood tissue was down-regulated, while showing up-regulated expressions in liver tissue (**Fig. 4.10**). Rapid translation of *RbSTAT2* mRNA into protein might be the reason for down-regulation in blood cells. However, the results of this study inferred a potential role of *RbSTAT2* in wound healing process.

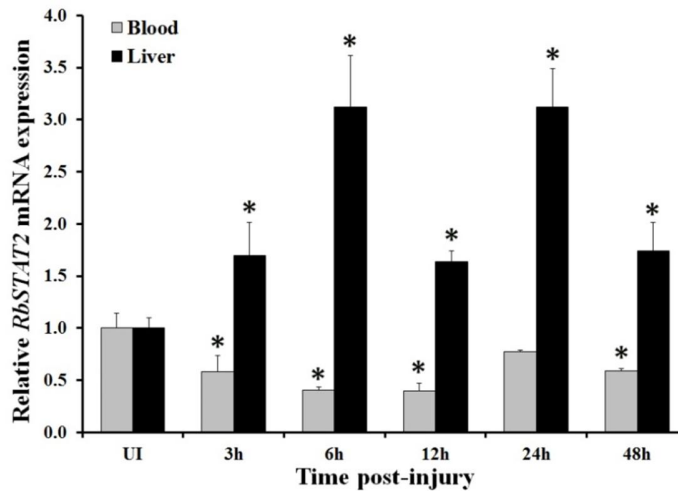


Fig. 4.10. Temporal mRNA expression profiling of RbSTAT2 in blood cells and liver tissue after tissue injury. The relative mRNA expression was calculated using rock bream β -actin as internal reference gene. The data was represented as mean \pm SD of triplicates, and results were statistically compared relative to the un-injured control (UI). Data with statistically difference at $P < 0.05$ are indicated by asterisks.

4.2.7. Temporal expression of *RbSTAT2* in response to the rRbIL-10

To assess the effect of IL-10 on *RbSTAT2* transcription, rRbIL-10 was introduced to the rock bream heart cells and analyzed the expression level. Results revealed the significant elevation of *RbSTAT2* transcription at 24 h post treatment, while detecting a suppressed expression at 12 h (Fig. 4.11). These results proposed that RbIL-10 might work as a significant cofactor for the expression of *RbSTAT2*, even though studies related to the interleukins and their associations with STAT2 are scarce.

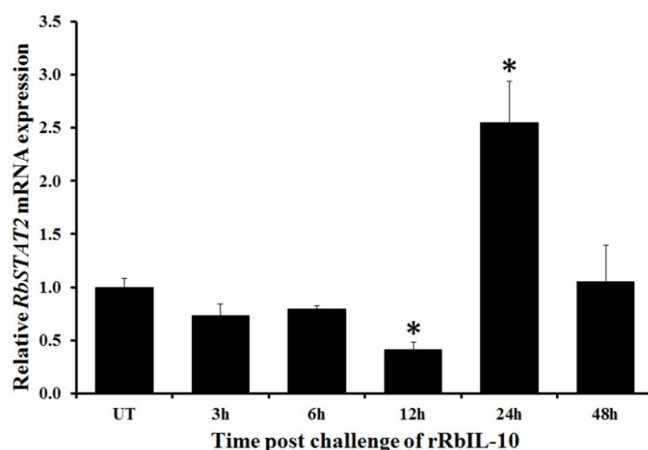


Fig. 4.11. Temporal expression profiling of RbSTAT2 in heart cells after in vitro challenge with rRbIL-10. The relative mRNA expression was calculated using rock bream β -actin as internal reference gene. The data was represented as relative mRNA expression which was normalized to the expression in MBP-treated control at each time points. The results are represented as mean \pm SD of triplicates and asterisks are indicated for statistically different data at $P < 0.05$.

4.2.8. Subcellular localization

Cellular localization of RbSTAT2 and nuclear translocation after poly I:C stimuli was examined in rock bream heart cells. For this purpose, RbSTAT2 was cloned into pEGFP-N1 vector and transfected to the rock bream cells seeded on 24-well plates as described in section 2.8. After 48 h of stimulation with poly I:C, cellular localization was observed via fluorescence microscope. Results revealed that RbSTAT2 protein was uniformly expressed in cytoplasm as a characteristic feature. Upon poly I:C stimulation, protein was not precisely translocated to the nucleus but it was localized near to the nucleus (**Fig. 4.12**). Previous study in turbot confirmed the nuclear translocation of STAT2 upon stimulation with poly I:C (Wang et al., 2013). Results of the present study may give an indication of signal transduction of RbSTAT2 from cell membrane to the nucleus. Nonetheless, further investigations are needed to be accomplished in order to understand the real signal transduction machinery of RbSTAT2 with the effect of various signals.

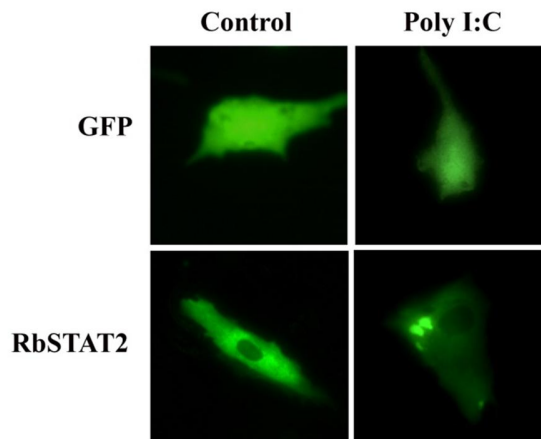


Fig. 4.12. Subcellular localization of RbSTAT2 in rock bream heart cells. Cells in the first row indicate the localization of GFP protein, where pEGFP-N1 empty vector was transfected. Cells in the second row indicate the localization of RbSTAT1 protein, where pEGFP-N1/RbSTAT1 vector was transfected.

4.3. Conclusion

Rock bream is one of the major edible fish species particularly for sashimi cultured in East Asian countries. Understanding of immune systems and their associated elements in rock bream is crucial not only for academic purposes but also for aquaculture industries. In this study, one of the important STAT paralog which was homologous to the STAT2 was identified from rock bream, and characterized structurally and functionally. *In silico* characterization, confirmed that RbSTAT2 indeed a homolog of STAT2 with high conservation among vertebrates sharing common structural features. Genomic structure comparison and phylogenetic study highlighted the distinguishable evolutionary path for fish and other vertebrates. Transcriptional analysis of *RbSTAT2* affirmed its potential role against bacterial and viral invasion, and tissue injury. Further studies conducted in rock bream heart cells with RBIV revealed its antiviral ability. In addition, transcriptional modulation was observed for the first time in fish species upon RbIL-10 stimulation. Subcellular localization and nuclear translocation of RbSTAT2 in response to the poly I:C will provide a possible sign for signal transduction.

CHAPTER 5

A homolog of teleostean signal transducer and activator of transcription 3 (STAT3) from rock bream, *Oplegnathus fasciatus*: structural insights, transcriptional modulation and subcellular localization

Abstract

Signal transducer and activator of transcription 3 (STAT3) is one of the crucial transcription factors in janus kinase (JAK)/STAT signaling pathway and it was previously considered as an acute phase response factor. Number of interleukins (ILs) such as IL-5, IL-6, IL-9, IL-10, IL-12 and IL-22 are known to be involved in activating of STAT3. In addition, various growth factors, pathogenic or oxidative stresses mediate the activation of wide range of functions via STAT3. In this study, a STAT3 homolog was identified and functionally characterized from rock bream (RbSTAT3), *Oplegnathus fasciatus*. *In silico* characterization revealed that the RbSTAT3 amino acid sequence shared highly conserved common domain architectural features including N-terminal domain, coiled coil domain, DNA binding domain, linker domain and Src homology 2 (SH2) domains. In addition, fairly conserved transcriptional activation domain (TAD) was located at the C-terminus. Comparison of RbSTAT3 with other counterparts revealed higher identities (> 90%) with fish orthologs. Genomic sequence of *RbSTAT3* was obtained from a bacterial artificial chromosome (BAC) library and it was identified as a multi-exonic gene (24 exons) as found in other vertebrates. Genomic structural comparison and phylogenetic studies evidently showed that the evolutionary route of teleostean and non-teleostean vertebrates were distinct. Quantitative real time PCR (qPCR) analysis revealed that the spatial distribution of *RbSTAT3* mRNA expression was ubiquitous and highly detected in blood, heart and liver tissues. Transcriptional modulation of *RbSTAT3* was examined in blood and liver tissues upon challenges with bacteria (*Edwardsiella tarda* and *Streptococcus iniae*), rock bream irido virus (RBIV) and immune stimulants (LPS and poly I:C). Significant changes in *RbSTAT3* transcription were also noticed, in response to the tissue injury. In addition, the transcriptional up-regulation of *RbSTAT3* was detected in rock bream heart cells upon recombinant rock bream IL-10 (rRbIL-10) treatment. Subcellular localization and nuclear translocation of rock bream STAT3 following poly I:C treatment were also demonstrated. Taken together, the results of the current study provide important evidences for potential roles for rock bream STAT3 in immune system and wound healing process.

5.1. Introduction

Signal transducer and activator of transcription (STAT) proteins play a vital role in biological system by activating the expression of specific genes or set of genes in response to a wide variety of internal and external stimuli. Signals from cytokines, growth factors or hormones are transduced following the dimerization of phosphorylated STATs and subsequent translocation into the nucleus, where they bind DNA response elements of target genes (Ihle, 1996). Seven STATs including STAT1, STAT2, STAT3, STAT4, STAT5a, STAT5b and STAT6 have been identified and well characterized in mammals (Stark and Darnell, 2012). All these STATs share common structural features with six conserved domains with different functions: N-terminal domain regulates the nuclear translocation (Strehlow and Schindler, 1998), coiled coil domain interacts with various proteins, DNA binding domain interacts with DNA, Src homology 2 (SH2) domain plays a vital role in signal transduction via phosphotyrosins, linker domain connects both DNA binding domain and SH2 domain, and transcriptional activation domain located at the C-terminal and regulates the transcriptional responses (Kisseleva et al., 2002).

STAT3 was identified in 1994 by two different groups independently. Initially, it was considered as an acute phase response factor activated by interleukin-6 (IL-6) (Akira et al., 1994) or a member of STAT family activated by epidermal growth factor and IL-6 (Zhong et al., 1994c). In addition, janus kinase 2 (JAK2), one of the member of JAK family, was identified as a major mediator of STAT3 phosphorylation (Aggarwal et al., 2006). Later studies have shown that, the signal transduction of mammalian STAT3 was initiated by a number of growth factors and cytokines such as growth hormone (Gronowski et al., 1995), IL-5 (Stout et al., 2004), IL-9 (Demoulin et al., 1996), IL-10 (Wehinger et al., 1996), IL-12 (Jacobson et al., 1995), IL-22 (Radaeva et al., 2004) and leptin (Vaisse et al., 1996). Apart from that, other factors including oxidative stress (Carballo et al., 1999), ultraviolet B (Ahsan et al., 2005), osmotic shock (Gatsios et al., 1998), and virus (Yoshida et al., 2002) activate the STAT3. The STAT3 is known to be the essential transcription factor that mediates pleiotropic activities including immune responses, cell proliferation, inflammation, embryo development, brain development, initiation of gene expression, and apoptosis (Takeda et al., 1997; Takeda et al., 1998; Alonzi et al., 2001; Levy and Lee, 2002; Yang et al., 2007b; Di Domenico et al., 2010). So far, very little information has been reported on fish STAT3, even though few fish species described the involvement of

immunobiological activities. *Siniperca chuatsi* (Guo et al., 2009), *Scophthalmus maximus* (Wang et al., 2011c) and *Epinephelus* spp (Huang et al., 2014) have demonstrated the possible role of STAT3 against viral/bacterial infections. Previous study in *Danio rerio* reported the involvement of STAT3 in regulation of cell migration during gastrulation (Yamashita et al., 2002). A recent study has shown the association of STAT3 with different forms of programmed cell death (Huang et al., 2015).

Rock bream (*Oplegnathus fasciatus*) is an economically important fish species in South Korean aquaculture. During the last decades, a great loss of fish production in aquaculture industry occurred due to the threat of viral and bacterial diseases (Park, 2009). Rock bream iridovirus (RBIV) causes the most eminent viral disease leading to the high mortality of rock bream in South Korea (Jung and Oh, 2000; Li et al., 2011). Edwardsiellosis and streptococcosis caused by *Edwardsiella tarda* and *Streptococcus iniae*, respectively are the devastating bacterial diseases identified in aquaculture industries (Sun et al., 2011; Park et al., 2012). Therefore, understanding of immune defensive mechanisms behind these microbial infections and other virulent factors is crucial in order to establish a sustainable rock bream industry.

In the current study, an ortholog of STAT3 identified from rock bream (RbSTAT3) was characterized at the cDNA and genomic DNA level. The spatial mRNA expression profile in different tissues and temporal mRNA expressions upon *in vivo* and *in vitro* challenges were also assessed. In addition, the mediation of RbSTAT3 on wound healing process was investigated by analyzing transcriptional profile following the tissue injury. Finally, the subcellular localization of RbSTAT3 under normal physiological condition and immune stress condition was examined.

Table 5.1. Description of primers used in this study

Primer name	Application	Sequence (5' -3')
RbSTAT3/BAC-F	BAC screening	ACCAGTTACAGCAGTTGGAGACCA
RbSTAT3/BAC-R	BAC screening	GTGTGACTCCTTATTGGCAGCGTA
RbIL-10/pMAL-F	Clone into pMAL-c5x	(GA) ₃ gaattcAGTCCCATGTGCAACAACCACTG – EcoRI
RbIL-10/pMAL-R	Clone into pMAL-c5x	(GA) ₃ aaagcttTCAATTAGAGGCCACTTGTTTTCGGAC - HindIII
RbSTAT3/qPCR-F	qPCR amplification	GACATCAGTGGAAAGACCCAGATCCA
RbSTAT3/qPCR-R	qPCR amplification	CGTAGAGTCTCCTCCCATCTCAGATTCA
RbSTAT3/GFP-F	Clone into pEGFP-N1	(GA) ₃ gaattcATGGCCCAGTGGAAACCAGTTAC - EcoRI
RbSTAT3/GFP-R	Clone into pEGFP-N1	(GA) ₃ ccgctgCATAGGTGATGCTACATCCATGTCCAAAGT - SacII
Rbβ-actin-F	qPCR internal control	TCATCACCATCGGCAATGAGAGGT
Rbβ-actin-R	qPCR internal control	TGATGCTGTTGTAGGTGGTCTCGT

Restriction sites in the cloning primers are shown with small case letters and indicated at the end of each primer sequence.

5.2. Results

5.2.1 *In silico* analysis of RbSTAT3

5.2.1.1. cDNA sequence characterization

A STAT3 homolog was identified from rock bream transcriptome data base following the NCBI BLAST analysis, and deposited in the GenBank. The full length *RbSTAT3* nucleotide sequence was 3652 bp in length and comprised an ORF of 2292 bp encoding a polypeptide of 764 aa with an estimated molecular mass of 87.4 kDa. The 5'-untranslated region (UTR) was 228 bp in length and the 1132 bp of 3'-UTR comprised a polyadenylation signal (³⁶³⁶AATAAA³⁶⁴¹) (Fig.5.1).

GAAAAGGCTGTACGTGCATTGGAGAGGTGTTCCCGTGCTGGCAAGAAAAGATATAGAGTTACGATCTTTTCTGTGTGTTCTCCCTCG 90
TTTTGTGGGTTGAATTTTTACAAAAGTCGTCACCTGACTGTACTGTCACTGTTTTTCTCGTAGAAAAGGTTTTTGTCTTCCAGGAGAAAC 180
TTTCCAAAAGAGTGACAACGAGCTAGGTTTGTGGAGGTGTGTGTACGATGGCCAGTGGCCAGTGAACAGGTACAGCAGTTGGAGACCAGGTAT 270
M A Q W N Q L Q Q L E T R Y
CTGGAGCACTCTACCCTTGTACAGTGCAGCTTCCCATGGAACACTACGCCAGTTCTTCCCGGTGGATTGAGAGTCCAGGATGGGCT 14
L E Q L Y H L Y S D S F P M E L R Q F L A P W I E S Q D W A 44
TACGCTGCCAATAAGGAGTCACACGCCACACTGGTGTCCACAACCTCTGGGAGAAATAGACCAGCAGTATAGCCGTTTTCTGCAGGAG 450
Y A A N K E S H A T L V F H N L L G E I D Q Q Y S R F L Q E 74
AACAATGTACTCTACCAGCACAACCTGCGCAGGATTAACAGCATCTGCAGAGCAAGTACTTGGAGAAGCCGATGGATATTGCCCGCATC 540
N N V L Y Q H N L R R I K Q H L Q S K Y L E K P M D I A R I 104
GTTGCCCGTGTCTGTGGGAGGAGCAAGACTGCTGCAGACTGCCACCTGCTGCACAGGATGGCCAGGCAGCACATCCACTGGGACA 630
V A R C L W E E Q R L L Q T A T S A A Q D G Q A A H P T G T 134
GTAGTGACAGAGAACAACAGATCCTGGAGCACAACTTCAAGACATCAGGAAGCGGGTGCAGGATATGGAACAGAAAGTAAAGTGCCT 720
V V T E K Q Q I L E H N L Q D I R K R V Q D M E Q K M K M L 164
GAGAAGTTGCAGGATGACTTACTTCAATTACAAGACTTTGAAAAGCCAAGGAGAGTTGCCAGGACCTAAATGGGAATAGCCAAACA 810
E N L Q D D D F D F N Y K T L K S Q G E L S Q D L N G N S Q A 194
GCTGTACCAGACAGAAATGGCTCAGCTGCAGCAGATGCTCAGCCCTGGACCAGCTCAGGAGCAAAATTGTACAGAGATGGGAGCC 900
A A T R Q K M A Q L E Q M L S A L D Q L R R Q I V T E M G G 224
TTGCTGACTGCCATGGATTATGTACAGAAAGCTGACAGATGAAGAATTAGCAGACTGGAAGAGAAGGCAGCAATATGCTGCATTGGA 990
L L T A M D Y V Q K N L T D E E L A D W K R R Q Q I A C I G 254
GGACCACCTAACATCTGCCTGGACCGCTCGAAACATGGATCAGTCCCTGGCTGAGTCCAGCTCCAGATTCTCGCAGAGATCAAGAAG 1080
G P P N I C L D R L E T W I T S L A E S Q L Q I R Q Q I K K 284
CTGGAGGAGCTTCCAGCAAGGTGTCTACAAGGAGACCCCATCCAGCACCAGCCCGCCCTGGAGGAGAAGATTGTGGACTTTGTC 1170
L E E L Q Q K V S Y K G D P I I Q H R P A L E E A I V D L F 314
AGAAACCTGATGAAGAGTCTTTTGTGGTCTGAAAGACAGCCTTGTATGCCCATGCATCCAGACAGACCTCTGGTTATAAAACGGGAGTG 1260
R N L M K S A F V V E R Q P C M P M H P D R P L V I K T G V 344
CAGTTCACAAATAAAGTCAAGTTACTGGTGAAGTTTCTGAACTCAATTACAGCTGAAAATTAAGTTTGCATTGACAAGGAATCTGGG 1350
Q F T N K V R L L V K F P E L N Y Q L K I K V C I D K E S G 374
GATGTGGCGCAATTCAGGGTCAAGAAATTAACATCTCGTACCAACAAAAGTATGAACATGGAGGAATCCAACAATGGGAGC 1440
D V A A I R G S R K F N I L G T N T K V M N M E E S N N G S 404
CTGTCCAGCAGTTTAAACACTTGACCTGAGAGAAGAGGTTGGTAATGGAGCCGCAATAGTATGCCTCTCTGATTGTTTACA 1530
L S A E F K H L T L R E Q R C G N G G R T N S D A S L I V T 434
GAGGAGCTCCACTTAACCTTTGAGACCGAAGTCTATCACCAGGTCTGAAGTTCGATCTGGAGACTCACTTCTTGCCTGTTGGTTGTC 1620
E E L H L I T F E T E V Y H Q G L K I D L E T H S L P V V V 464
ATTTGCAACATCTGCCAGATGCCAAGCCTGGGTTCCATCTCGTGGTACAACATGCTCAACACCACCAAGAAATGTAACATTCTTC 1710
I S N I C Q M P N A W A S I L W Y N M L T N H P K N V F F 494
ACCAAGCTCCAGTGGGACATGGGATCAAGTGGCTGAGGTTCTTAGTGGCAGTTTTCTCCACAACCAAGAGAGGCTGACCATTGAA 1800
T K P P V G T W D Q V A E V L S W Q F S S T T K R G L T I E 524
CAGCTCACCACTGGCTGAGAAATTAAGGCTTGTGCAACTACTGGCTGTCAGATCACTTGGGCCAAGTTCTGTAAGGAAAAC 1890
Q L T T L A E K L L G P C V N Y S G C Q I T W A K F C K E N 554
ATGGCTGGCAAGGCTTCTCTTCTGGTGGGCTGGACAACATCATTGACCTGGTGAAGAAATATATCTGGCAGCTGGGAATGAAGGG 1980
M A G K G F S F W V W L D N I I D L V K K Y I L A L W N E G 584
TATATCATGGGCTTATCAGTAAGGAGAGGAGGGCCATCTTAGTCCAAAACCTCCTGGCACTTTTCTGCTGGCTTCACTGAGAGC 2070
Y I M G F I S K E R E R A I L S P K P P G T F L L R F S E S 614
AGCAAGGAGGAGGCATTACATTACATGGGTAGAGAAAGACATCAGTGGAAAGACCCAGATCCAGTCACTGGAGGCCTACACCAAGCAG 2160
S K E G G I T F T W V E K D I S G K T Q I Q S V E P Y T K Q 644
CAGCTCAACAGCATGCTTTCCCGACATCATATGGGCTACAAGATTATGGATGCCACCAACATCCTGGTTTCACTCTGTGTACCTC 2250
Q L N S M S F A D I I M G Y K I M D A T N I L V S P L V Y L 674
TACCCTGAAATCCCCAAGAGGAAAGCTTTGGGAAATCTGCAGACCAAGCAGCTCCTGAATCTGAGATGGGAGGAGACTCTACGGG 2340
Y P E I P K E E A F G K Y C R P E A A P E S E M G G D S T G 704
ACTATTGACCCATACTGAAGACAAAGTTCATCTGTGTACCCCCAAAACCTGGAACACCAGTGACCTGTCCCATGTCGCTCCG 2430
T I Q P Y L K T K F I C V T P T N S G N T S D L F P M S P R 734
ACCCTCGACTCCCTGATGCACAATGAAGCTGAAGTAAATCCAGGACATTTGGATTCACTCACTTGGAGATGGATGATGATCAGTATG 2520
T L D S L M H N E A E A N P G H L D S L T L D M D V A S P M 764
TGAAGACATTCGTCAGTCTCCTCATCTCTTTCTTCTTGTGGGATTTGATGTTATGTTGTGATGGAGGATGTGACGATGATTTCTC 2610
*

TCTCCCTATGTACACAGTCTGCCTGTACAGTTTGTCTGTCTGTGTAATAATGATTTCACTTTCACATCATAGAAAATTAGATGA 2700
TTTTGAAAGATATTTTAAAAAAGCATGCCCATTATTTAGGTTTTTCTGTCCACTGGTAGCTTAGTGTGAAACTGTTGACTGAT 2790
ACTGACCTGTGATTTCTGCTCCCATCAGTACTTTCCCATCTTCATAGATGGCTTAAGTACCTATTAAGTATCTGGAATTTGATTTT 2880
TGAGAACATGTATTTTTCGGTGTGACTTTTAAATGGTAAATGTAATGAGAGTAAATTTGTTGATAGTACGCGACTTTCAAAATTGT 2970
ACCTTGACGATTTTATGCAATTAATGGTCTCTCAGTATTTTTGTGCGATTTTTTAAATCCCTGTCAAATGTAATGTCACGGGTGTT 3060
CTCAATACCTTTGATTTCAATTAATGTTCTGTTTCATTATGGGTTTTTATCTCAAAATCGAATATTTCTTATTTCTCAGAGCC 3150
ATTTGAAGTGTGAAGACATTTCTGAGGTTATTTTCCAGTAAGCTCTTTTTTCCCTTATAGTGGTGTGAGAAATACATAACATAACCG 3240
GTAAAAGTTGGTCTGAAAGCAGTTTCTGTCACTCCCATTTAAATACTGTCATTGTTGATCGTGTGAAATGCACTTGTCTGGAAATG 3330
AGCAGTTTGTATTTTTGTTGGCTGAATTCACCTGATGTGACCAGATGTAAATCATTATGACCAATTTATTTAGGACAAACT 3420
TGTTATCAAAAATAACCATGGATTTAAGAAAGATATTTCACTTCAACAGAGTGTACACAGTAAGGTGTGACGGTGTACTTTTAAAC 3510
TTTCTGACACTTGAGTAAACCTGTGAGTTTAAATGCAAGCCAGTTTGTCTGCTGCCATGAAATGTTGAGAGCTTTTCTGTAA 3600
AATATGCTGTAACATTTCAATTTTGAACAGAGGCC**AATAAA**ATCAAGTTAGC 3652

Fig. 5.1. Nucleotide and deduced amino acid sequence of RbSTAT3. Translation start (ATG) and stop (TGA) codons are red color letters. Polyadenylation signal at the 3'-UTR is bold italics and underlined.

5.2.1.2. Homology analysis

The amino acid sequence of RbSTAT3 was compared with various orthologs belong to the wide array of taxonomical groups in vertebrates, and revealed that most of the residues are completely conserved except a set of residues at the C-terminus. The characteristic domain regions of RbSTAT3 can be marked according to the multiple sequences alignment results and the data obtained from web based tools. The first five conserved domains, including N-terminal domain, coiled coil domain, DNA binding domain, linker domain and Src homology 2 (SH2) domain, were strongly conserved. However, the C-terminal region belongs to transcriptional activation domain (TAD) was not conserved well. Pairwise sequence analysis revealed that RbSTAT3 shared greater than 90% identity with fish homologs, while showing higher than 84% identity with mammalian homologs (**Fig. 5.2**). In addition, the CDD in NCBI revealed that several amino acid residues important for phosphotyrosine (Lys⁵⁹², Arg⁶¹⁰, Ser⁶³⁷ and Glu⁶³⁹) and hydrophobic binding pockets (Val⁶³⁸ and Ile⁶⁵⁴) and, homodimer interface (Ser⁶⁴⁸, Met⁶⁴⁹ and Phe⁷¹⁴) were conserved. Further the completely conserved tyrosine (Y⁷⁰⁹) residue which is phosphorylated during activation was also identified at the end of SH2 domain region (**Fig. 5.3**). The homology model of RbSTAT3 was generated by SWISS-MODEL, and compared with its template of mouse ortholog which shared 90.32% identity with RbSTAT3. Results revealed that the structural topology of RbSTAT3 was more or less similar with the mammalian counterpart (**Fig. 5.4**).



Fig. 5.2. Multiple sequence alignment of RbSTAT3 amino acid sequence with other orthologs from different taxonomical origins. Identical residues to the RbSTAT3 are marked with periods. Domain regions are marked with different colored line at the top of the alignment. The percentage of identity (I%) and similarity (S%) of RbSTAT3 with other counterparts are at the C-terminus.

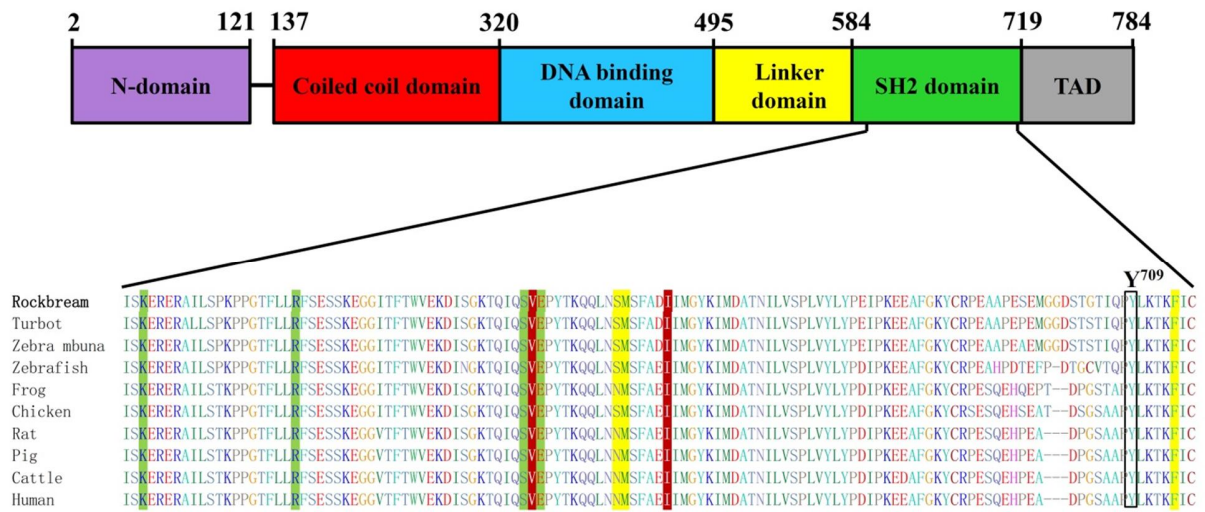


Fig. 5.3. Domain structure of RbSTAT3 and multiple alignments with biologically important binding/active sites in SH2 domain. Phosphotyrosine and hydrophobic binding pockets are shaded with green and reddish brown color, respectively. Amino acid residues belong to the homodimer interface are highlighted in yellow color. Characteristic site for phosphorylation (Tyrosine) is marked with box and label as Y⁷⁰⁹.

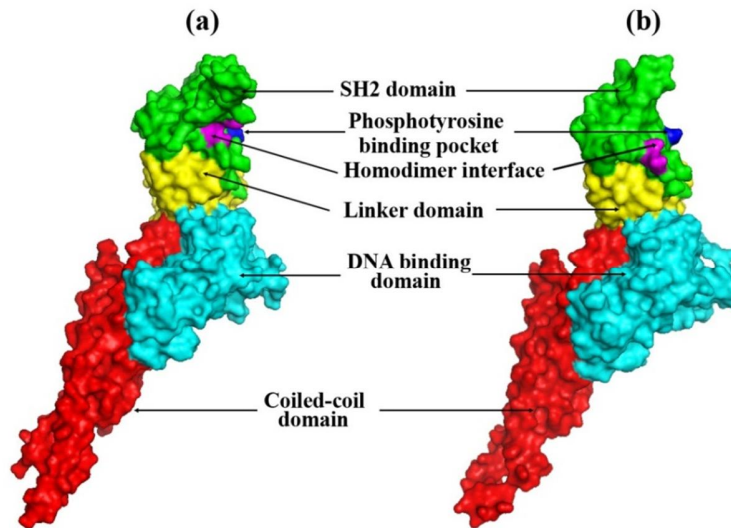


Fig. 5.4. Homology model of RbSTAT3 (a) and mouse STAT3 (b). Topological surfaces of each domain region were highlighted with different colors. Residues important for the phosphotyrosine binding pocket and homodimer interface are marked with blue and pink colors, respectively. The 3D structures were modeled by SWISS-MODEL and decorated by PyMOL molecular graphic software version 1.3.

5.2.1.3 Phylogenetic analysis

To interpret the evolutionary relationship among the STAT3 members and origin of RbSTAT3 in the context of biological evolution, a phylogenetic tree was constructed based on the sequences of available orthologs in the NCBI. In addition, a STAT member identified from slime mold (*Dictyostelium discoideum*) was used as an out group of the phylogenetic tree. Rock bream STAT3 clustered with other fish members in the fish clade, while showing a closer relationship with zebra mbuna (*Maylandia zebra*) STAT3 which shared the highest identity (96.7%) with RbSTAT3 (Fig. 5.5). Interestingly, the fish and other vertebrates diverged into two distinct clusters indicating their molecular evolution has possibly occurred independently from a common ancestor.

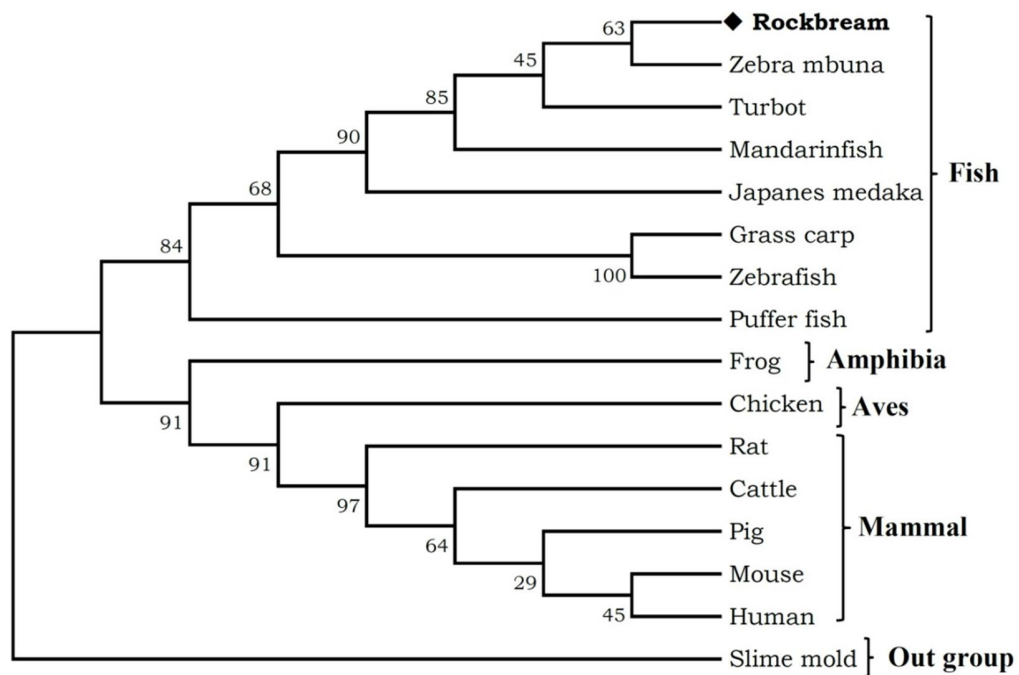


Fig. 5.5. Phylogenetic tree based on the STAT3 amino acid sequences from various taxonomical origins. The rooted phylogenetic tree was constructed by using NJ method and the bootstrap confidence was calculated from 5000 replications. The numbers at the each nodes are represented the bootstrap confidence values (%). The accession numbers for the selected species as follows; Zebra mbuna (XP_004552345), Turbot (ACX69847), Mandarinfish (ACU12485), Japanese medaka (AAT64912), Grass carp (AGC70812), Zebrafish (NP_571554), pufferfish (AAL09415), Frog (NP_001090202), Chicken (NP_001026102), Rat (NP_036879), Cattle (AAI09482), Pig NP_001038045), Mouse (NP_998824), Human (NP_644805) and Slime mold (O00910).

5.2.1.4 Genomic sequence analysis

The complete genomic sequence of *RbSTAT3* was obtained from the BAC library and it was found that the cDNA sequence was distributed within 24 exons disrupted by 23 introns. The comparison of *RbSTAT3* genomic structure with other homologs revealed that 16 exons in the CDS were completely conserved among all the species analyzed, while 20 conserved exons were noted among fish counterparts (**Table 5.2** and **Fig. 5.6**). First exon of all the species comprised noncoding nucleotides in its entirety. In addition, initial part of the second exon and ending part of the last exon also comprised of noncoding nucleotides. Remarkably, the third exon of the fish species has been separated into two different exons in other vertebrate species. Further, the twenty second exon of fish species has been lost in the other fish species as marked in **Table 5.2**.

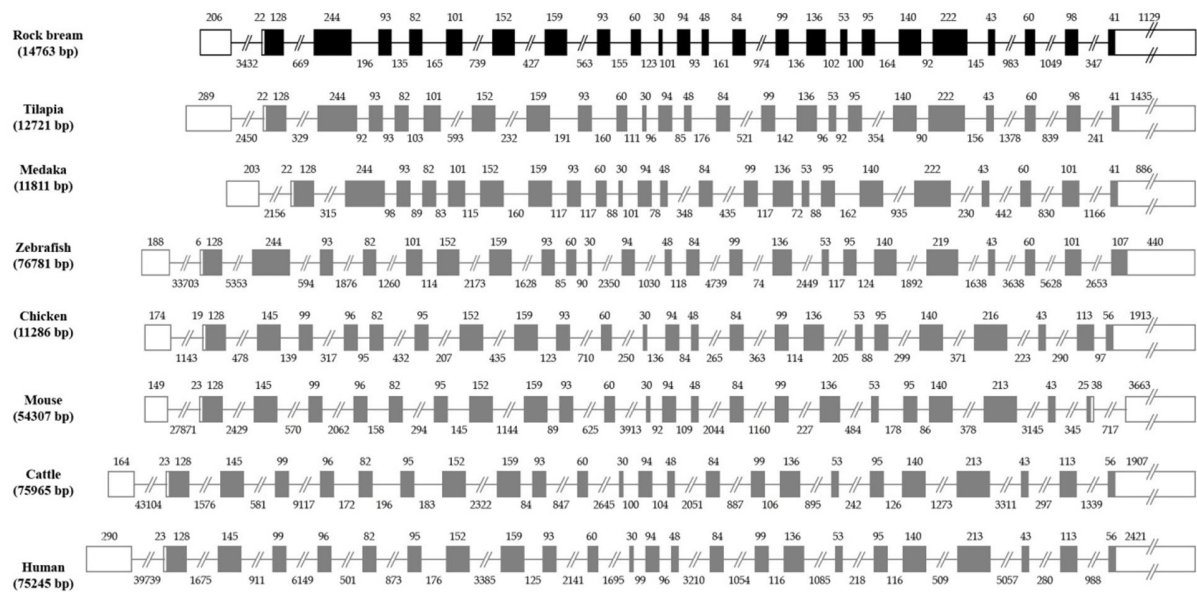


Fig. 5.6. Comparison of genomic organization of *RbSTAT3* with other counterparts. The boxes represent the exons, whereas the lines between them indicate the introns. Coding regions and un-translated regions are indicated by filled and empty boxes, respectively. genomic sequences of other species were obtained from Ensemble data base and their accession numbers are as follows; Tilapia: ENSONIT0000001452, Medaka: ENSORLT0000005086, Zebrafish: ENSDART00000104519, Chicken: ENSGALT00000005170, Mouse: ENSMUST00000127638, Cattle: ENSBTAT00000028687, Human: ENST00000264657.

Table 5.2. Exon organization in genomic structure of fish and higher vertebrates.

	E1	E2	E3	E4	E5	E6	E7	E8	E9	E10	E11	E12	E13	E14	E15	E16	E17	E18	E19	E20	E21	E22	E23	E24			
Rock bream	206	22	128	244	93	82	101	152	159	93	60	30	94	48	84	99	136	53	95	140	222	43	60	98	41	1129	
Tilapia	289	22	128	244	93	82	101	152	159	93	60	30	94	48	84	99	136	53	95	140	222	43	60	98	41	1435	
Medaka	203	22	128	244	93	82	101	152	159	93	60	30	94	48	84	99	136	53	95	140	222	43	60	101	41	886	
Zebrafish	188	6	128	244	93	82	101	152	159	93	60	30	94	48	84	99	136	53	95	140	219	43	60	101	107	440	
Chicken	174	19	128	145	99	96	82	95	152	159	93	60	30	94	48	84	99	136	53	95	140	216	43		113	56	1913
Mouse	285	23	128	145	99	96	82	95	152	159	93	60	30	94	48	84	99	136	53	95	140	213	43		113	56	1995
Cattle	164	23	128	145	99	96	82	95	152	159	93	60	30	94	48	84	99	136	53	95	140	213	43		113	56	1907
Human	290	23	128	145	99	96	82	95	152	159	93	60	30	94	48	84	99	136	53	95	140	213	43		113	56	2421
	E1	E2	E3	E4	E5	E6	E7	E8	E9	E10	E11	E12	E13	E14	E15	E16	E17	E18	E19	E20	E21	E22		E23	E24		

Sizes of the exons in CDS of fish and higher vertebrates are highlighted with dark gray and light gray colors, respectively. The exon numbers corresponding to the fish and higher vertebrates are presented in the top and bottom rows, respectively. Un-shaded regions of the table in either side indicated sizes of exons in UTRs.

5.2.1.5 Putative promoter characterization

The 5'-upstream region (~2 kb) of *RbSTAT3* gene obtained from the BAC clone was analyzed by AliBaba online prediction tool to ascertain the potential TFBS. As shown in the **Fig. 5.7**, various *cis*-regulatory elements that are essential for the binding of transcription factors such as nuclear factor I (NF-1), nuclear factor- κ B (NF- κ B), specificity protein 1 (SP1), c-Jun, GATA binding factor 1 (GATA-1), octamer transcription factor 1 (Oct-1), CCAAT-enhancer binding protein alpha and beta (C/EBP α and β), member of ETS oncogene family (Elk-1) and interferon consensus sequence binding protein (ICSBP) were present in the putative promoter region of *RbSTAT3*.

TAAAGATCATGAAGCCTTAAAAGAATCAGTAGTCCACCAGTGTGAAAGTTATTCTATATTATGTGGGAAATATCTCTGTCTACT -5579
GTATTCTGTGCTCTTAATTTGTCAATTTGTCAAAATTTAGCTACAATAATAAGAACTCAAAGCTGATA**TCAGTGTAACT**TAGAATG -5489
TAACCTTTGCTGCGGTGTGCTTTAC**AGTGCATGCT**TGAAAACACGGTTTGATCATCATTTGCTGTAACGTTTGTGATGATACTACCAT -5399
Oct-1
GCTGTATTTATTGCATCGGGACATGTTG**TCCTCACCAGCTTCCACATGGCAC**ACCTCTGCACAGAGGAGAGACAAACGACTGTGTACC -5309
SPI NF-1
ACGGTCACAGCTCATCAGTGCATTGTCACATCCCTATTAATTTTCCCGAGGTAATTGCAGTCAGAAAAATGATGGTCCGGAGAGCG -5219
AGATGACAGTTTAACTGACTACTGTAACACGCGGAGATGCAATGTCATTCTAAACGCAGTCAAAGCGAGACAGCACACTGCCGAGTT -5129
TTATGAATGCCGTGTCAGGATACCAGAACAGCATGATCC**AGTCCACAAC**ATTTTTGCAGAGACCAGGTGCAAGCTTGTATACTTCTTCT -5039
C/EBP α
TAAGTATAAAACGAATTAATTCAGATTCATAAAATGACAATCGTGAAGAT**TAGAGGAAGC**TATGATAATT**GAATTGTGAT**CATTCTGAG -4949
Elk-1 c-Jun
CCTGTGTAACAA**ACATTGGCAA**TGTTTCAGTGTGCGCACTTTTGTATCATGTGGGCAAGCACACAGGGCTCCGGTCAGGAAGGAGGTG -4859
NF-1
AATGTACTGTACAGCTTCCATTTCCCTCCCTGGAGACTGTGAGTGTGATCTTGTATGTTGGAGTAGGCACGCAGAAAGCCACCGTGTAGCAT -4769
GGAAACACATTAATAAATCAATGGGCTGGAGAATGCAATTAAGGAGAGTGTCCCTTTGAGCACTGAGCAGGGTGGAGAACAGGGAGAA -4679
GGACAGAGAGAAAGGGTGTGTGATCT**GTCTGTGTGT**GTGTGTGTGTGTGATtGTGAAGAGTAAG**TATGTGCATA**CCATATACCCACA -4589
SPI Oct-1
CTGACATTTCAATAAACTCTATGTTTATAGAGCGAAGAAACCAATTACAGGCCTGTGAAATCACATCAAAATTATAAAAGTATTATCTTT -4499
TATATTGATTTTACATGCTAGCACATCAAATACTGAAACACTTG**TAAGATATTG**TCCCTTTTACAAAAAAGTGTGTTTTTGCCA -4409
GATA-1
CCATGTATATTTGCTTGTGTTGGAGCTTCTGGTCATTAATAAACTGAACAGCCTGTATAAGCGTAGGTAGACCATGCACAGCTTAT -4319
ATAAAGACATTGTGATGTTGGCTGCAGCCACACAGTGTGACACAA**ATTGGGTGTT**ATTGATTACTACTCAAATAATGAAGCTTGCCTTTT -4229
C/EBP β
CTGTGTGTTCAAGGCCACTTTTGGCCACTTCAGTATAATAAAAGCTTACTAAACAACATATACTGCCTGTTA**TTTTTATTTT**ATTATTA -4139
Oct-1
TCTTATGAGCCTTTTATATATCTGACTACACTATTAGTGTACTACTAATGATTTTAT**TTTTATTGCTCA**CCTACTGCGGAGGAGAAGCTCG -4049
C/EBP α
GGCAAACCAGCCGCT**GGATTAAGAT**TAAGAGCGGCAATAATGAACAGCACTGGTGTATTAAACTCTTGATGACGTCGATGCTGCCAGT -3959
GATA-1
AACT**TCAGATGACT**TCCAGGCTGGCTGTCCGTCGAAGCGCAC**GCACCTCCCTCCGGC**CGGGCCTACTCCGGGTCCACCCCGGGGAGGG -3869
c-Jun SPI
CGCGCTGTGGGAACAGCGCAGTTGGACAGCAGTAAACACGACGTTCTCAACCAACCTCGC**CGTGGAGTCC**CGCCTCTCTGCTTTAAG -3779
NF- κ B
ATGCATTTCT**GATTGGCTAC**AGTAGATGTAGCGGCTAGTATTGGCTGTGGAGGTGTCAATAAAGTAGTTTATGGGGTTGTCTGGCTGGA -3689
NF-1
AGGACTGCAATGTAGGAGATGTTAGTT**GAAAAGTCTGTACGTGCATTTGGAGAGGTGTTTCCCGTGTGGCAAGAAAAGATATAGAGTT** -3599
ACGATCTTTTTCTGTGCGTTCTCCCTCGTTTTTGTGGGTGAATTTTACAAAAGTCGTCAGTACTGTTACTGTCAGTGTTTTTGTGCT -3509
AGAAAGTTTTTTGTTTTACGGAGAAACTTTCCAAAAGAGTGACAACGAGCTAGgt..ag**GTTTGTGGAGGTGTGTGTCAGATG**CCCA +8
1st exon ← 3432 → 2nd exon
GTGGAACCAAGTTACAGCAGTTGGAGACCAGGTATCTGGAGCACTCTACCCTGTACAGTACAGCTTCCCATGGAACTACGGCAGTT

Fig. 5.7. Putative promoter proximal region at the 5' flanking region of RbSTAT3 gene. The first and second exon regions are shaded with gray color and, 5' and 3' splice sites (gt and ag, respectively) in the first intron are shown as small case letters. The position of the nucleotides in the sequence are marked relative to the translation initiation site (ATG) shown by white color letters. Transcription factor binding sites predicted by AliBaba 2.1 program are marked with green color letters and indicated at below the sequence.

5.2.2 Expression patterns of *RbSTAT3* mRNA

The expression of *RbSTAT3* transcripts was examined by SYBR Green qPCR and dissociation curve was analyzed for all the assays. The results revealed that the dissociation curve had a single peak for both *RbSTAT3* and β -actin suggesting that the amplification was target specific.

5.2.2.1 Tissue specific expression pattern

As determined by the qPCR, *RbSTAT3* transcripts were ubiquitously expressed in all the tissues examined with different levels under normal physiological conditions. The expression of *RbSTAT3* transcripts was remarkably higher in the blood cells followed by heart and liver tissues respectively with 240-, 180- and 167-fold, when compared to the tissue with the lowest mRNA levels. Meanwhile, *RbSTAT3* mRNA was moderately expressed in gills, brain, spleen, kidney, and intestine tissues (Fig. 5.8).

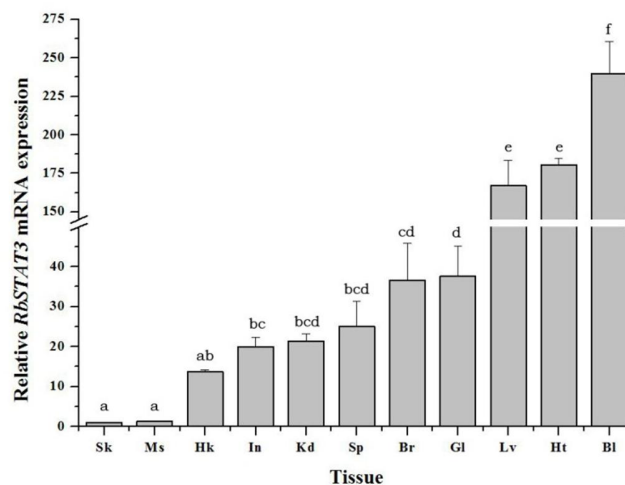


Fig. 5.8. Tissue specific expression of *RbSTAT3* in healthy fish under normal physiological condition. The rock bream β -actin was used as an internal reference gene to normalize the relative mRNA expression. Eleven different tissues including skin (Sk), muscle (Ms), head kidney (Hk), intestine (In), kidney (Kd), spleen (Sp), brain (Br), gill (Gl), liver (Lv), heart (Ht) and blood cells (Bl). The results are reported as mean \pm standard deviation (SD) of triplicates. Statistical analysis was performed by one-way ANOVA followed by Duncan's Multiple Range Test. Data with small case letters are indicated the significant differences at $P < 0.05$ among different tissues.

5.2.2.2 Expression patterns after *in vivo* immune challenges

The transcriptional modulation of *RbSTAT3* was assessed in response to the common pathogenic viral (RBIV), bacterial (*E. tarda* and *S. iniae*) and immune stimulants (LPS and poly I:C) in rock bream blood cells (**Fig. 5.9a**) and liver tissue (**Fig. 5.9b**). Upon RBIV infection, no significant ($P < 0.05$) changes were observed in blood at any time points analyzed. However, significantly elevated mRNA levels were detected after 6 h post injection (p.i.) (2.7-fold) and 48 h p.i. (1.6-fold) in liver tissues. Following the injection of poly I:C (a mimic of double stranded virus), the expression of *RbSTAT3* transcripts in blood cells was up-regulated at 6 h and peaked at 12 p.i. (4.4-fold). Subsequently, the level of expression reached to the basal level. In contrast, no significant ($P < 0.05$) changes of *RbSTAT3* expression was detected in liver except at 48 h p.i. (1.4-fold) of poly I:C. In the case of LPS challenge experiments, the expression of *RbSTAT3* peaked at 12 h p.i. (4.36-fold) in blood and 24 h p.i. (3.4-fold) in liver tissues. Upon pathogenic bacterial infections, the level of *RbSTAT3* transcription was up-regulated at the middle and late phase of the experiments. After *E. tarda* infection, the highest level of *RbSTAT3* transcripts was detected at 24 h p.i. (3.6-fold) in blood, while strongest expression was observed at 6 h p.i. (3.6-fold) in liver. Meanwhile, the highest expression against *S. iniae* infection was observed at 24 h p.i. (2.01-fold) in blood and 6 h p.i. (3.4-fold) in liver.

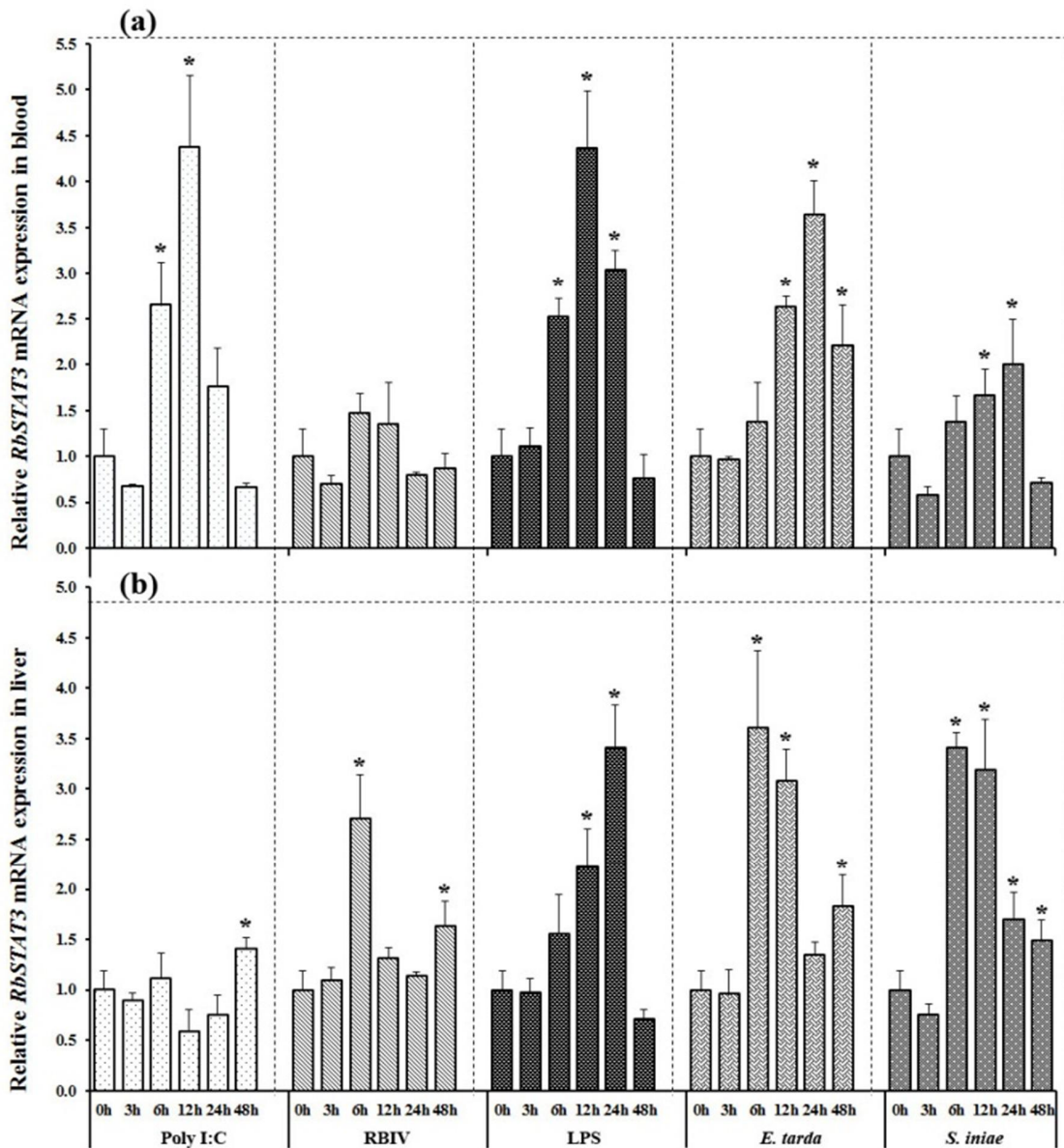


Fig. 5.9. Expressional patterns of RbSTAT3 in blood (a) and liver (b) after in vivo immune challenge experiments. The rock bream β -actin was used as an internal reference gene to calculate the relative mRNA expression. The fold change relative to mRNA expression at each time was compared with the corresponding PBS-injected control and represented as relative fold changes. The vertical bars represent the mean \pm standard deviation (SD) of triplicates, and results were statistically compared relative to the un-injected control (0 h) using t-test. Data with statistically difference at $P < 0.05$ are indicated by asterisks.

5.2.2.3 Expression patterns after injury challenges

The temporal expression profile of *RbSTAT3* mRNA in blood cells and liver tissue were detected with controversial results. As shown in **Fig. 5.10**, the expression of *RbSTAT3* transcripts were significantly elevated at 3 h post-injury in rock bream liver tissue, and the transcription was continually up-regulated until 48 h, except at 12 h compared to the un-injured control. The highest transcription was examined at 24 h post injury. In contrast, the expression of *RbSTAT3* in blood cells was observed with periodical down-regulations. While showing down-regulations at 3, 12 and 48 h, the expression in other time points remained as similar as the un-injured control.

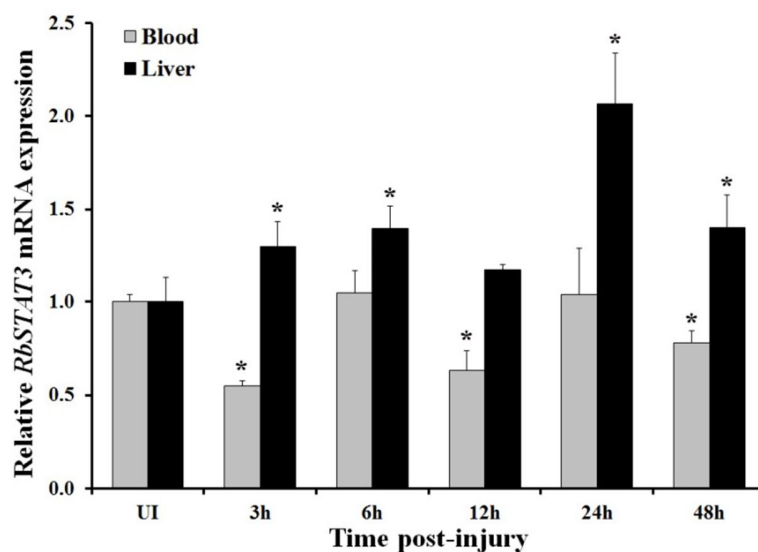


Fig. 5.10. The expressional patterns of *RbSTAT3* in blood cells and liver tissue in response to the injury. The rock bream β -actin was used as an internal reference gene to calculate the relative mRNA expression. The fold change of expression at each time point was compare with un-injured control (UI) and represented as relative mRNA expression. The vertical bars represent the mean \pm standard deviation (SD) of triplicates, and results were statistically compared relative to the un-injured control (UI) using t-test. Data with statistically difference at $P < 0.05$ are indicated by asterisks.

5.2.2.4 Expression patterns after *in vitro* challenges

In order to determine the impact of interleukin-10 on *STAT3* transcription, the level of mRNA expression was examined after treating rock bream heart cells with rRbIL-10. Results revealed that the expression of *RbSTAT3* mRNA was significantly ($P < 0.05$) up-regulated after 24 h post-treatment of rRbIL-10, while showing a down-regulated expression at 12 h (Fig. 5.11). Subsequently, the expression reached the basal level at 48 h.

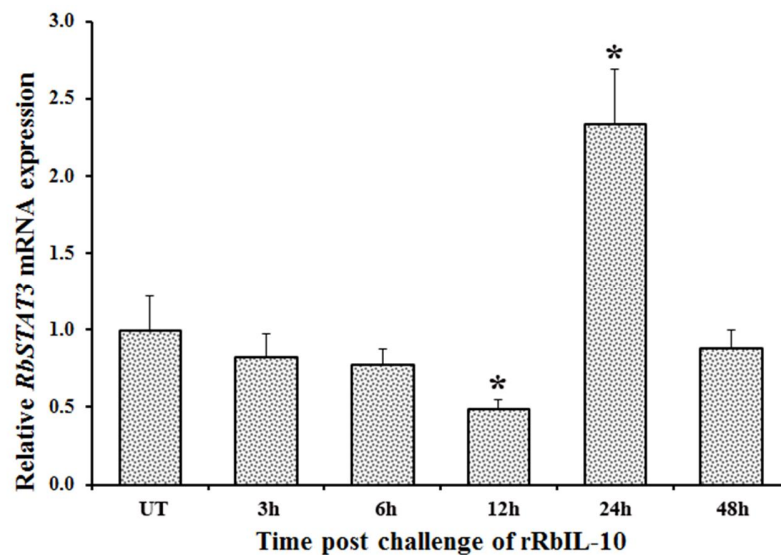


Fig. 5.11. The expressional patterns of RbSTAT3 in heart cells upon *in vitro* challenge with rRbIL-10. The rock bream β -actin was used as an internal reference gene to calculate the relative mRNA expression. The fold change in mRNA expression is represented as relative to mRNA level of MBP-treated cells at each time point. The vertical bars represent the mean \pm standard deviation (SD) of triplicates, and results were statistically compared relative to the untreated control (UT) using t-test. Data with statistically difference at $P < 0.05$ are indicated by asterisks.

5.2.3. Subcellular localization

To examine the localization of RbSTAT3 protein in the cells, a system containing GFP tag was used. The construct of pEGFP-N1/RbSTAT3 was transfected into rock bream heart cells and observed under the fluorescence microscope. Results revealed that RbSTAT3 was evenly distributed in cytoplasm, while mock control (only GFP protein) showed in whole cell (Fig. 5.12). Upon poly I:C stimulation the RbSTAT3 seems to be concentrated in nucleus.

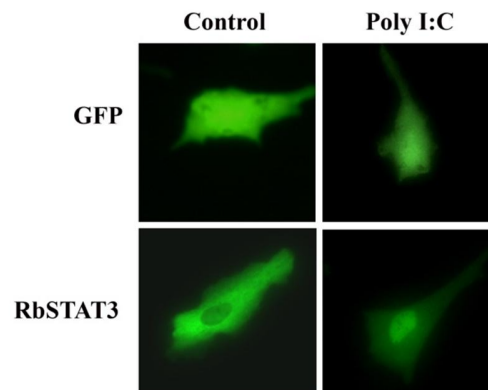


Fig. 5.12. Subcellular localization of RbSTAT3 in rock bream heart cells. Cells in the first row indicate the localization of GFP protein, where pEGFP-N1 empty vector transfected. Cells in the second row indicate the localization of rock bream STAT3 protein, where pEGFP-N1/RbSTAT3 vector transfected. The nuclear translocation of RbSTAT3 upon poly I:C stimulation is clearly depicted in the cells in the second row.

5.3. Discussion

STAT3, which is also known as an acute phase response element, is an essential and multifunctional member of the STAT family, activated via JAK2 upon stimulation with various factors. It has been broadly studied in mammals, and reported that STAT3 plays vital roles in various responses such as embryogenesis, hematopoiesis, neurogenesis, immune, and inflammatory responses (Hirano et al., 2000; Levy and Lee, 2002). Even though few studies have been focused on the immune responses of fish STAT3 against microbial infections (Guo et al., 2009; Wang et al., 2011c; Huang et al., 2014), the major functional aspects of STAT3 in fish species remain to be explored. In the present study, a member homologous to the STAT3 was identified from rock bream, and characterized structurally and functionally. The RbSTAT3 shared the common structural topology similar to other STAT orthologs comprising six common domains. Protein sequence comparison revealed that the aa residues of RbSTAT3 were highly conserved particularly in N-terminal domain, DNA binding domain, linker domain and SH2 domain. More importantly, the functional residues localized in SH2 domain and tyrosine residue that is a characteristic residue for the phosphorylation were completely conserved among different taxonomical groups. Three dimensional homology model of RbSTAT3 also displayed structural conservation. Collectively, these structural features suggest that the functional aspects of RbSTAT3 might be highly conserved from mammals to fish.

The comprehensive study of phylogeny and genomic organization of a particular gene might be essential to understand its molecular evolution. The NJ phylogenetic tree clearly depicted that the evolution of *STAT3* in fish and other vertebrates has distinctly occurred. These results were also consistent with the previous reports (Wang et al., 2011c; Huang et al., 2014). As shown in **Table 5.2**, the markedly different genomic organization could be observed between fish and other vertebrates. Specifically, the intron addition at the 5' region and exon deletion at the 3' region have taken place during the evolution. These results evidently support the notion of distinct evolution of *STAT3* in fish and other vertebrates.

Study of TFBSs at the promoter region might be an important feature to understand the transcription potential of a particular gene. In the current study, various possible TFBSs were predicted by the computational tools at the 5'-proximal region of *RbSTAT3*, and they were known to be involved in diverse immune functions. It has been reported that most of the transcription factors such as NF-1 (Xu et al., 2005), NF- κ B (Oeckinghaus and Ghosh, 2009), AP-1 (Foletta et al., 1998), C/EBP (Wedel and Ziegler-Heitbrock, 1995; Lekstrom-Himes and Xanthopoulos, 1998), GATA1 (Ferreira et al., 2005), Oct-1 (Kemler and Schaffner, 1990; Tantin et al., 2005), and ICSBP (Horiuchi et al., 2012) are crucial for the various immune/stress related functions. Previous study in human *STAT3* reported the presence of several transcription factors including CRE/ATF (c-AMP responsive element/activating transcription factor), SBE (Smad-binding element) and GC boxes (Kato et al., 2000). However, additional studies are required to be carried out, in order to understand the real TFBSs in *STAT3*, since there are limited studies available about the promoter region of *STAT3* gene.

The analysis of mRNA expression in different tissues under normal physiological conditions will be supportive to understand the possible biological roles of specific genes. The expression of *STAT3* transcripts was analyzed in a few fish species, and reported the ubiquitous expression in various tissues with different levels. Previous reports on turbot (Wang et al., 2011c), grass carp (Guo et al., 2013), and orange spotted grouper (Huang et al., 2014) demonstrated that the highest expression of *STAT3* transcripts were in liver tissue. Meanwhile, higher amount of *STAT3* transcripts from mandarin fish was observed in gonad, followed by spleen and heart tissues (Guo et al., 2009). In the present study, the *RbSTAT3* transcripts were highly detected in blood, heart and liver tissues. In addition, Oates *et al* (Oates et al., 1999) has reported the highest expression

of *STAT3* in liver tissue of zebrafish embryo. These evidences indicate the significant role of *STAT3* in diverse tissues, particularly in the liver.

To examine the immune defensive role of *STAT3* under pathologic conditions, the level of *RbSTAT3* transcripts was determined in liver and blood following *in vivo* stimulation with live bacteria, virus and PAMPs. Results showed that the *RbSTAT3* mRNA expression was significantly elevated in the middle and late phase of the experiment. These results were in accordance with some of the previous studies. The mRNA expression analysis of *STAT3* from mandarin fish demonstrated significantly up-regulated expression at the late phase of the experiment (48 – 120 h) upon poly I:C challenge (Guo et al., 2009). Meanwhile, Wang *et al* (Wang et al., 2011c) has reported that significant inductions of turbot *STAT3* transcripts at the middle phase of the experiment (6 - 12 h) after *Vibrio anguillarum* and lymphocystis disease virus (LCDV) infection. Recent study in orange spotted grouper also reported the significantly induced *STAT3* transcription at 12 - 24 h post infection of Singapore grouper iridovirus (SGIV) (Huang et al., 2014). In fact, number of studies has documented the activation of *STAT3* signaling in response to the various types of viruses (McCartney et al., 2013; Okemoto et al., 2013; Reitsma and Terhune, 2013; Trilling et al., 2014). These findings intimate that *STAT3* is a vital component for the organism to defend invading microbial organisms. In the context of present study, the *RbSTAT3* might play a potent role against bacterial and viral attack.

Wound healing is a most essential process in replacing the damaged cells and tissue layers in living organisms. In biological systems, it is a complex and dynamic process taking place via a cascade of biochemical events encompassing three main phases including inflammation, proliferation and remodeling (Stadelmann et al., 1998). These biological processes are known to be mediated by a vast array of elements including cytokines (Filkor et al., 2015), stem cells, growth factors (Pikula et al., 2015) and many signaling molecules (Xu and Yu, 2011; Portou et al., 2015). A number of studies have reported on the involvement of *STAT3* in the wound healing processes. Dauer *et al* (Dauer et al., 2005) described the *STAT3* as a crucial factor in regulating genes that are important for the wound healing and cancer. Meanwhile, several other studies reported the great impact of *STAT3* on lung injury (Gao et al., 2004), liver injury (Wang et al., 2011a), and ischemic and traumatic injury in brain, spinal cord and peripheral nerves (Dziennis and Alkayed, 2008). The mechanisms and crucial factors behind wound healing

process are poorly studied in teleost models. In the current study, transcription of *RbSTAT3* was assessed in response to the tissue injury, and observed significant changes in expression at different time points indicate a possible role of RbSTAT3 in wound healing. However, a broad spectrum of study is required in order to understand the real mechanism of STAT3 associated with wound healing process.

The interleukins are cytokines involved in activating various signaling pathways, one of which is JAK/STAT signaling cascade and activated via complex of interleukin receptors. Previous studies in mammals have described that the IL-10, an anti-inflammatory cytokine, activates the JAK1 and TYK2 (tyrosine kinase 2) associated with IL-10 receptors. Afterwards, STAT3 phosphorylates and transduces the signals for related anti-inflammatory actions (Riley et al., 1999; Mosser and Zhang, 2008). Past study on memory cells revealed that STAT3 play a vital role in functional maturation of memory CD8⁺ T cells via IL-10–IL-21–STAT3 signaling pathway (Cui et al., 2011). Liu et al (Liu et al., 2013) reported the influential impact of IL-10 on TLR-MyD88-STAT3 pathway in human B cells over phosphorylation of STAT3. Nonetheless, the functional aspects of teleostean STAT3 and their links with other signaling modules are very scarce. As a fundamental aspect, the expression level of *RbSTAT3* transcripts was investigated in response to the rRbIL-10. Results revealed that the expression of *RbSTAT3* mRNA was conceivably modulated by rIL-10 protein. To understand the real mechanism of triggered *STAT3* expression by IL-10, and subsequent functional features of STAT3, broader studies are needed to be conducted.

It is well-known that all the STAT proteins are generally located in cytoplasm under normal physiological conditions. Upon various stimuli, they will translocate into the nucleus in order to deliver the signal and activate subsequent functional processes (Lau et al., 2000; Sotillos et al., 2008). However, as per our knowledge no studies showing the localization of teleostean STAT3 counterparts are reported. In the current study, we investigated the subcellular localization of rock bream STAT3 in cytoplasm and translocation into the nucleus upon poly I:C stimulation. The results were as expected and indicated the characteristic signal transduction in response to the stimulus.

5.4. Conclusion

Hereby, we present the molecular characteristics and functional insights of a teleostean STAT3 ortholog, which is an important transcription factor of JAK/STAT signaling cascade, from rock bream. Bioinformatics of RbSTAT3 revealed that it is highly conserved among vertebrates, and shared common domain architectural features. In addition, comparison of genomic organization and phylogenetic studies of STAT3 with different taxonomical lineages provided strong information for distinct evolutionary paths for teleost and other vertebrate origins. The ubiquitous expression of *RbSTAT3* transcripts in different tissues of healthy fish implied its crucial biological importance in rock bream. Comprehensive studies of transcriptional analyses of RbSTAT3 in response to the microbial pathogens, PAMPs, interleukins (RbIL-10) and injury further support its essential roles in immune and wound healing mechanisms.

CHAPTER 6

Genomic structure and immunological response of STAT4 family member from Rock bream (*Oplegnathus fasciatus*)

Abstract

The Janus tyrosine kinase (JAK)/signal transducer and activator of transcription (STAT) signaling pathway plays a critical role in host defense against viral and bacterial infections. STAT proteins are a group of transcription factors that translocate into the nucleus and critical for the induction of many genes crucial for the allergic cascade and immune defense. In the present study, a member of STAT4 family was identified from rock bream (RbSTAT4) at genomic level and investigated its transcriptional regulation in response to the different pathological stimuli under *in-vivo* conditions to the first time in fish. The genomic sequence of the RbSTAT4 is around 15.6 Kb in length, including the putative core promoter region and 24 exons interrupted by 23 introns. Bioinformatics analysis of RbSTAT4 identified the presence of typical and conserved features of the STAT4 family, including STAT_int domain, STAT alpha domain, STAT bind domain, linker domain, SH2 domain and transcriptional activation domain. According to the phylogenetic analysis, RbSTAT4 exhibited a closest evolutionary proximity with the STAT4 member from mandarin fish (*Siniperca chuatsi*). Transcript profile of RbSTAT4 in healthy rock breams was detected as a ubiquitous expression in eleven different tissues examined, where liver and spleen showed moderate expression compared to the highest expression level detected in gill tissue. Time-course *in-vivo* immune stimulation with LPS, poly I:C, live *Edwardsiella tarda* and rock bream iridovirus caused significant transcriptional regulation of the RbSTAT4 expression in gill, head kidney and spleen tissues, suggesting that RbSTAT4 might involve in immune regulation mechanisms and/or signaling cascades, orchestrate against both bacterial and viral pathogens.

6.1. Introduction

Mariculture is one of the rapid developing worldwide industries which provides valuable source of essential fatty acids and essential amino acids along with enriched source of other nutrients. Many edible fish species are used either through culturing or capture fisheries; from which rock bream (*Oplegnathus fasciatus*) is known to be a highly consumed and one of the most economically important fish species, mostly in eastern Asia, both from capture fisheries and mariculture industry. However, production losses were also increased in recent years with the growing and intensified mariculture industry due to the occurrence of many infectious diseases. Especially, Edwardsiellosis caused by *Edwardsiella tarda* (Mohanty and Sahoo, 2007) and Iridoviral disease caused by rock bream iridovirus (RBIV) (Do et al., 2004) are frequently taking place, causing a significant mortality of farmed rock breams. In this regard, disease control plays an important and critical role to minimize the production losses which target basically either by pathogen control with chemotherapeutics or by host control with vaccines and immune stimulants (Park, 2009). The studies on immunogenetics will provide more precise approaches to develop new strategies of efficient disease control.

Immune system of an organism plays critical and indispensable roles; from which the innate immune system of fish relies on both cellular and humoral responses that are mediated via the activation of several signaling pathways, already identified in mammals (Stein et al., 2007). The Janus tyrosine kinase (JAK)/signal transducer and activator of transcription (STAT) signaling pathway plays a critical role in host defense against viral and bacterial infections. The JAK/STAT signaling cascade is activated as a response to the various chemical signals induced by interferons (IFNs), interleukins (IL), growth factors, or other chemical messengers. STAT proteins are a group of transcription factors that transmit signals to the nucleus and critical for the induction of many genes crucial for the allergic cascade and immune defense. The members of the STAT family are found to be involved in cell proliferation, apoptosis, survival, immune functions and certain aspects of tissue differentiation (Bowman et al., 2000; Bromberg and Darnell, 2000). In mammals STAT proteins were grouped into seven families, STAT1, STAT2, STAT3, STAT4, STAT5a, STAT5b and STAT6, each STAT was found to be bound with different DNA sequences in the promoter region of target gene.

STAT4 is an important element in mediating interleukin (IL)-12 responses, and it has been most extensively investigated in both human and murine T lymphocytes (Yamamoto et al., 1994;

Zhong et al., 1994a; Wurster et al., 2000). Many studies have been reported that Th1 cell differentiation requires the STAT4 activation through IL-12 signaling cascade and STAT4 was reported to bind directly with genes involved in Th1 cell differentiation, including Bcl6 and IL-21 (O'Shea and Plenge, 2012). STAT4 was also reported to be in conjunction with STAT1 in order to produce IFN γ and enhance the expression of T-box (T-bet) in Th1 cell differentiation through the IL-12 signaling cascade (Thieu et al., 2008). Although STAT4 is activated by both IL-12 and type I interferon IFN α/β in human, it is activated only by IL-12 in mice (Bacon et al., 1995; Jacobson et al., 1995; Cho et al., 1996). In addition to T lymphocytes, STAT4 was also reported to express by different immune cells including B lymphocytes (Durali et al., 2003), natural killer (NK) cells (Wang et al., 2000), dendritic cells, monocytes and macrophages (Frucht et al., 2000; Fukao et al., 2001). However the role of STAT4 in teleosts is not well understood and no STAT or IL gene from rock bream has been identified yet. In this study, the genomic organization of STAT4 gene from rock bream was identified and its temporal mRNA expression was investigated in animals challenged with different immune stimuli, derived from both bacterial (*Edwardsiella tarda* and LPS) and viral (rock bream iridovirus and poly I:C) origins.

Table 6.1. Primers used in this study

Primer name	Application	Sequence (5' -3')
<i>RbSTAT4/BAC-F</i>	BAC screening	TCAGACTCCTGGAACATGTGGACT
<i>RbSTAT4/BAC-R</i>	BAC screening	ATTGACTCATCGTTAGCCGCTGTG
<i>RbSTAT4/qPCR-F</i>	qPCR amplification	TTGTGAGTAAAGAGATGGAGCG
<i>RbSTAT4/qPCR-R</i>	qPCR amplification	AACTTCACCTCCCCATTGTC
<i>β-actin</i>	qPCR of internal reference	TCATCACCATCGGCAATGAGAGGT
<i>β-actin</i>	qPCR of internal reference	TGATGCTGTTGTAGGTGGTCTCGT
<i>RbIL-10/pMAL-F</i>	Clone into pMAL-c5x	(GA)3gaattcAGTCCCATGTGCAACAACCACTG - EcoRI
<i>RbIL-10/pMAL-R</i>	Clone into pMAL-c5x	(GA)3aagcttTCAATTAGAGGCCACTTGTTCGGAC - HindIII

Restriction sites in the cloning primers are shown with small case letters and indicated at the end of each primer sequence.

6.2. Results and Discussion

6.2.1. Genomic and cDNA sequence identification

Complete genomic sequence around 15.6 Kb, including the putative promoter sequence (~1 Kb) was identified from rock bream BAC library screening and sequencing. This sequence was

deposited in GenBank under accession number KC521467. Genomic structure of RbSTAT4 is comprised of 24 exons and 23 introns, in which 5' untranslated region (UTR) was split into two exons (Fig. 6.1). However, coding region of the RbSTAT4 is split into 23 exons, which is compatible with genomic structure organizations of several other teleost species. Moreover, almost all the exons exhibited identical length either to stickleback or zebrafish genomic architectures, except the last exon which was found to be bit smaller in length. Although some exons exhibited identical lengths to other STAT4 orthologous from avian and mammalian species, the number of exons was varied between species. However, all the teleost species compared in this study exhibited more or less similar genomic structure for STAT4 orthologs.

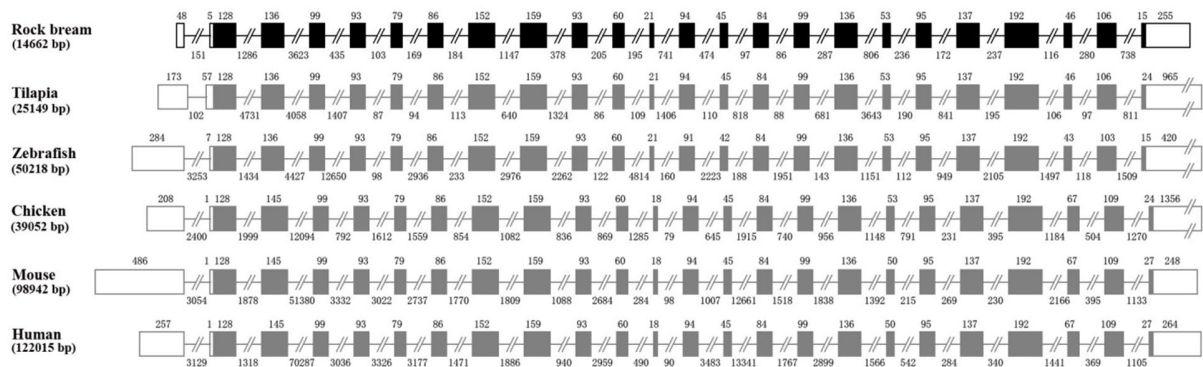


Fig. 6.1. Schematic representation of the STAT4 genomic structures. UTRs, coding regions and introns are denoted by white boxes, black boxes and black lines respectively.

Putative promoter region analysis of RbSTAT4 indicated the presence of several important transcription factor (TF) binding sites which are involved in the downstream gene regulation for various stimuli including cytokines, growth factors, stress, and pathogen infections (Fig. 2). For examples, octamer transcription factor-1 (Oct-1), activator protein 1 (AP-1), specificity protein 1 (Sp1), c-jun, interferon consensus sequence binding protein (ICSBP), upstream stimulating factor (USF), nuclear factor of activated T-cells, cytoplasmic 3 (NF-ATc3), nuclear factor kappa B (NF- κ B) and nuclear factor 1 (NF-1) like transcription factors are proven to be involved in activation of immune response genes. Moreover, NF-ATc3 and NF- κ B were reported to involve in transcriptional regulation of genes acting on T-cell activation and Th1 and Th2 cell differentiation (Serfling et al., 2000; Shinohara et al., 2009; Urso et al., 2011). Transcription of most of the protein coding genes was facilitated by the TATA-elements. Although there was no

evidence of TATA-box closer to the transcription start site in the putative promoter sequence of the RbSTAT4, there was a TBP binding region around -285 bp up-stream to the transcription start site. However, a considerable number of human core promoters were also recorded without TATA-like elements and rich in Sp1-binding sites (Yang et al., 2007a), which were prominently identified in predicted RbSTAT4 core-promoter region (**Fig. 6.2**).

Complete cDNA sequence of RbSTAT4 is comprised of 2516 bp together with a 53 bp 5' UTR sequence, a 2205 bp open reading frame (ORF) sequence which encodes for 735 amino acid polypeptide and a 255 bp 3' UTR sequence.

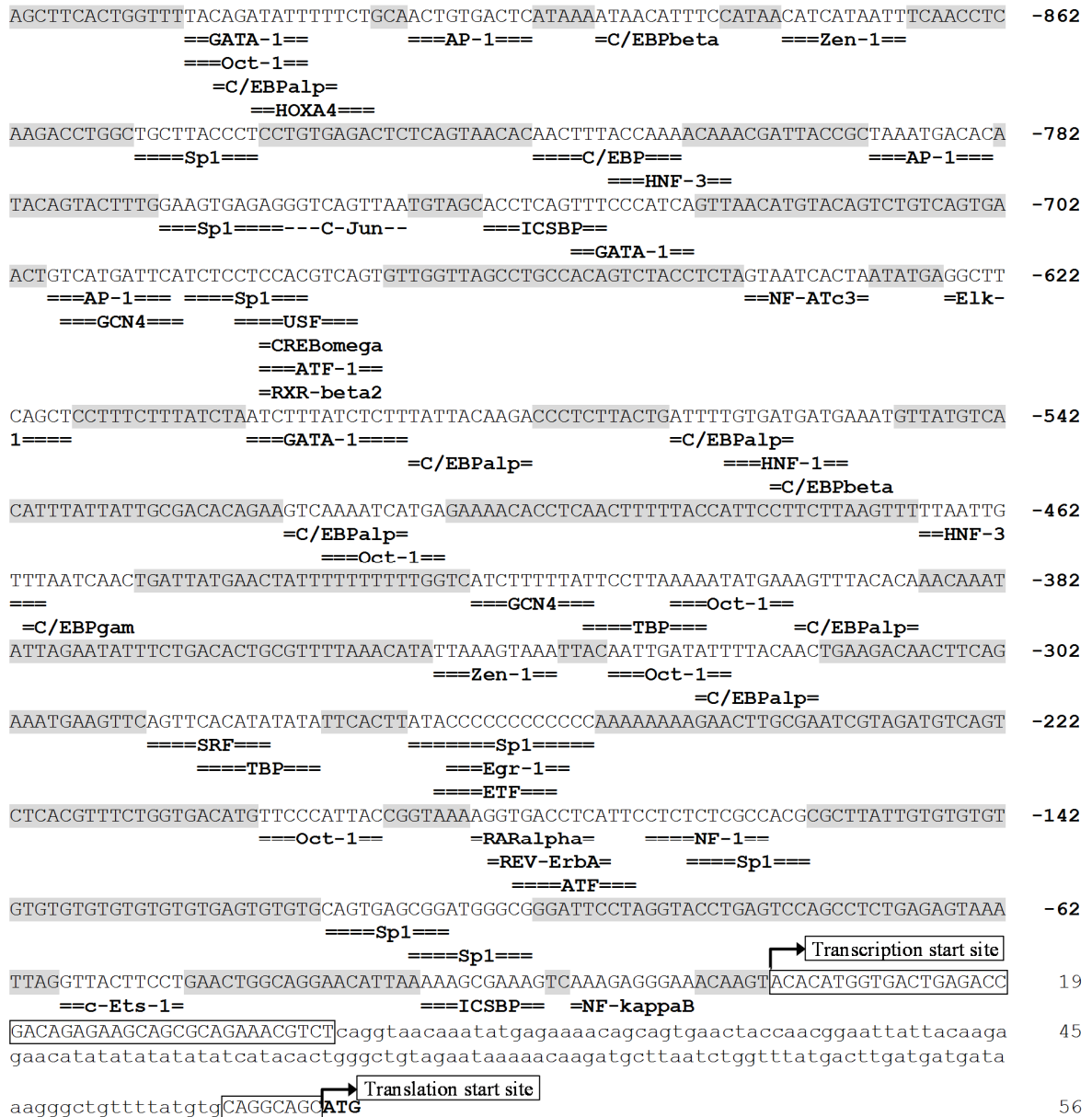


Fig. 6.2. Putative promoter region and transcription factor binding sites of the RbSTAT4. Respective transcription factors are indicated exactly below the TF binding site. Transcription start site and translation start site are marked with a bend arrow. 5' UTR sequence is boxed and first intron sequence is showed in small letters.

6.2.2. Sequence characterization

RbSTAT4 amino acid sequence analysis showed that the presence of characteristic conserved domains of the STAT4 members including N-terminal interaction (STAT_int) domain, STAT alpha (coiled-coil) domain, STAT bind (DNA binding) domain, linker domain, Src homology2 (SH2) domain and transcriptional activation domain. Moreover, within SH2 domain phosphotyrosine binding pocket, hydrophobic binding pocket and homodimer interface polypeptide binding sites were identified. Additionally, a crucial element for dimerization, tyrosine residue (Tyr⁶⁸⁴) which is phosphorylated by JAKs during the activation was well conserved within the transactivation domain (Murphy et al., 2000). However, other conserved phosphorylation residue, serine (Ser) in transactivation domain is replaced by threonine (Thr⁷¹⁴) in most of the analyzed fish species except in *Salmo salar* (Fig. 6.3). This phosphorylation site also reported to involve in regulation of STAT4 function by serine/threonine phosphorylation (Bacon et al., 1995; Santos and Costa-Pereira, 2011). Conserved NH₂-terminal domain of the STATs was reported to play a critical role in DNA binding which was not essential for dimerization (Xu et al., 1996). STAT4 is believed to bind to IFN γ activated sites (GASs) as a dimer stabilized through N-terminal domain interactions. However, a mutation of the N-domain in tryptophan residue W37 was reported to interrupt the dimer formation which leads to a prevention of IFN α induced tyrosine phosphorylation and nuclear translocation of the STAT4 (Murphy et al., 2000). Moreover, methylation of a conserved arginine (Arg-31) at N-terminal was reported to enhance the DNA binding activity in STAT1 in response to interferon stimulations (Mowen et al., 2001). Similarly, these two conserved Arg³¹ and Trp³⁷ residues were found at the same locations in RbSTAT4 also suggesting its conserved functional properties. However, STAT4 N-domain was reported to possess an unusual architecture (Vinkemeier et al., 1998). SH2-phosphotyrosine site is important for the interaction between two STAT molecules in order to form active dimers which translocate to the nucleus and activate the target gene expressions (Darnell et al., 1994).

According to the pairwise sequence alignment, RbSTAT4 showed very high amino acid identity and similarity with those of other fish species (highest identity to *Siniperca chuatsi*) and moderate identity and similarity with those of other mammalian and avian species (Fig. 6.3). However, similar to the previous reports, carboxy terminal region exhibited higher variation among different homologues, which plays a critical role for transcriptional activation by

phosphorylation (Becker et al., 1998). Multiple sequence alignment results revealed the clear conservation of most of the characteristic features of the STAT4 members discussed above. In evolutionary analysis, we used members representing all STAT family proteins distributed among mammals, avian, amphibian and fish species (total of 42 members). All the STAT families showed closer relation to each other with higher bootstrap values. RbSTAT4 was clustered within fish STAT4 clade, which is suggesting its orthologous nature in the STAT4 family (**Fig. 6.4**). Moreover, STAT4 clade showed a closer evolutionary relation to the STAT1 clade.

N-Domain

Rock bream MSQWQKIQQLERLLEHVDLDDNFPMDI... 117
Mandarinfinsh MSQWQKIQQLERLLEHVDLDDNFPMDI... 117
Salmon MSQWQKIQQLERLLEHVDLDDNFPMDI... 117
Zebrafish MSQWQKIQQLERLLEHVDLDDNFPMDI... 117
Frog MSQWQKIQQLERLLEHVDLDDNFPMDI... 117
Green anole MSQWQKIQQLERLLEHVDLDDNFPMDI... 120
Chicken MSQWQKIQQLERLLEHVDLDDNFPMDI... 120
Mouse MSQWQKIQQLERLLEHVDLDDNFPMDI... 120
Cattle MSQWQKIQQLERLLEHVDLDDNFPMDI... 120
Human MSQWQKIQQLERLLEHVDLDDNFPMDI... 120

Coiled coil domain

Rock bream MQEGGPLEKSLQNSVAFERKQNMDSR... 236
Mandarinfinsh MQEGGPLEKSLQNSVAFERKQNMDSR... 236
Salmon MQEGGPLEKSLQNSVAFERKQNMDSR... 236
Zebrafish MQEGGPLEKSLQNSVAFERKQNMDSR... 236
Frog MQEGGPLEKSLQNSVAFERKQNMDSR... 239
Green anole MQEGGPLEKSLQNSVAFERKQNMDSR... 239
Chicken MQEGGPLEKSLQNSVAFERKQNMDSR... 239
Mouse MQEGGPLEKSLQNSVAFERKQNMDSR... 239
Cattle MQEGGPLEKSLQNSVAFERKQNMDSR... 239
Human MQEGGPLEKSLQNSVAFERKQNMDSR... 239

DNA binding domain

Rock bream RRQQAIAIGGPLITGLDQLS... 356
Mandarinfinsh RRQQAIAIGGPLITGLDQLS... 356
Salmon RRQQAIAIGGPLITGLDQLS... 356
Zebrafish RRQQAIAIGGPLITGLDQLS... 356
Frog RRQQAIAIGGPLITGLDQLS... 359
Green anole RRQQAIAIGGPLITGLDQLS... 359
Chicken RRQQAIAIGGPLITGLDQLS... 359
Mouse RRQQAIAIGGPLITGLDQLS... 360
Cattle RRQQAIAIGGPLITGLDQLS... 360
Human RRQQAIAIGGPLITGLDQLS... 359

Linker domain

Rock bream EPRNLAFFGNPPRATNSQLSEVL... 593
Mandarinfinsh EPRNLAFFGNPPRATNSQLSEVL... 593
Salmon EPRNLAFFGNPPRATNSQLSEVL... 593
Zebrafish EPRNLAFFGNPPRATNSQLSEVL... 592
Frog EPRNLAFFGNPPRATNSQLSEVL... 595
Green anole EPRNLAFFGNPPRATNSQLSEVL... 595
Chicken EPRNLAFFGNPPRATNSQLSEVL... 595
Mouse EPRNLAFFGNPPRATNSQLSEVL... 594
Cattle EPRNLAFFGNPPRATNSQLSEVL... 594
Human EPRNLAFFGNPPRATNSQLSEVL... 594

SH2 domain and **TAD domain**

Rock bream FLLSSESHLGGITFTWVNDNG... 704
Mandarinfinsh FLLSSESHLGGITFTWVNDNG... 704
Salmon FLLSSESHLGGITFTWVNDNG... 700
Zebrafish FLLSSESHLGGITFTWVNDNG... 699
Frog FLLSSESHLGGITFTWVNDNG... 715
Green anole FLLSSESHLGGITFTWVNDNG... 712
Chicken FLLSSESHLGGITFTWVNDNG... 712
Mouse FLLSSESHLGGITFTWVNDNG... 712
Cattle FLLSSESHLGGITFTWVNDNG... 714
Human FLLSSESHLGGITFTWVNDNG... 714

	I%	S%
Rock bream	100.0	100.0
Mandarinfinsh	95.7	98.1
Salmon	80.4	89.3
Zebrafish	77.7	88.3
Frog	75.9	74.2
Green anole	58.8	77.6
Chicken	59.9	78.5
Mouse	58.5	76.6
Cattle	59.8	77.1
Human	59.9	77.4

Fig. 6.3. Multiple sequence alignment and pairwise comparison of RbSTAT4 with other STAT4 members. Residues in phosphotyrosin binding pocket and hydrophobic binding pocket are marked with blue and purple color, respectively. Completely identical and similar residues among all species are marked with asterisk (*) colon (:), respectively. The conserved residues among fish and mammals were shaded with gray and black colors separately. Conserved Tyr residue phosphorylation site is showed in red color box. Percent of identity (I%) and similarity (S%) of RbSTAT4 with other species are shown at the end of each sequences.

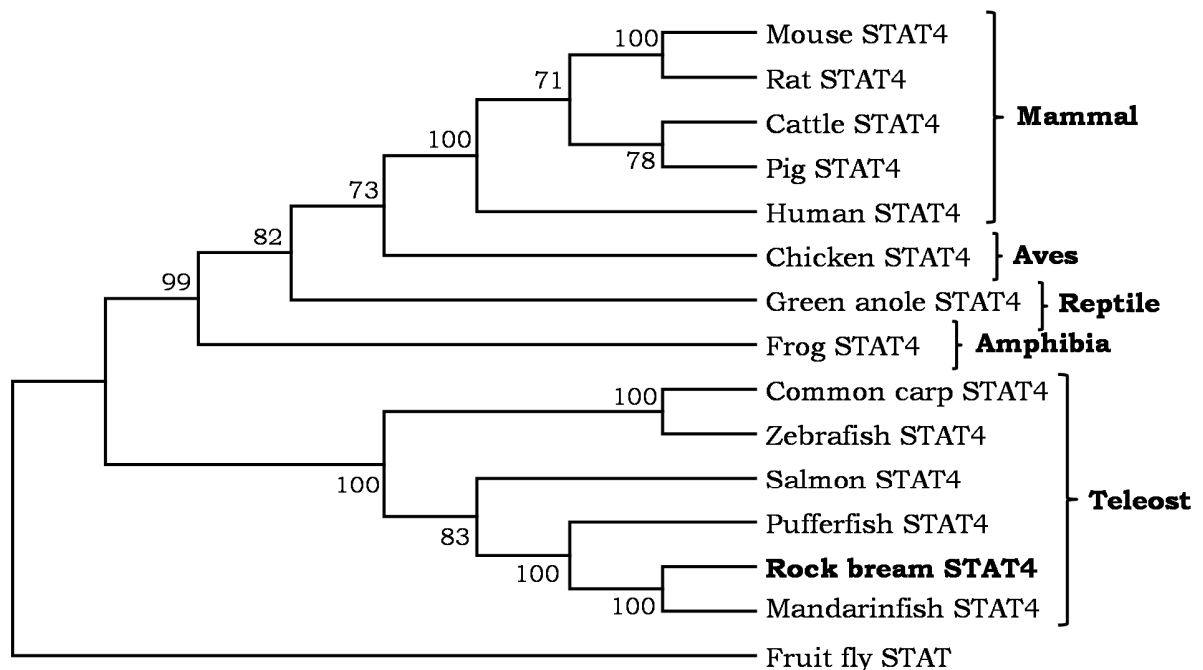


Fig. 6.4. Evolutionary relationship analysis of the RbSTAT4 with other members in the STAT4 family proteins. The tree is based on the alignment corresponding to the full-length amino acid sequences by ClustalW and MEGA (version 5). The numbers at the branches denote the bootstrap majority consensus values on 1000 replicates.

6.2.3. Tissue specific gene expression

RbSTAT4 was ubiquitously expressed in eleven different tissues examined in healthy rock breams. As lower level of expressions in most of the tissues including kidney, head kidney, intestine, brain, blood, heart, skin, and muscle were detected where muscle showed the lowest expression. However, in liver and spleen it was detected as moderate expression while the gill tissue showed highest (~35 fold compared to the blood) mRNA expression (Fig. 6.5). Although, STAT4 was reported to have a restricted distribution mainly within hematopoietic tissues

including thymus and spleen, myeloid cells and developing spermatogonia (Yamamoto et al., 1994; Zhong et al., 1994a), a recent study from mandarin fish showed its ubiquitous expression in different tissues similar to the RbSTAT4 (Guo et al., 2009).

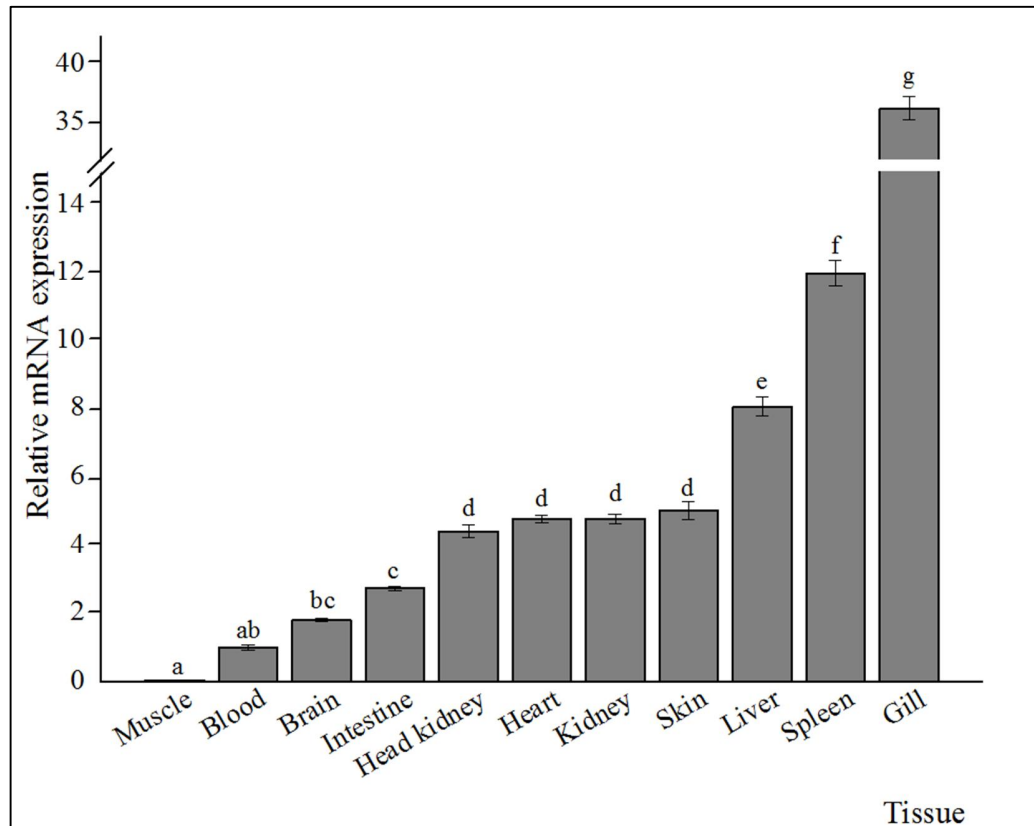


Fig. 6.5. Tissue-specific mRNA expression of the RbSTAT4 in healthy rock breams. Analysis of the mRNA level was carried out by qPCR and relative expressions were calculated compared to the mRNA level detected in blood. Data are represented as means \pm standard deviation ($n=3$). Statistical analysis was performed by one-way ANOVA followed by Duncan's Multiple Range test using the SPSS 16.0 program. Data with different letters are significantly different ($P < 0.05$) among different tissues.

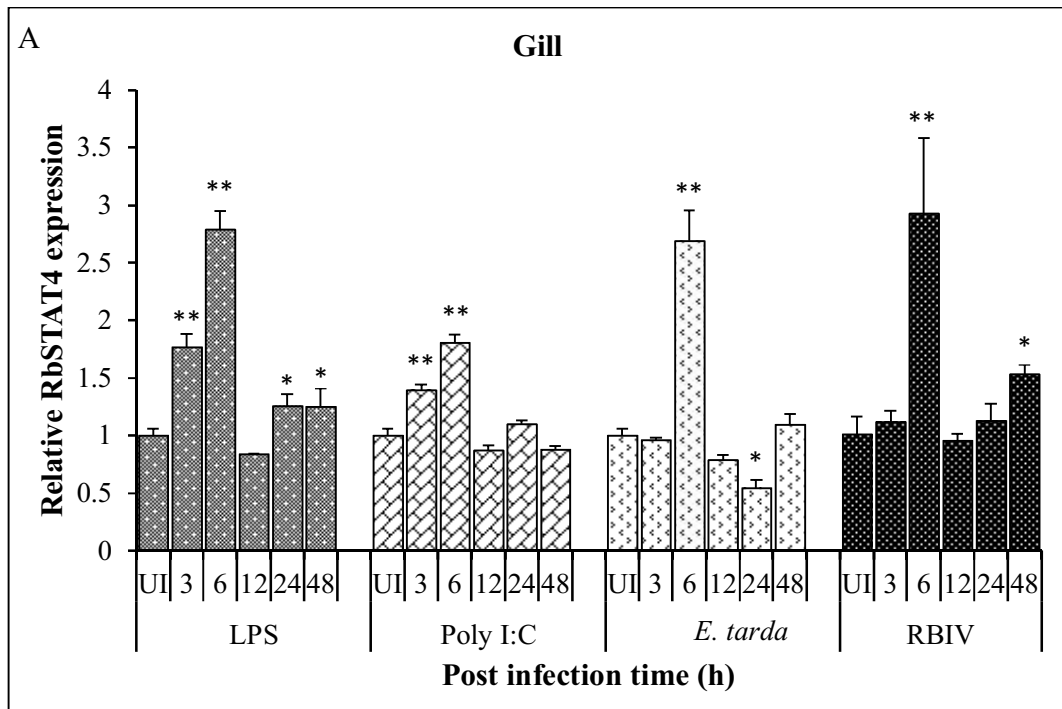
6.2.4. Regulated gene expression after immune stimulation

Three immune related tissues were selected for the temporal expression analysis in response to immune stimulations in the present study. Gill is an important organ involved in respiration as well as in immune regulation which is frequently exposed to the external environment. Head kidney and spleen are two important lymphoid and hematopoietic tissues, which involved in both innate and adaptive immune responses. LPS is a well-known endotoxin, Gram-negative bacterial cell wall component which was reported to induce the JAK/STAT signaling in mosquitoes (Lin

et al., 2004). After the LPS injection, a significant ($P < 0.05$) induction of relative RbSTAT4 expression was detected in gill tissue from 3 h of post infection (p.i.) to 48 h p.i., except at 12 h p.i. which was not significantly differed from basal expression (**Fig. 6.6A**). Similarly, in head kidney also showed a significant induction of relative RbSTAT4 expression at 3 h p.i. as an acute response and a significant down-regulation at 24 h p.i., while all other time points showed a basal level expression (**Fig. 6.6B**). However, in spleen it was continuously down-regulated after 3 h p.i. (**Fig. 6.6C**). A similar study with LPS stimulation reported only a mild change in STAT transcript level in shrimp (Chen et al., 2008), however, IL-12 or IFN α mediated IFN γ secretion was reported as a result of up-regulated STAT4 expression in response to LPS stimulation during the dendritic cell maturation or monocyte activation (Frucht et al., 2000). A synthetic analog of double-stranded RNA virus, poly I:C infection in rock breams showed a generally up-regulated expression pattern of the RbSTAT4 in all three tissues, except at 12 h p.i. in spleen where it was significantly down-regulated (**Fig. 6.6**). Poly I:C infection caused both acute and late responses in the head kidney tissue. However, in gill it was detected as early phase response compared to the late phase response detected in the spleen. This result is in agreement with a previous time-course study on poly I:C induction of MFF-1 cells showed a significantly induced expression of mSTAT4 from 6 h onwards (Guo et al., 2009).

In the case of live bacterial infection (*E. tarda*), head kidney showed significant up-regulation of the relative RbSTAT4 expression from 6 h to 24 h p.i., while in other two tissues it was only at 6 h p.i. However, in spleen the RbSTAT4 expression showed a dynamic behavior in response to the *E. tarda* infection (**Fig. 6.6C**). As a result of bacterial challenges, transcriptional activation and translocation of STATs to the nucleus were reported in insects (Barillas-Mury et al., 1999; Agaisse et al., 2003; Kim et al., 2011). Moreover, it was reported that JAK/STAT signaling is involved in both anti-bacterial and anti-viral responses in insects (Barillas-Mury et al., 1999; Lin et al., 2004; Dostert et al., 2005). Although *E. tarda* infection caused a significant induction of RbSTAT4 expression in head kidney, live RBIV infection did not cause any significant difference to the RbSTAT4 expression throughout the experimental period (**Fig. 6.6B**). However, in gill RbSTAT4 expression was detected as significant induction at 6 h and 48 h p.i. while, in spleen it induced at 6-12 h of p.i. (**Fig. 6.6A and C**). Similarly, transcriptional induction of STAT4 was reported in infectious pancreatic necrosis virus (IPNV) infected zebrafish embryonic cells (Wang et al., 2011). Moreover, WSSV infection also showed an increased level of

phosphorylated STAT in lymphoid organs of shrimp, although it showed a decreased transcriptional level of shrimp STAT (Chen et al., 2008). Furthermore, a dynamic regulation of the STAT4 phosphorylation through the type 1 IFNs was observed after a viral infection in mice (Nguyen et al., 2002a).



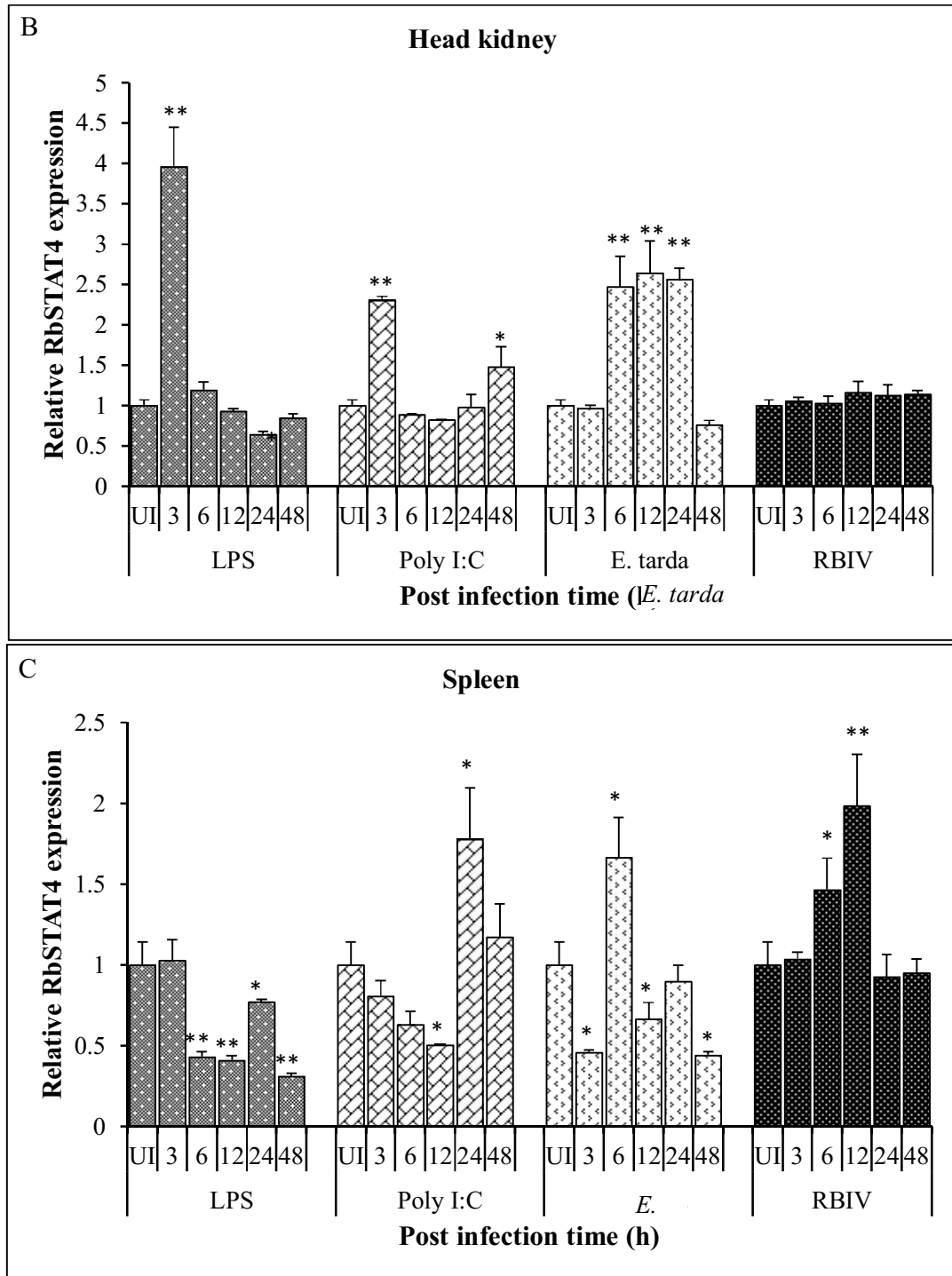


Fig. 6.6. Relative mRNA expression of RbSTAT4 in response to LPS, poly I:C, *E. tarda* and RBIV infections in (A) gill, (B) head kidney and (C) spleen tissues. The mRNA levels were detected by qPCR and data are represented as means \pm standard deviation (n=3). Statistical analysis was performed by t-test and asterisks indicate significant differences (* $P < 0.05$; ** $P < 0.01$) to the un-injected control (UI).

6.2.5. Regulated gene expression after tissue injury

The expression profile of *RbSTAT4* mRNA in blood cells and liver tissue were detected with controversial results. As shown in **Fig. 6.7**, the expression of *RbSTAT4* transcripts were significantly elevated at 6 h post-injury in rock bream liver tissue, while showing no changes in other time points compare to the un-injured control. In the case blood cells, *RbSTAT4* expression was significantly suppressed from 3 h to 24 h post injury and at 48 h reached to the normal expression level. The results of this study indicate that *RbSTAT4* may involve in wound healing process, and particularly blood cells showed more potent effect. However, the real mechanism behind this is yet to be elucidated.

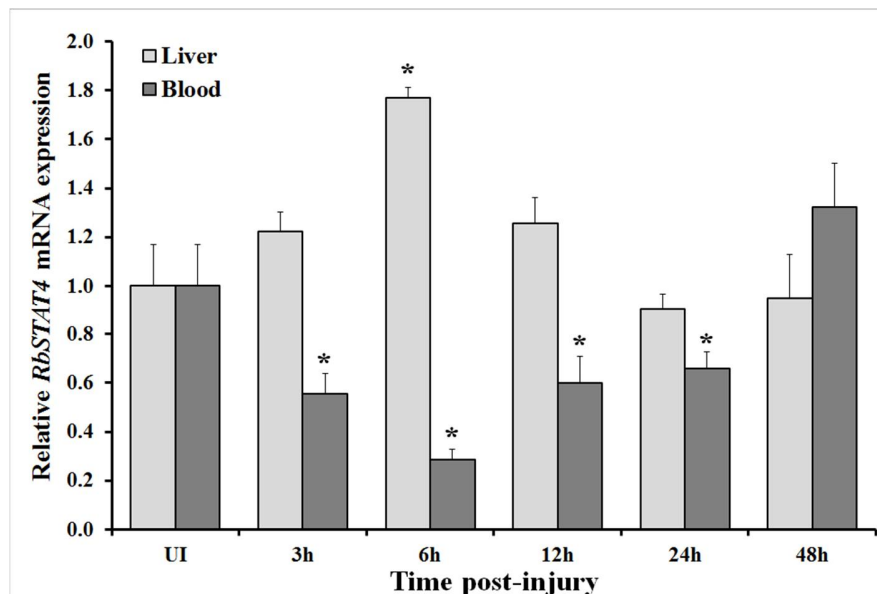


Fig. 6.7. Relative mRNA expression of *RbSTAT4* in blood cells and liver tissue in response to the injury. The rock bream β -actin was used as an internal reference gene to calculate the relative mRNA expression. The fold change of expression at each time point was compare with un-injured control (UI) and represented as relative mRNA expression. The vertical bars represent the mean \pm standard deviation (SD) of triplicates, and results were statistically compared relative to the un-injured control (UI) using t-test. Data with statistically difference at $P < 0.05$ are indicated by asterisks.

6.2.6. Regulated gene expression after *in vitro* challenges

In order to determine the impact of interleukin-10 on *STAT4* transcription, the level of mRNA expression was examined after treating rock bream heart cells with rRbIL-10 protein. Results revealed that the expression of *RbSTAT4*mRNA was significantly ($P < 0.05$) up-regulated after 3

h post-treatment and peaked at 6 h post treatment of rRbIL-10, while showing a down-regulated expression at 48 h (Fig. 6.8).

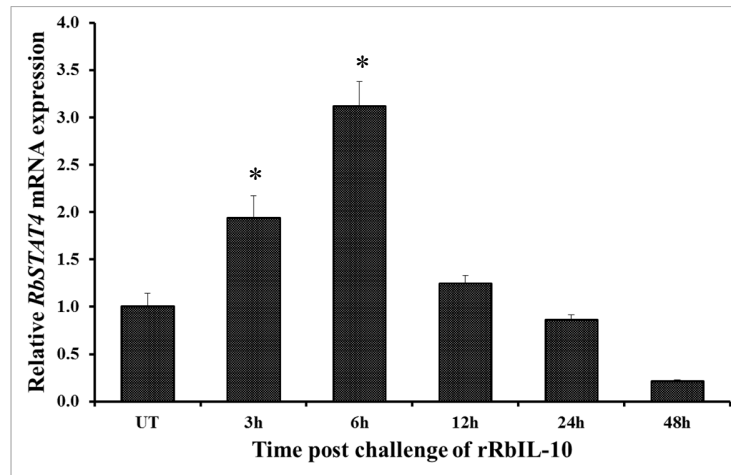


Fig. 6.8. Relative mRNA expression of *RbSTAT4* in heart cells upon in vitro challenge with rRbIL-10. The rock bream β -actin was used as an internal reference gene to calculate the relative mRNA expression. The fold change in mRNA expression is represented as relative to mRNA level of MBP-treated cells at each time point. The vertical bars represent the mean \pm standard deviation (SD) of triplicates, and results were statistically compared relative to the untreated control (UT) using t-test. Data with statistically difference at $P < 0.05$ are indicated by asterisks.

Previous studies have been shown that the expression of STAT4 could be modulated by various interleukins. IL-12 is a key immunoregulatory cytokine that coordinates innate and adaptive immune responses through STAT4 activation, which produced mainly by macrophages and dendritic cells in addition to the monocytes, B cells and neutrophils in response to pathogenic infections, including bacteria, virus, fungi and parasites (Watford et al., 2004). In addition, microbial products also reported to induce the T-cell independent IL-12 production via Toll-like receptor signaling (Medzhitov, 2001; Barton and Medzhitov, 2002), which helps us to suggest that RbSTAT4 may involve in immune mechanisms for both bacterial and viral infections. IFN γ is a well-known effector cytokine involved in control of intracellular viral infections, activated by STAT4 through the IL-12 signaling pathway (Laing and Hansen, 2011). However, both IL-12 and IFN γ are yet to be discovered in the rock bream genome.

In addition to the IL-12, IL-23 and type 1 IFNs also reported to activate the STAT4 directly, to induce the IFN γ production during the viral infections in mice, and STAT4 was reported to bind with 5'-upstream sequence of the murine IFN and human perforin genes (Nguyen et al., 2002; O'Shea and Plenge, 2012; Yamamoto et al., 2002). Hence, here we compared the RbSTAT4 expression results with our previous data on type 1 IFN mRNA expressions against the four types of infections in head kidney tissue (Wan et al., 2012). Similar to the RbSTAT4 expressions, both IFN1 and IFN2 also showed induced transcriptional levels in response to all four challenges. More specifically, *E. tarda* infection caused significant elevation of both IFN2 and RbSTAT4 expressions at the same time points. Moreover, both IFN1 and IFN2 showed only mild regulations at some time points in response to RBIV infection, where RbSTAT4 did not respond to the RBIV infections in head kidney suggesting the link between type 1 IFNs and STAT4. This suggestion is in agreement with a clear relationship observed between STAT4 activation by the IFN- α/β for IFN- γ production in lymphocytic choriomeningitis virus (LCMV) infected mice (Nguyen et al., 2002).

Furthermore, STAT4 was reported to enhance the interferon regulatory factor-1 (IRF-1) gene transcription by binding to the IRF-1 promoter in human NK and T-cells (Coccia et al., 1999; Galon et al., 1999). IRF-1 is a transcription factor involved in regulation of IFN genes and IFN-inducible genes in Th1 responses through regulation of T-cell maturation, Th1 and NK cell development (Coccia et al., 1999), and to date transcriptional regulation of IRF-1 was reported from different fish species in response to viral infections (Collet et al., 2003; Yabu et al., 1998; Yao et al., 2010). In the present study, we compared the rock bream IRF-1 mRNA expression (Accession no. GQ903769) in gill tissue after the poly I:C infections. Similar to the RbSTAT4 expressions detected in gills, rock bream IRF-1 also showed a significant up-regulation of mRNA expression after the poly I:C infections throughout the experimental period with higher magnitude and exactly similar pattern of expression to the RbSTAT4 (un-published data), suggesting the involvement of RbSTAT4 in viral response gene regulation.

6.3. Conclusion

Herein, we identified a member of the STAT4 family; RbSTAT4 from the rock bream at genomic level and investigated the time-course expression against the *in-vivo* infection of two

different immune stimulants (LPS and poly I:C) and real pathogens (*E. tarda* and rock bream iridovirus) to the first time in a fish species. According to the transcriptional regulation of RbSTAT4 observed in this study, we suggest that RbSTAT4 might involve in immune regulation mechanisms and/or signaling cascades functioning against both bacterial and viral pathogens in rock bream. In addition, the expression of RbSTAT4 was significantly modulated after tissue injury. Further the RbIL-10 also showed great impact for the expression of RbSTAT4. Hence, the findings of this study will help to extend the knowledge on diverse biological functions of the STAT4 family members with respect to their immune regulation mechanisms in teleost species. Nevertheless further investigations are required to clarify the detailed involvement of STAT4 in immune regulation in teleosts, along with the other members of the respective signaling pathways.

CHAPTER 7

Two teleostean signal transducer and activator of transcription 5 (STAT5) orthologs from rock bream *Oplegnathus fasciatus*: Genomic structure, transcriptional modulation and subcellular localization

Abstract

Signal transducer and activator of transcription (STAT) family members are key signaling molecules that transduce the cellular responses from cell membrane to nucleus upon janus kinase (JAK) activation. Even though the seven STAT members have been reported and extensively studied in mammals, limited studies are available for the STAT genes in teleosts. In this study, we have identified and characterized two STAT paralogs homologous to the STAT5 from rock bream, *Oplegnathus fasciatus*, and designated as RbSTAT5-1 and RbSTAT5-2. In comparison of deduced amino acid sequence of RbSTAT5-1 (786 aa) and RbSTAT5-2 (786 aa) with other counterparts revealed the conserved residues important for functions and, typical domain regions including N-terminal domain, coiled coil domain, DNA binding domain, linker domain, Src homology 2 (SH2) domain and trans activation domain (TAD) as mammalian counterparts. Analysis of gene phylogeny revealed that RbSTAT5-1 and RbSTAT5-2 were clustered in separate groups in fish clade indicating distinct evolution. According to the genomic structure of *RbSTAT5-1*, the coding sequence was distributed into eighteen exons with seventeen introns. The immunologically essential transcription factor binding sites such as ICSBP, ISGF-3, GATA-1, HNF-3, SP1, C/EBP, Oct-1, AP1, c-Jun, IRF-1 and NF- κ B were predicted at the 5'-proximal region of the *RbSTAT5-1* gene. The expression level of *RbSTAT5-1* and *RbSTAT5-2* mRNA was measured in different tissues and revealed that the highest level of both *RbSTAT5s* transcripts was detected in blood cells. The temporal expressions of *RbSTAT5s* were analyzed upon live bacterial, viral and PAMPs stimulations and, revealed the significant elevations indicating their immune modulation. In addition, expressional analysis in injured fish also implied the potential role of RbSTAT5s in wound healing process.

7.1. Introduction

The Janus kinase/signal transducer and activator of transcription (JAK/STAT) signaling cascade which comprises of 3 main components including receptors, JAK and STAT, is an important to transmit the information received from extracellular peptides to the nucleus (Aaronson and Horvath, 2002). In mammals, the JAK/STAT pathway is the principal signaling system in response to the wide array of cytokines and growth factors and, mediates the various biological events such as immune responses, proliferation, differentiation, cell migration, apoptosis and cell survival (Rawlings et al., 2004; Harrison, 2012; Richard and Stephens, 2014).

The STAT proteins are key transcription factors that transduce the signals into the nucleus upon phosphorylation via JAK activation. Once the activated STAT proteins reach to the nucleus, they can interact with the corresponding transcription factor binding sites of promoters that belong to the cytokine inducible genes and activate the transcription (Darnell et al., 1994; Mitchell and John, 2005). Up to date, there are seven STAT members (STAT1, STAT2, STAT3, STAT4, STAT5a, STAT5b and STAT6) were identified and well documented in mammals (Stark and Darnell, 2012). Structurally these all STATs are resemble and shared common topological domains including N-terminal domain, coiled coil domain, DNA binding domain, linker domain, Src homology 2 (SH2) domain and transcriptional activation domain even though they functionally unlike (O'Shea et al., 2002).

The STAT5 protein, one of the most important members of the STAT family, is activated in response to the wide range of cytokines and hormones such as interleukin-2 (IL-2), IL-3, IL-5, IL-7, IL-9, IL-15 erythropoietin, thrombopoietin, growth hormone and prolactin (Teglund et al., 1998; Takeda and Akira, 2000). In mammals, two closely related isoforms referred as STAT5a and STAT5b, have been identified and showed their specific functions using STAT5a and STAT5b knockout mice. The STAT5a is crucial for the Prl-mediated mammary gland development, whereas STAT5b is essential for the sexually dimorphic growth (O'Shea et al., 2002).

The identification and functional investigations of members in teleostean JAK/STAT signaling cascade is not completed yet. Studies reporting the structural characteristics and functional aspects of teleostean STAT5 are very limited. Genomic structural characterization of STAT5 ortholog has been reported by Sung *et al*, from pufferfish, and showed the high conservation

with mammalian counterparts (Sung et al., 2003). Meanwhile, another study described that two STAT5 isoforms identified from zebrafish have been undergone independent gene duplication (Lewis and Ward, 2004). In addition, several JAK and STAT members including STAT5 have been identified from mandarin fish, and demonstrated their structural features and functional role in response to the poly I:C (Guo et al., 2009).

Rock bream, *Oplegnathus fasciatus* is one of the most important marine teleost fish commercially cultured in Republic of Korea. During the past decades, the frequent disease outbreaks were observed due to the habitat contaminated with chemicals and microbial pathogens and, thereby caused great effect for the fish production. Investigation of signaling cascades like JAK/STAT that has not been completely established in fish might be essential for the improvement of health management and disease control of rock bream culturing. In the present study, two members of STAT family homologous to STAT5 was identified from rock bream and characterized in cDNA and genomic level. To understand the molecular evolution, comprehensive sequence analysis was conducted in terms of phylogeny and genomic organization with other STAT5 family members. For the functional aspects, spatial expression in several adult tissues and, temporal expression in adult liver and blood cells upon pathogenic and PAMPs stresses and following tissue injury were investigated.

Table 7.1. Primers used in this study

Primer	Purpose	Sequence, 5'-3'
<i>RbSTAT5-1-F</i>	BAC screening	AGTCCCAGTTTAGTGTGGAGGCA
<i>RbSTAT5-1-R</i>	BAC screening	AAGCACCTTATCTGGCACGAGGAA
<i>RbSTAT5-2-F</i>	BAC screening	AGAGCTTACCTGGACGCAACTTCA
<i>RbSTAT5-2-R</i>	BAC screening	TGGTGCTTGTTTACAAAGCCCAGG
<i>RbSTAT5-1-F</i>	qPCR amplification	GCCAATCCAGACCCAGCAAGT
<i>RbSTAT5-1-R</i>	qPCR amplification	TACATGCCTCGCCACGTCC
<i>RbSTAT5-2-F</i>	qPCR amplification	CAGTGGAGGAACTCCTACGTTTCATGG
<i>RbSTAT5-2-R</i>	qPCR amplification	CACGTCCATCGTGTCGTCCAG
<i>Rb b-actin F</i>	qPCR internal reference	TCATCACCATCGGCAATGAGAGGT
<i>Rb b-actin R</i>	qPCR internal reference	TGATGCTGTTGTAGGTGGTCTCGT
<i>RbSTAT5-1/pcDNA-F</i>	Clone into pcDNA3.1(+)	(GA) ₃ gaattcATGGCAGTGTGGATCCAGGC - EcoRI
<i>RbSTAT5-1/pcDNA-R</i>	Clone into pcDNA3.1(+)	(GA) ₃ ctcgagGGTCAAGGGTCAGGACTGTTGG - XhoI
<i>RbSTAT5-2/pcDNA-F</i>	Clone into pcDNA3.1(+)	(GA) ₃ ggtaccATGGCAATGTGGATCCAGGCC - KpnI
<i>RbSTAT5-2/pcDNA-R</i>	Clone into pcDNA3.1(+)	(GA) ₃ ctcgagTCAGGACTGCTGACTGCTCCA - XhoI
<i>RbIL-10/pMAL-F</i>	Clone into pMAL-c5x	(GA) ₃ gaattcAGTCCCATGTGCAACAACCACTG - EcoRI
<i>RbIL-10/pMAL-R</i>	Clone into pMAL-c5x	(GA) ₃ aagcttTCAATTAGAGGCCACTTGTTTTCGGAC - HindIII

Restriction sites in the cloning primers are shown with small case letters and indicated at the end of each primer sequence.

7.2. Results

7.2.1. Characteristics of RbSTAT5-1 and RbSTAT5-2 cDNA sequences

7.2.1.1. Primary sequence characterization

Two cDNA sequences (*RbSTAT5-1* and *RbSTAT5-2*) bearing complete CDS homologous to the *STAT5* were identified from rock bream transcriptome database. The complete CDS of *RbSTAT5-1* gene (4467 bp) was composed 2358 bp excluding stop codon and encoded for 786 aa poly peptide. The molecular mass and theoretical isoelectric point (*pI*) of predicted protein of RbSTAT5-1 was 89.8 kDa and 6.04, respectively. In addition, 45 bp of 5'-untranslated region (UTR) and 2064 bp of 3'-UTR were obtained (**Fig. 7.1a**). Meanwhile, the cDNA contig of *RbSTAT5-2* (2718 bp) was also known to be contained a CDS of 2358 bp excluding stop codon and coded for 786 aa poly peptide with 89.5 kDa of molecular mass and 6.01 of *pI*. The 5'- and 3'-UTR of *RbSTAT5-2* were 139 bp and 221 bp in length, respectively (**Fig. 7.1b**).

AGAGTTTCTCTGTACATGTAAACAGAGCTGAAGCCAGAGATGGCAGTGTGGATCCAGCCACGACCTCCAGGGAGATGCTCCGACCAGATGC 100
M A V W I Q A Q Q L Q G D A L H Q M
AGTCTCTGACCGTCCAGCTTCCCACTTGGAGTGGCATTATCTGTCCAGTGGATAGAGGCCAGCTCTGGATGCCATAGACCTGGAGAACCACA 200
Q S L Y G Q H F P I E V R H Y L S Q W I E G Q L W D A I D L E N P Q
GGAGGAGTTCAAGGCCAAACGCTTCTGGACAGTCTGATCCAGGAGCTGCAGAAAGGCCGAGCAGGAGGGAGGAGCGGCTTCTTCAAAATC 300
E E F K A K R L L D S L I Q E L Q N K A E H O V G E D G F L L K I
AACTGGACACTAGCCAGCCAGCTCAAGAGCAGTATGACCCGCTGTCTCTGGAGTGGTCCGATGCATCAAAACATCTCTACACAGAGCAGAGGC 400
K L G H Y A S Q L K S T Y D R C P L E L V R C I K H I L Y T E O R
TGCTCAGAGGCCACCAATTTGAGCTCTCCAGTGGCGGGATGATGGACAGCATGTCTCAGAAATACCAACAGATCAACCAAGCTTTTGGAGGAGCTTCG 500
L V R E A T N S S S P V G G M M D S M S O K Y Q Q I N Q A F E E L R
CCTGCTCACCAGGACCTGAGAAATGATCTCCGCAAGCTCCAGCACAACCAGGACTTTCATCATCCAGTACCAAGAGGCTCCCGATCCAGGCTCAG 600
L L T Q D T E N D L R K L Q H N Q E Y F I I Q Y Q E S L R I Q A Q
CTAACCGCTGGCCGCGCTTCCCTCCGCTGACCGACAGCTACCGGAGCCAGCCCTTCTCAGCAAGAGAGCCACTGTGGAGGATGCTGACAGAGAGG 700
L T S L A A L P P A D R Q L R E P A L L S K R A T V E A W L T R E
CCAAACACTACAGAAATCAGACTGGACCTGGCAGAAAGCAGAAACACTGCAGCTGTGGAGGAGCAGGACCATCATCTGGATGACGAGCT 800
A N T L O K Y R L D L A E K H Q K T L O L L R K Q O T I I L D D E L
GATCCAGTGGAGAGCCGCAACAGCTGGCAGCAACGGGGCCCAAGAGGGAGCCCTGGACATCTGTCAGTCTGGTGGAGAGCTGGCAAAACT 900
I Q W K R R Q Q L A G N G G P P E G G L D I L Q S W C E K L A E T
ATCTGGCAAAACAGGACAGATTCGAGGCGCAGAGCCTCAGACACAGCTGCCATCCCGCCCTTGAAGAGCTCTCAACAGCTCAACAGTA 1000
I W Q N R Q Q I R R A E H L R Q O L P I P G P I E E L L N E L S
CTATCAGATATCATCTCAGCATTTGTCACAGCCTTTCATATTGAGAAACAGCCTCCACAGTGTCAAAAACCCAGACAGGTTTGTCTCAAGCT 1100
T I T D I S A L V T S T F I I E K Q P P Q V L K T Q T K F A A T V
GCCTCTTAGTGGTGGAAATGAACTGACATGAATCTCCCGAGGTCAAAAGCCACATCATATTGAAACAGGCAAGCCCTGCTGAGAAAC 1200
R L L V G G K L N V H M N P P Q V K A T I I S E Q Q A K A L L K N
GAGAACACAGGAATGACAGCTGGGAAATCTCAACAATACTGTGTGATGGATACACAGACTACAGCAGCTCAGCCCTCAGGACCAAGCA 1300
E N T R N D S S G E I L N N N C V M E Y H Q T T G T L S A H F R N
TGCTTTGAGAGGATCAAGAGCTGGACAGGCGAGCAGAACTGTACAGAAAGAGGTCACCATCTGTTCGAGTCCAGGTTAGTGTGGAGG 1400
M S L K R I K R S D R R G A E S V T E E K F T I L F E S Q F S V G G
CAATGAGCTTGTGTTCAAGTGAAGAGCTTATCACTTCTGTAGTGGATAGTTCACGCTAGCCAGACAAATATTCACAGCAACTGTGTGGAG 1500
N E L V F Q V K T L S L P V V V I V H G S Q D N N A T A T V L W D
AATGCTTTGAGAGGCGGAGCGGCTTCTCTGTCGCAAGTAAAGTCTTTGGCTCAGCTGTGTGATGCCATCAATGAAGTACAAGGCTGAGG 1600
N A F A E P G R V P F L V P D K V L W P Q L C D A I N M K Y K A E
TACAGAGTAAACGAGCCTGTCTGAGGAGAACTGGTCTTCTGCTCAAAGGCCCTCAGCAGCTCCAGCAACCAACCTGAAAGCTACCCGAACTGAC 1700
V Q S N R G L S E E N L V F L A Q K A F S S S S N N P E D Y R N M T
TATGACTTGTGACAGTTTAAACAGGAAAGCTTCCAGGAGGAGCTTACATTTTGGCAGTGGTTTGTAGTGTGATGGAATCACAAGAAAGCATCTC 1800
M T W S Q F N R E S L P G R S F T F W Q W F D G V M E L T K K H L
AAACCACTGAAAGCAGGACCATATTAGGCTTTTGAACAAGCAGCAGCTCAGGACATGTCGATGCCAAACCAACCGTACTTCTCTGCGCT 1900
K P H W N D G A I L G F V N K Q Q A Q D M L M S K P N G T F L L R
TTAGTACTTGAAGTGGAGAAATCAAAATGCCCTGGTGGCAAAATCTCAACAAGCAGGTGAGAGAAATGGTTTGAAGCACTGACCTACACAAC 2000
F S D S E I G G I T I A W V A E N P N K A G E R M V W N L M P Y T T
CAAAAGCTTCCATTCCTGCTGGCTGACCGCATCAGCGATCTCAATCACTTCTGTCTCTACCCCGCAGCAGCAAGGAGGAGGTTTCTCCAAA 2100
K D F S I R S L A D R I S D L N H L L F L Y P D R P K D E V F S K
TATTACACCCCACTTCCAAAGCAGTGGACGCTAGCTGAAACCAAAATTAACAAGTGGTCCAGTGTGCCACAGCAATCCAGCCAGCA 2200
Y Y T P P L S K A V D G Y V K P Q I K Q V V P E F A T A N P D P A
GTGGAGAACCAACTTATGATCAGCGCCCTCCAGCAGCTGCAATCACTCAGCCTCAGCAGCATATACCCACTATGAGTGAATCTATGTTGGA 2300
S G N P T Y M D H G A S P A P V N H P H T Y G I Y P P M S D S M L D
CCCGAGCGGAGACTTCCAGCTGACAGCAGCATGAGCTGGCGGCGCATGTAGAGGAGCTACTCCGCGCGCTGTAGAGAGCCAGTGGCGCGCCCAACAG 2400
A D G D F D L D D T M D V A R H V E E L L R R P V E S Q W G G Q Q
TCTGAGCCCTTGACATTTAAACCGGACACACCAAAACCCCTGCCCTCCCAACCTGCGCCACTGCAATTTGATGTTTAAATCCATTTCA 2500
S *

TTTCTCTTTTTTTCAGCTAGCTATAATGTGAAATGTAATAAGTGGTGTGATTTTTTTTCTTCCAGCATGAGAGCATGCATGTCAGTGACTTCTCTT 2600
AGTTTTATTTGTGTCCATAGGTGTTTGTAAAAACAGACTAGGCATAATGCAAAACCTCAGGTGTACAGTATTGTGAAAAAGAAATGTCATTCACATTTGT 2700
CATGCAATTTCAATTTGATTTTGAACAGATTTTCAAAAAAATGCTACTGTATGAAGTCAATTTAACAGTTGAAATGTTTTCATTTTGTATATTTTCTTC 2800
TTTGTAAATGGGTTATGATGATTTTGTAGTGAATTTGAACTTGCCTTTTGAACAAAAAAGAACTTAAATGGAGAGTTTGTCTTTTGTCTTAAACA 2900
TTATCTGATTTACTGCTGACAGATTTACAGTCACTTTTCAAAATCATAACACTAAAGCAGAGTGAATCTCTTGTCTGACCTGACAGC 3000
ACACACATCAGCAGCAGTACACATGGCAAGTGTACAGTATTTTGTCTGATTTTGTTCACAGCTGAAACCCAGGAGGGGGTTTATGCACTCCCTC 3100
GCTCTCAGAGGCTATTGCTCTCTTGTACACAAATGCAAACTAAGCATTTACCCAGGCTGCTGCTGTCTCTCAGGTCCTCTGTTCTC 3200
TCATCAATGCTCCATTTACTTACTGACAGCTGTGTTACTATTGGTCTGTGTTGTTCTGACACATTCACACAGTAGGTACCTTTATTTGG 3300
GTTTTGCTTGTAAATTTGTGTTAATGTGTGGAAGAAGTCCCTTGTGCCCCGAGGCTAATCTGCTGCTGTTTATGCTTGAACCACTACCTG 3400
TGAAGTCTAGAGGATGAAAGTGTACATGCTGCTGGTATGCTGAAATTTCCGGGCTCTGCTGCTCTTCTGACTCTCTGCTTATCCGTCACCTTG 3500
CCCCCTAGCTGTGTCAGACTGTGGCAAAACAGCATGTGCAAGTCTGCTGATGACAACTGGGCAACAGCAGCTGAAAGTGGAGGCAATAGATA 3600
GATTCATGACAGCTTTGAGTGTGTCACAGACTACTAGCCGCTGGGCCACATATAGAGCTCAAGGATGTAGTGCCTTTGTTATTGTTGCAAGATTAGT 3700
TTTCTTCTCCCCCACTTTTCTACACATAAAAGATAACAAATACATTAAGTCTGATAGAACAGTTGACACACAAATAGAGAAATATGCTGTGACA 3800
ACAGCTTGCACCTCAGGAATGAATGCTTGTGCTAGCTGATGATAAGCCAAATAGAAATATATCTATGATACAGAAATATGAAATTTATTTCTCTA 3900
TCATAATCTATTTTATTTATTTCTCTGCACTCCCTGTTGAAATGTAACCCCTTTTGCATGACCTGTTAAGGATTTACGTACAAATGGATCCCTCAGG 4000
CTGACGCAAGTTTCAAGTCTGCTGCAAAAGAAAGTACCAAGTGAAGAAAGCAGACAGCACTGGAATCAGAGAAAGAAATTTAGTATGACTTTTGTGT 4100
TTTCCAAACAGACATTTACAGTATTAATAATTTCCCTGCTATCTTTTCTTCTTCTGAAACATTTTGTGATCTGCTTTCTTTCTGTTTGTAA 4200
GTCTCAAGCTACATGGGAGCTGTGTGATACACCTTACCATATTCTCATCATTTTACGCTTTGTTCCACTGTAGACTGTGATTTTGTGACGA 4300
TGTAGATGGCCCTGCGTCTGTGATGTATGATCATGTTTGTGGATTTGATTTAACACTTGGAGGTTTCCAAAGAAATAGCTGTGAGTTGAAAG 4400
AAGAAAAAAGTTTTATAAATAATTTAACTCAACATGTAGAAGTACAGAAGATTTTGTGATCACT 4467

Fig. 7.1a

```

AGAAGGCGATAAAGTAGTGGCGATGTGATATGTACGTCAAAACCACTGTGTTAGGTTTAAAGTGTACTTGTATGCTGTCGGTGTCTCATGGTG 100
TTGCTGTAAGGTGTGTCTGCTCTCTTAAAGGAAGCACCATGGCAATGTGGATCCAGGCCAGCAGCTGCAGGGTGAGGCGTTGCACCAGATGCAGGCC 200
M A M W I Q A Q Q L Q G E A L H Q M Q A
TGTACGGCCAGCACTTTCCCATAGAGGTGCGACACTACTGGCCAGTGGATTGAGAGCCAGCTCTGGGATTCAGTGGAGTTGGACAAACCCAGCGGAGGA 300
L Y G Q H F P I E V R H Y L A Q W I E S Q L W D S V E L D N P A E E
AGCTAAAGCCAGCGCTGTCTAGACAACTGTGGCCGAGCTGCAGAGGAAAGCCAGCTTCAGGGAGGAGAGACGGCTTCTCTCTCAAGATCAAGCTG 400
A K A K R L L D N L V A E L Q R K A Q L Q G G E D G F L L K I K L
GGCCACTATGCCAACAGCTCAAGAGCACTTATGACCCTGTCTTGGAGCTTGTGGCGTGTATAAAACACATCTGCAGTCAGAGCAGAGGCTGGTTC 500
G H Y A N Q L K S T Y D R C P L E L V R C I K H I L Q S E Q R L V
AAGAAGCTACAAATGCCAGCTGTGGAGTGGGGCGGCGCATGGACAGCTGTACAGCGTCCACAGCAGATCAACAGCGCTTTTGGAGCTCCGCT 600
Q E A T N A S C G S G G Q A M D S L S Q R H Q Q I N Q A F E E L R L
GGCAACCCAGGAGACTGAGAATGAACCTGAGAAAGCTGCAGCAGCAGCCAGGAGTACTTTATCATCCAGTACCAGGAGAACCTGGCGCTCCAGGCCAGCTG 700
A T Q E T E N E L R K L Q H S Q E Y F I I Q Y Q E N L R I Q A Q L
AGCACCTGTCTTCACTGCTCCAGCTGAGCGCCACCCAGCCGGAGACCACTGCAGAGCAAGAGGCCACTGTGGAGCTGCTCCACAGAGAAAGCCA 800
S S L S S L P P A E R T Q R E T T L Q S K R A T V E A W L T R E A
GCACACTACAGAAATACAGGCTTGTATGTCCAGAACACACAGAAAGCCCTGACCCTGCTGAGGAGCAGCAGACTGTGATCTCGATGAGGAACTCAT 900
S T L Q K Y R L D L S E Q H Q K T L T L L R K Q Q T L I L D E E L I
CCAGTGGAAAGAGGAGCAGCTGGCTGCAATGGGGTCTCATGAGGGGGACTGGATGTCCTCAATCTGGTGTGAGAACTGGCTGACCTGATC 1000
Q W K R R Q Q L A G N G G P H E G G L D V L Q S W C E K L A D L I
TGGCAGAACCCGCAACAGATCCGGCTGTGAACTTAACCCAGCAGCTTCTTCCAGGCCCATGGAAGAGTTCCTGAGCAAACTCAACGCTGACADA 1100
W O N R Q Q I R R C E H L T Q Q L P L P G P M E E L L S K L N D
TCAGTATATCATTTCCGCCCTGGTTACAGCACTTTCATCATTTGAAAAACAGCCGCCAGGTATTAAGAACCCAGACCAAGTTTCCAGCCACAGTGG 1200
I T D I I S A L V T S T F I I E K Q P P Q V L K T Q T K F A A T V R
CCTTCTGGTGGGTGGGAGCTTAATGTCCACATGAACCCACTCAGGTCAAGGCTGTCTATTTAGCGAGCAGCAGGCCAAAGCTGTGTGAAAGATGAG 1300
L L V G G K L R L N V H M N P P Q V K A V I V S E Q Q A K A L L K N E
AGCACACAGTGAAGCAGTGGAGAAATCTCAACAACAACCTGTGTGATGGAGTATCACCAGGCCACTGGCACCTCAGTGCACACTTCAGAAACATGT 1400
S T H S E S S G E I L N N N C V M E Y H Q A T G T L S A H F R N M
CACTGAAGCGGATCAAGCTTCGACCGTTCGAGGTGCAGAGTCAAGTGCAGGAGGAGAAAGTTACAGTTCCTGTTGAATCACAGTTCAGCGTGGGGGCAA 1500
S L K R I K R S D R R G A E S V T E E K F T V L F E S Q F S V G N
CGAGCTGTCTTCCATGTCAAAACCTTATCACTGCCTGTGTGTGATGTCCTCATGGCAGTCAAGACAACAATGCCACAGCAACAGCTCTGTGGGCAAC 1600
E L V F H V K T L S L P V V V I V H G S Q D N N A T A T V L W D N
GCCTTTGCTGAGCCAGGAGGCTGCCCTTTCATGCTGCCAGACAAGGTGCTGTGGCCAGCCTGTGGAGGCCCTCGATATGAAGTACAAGCGGAGATGC 1700
A F A E P G R V P F I V P D K V L W P Q L C E A L D M K Y K A E M
ACAGCGGGCTGGCCGTGCAGAGGATAACCTGGCTTTCCTGGCACAGAAAGGCTTTTACTAACAGCAGCAATAACCCAGAGGATTACCGTAACATGACCAT 1800
H S G R G L S E D N L V F L A Q K A F T N S S N N P E D Y R N M T I
ATCCTGGGCGGAGTCAAGCGGAGAGCTTACCTGGAGCAGCTTCACTTCTGGCAGTGGTGTGATGGAGTGTGGAATCATGAAGAAACATCTCAAG 1900
S W A Q F N R E S L P G R N F T F W Q W F D G V V E L M K K H L K
CCTCACTGGAATGATGGGCCATCTGGCTTTTGTAAACAAGCACAGGACATGCTGCTGTCACCAACCCAGCCCTTCTGCTGAGATTC 2000
P H W N D G A I L G F V N K H Q A Q D M L L S K P N G T F L L R F
CGCAGCTCGAGATTGGAGCATCAATCGCTGGGTGGCTGAGAACCCCAACAAACAGGTTGAGAGGCTGTGTGGAACCTGTGCTTATACAAACAAA 2100
S D S E I G G I T I A W V A E N P N K P G E R L V W N L L P Y T T K
GGACTTCTCAATTCCTCCCTGGCTGATGATCAGGACCTGAACCACTTCTGTTTCTTACCCTGACCGGCCAAAGACGAGGCTTTCGCGAAGTAT 2200
D F S I R S L A D R I S D L N H L L F L Y P D R P K D E V F A K Y
TACACCCCTCCACTCTCAAAGCAGTGGATGATGATAAGTAAACACAGATCAAAACAGTGTGGCAGAAATCACACCCCAACCCAGAAACCCAGTGGAG 2300
Y T P P L S K A V D G Y V K P Q I K Q V V P E F T T P N P E P S G
GAACTCTACGTTATGGACACAGCCGCTTCTCTCTGTGAACCAACCCCAACCTTTGGTGTCTACCTTCTATGAGTGACACCATGTTGGATGCAGA 2400
G T P T F M D Q T A S P S V N H P N N F G V Y P S M S D T M L D A D
TGAAGACTTCGACCTGGAGCAGCAGATGAGCTGGCCCGCATGTGGAGGAATGCTCCGCCGCTATGGCCAAACAGTGGAGCAGTCCAGCAGTCCGTA 2500
E D F D L D D T M D V A R H V E E L L R R P M A N Q W S S Q Q S *
ACCTGAAACCTGCACACTTCAGTCTTCTCCACTTATCTAAACAGAAACCCACACCTGTAAITCTACTGGACTGCAACCCAGAGAAATTTCTC 2600
GTCTTCATCAGTCACTTGGCGGATCCACATCAAACTCACCTTCTCAGTTTGTAGCTGCCACAGGAGATTTTAAAGAGAACAGGTTGGGTAAATG 2700
AATAACTGTCTACTTGC 2718

```

Fig.7.1b

Fig. 7.1. Nucleotide and deduced amino acid sequence of RbSTAT5-1 (a) and RbSTAT5-2 (b). Translation start (ATG) and stop (TGA) codons are red color letters.

2.1.2. Homology analysis of RbSTAT5s

Homology analysis was performed by comparing of amino acid sequence of RbSTAT5 with available orthologs from number of species belong to the different taxonomical lineages. Pairwise sequence analysis revealed that both RbSTAT5 isoforms were shared highest identity with STAT5 orthologs from fish lineage (> 80%) as expected while showing low identity percentage with higher vertebrates (73 – 81%). The highest identity of RbSTAT5-1 and RbSTAT5-2 was presented with mandarin fish (98.9%) and damselfish (98.0%), respectively. In

the sense of RbSTAT5s, they shared with comparatively higher identity (85.1%) and similarity (94.7%) with each other (Supplementary table 2).

Table 7.2. Percentage of identity (I%) and similarity (S%) of interspecies amino acid sequences in comparison with RbSTAT5-1 and RbSTAT5-2 sequences

Scientific name	Common name	Gene name	Accession number	RbSTAT5-1		RbSTAT5-2	
				I%	S%	I%	S%
<i>Oplegnathus fasciatus</i>	Rock bream	RbSTAT5-1		100.0	100.0	85.1	94.7
<i>Oplegnathus fasciatus</i>	Rock bream	RbSTAT5-2		85.1	94.7	100.0	100.0
<i>Siniperca chuatsi</i>	Mandarinfish	STAT5	ACU12487	98.9	99.4	84.9	94.1
<i>Tetraodon fluviatilis</i>	Pufferfish	STAT5	AAL09417	96.7	98.5	83.6	93.8
<i>Salmo salar</i>	Salmon	STAT5b	NP_001167288	96.1	97.8	85.1	94.3
<i>Oncorhynchus mykiss</i>	Rainbowtrout	STAT5	NP_001117733	95.8	97.8	85.2	94.4
<i>Stegastes partitus</i>	Damsel fish	STAT5b-like	XP_008277551	85.3	94.9	98.0	99.4
<i>Oreochromis niloticus</i>	Nile tilapia	STAT5b-like	XP_003454095	84.2	94.1	95.2	97.8
<i>Ctenopharyngodon idella</i>	Grass carp	STAT5b	ACK75717	95.3	97.3	84.5	93.8
<i>Danio rerio</i>	Zebrafish	STAT5a	NP_919368	94.0	96.8	83.7	93.4
<i>Danio rerio</i>	Zebrafish	STAT5b	NP_001003984	83.0	93.1	80.0	92.4
<i>Xenopus laevis</i>	Frog	STAT5b	NP_001084677	79.5	90.3	75.2	88.2
<i>Gallus gallus</i>	Chicken	STAT5b	NP_990110	78.7	90.6	75.8	89.1
<i>Mus musculus</i>	Mouse	STAT5a	AAQ75421	77.6	88.7	74.0	87.6
<i>Mus musculus</i>	Mouse	STAT5b	NP_035619	80.2	90.6	75.5	88.7
<i>Rattus norvegicus</i>	Norway rat	STAT5a	NP_058760	77.4	88.7	73.5	87.1
<i>Rattus norvegicus</i>	Norway rat	STAT5b	NP_071775	79.9	90.6	75.3	88.9
<i>Bos taurus</i>	Cattle	STAT5a	NP_001012691	77.8	88.7	73.7	87.4
<i>Bos taurus</i>	Cattle	STAT5b	NP_777042	80.4	90.7	75.3	89.3
<i>Sus scrofa</i>	Pig	STAT5a	NP_999455	77.5	88.4	73.9	87.6
<i>Homo sapiens</i>	Human	STAT5a	EAW60819	77.8	88.4	74.3	87.7
<i>Homo sapiens</i>	Human	STAT5b	NP_036580	79.9	90.3	75.9	89.2

Multiple sequence alignment analysis also further confirmed the high conservation of STAT5 orthologs. As shown in **Fig. 7.2**, residues among fish lineages as well as among other vertebrates were more or less similarly conserved. Characteristic domain regions including N-terminal domain, coiled-coil domain, DNA binding domain, linker domain, SH2 domain and TAD domain were recognized. Completely or partly conserved residues important for phosphotyrosine binding pocket (Lys⁶⁰⁰, Arg⁶¹⁸, Asn⁶⁴⁶ and Met⁶⁴⁸ in RbSTAT5-1 and Lys⁶⁰¹, Arg⁶¹⁹, Asn⁶⁴⁷ and Leu⁶⁴⁹), and completely conserved residues in hydrophobic binding pocket (Leu⁶⁴⁷ and Arg⁶⁶³ in RbSTAT5-1 and Leu⁶⁴⁸ and Arg⁶⁶⁴ in RbSTAT5-2) were identified based on the conserved domain database (CDD) in NCBI. Tyrosine residue which is phosphorylated during activation was completely conserved and identified in TAD domain region of RbSTAT5-1 (Tyr⁶⁹⁸) and RbSTAT5-2 (Tyr⁶⁹⁹).

N-terminal domain

RbSTAT5-1 MAWVIAQAQQLGQALHQMQLYQGHFPVEVRHYLSQWIEQSQWDSVLELNPVEEAKKRLDLSLVELOKKAHQVGEDGFLKIKLGHYATQKSTYDRCPLELVRCTRHHLYEORLVREATNCSGSGQAMDLSQ 139
RbSTAT5-2 MAWVIAQAQQLGQALHQMQLYQGHFPVEVRHYLSQWIEQSQWDSVLELNPVEEAKKRLDLSLVELOKKAHQVGEDGFLKIKLGHYATQKSTYDRCPLELVRCTRHHLYEORLVREATNCSGSGQAMDLSQ 140
ScSTAT5 MAWVIAQAQQLGQALHQMQLYQGHFPVEVRHYLSQWIEQSQWDSVLELNPVEEAKKRLDLSLVELOKKAHQVGEDGFLKIKLGHYATQKSTYDRCPLELVRCTRHHLYEORLVREATNCSGSGQAMDLSQ 139
TfSTAT5 MAWVIAQAQQLGQALHQMQLYQGHFPVEVRHYLSQWIEQSQWDSVLELNPVEEAKKRLDLSLVELOKKAHQVGEDGFLKIKLGHYATQKSTYDRCPLELVRCTRHHLYEORLVREATNCSGSGQAMDLSQ 139
SpSTAT5-L MAWVIAQAQQLGQALHQMQLYQGHFPVEVRHYLSQWIEQSQWDSVLELNPVEEAKKRLDLSLVELOKKAHQVGEDGFLKIKLGHYATQKSTYDRCPLELVRCTRHHLYEORLVREATNCSGSGQAMDLSQ 140
OnSTAT5-1 MAWVIAQAQQLGQALHQMQLYQGHFPVEVRHYLSQWIEQSQWDSVLELNPVEEAKKRLDLSLVELOKKAHQVGEDGFLKIKLGHYATQKSTYDRCPLELVRCTRHHLYEORLVREATNCSGSGQAMDLSQ 140
X1TAT5b MAWVIAQAQQLGQALHQMQLYQGHFPVEVRHYLSQWIEQSQWDSVLELNPVEEAKKRLDLSLVELOKKAHQVGEDGFLKIKLGHYATQKSTYDRCPLELVRCTRHHLYEORLVREATNCSGSGQAMDLSQ 139
GgSTAT5b MAWVIAQAQQLGQALHQMQLYQGHFPVEVRHYLSQWIEQSQWDSVLELNPVEEAKKRLDLSLVELOKKAHQVGEDGFLKIKLGHYATQKSTYDRCPLELVRCTRHHLYEORLVREATNCSGSGQAMDLSQ 139
MmSTAT5a MAWVIAQAQQLGQALHQMQLYQGHFPVEVRHYLSQWIEQSQWDSVLELNPVEEAKKRLDLSLVELOKKAHQVGEDGFLKIKLGHYATQKSTYDRCPLELVRCTRHHLYEORLVREATNCSGSGQAMDLSQ 139
MmSTAT5b MAWVIAQAQQLGQALHQMQLYQGHFPVEVRHYLSQWIEQSQWDSVLELNPVEEAKKRLDLSLVELOKKAHQVGEDGFLKIKLGHYATQKSTYDRCPLELVRCTRHHLYEORLVREATNCSGSGQAMDLSQ 139
HsSTAT5a MAWVIAQAQQLGQALHQMQLYQGHFPVEVRHYLSQWIEQSQWDSVLELNPVEEAKKRLDLSLVELOKKAHQVGEDGFLKIKLGHYATQKSTYDRCPLELVRCTRHHLYEORLVREATNCSGSGQAMDLSQ 139
HsSTAT5b MAWVIAQAQQLGQALHQMQLYQGHFPVEVRHYLSQWIEQSQWDSVLELNPVEEAKKRLDLSLVELOKKAHQVGEDGFLKIKLGHYATQKSTYDRCPLELVRCTRHHLYEORLVREATNCSGSGQAMDLSQ 139

Coiled coil domain

RbSTAT5-1 KYQOINQAFEEELRLTQDTENELKRLQIQEYFIQOYESLRIOAQLSLSLALPPADRLQREPAISKRRTVEWVIREANFLQKYRLDIAEHHOKTLLLRKQOITLDELQWKRROQLAGNGGPEGLDLQSWIC 279
RbSTAT5-2 KYQOINQAFEEELRLTQDTENELKRLQIQEYFIQOYESLRIOAQLSLSLALPPADRLQREPAISKRRTVEWVIREANFLQKYRLDIAEHHOKTLLLRKQOITLDELQWKRROQLAGNGGPEGLDLQSWIC 280
ScSTAT5 KYQOINQAFEEELRLTQDTENELKRLQIQEYFIQOYESLRIOAQLSLSLALPPADRLQREPAISKRRTVEWVIREANFLQKYRLDIAEHHOKTLLLRKQOITLDELQWKRROQLAGNGGPEGLDLQSWIC 279
TfSTAT5 KYQOINQAFEEELRLTQDTENELKRLQIQEYFIQOYESLRIOAQLSLSLALPPADRLQREPAISKRRTVEWVIREANFLQKYRLDIAEHHOKTLLLRKQOITLDELQWKRROQLAGNGGPEGLDLQSWIC 280
SpSTAT5-L RHQOINQAFEEELRLTQDTENELKRLQIQEYFIQOYESLRIOAQLSLSLALPPADRLQREPAISKRRTVEWVIREANFLQKYRLDIAEHHOKTLLLRKQOITLDELQWKRROQLAGNGGPEGLDLQSWIC 280
OnSTAT5-1 RHQOINQAFEEELRLTQDTENELKRLQIQEYFIQOYESLRIOAQLSLSLALPPADRLQREPAISKRRTVEWVIREANFLQKYRLDIAEHHOKTLLLRKQOITLDELQWKRROQLAGNGGPEGLDLQSWIC 280
X1TAT5b KHILOINQTFEELRLTQDTENELKRLQIQEYFIQOYESLRIOAQLSLSLALPPADRLQREPAISKRRTVEWVIREANFLQKYRLDIAEHHOKTLLLRKQOITLDELQWKRROQLAGNGGPEGLDLQSWIC 279
GgSTAT5b KHILOINQTFEELRLTQDTENELKRLQIQEYFIQOYESLRIOAQLSLSLALPPADRLQREPAISKRRTVEWVIREANFLQKYRLDIAEHHOKTLLLRKQOITLDELQWKRROQLAGNGGPEGLDLQSWIC 279
MmSTAT5a KHILOINQTFEELRLTQDTENELKRLQIQEYFIQOYESLRIOAQLSLSLALPPADRLQREPAISKRRTVEWVIREANFLQKYRLDIAEHHOKTLLLRKQOITLDELQWKRROQLAGNGGPEGLDLQSWIC 279
MmSTAT5b KHILOINQTFEELRLTQDTENELKRLQIQEYFIQOYESLRIOAQLSLSLALPPADRLQREPAISKRRTVEWVIREANFLQKYRLDIAEHHOKTLLLRKQOITLDELQWKRROQLAGNGGPEGLDLQSWIC 279
HsSTAT5a KHILOINQTFEELRLTQDTENELKRLQIQEYFIQOYESLRIOAQLSLSLALPPADRLQREPAISKRRTVEWVIREANFLQKYRLDIAEHHOKTLLLRKQOITLDELQWKRROQLAGNGGPEGLDLQSWIC 279
HsSTAT5b KHILOINQTFEELRLTQDTENELKRLQIQEYFIQOYESLRIOAQLSLSLALPPADRLQREPAISKRRTVEWVIREANFLQKYRLDIAEHHOKTLLLRKQOITLDELQWKRROQLAGNGGPEGLDLQSWIC 279

DNA binding domain

RbSTAT5-1 EKLAETIWNQROOIRRAEHLQOQLPQGVVEELKLNATTDIISALVTSFTIIEKQPPVQLKTQTKFAATVRLVGGKLVNHNPPQVAKTIISEQAKALKNENRDNSSGIEINNCVMIEHQTGLSAHFNM 419
RbSTAT5-2 EKLAETIWNQROOIRRAEHLQOQLPQGVVEELKLNATTDIISALVTSFTIIEKQPPVQLKTQTKFAATVRLVGGKLVNHNPPQVAKTIISEQAKALKNENRDNSSGIEINNCVMIEHQTGLSAHFNM 420
ScSTAT5 EKLAETIWNQROOIRRAEHLQOQLPQGVVEELKLNATTDIISALVTSFTIIEKQPPVQLKTQTKFAATVRLVGGKLVNHNPPQVAKTIISEQAKALKNENRDNSSGIEINNCVMIEHQTGLSAHFNM 419
TfSTAT5 EKLAETIWNQROOIRRAEHLQOQLPQGVVEELKLNATTDIISALVTSFTIIEKQPPVQLKTQTKFAATVRLVGGKLVNHNPPQVAKTIISEQAKALKNENRDNSSGIEINNCVMIEHQTGLSAHFNM 419
SpSTAT5-L EKLAETIWNQROOIRRAEHLQOQLPQGVVEELKLNATTDIISALVTSFTIIEKQPPVQLKTQTKFAATVRLVGGKLVNHNPPQVAKTIISEQAKALKNENRDNSSGIEINNCVMIEHQTGLSAHFNM 420
OnSTAT5-1 EKLAETIWNQROOIRRAEHLQOQLPQGVVEELKLNATTDIISALVTSFTIIEKQPPVQLKTQTKFAATVRLVGGKLVNHNPPQVAKTIISEQAKALKNENRDNSSGIEINNCVMIEHQTGLSAHFNM 420
X1TAT5b EKLAETIWNQROOIRRAEHLQOQLPQGVVEELKLNATTDIISALVTSFTIIEKQPPVQLKTQTKFAATVRLVGGKLVNHNPPQVAKTIISEQAKALKNENRDNSSGIEINNCVMIEHQTGLSAHFNM 419
GgSTAT5b EKLAETIWNQROOIRRAEHLQOQLPQGVVEELKLNATTDIISALVTSFTIIEKQPPVQLKTQTKFAATVRLVGGKLVNHNPPQVAKTIISEQAKALKNENRDNSSGIEINNCVMIEHQTGLSAHFNM 419
MmSTAT5a EKLAETIWNQROOIRRAEHLQOQLPQGVVEELKLNATTDIISALVTSFTIIEKQPPVQLKTQTKFAATVRLVGGKLVNHNPPQVAKTIISEQAKALKNENRDNSSGIEINNCVMIEHQTGLSAHFNM 419
MmSTAT5b EKLAETIWNQROOIRRAEHLQOQLPQGVVEELKLNATTDIISALVTSFTIIEKQPPVQLKTQTKFAATVRLVGGKLVNHNPPQVAKTIISEQAKALKNENRDNSSGIEINNCVMIEHQTGLSAHFNM 419
HsSTAT5a EKLAETIWNQROOIRRAEHLQOQLPQGVVEELKLNATTDIISALVTSFTIIEKQPPVQLKTQTKFAATVRLVGGKLVNHNPPQVAKTIISEQAKALKNENRDNSSGIEINNCVMIEHQTGLSAHFNM 419
HsSTAT5b EKLAETIWNQROOIRRAEHLQOQLPQGVVEELKLNATTDIISALVTSFTIIEKQPPVQLKTQTKFAATVRLVGGKLVNHNPPQVAKTIISEQAKALKNENRDNSSGIEINNCVMIEHQTGLSAHFNM 419

Linker domain

RbSTAT5-1 SLKRIKRSRRGAEVTEEFKTLFESQFSVGNELVFOVKTLSPVWIVHGSQDNATATVLDNFAEAPGRVFPVDPKVLWPOLGALNMFKAIEVQSRGLSDENLFLAOKAFSSSSNPEYRMTITWSAQFN 559
RbSTAT5-2 SLKRIKRSRRGAEVTEEFKTLFESQFSVGNELVFOVKTLSPVWIVHGSQDNATATVLDNFAEAPGRVFPVDPKVLWPOLGALNMFKAIEVQSRGLSDENLFLAOKAFSSSSNPEYRMTITWSAQFN 560
ScSTAT5 SLKRIKRSRRGAEVTEEFKTLFESQFSVGNELVFOVKTLSPVWIVHGSQDNATATVLDNFAEAPGRVFPVDPKVLWPOLGALNMFKAIEVQSRGLSDENLFLAOKAFSSSSNPEYRMTITWSAQFN 559
TfSTAT5 SLKRIKRSRRGAEVTEEFKTLFESQFSVGNELVFOVKTLSPVWIVHGSQDNATATVLDNFAEAPGRVFPVDPKVLWPOLGALNMFKAIEVQSRGLSDENLFLAOKAFSSSSNPEYRMTITWSAQFN 559
SpSTAT5-L SLKRIKRSRRGAEVTEEFKTLFESQFSVGNELVFOVKTLSPVWIVHGSQDNATATVLDNFAEAPGRVFPVDPKVLWPOLGALNMFKAIEVQSRGLSDENLFLAOKAFSSSSNPEYRMTITWSAQFN 560
OnSTAT5-1 SLKRIKRSRRGAEVTEEFKTLFESQFSVGNELVFOVKTLSPVWIVHGSQDNATATVLDNFAEAPGRVFPVDPKVLWPOLGALNMFKAIEVQSRGLSDENLFLAOKAFSSSSNPEYRMTITWSAQFN 560
X1TAT5b SLKRIKRSRRGAEVTEEFKTLFESQFSVGNELVFOVKTLSPVWIVHGSQDNATATVLDNFAEAPGRVFPVDPKVLWPOLGALNMFKAIEVQSRGLSDENLFLAOKAFSSSSNPEYRMTITWSAQFN 559
GgSTAT5b SLKRIKRSRRGAEVTEEFKTLFESQFSVGNELVFOVKTLSPVWIVHGSQDNATATVLDNFAEAPGRVFPVDPKVLWPOLGALNMFKAIEVQSRGLSDENLFLAOKAFSSSSNPEYRMTITWSAQFN 559
MmSTAT5a SLKRIKRSRRGAEVTEEFKTLFESQFSVGNELVFOVKTLSPVWIVHGSQDNATATVLDNFAEAPGRVFPVDPKVLWPOLGALNMFKAIEVQSRGLSDENLFLAOKAFSSSSNPEYRMTITWSAQFN 559
MmSTAT5b SLKRIKRSRRGAEVTEEFKTLFESQFSVGNELVFOVKTLSPVWIVHGSQDNATATVLDNFAEAPGRVFPVDPKVLWPOLGALNMFKAIEVQSRGLSDENLFLAOKAFSSSSNPEYRMTITWSAQFN 559
HsSTAT5a SLKRIKRSRRGAEVTEEFKTLFESQFSVGNELVFOVKTLSPVWIVHGSQDNATATVLDNFAEAPGRVFPVDPKVLWPOLGALNMFKAIEVQSRGLSDENLFLAOKAFSSSSNPEYRMTITWSAQFN 559
HsSTAT5b SLKRIKRSRRGAEVTEEFKTLFESQFSVGNELVFOVKTLSPVWIVHGSQDNATATVLDNFAEAPGRVFPVDPKVLWPOLGALNMFKAIEVQSRGLSDENLFLAOKAFSSSSNPEYRMTITWSAQFN 559

SH2 domain

RbSTAT5-1 RESLPGRSFTFWQFDGMEVLLKHKHKEPHNDGAILGFVNIQAQDMLSKPNGTFLFRSDSEIGGTTIAWVAENPKAGERVWNLVPTTKDFSTRSLADRLSDNLHLLYDPDRPKDEVSNYTPP ----LSKA 694
RbSTAT5-2 RESLPGRSFTFWQFDGMEVLLKHKHKEPHNDGAILGFVNIQAQDMLSKPNGTFLFRSDSEIGGTTIAWVAENPKAGERVWNLVPTTKDFSTRSLADRLSDNLHLLYDPDRPKDEVSNYTPP ----LSKA 695
ScSTAT5 RESLPGRSFTFWQFDGMEVLLKHKHKEPHNDGAILGFVNIQAQDMLSKPNGTFLFRSDSEIGGTTIAWVAENPKAGERVWNLVPTTKDFSTRSLADRLSDNLHLLYDPDRPKDEVSNYTPP ----LSKA 694
TfSTAT5 RESLPGRSFTFWQFDGMEVLLKHKHKEPHNDGAILGFVNIQAQDMLSKPNGTFLFRSDSEIGGTTIAWVAENPKAGERVWNLVPTTKDFSTRSLADRLSDNLHLLYDPDRPKDEVSNYTPP ----LSKA 694
SpSTAT5-L RESLPGRSFTFWQFDGMEVLLKHKHKEPHNDGAILGFVNIQAQDMLSKPNGTFLFRSDSEIGGTTIAWVAENPKAGERVWNLVPTTKDFSTRSLADRLSDNLHLLYDPDRPKDEVSNYTPP ----LSKA 695
OnSTAT5-1 RESLPGRSFTFWQFDGMEVLLKHKHKEPHNDGAILGFVNIQAQDMLSKPNGTFLFRSDSEIGGTTIAWVAENPKAGERVWNLVPTTKDFSTRSLADRLSDNLHLLYDPDRPKDEVSNYTPP ----LSKA 695
X1TAT5b RENLPGWNYTFWQFDGMEVLLKHKHKEPHNDGAILGFVNIQAQDMLSKPNGTFLFRSDSEIGGTTIAWKFDSP ----ERLFWNLVPTTKDFSTRSLADRLGDLNLVYVFPDRPKDEVSKYTPVLCN ----PSK 692
GgSTAT5b RENLPGWNYTFWQFDGMEVLLKHKHKEPHNDGAILGFVNIQAQDMLSKPNGTFLFRSDSEIGGTTIAWKFDSP ----ERLFWNLVPTTKDFSTRSLADRLGDLNLVYVFPDRPKDEVSKYTPVLCN ----PSK 695
MmSTAT5a RENLPGWNYTFWQFDGMEVLLKHKHKEPHNDGAILGFVNIQAQDMLSKPNGTFLFRSDSEIGGTTIAWKFDSP ----ERLFWNLVPTTKDFSTRSLADRLGDLNLVYVFPDRPKDEVSKYTPVLCN ----PSK 690
MmSTAT5b RENLPGWNYTFWQFDGMEVLLKHKHKEPHNDGAILGFVNIQAQDMLSKPNGTFLFRSDSEIGGTTIAWKFDSP ----ERLFWNLVPTTKDFSTRSLADRLGDLNLVYVFPDRPKDEVSKYTPVLCN ----PSK 695
HsSTAT5a RENLPGWNYTFWQFDGMEVLLKHKHKEPHNDGAILGFVNIQAQDMLSKPNGTFLFRSDSEIGGTTIAWKFDSP ----ERLFWNLVPTTKDFSTRSLADRLGDLNLVYVFPDRPKDEVSKYTPVLCN ----PSK 690
HsSTAT5b RENLPGWNYTFWQFDGMEVLLKHKHKEPHNDGAILGFVNIQAQDMLSKPNGTFLFRSDSEIGGTTIAWKFDSP ----ERLFWNLVPTTKDFSTRSLADRLGDLNLVYVFPDRPKDEVSKYTPVLCN ----PSK 695

TAD domain

RbSTAT5-1 VDGVKPQIKQVPEEFTNPFASQNTYMDHGSAPVWPHHTYGYEYVNSMLDADDFDLDITMDVARHVEELLRRPPIAN ----QWISQOOS ---- 786
RbSTAT5-2 VDGVKPQIKQVPEEFTNPFASQNTYMDHGSAPVWPHHTYGYEYVNSMLDADDFDLDITMDVARHVEELLRRPPIAN ----QWISQOOS ---- 786
ScSTAT5 VDGVKPQIKQVPEEFTNPFASQNTYMDHGSAPVWPHHTYGYEYVNSMLDADDFDLDITMDVARHVEELLRRPPIAN ----QWISQOOS ---- 786
TfSTAT5 VDGVKPQIKQVPEEFTNPFASQNTYMDHGSAPVWPHHTYGYEYVNSMLDADDFDLDITMDVARHVEELLRRPPIAN ----QWISQOOS ---- 785
SpSTAT5-L VDGVKPQIKQVPEEFTNPFASQNTYMDHGSAPVWPHHTYGYEYVNSMLDADDFDLDITMDVARHVEELLRRPPIAN ----QWISQOOS ---- 786
OnSTAT5-1 VDGVKPQIKQVPEEFTNPFASQNTYMDHGSAPVWPHHTYGYEYVNSMLDADDFDLDITMDVARHVEELLRRPPIAN ----QWISQOOS ---- 786
X1TAT5b TDG VKPQIKQVPEEFTNPFASQNTYMDHGSAPVWPHHTYGYEYVNSMLDADDFDLDITMDVARHVEELLRRPPIAN ----QWISQOOS ---- 781
GgSTAT5b VDG VKPQIKQVPEEFTNPFASQNTYMDHGSAPVWPHHTYGYEYVNSMLDADDFDLDITMDVARHVEELLRRPPIAN ----QWISQOOS ---- 787
MmSTAT5a VDG VKPQIKQVPEEFTNPFASQNTYMDHGSAPVWPHHTYGYEYVNSMLDADDFDLDITMDVARHVEELLRRPPIAN ----QWISQOOS ---- 793
MmSTAT5b ADG VKPQIKQVPEEFTNPFASQNTYMDHGSAPVWPHHTYGYEYVNSMLDADDFDLDITMDVARHVEELLRRPPIAN ----QWISQOOS ---- 786
HsSTAT5a VDG VKPQIKQVPEEFTNPFASQNTYMDHGSAPVWPHHTYGYEYVNSMLDADDFDLDITMDVARHVEELLRRPPIAN ----QWISQOOS ---- 794
HsSTAT5b VDG VKPQIKQVPEEFTNPFASQNTYMDHGSAPVWPHHTYGYEYVNSMLDADDFDLDITMDVARHVEELLRRPPIAN ----QWISQOOS ---- 787

Fig. 7.2. Multiple amino acid sequence alignment of RbSTAT5-1 and RbSTAT5-2 with other counterparts from various taxonomical origins. Completely conserved aa residues among all the species analyzed are marked with asterisks at the bottom of the alignment. Completely conserved residues among fish species and mammals are shaded with black and gray color, respectively. The regions characteristic for domains are shown by different colored lines on top of the alignment. Amino acid residues important for phosphotyrosine binding pocket and hydrophobic binding pocket are shaded with blue and green color, respectively. Tyrosine residue (Tyr⁶⁹⁸ and Tyr⁶⁹⁹, respectively) that phosphorylates during activation was shaded by red color.

The tertiary structures of RbSTAT5-1 and RbSTAT5-2 were modeled by SWISS-MODEL automated modeling server based on the crystal structure of mouse STAT5a (Neculai et al., 2005), and revealed the similar structural topology as depicted in **Fig. 7.3**. Amino acid residues reside in phosphotyrosine binding pocket and hydrophobic binding were found to be in similar locations of the each model.

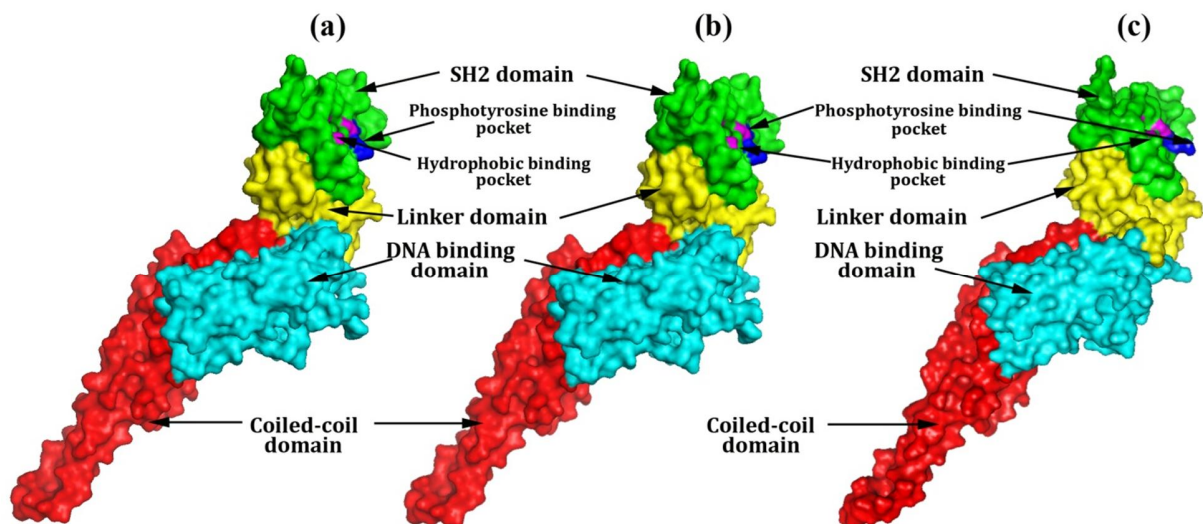


Fig. 7.3. Surface representations of RbSTAT5-1 (a), RbSTAT5-2 (b) and Mouse STAT5 3D homology models. The domain regions were highlighted with different surface colors and residues important for the phosphotyrosine binding pocket and hydrophobic binding pocket are marked with pink and blue color, respectively. The images were generated from SWISS-MODEL and visualized by PyMOL molecular graphic software version 1.3.

7.2.1.3. Phylogenetic analysis of RbSTAT5s

To understand the molecular evolution of STAT5, a phylogenetic tree was constructed based on the NJ method. According to the phylogenetic analysis, STAT5 members from fish species and other vertebrates were distinctly clustered (**Fig. 7.4**). Interestingly, mammalian STAT5a and STAT5b orthologs were separately claded within mammalian group. Meanwhile, STAT5 counterparts from fish origins also seemed to be evolved as two groups. The RbSTAT5-1 and RbSTAT5-2 were clustered in each fish group.

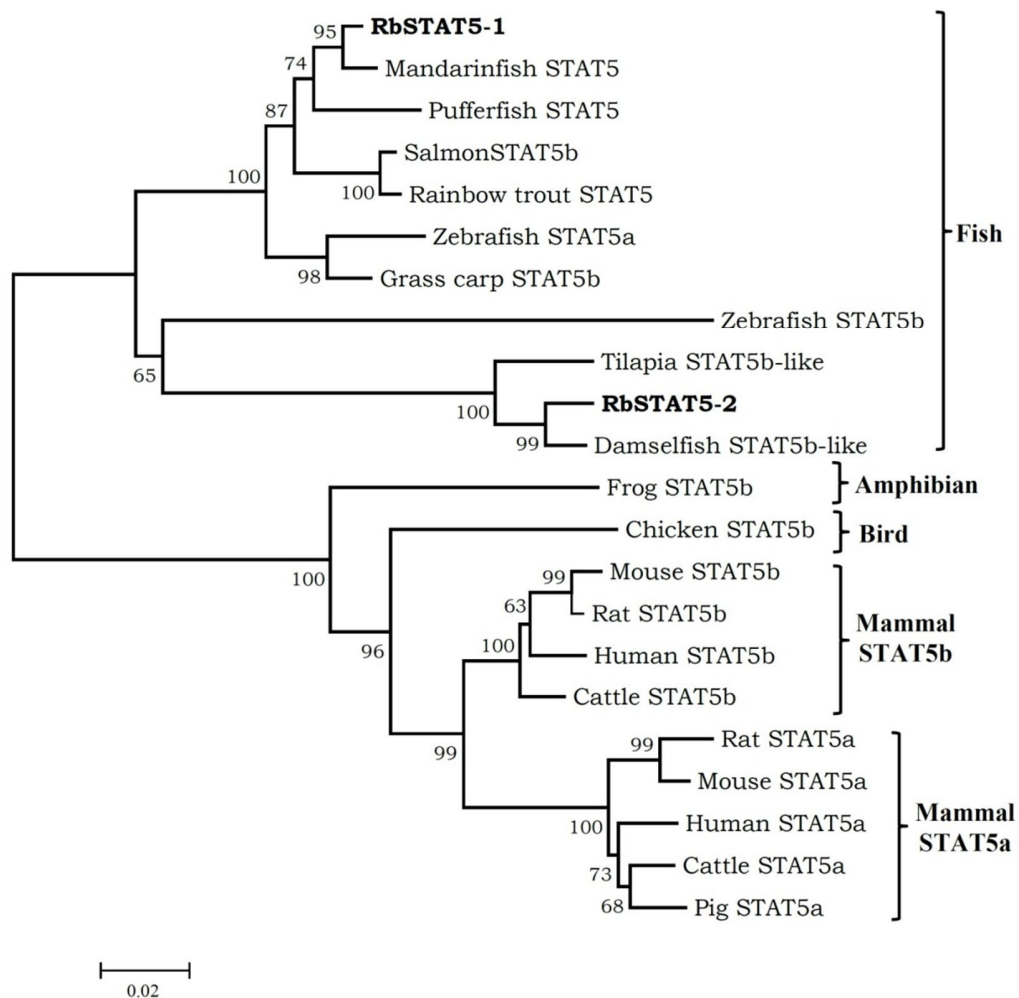


Fig. 7.4. Phylogeny of RbSTAT5-1 and RbSTAT5-2. The un-rooted phylogenetic tree was constructed using ML method based on the ClustalW alignment of core sequences of STAT5 family members from various taxonomical origins. The numbers at the each nodes are represented the bootstrap confidence values (%) according to the 5000 bootstrap replications.

7.2.2. Characteristics of RbSTAT5-1 genomic sequence

BAC library screening was able to identify only RbSTAT5-1 genomic structure, while RbSTAT5-2 genomic sequence is remained to be elucidated. The identified genomic sequence of RbSTAT5-1 was found to be with 19 exons interrupted by 18 introns. The coding sequence of RbSTAT5-1 was covered by 18 exons.

7.2.2.1. Comparative organization of RbSTAT5-1 genomic structure

In comparison of genomic organization of RbSTAT5-1 with other counterparts revealed that all fish species composed of 18 exons at their CDS region except in tilapia STAT5b. Interestingly, the sizes of fifteen exons from 5'-region in CDS were completely identical in all fish STAT5 counterparts except in tilapia STAT5b. In comparison with fish and mammals genomic structure organization of STAT5 revealed that first fourteen exons in CDS region were completely identical. In addition, exon number 15 in the CDS region of mammalian STAT5 clearly showed the distinguishable size as STAT5a (156 bp) and STAT5b (171 bp) (**Fig. 7.5**).

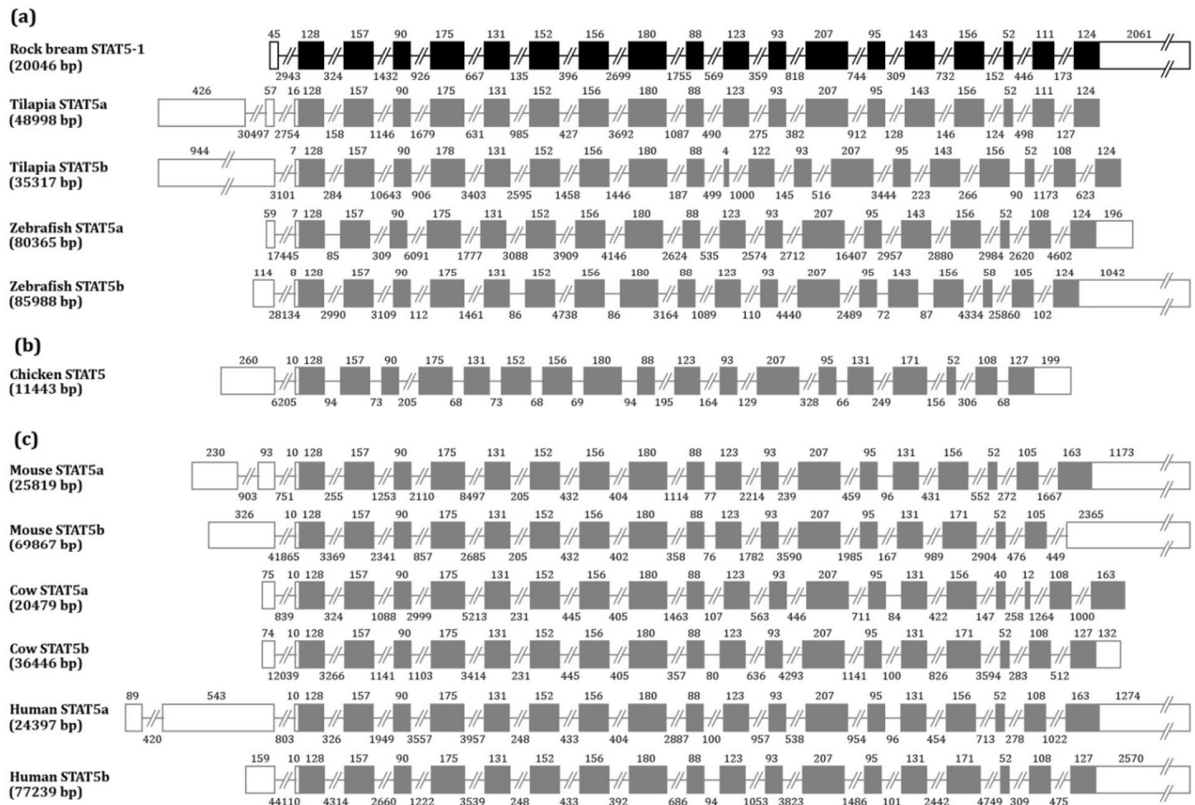


Fig. 7.5. Schematic representation of genomic structure comparison of RbSTAT5-1 and RbSTAT5-2 with fish (a), bird (b) and mammalian (c) counterparts. The exons and UTRs are represented by solid and empty boxes, respectively. The introns are shown by lines connecting each box. Numbers indicated in the top and bottom of the genomic structures are denoted for size of the exon and intron, respectively.

7.2.2.2. Putative promoter of RbSTAT5s at 5'-proximal region

To examine the potential TFBSs which can control the transcription of RbSTAT5-1, ~2 kb of 5'-flanking region was analyzed using AliBaba web based server. The TATA box-binding protein (TBP)-binding site was predicted at the upstream of 5'-UTR, although TATA box was not apparently present. Number of TFBSs including CCAAT enhancer binding protein alpha (C/EBP α), C/EBP β , C/EBP γ , interferon consensus sequence-binding protein (ICSBP), GATA-binding factor-1 (GATA-1), octamer transcription factor-1 (Oct-1), nuclear factor 1 (NF-1), specificity protein 1 (SP1), hepatocyte nuclear factor-3 (HNF-3), nuclear factor kappa B (NF- κ B), interferon-stimulated gene factor 3 (ISGF3), interferon regulatory factor 1 (IRF-1), activating protein (AP-1) and c-Jun (a member of AP-1) were identified in the putative promoter region (**Fig. 7.6**).

TATTTTTGTACGTTTCATTGTAAAGTTCATTGCTGAGATCTCACACGTGGTAACCAGGCTGTGTCAAACTGAAAATATCACCTAACAAATTTGTAAACAT 100
 TTGTTATAAATATCCATCAGATTCTCGGTCAACTCTTGACTATGTCTACACTAAGCTGTCTAAAGTTTTAAAATGCCATTAATGCGTGGAAACGACTTA 200
 GCAGTAGCAGTTCAGGTTGTTTTCATAAAGATCTCTTCCACAGTGACACACCTGAACAACAGGGAAATGGCATAATCTCTTCTCTTCGTCTCTTTT 300
 CAGTTGGCAAAACACAAAACCTACGTCACAGCCAACAGCTGATAAGAAGTGGGACAGACGCCTGTTATTCTGTATAGTCTCAGCCTATTAACCTCCGTT 400
 C/EBP α
CTGCTCTGCTCTCTGTGATGATCTACTGTATACTGTGTTTAAATGCAGCCGAACTCACAATATAGTTGTTCTCATTGTCAGACAATGGAAAGTGATGA 500
 SP1 **Oct-1**
 AACTGTGGCTTAATCGTGGTGGCCATAAACTACTACAGTCATCCCAAGCTGCTGCGCTGCTGTTTATAAAAACAATTTTATGATCGAGACGTCG 600
 SP1
 TCTGACAAAATCAACATAAATAGAGGTTAAATAACAAGGACTGTGCTGTGTGATCGGCTATATTGACATTTTAAAAAGTACTCACTGTCGGACTCACGATG 700
 C/EBP α
 GACAGAAAAAACGATCAAAATCAATGCAGCAGAAATCAGAGATATCGTCTTTTTCCACATGAATTGCTCTCCCTTCCTTCTGGTGCCTACATTACCACA 800
 GATA-1 NF-1 **Oct-1**
 ATGCCACAGTTAGCGCGGAGATTCTGGTGTGTTTCTCAAGCCGTAGCCTCAAGCAATGATGAGGTTTGTAAGCTCCCCAGATTTTTTTTCAATTTT 900
 SP1
 AAACCTGCGAGTCTTCAGTTCCAACCGCCGCTCCCTCAAGTGCACCTATCAGACTTTGCCAGCTCCCTCTGGAGCCAAAAACGCTTTTATACAACAGTT 1000
 AP-1 NF- κ B
 TTCACATATGTACAAGTACTCCATAAGACTTGTAACCGACTTACATTTGTGTAAATCGATGGAGTTCCCTTTAAAGTGATCGATCAGAGAAAGTTAG 1100
 C/EBP γ ISGF-3 IRF-1
 AGGTGACAGAAAGTTCTTAACTTATCTTACTGCCAGTGTTTTAAAAATGTATCCACTCTGGAGCCCGTTTTTTTTTAGTGAGGACAGAGGGCTCAAGCGGA 1200
 HNF-3
 GAGGAAACATATGCGTTTTTAAATTTAACGAGCCTGATGGGACAAAACCTTTTGACCTACTGTACTTGTCTGTAGTTGTGCACTGACGGCCAATGAGGG 1300
 NF- κ B C/EBP β
 ATTATTAGCAACACTTTTACGTCCAGCTAATCTGGCTGGGCTGTGCGCTATGCGATGATAAACCTGACTGCTTGTTCTTGTGCCCTGTGGACC 1400
 Sp1
 TATTTTTGGCGATGTCACCATGTTTCAAGATCTTAGCAAATACCTTTGGTGAGAACTATGTTTATCATGACCGATAGAACCAGCAGCCAGAGCCAAGAAAGT 1500
 NF-1 GATA-1 NF-1
 AAAACCAAGTTGTAATGAACAATATTTTTCTTTAATTTGTGATGTAATTAAGACGATCTGTTTTCATGCAATTATATTTGAAAACAGCTTTCTGGACA 1600
 C/EBP α **Oct-1**
 CATCTCCAACATCTCTGCTTGCTGTCTTTGCTTGCCTTGCATGTTTAAATGCAACAGCTCCAAGATCACTATAGCATCACATAGTGAGTTTCGCCTGTG 1700
 C/EBP α
 TACTTCTCAGTTTTGGGAAAGTTCATAAATAGGTTGTTATGTTGACGTCATGAAGAGAACTGGAATGAAGAGAATCTGTTCAAGTTGACTTTCCCTTTC 1800
 GATA-1
 ACCCTTTCAGTCTCTTTCTCATTCTTTTGTGTAATACTCCGGTCCTTGTGAAAAAGATAGCTTCTCAGAAGCACCAGATTGACTCATTCTCTCT 1900
 ICSBP TBP
 TTGCTTTCT 2000
 CTCTTTAGAGTTTCTCTGCTGTTACATGGTAAACACAGAGCTGAAGGCAAGAGgt... agATGCAGTGTGGATCCAGGCCAGCAGCTCCAGGGAGATG 2053
 Exon 1 Intron Exon 2

Fig. 7.6. Putative promoter proximal region of RbSTAT5-1. Predicted transcription factor binding sites are shown by underlined purple color letters and indicated below the sequence. The first and second exon regions and the first intron regions are marked. The splicing sites (gt and ag) are shown in the intron gap. The start codon (ATG) located in the second exon is shown by white color letters with black background.

7.2.3. Transcriptional profile of *RbSTAT5-1* and *RbSTAT5-2*

Quantification of gene transcription was assessed by SYBR Green qPCR and rock bream β -actin was used as an internal reference gene to normalize the expression of each gene. The specificity of the gene amplification was affirmed by the occurrence of single peak for each of the *RbSTAT5* gene as well as for internal control gene β -actin during last step of the qPCR program.

7.2.3.1. Expression of *RbSTAT5s* mRNA in tissues of healthy juvenile fish

The expression of *RbSTAT5-1* and *RbSTAT5-2* mRNA was ubiquitous with different levels according to the qPCR results. Transcriptional profile showed that the level of transcription of *RbSTAT5-1* was comparatively higher than *RbSTAT5-2*. In the case of *RbSTAT5-1*, levels of transcripts were highest in blood cells followed by liver and heart compare to the lowest expressed skin tissue. Similarly, *RbSTAT5-2* was highly expressed in blood cells, while heart and liver showed moderate expression compare to the lowest expressed muscle (**Fig. 7.7**).

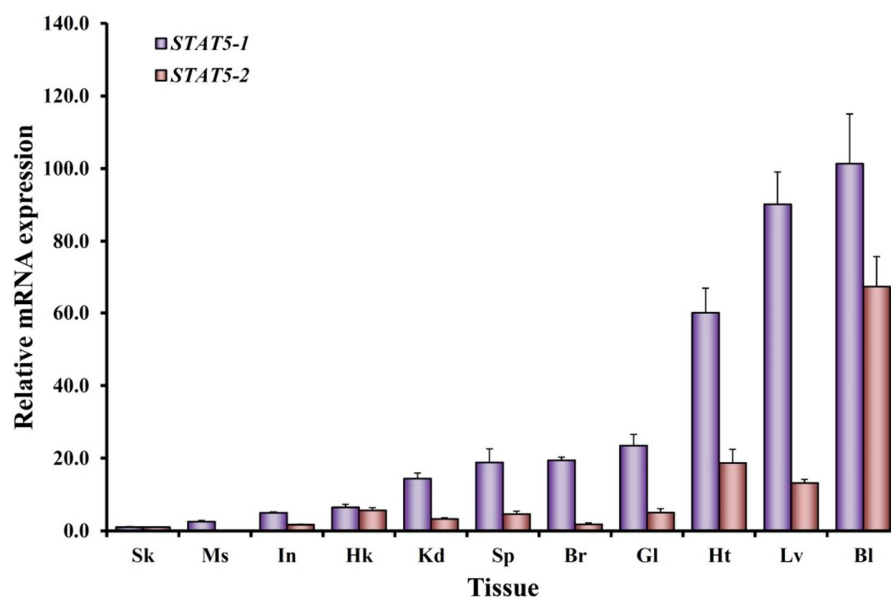


Fig. 7.7. Tissue-specific expression of rock bream *STAT5-1* and *STAT5-2* transcripts in healthy fish. The level expression was examined by SYBR Green qPCR and, rock bream β -actin was used as an internal reference gene to calculate the relative mRNA expression. Based on the results, the calculation was performed using Livak method and values were compared relative to muscle which showed lowest expression. Eleven different tissues including muscle (Ms), skin (Sk), head kidney (Hk), kidney (Kd), brain (Br), gill (Gl), intestine (In), spleen (Sp), liver (Lv), heart (Ht) and blood cells (Bl) were used. The results are reported as mean \pm standard deviation (SD) of triplicates.

7.2.3.2. Expression of RbSTAT5s mRNA in immune challenged fish

To examine the transcriptional modulation of *RbSTAT5s*, the level of mRNA expression was investigated in liver and blood cells after viral, bacterial and PAMPs stimulations. The qPCR analysis revealed that the expression of *RbSTAT5-1* mRNA was significantly ($P < 0.05$) down-regulated at 12 h post injection (p.i) of poly I:C compare to the un-injected control in liver tissue. Next the expression was gradually increased and peaked at 48 h p.i (2.6-fold) (Fig. 7.8a). In the case of blood cells, the expression of *RbSTAT5-1* was up-regulated at 3 h and 12 h p.i of poly I:C, while showing down-regulation at 6h (Fig. 7.8b). RBIV injection was caused to induce the expression of *RbSTAT5-1* at 6 h, 24 h and 48 h in liver tissue, although suppression was observed at 12 h p.i. In contrast, the *RbSTAT5-1* mRNA expression was suppressed at 6 h and 24 h p.i of RBIV, while showing significant elevation at 12 h p.i. Upon LPS stimulation, significantly down-regulated expression of *RbSTAT5-1* mRNA was observed at 12 - 48 h p.i in liver tissue. However, in blood cells, significantly up-regulated expression was detected at 3 h and 12 h p.i of LPS, while detecting a suppressed expression at 6 h p.i. Upon Gram-negative bacterial pathogen *E. tarda* infection, the expression of *RbSTAT5-1* mRNA was peaked at 6 h in both liver (2.07-fold) and blood cells (2.5-fold). Meanwhile, significantly down-regulated expression was observed during 12 - 48 h p.i of *E. tarda* only in liver tissue. In the case of Gram-positive *S. iniae* challenge experiment, elevated expression of *RbSTAT5-1* was detected at 6 h and 48 h, while showing suppressed expression at 12 - 24 h p.i in liver tissue. Whereas, the up-regulated expression at 3 h and down-regulated expression at 6 h was observed after injection of *S. iniae* in blood cells.

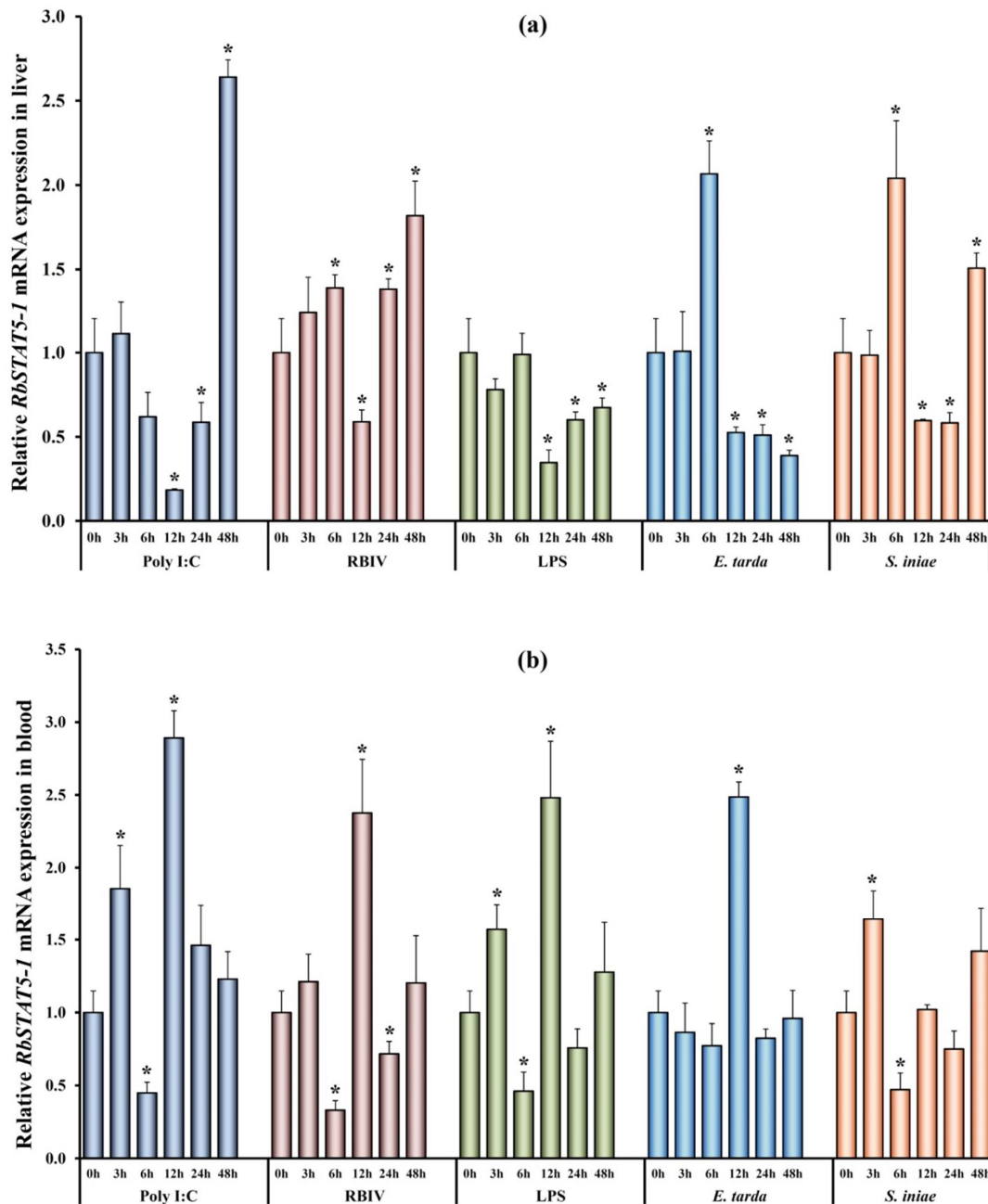


Fig. 7.8. The expressional patterns of RbSTAT5-1in (a) liver and (b) blood tissues after in vivo immune challenges. The rock bream β -actin was used as an internal reference gene to calculate the relative mRNA expression. The fold change of mRNA expression at each time point was compared with the PBS-injected control at corresponding time points and, represented as relative fold changes. The results are reported as mean \pm standard deviation (SD) of triplicates, and results were statistically compared relative to the un-injected control (0 h) using t-test. Data with statistically difference at $P < 0.05$ are indicated by asterisks.

Interestingly, more or less similar expression pattern of *RbSTAT5-2* was observed in both liver and blood cells (**Fig. 7.9**) except down-regulated expression was detected at 6 h in liver tissue. Upon poly I:C injection, the expression of *RbSTAT5-2* mRNA was raised at 3 h, 24 h and 48 h p.i in liver tissue (**Fig. 7.9a**), while showing continues up-regulation (12 – 48 h) in blood cells (**Fig. 7.9b**). Similarly, significant up-regulation was observed continuously from 12 – 48 h p.i of RBIV in liver and blood cells. Upon LPS stimulation, the expression of *RbSTAT5-2* was significantly elevated at 12 h and 24 h p.i in liver tissues. However, no significant changes were detected in blood cells after LPS injection. Meanwhile, significantly elevated expression (at 6 - 12 h) of *RbSTAT5-2* was detected only in blood cells upon *E. tarda* infection. *S. iniae* bacterial infection was caused to increase the expression of *RbSTAT5-2* in liver tissue from 12 h – 48 h, while in blood cells from 6 h – 48 h p.i. Overall expression of *RbSTAT5-2* was clearly depicted as late phase up-regulated transcriptions.

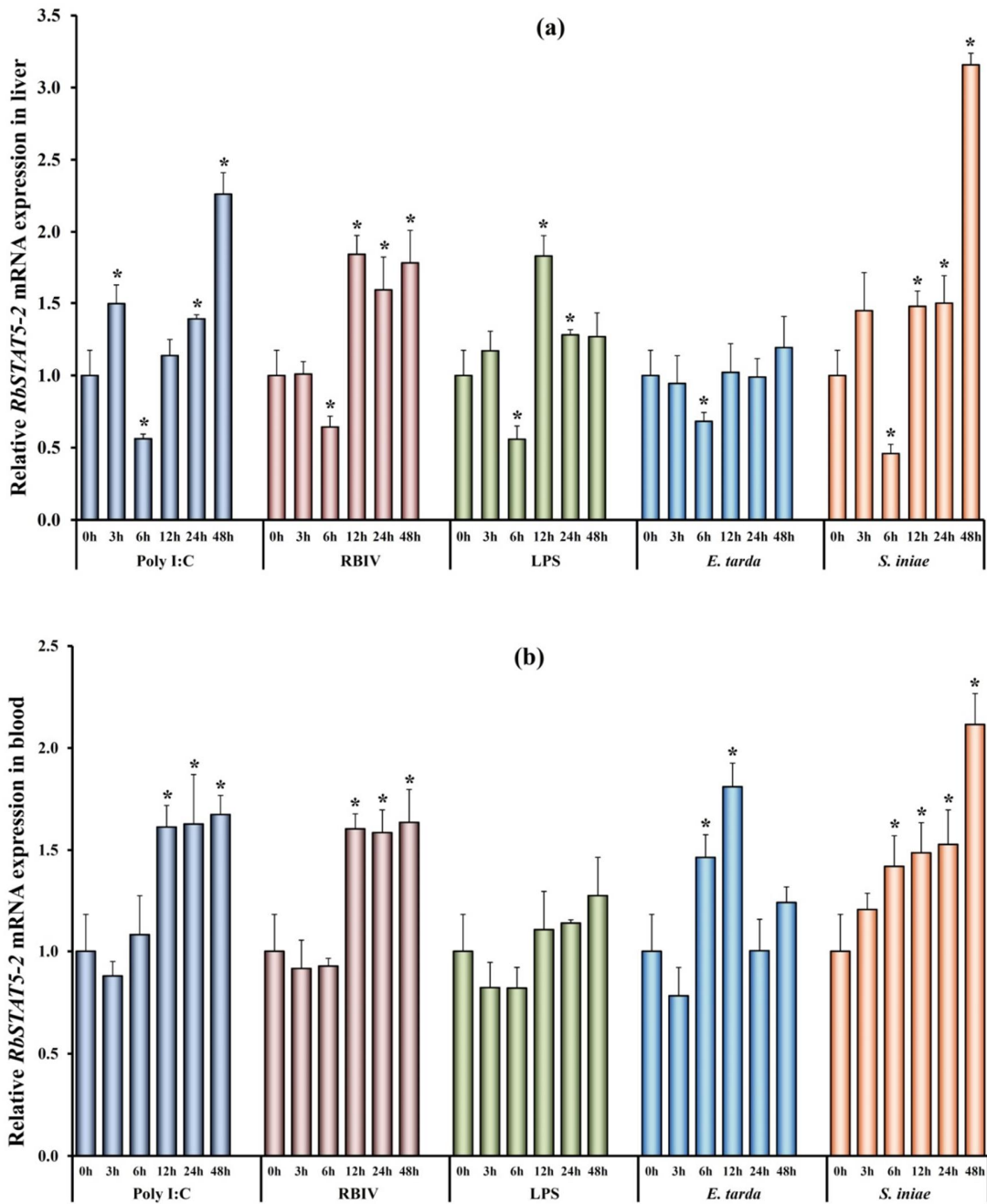


Fig. 7.9. The expressional patterns of RbSTAT5-2 in (a) liver and (b) blood tissues after in vivo immune challenges. The rock bream β -actin was used as an internal reference gene to calculate the relative mRNA expression. The fold change of mRNA expression at each time point was compared with the PBS-injected control at corresponding time points and, represented as relative fold changes. The results are reported as mean \pm standard deviation (SD) of triplicates, and results were statistically compared relative to the un-injected control (0 h) using t-test. Data with statistically difference at $P < 0.05$ are indicated by asterisks.

7.2.3.3. Expression of RbSTAT5s mRNA in injured fish

Transcriptional changes of RbSTAT5-1 and RbSTAT5-2 was examined in liver tissue and blood cells after tissue injury. The qPCR results showed that fairly similar expression patterns for both RbSTAT5s. The down-regulated expression of RbSTAT5-1 mRNA was observed at 12 h in liver tissue subsequent up-regulations at 24 - 48 h post injury (**Fig. 7.10a**). In the case of expression profile of RbSTAT5-2 in liver tissue, 6 - 12 h down-regulations and then 24 - 48 h up-regulations were observed (**Fig. 7.10b**). Compare to the un-injured control, significantly down-regulated expressions were detected at all the experimental time points except 24 h for RbSTAT5-1, while showing similar down-regulated expressions for all time points except at 6 h for RbSTAT5-2.

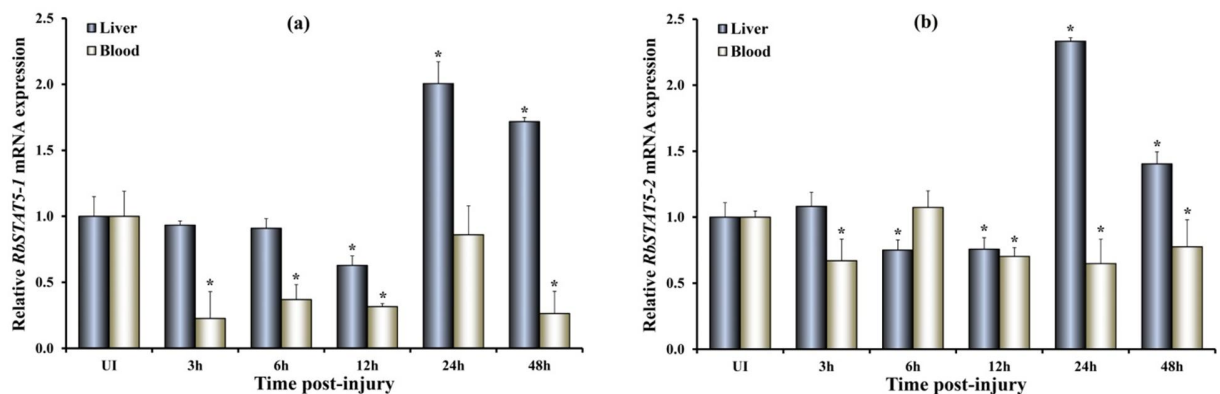


Fig. 7.10. The expressional patterns of RbSTAT5-1 (a) and RbSTAT5-2 (b) in liver tissues and blood cells after injury. The fold change of mRNA expression at each time point was compared with the un-injured control (UI) and, represented as relative fold changes. The results are reported as mean \pm standard deviation (SD) of triplicates, and results were statistically compared relative to the un-injured control (UI) using t-test. Data with statistically difference at $P < 0.05$ are indicated by asterisks.

7.2.3.3. Expression of RbSTAT5s mRNA in injured fish

Based on the qPCR results, the expression of *RbSTAT5-1* and *RbSTAT5-2* transcripts were not significantly altered compare to the untreated samples, except at 48 h post treatment of rRbIL-10 for *RbSTAT5-1* transcription.

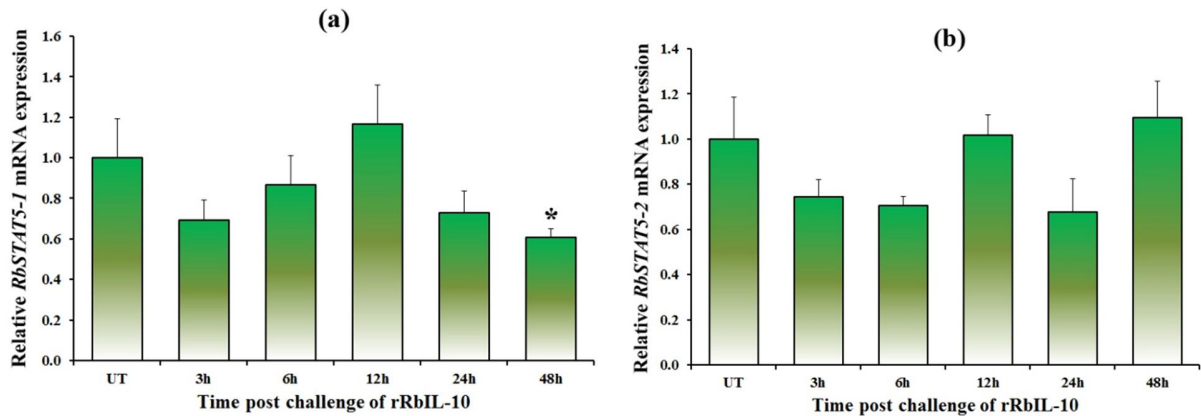


Fig. 7.11. The expressional patterns of RbSTAT5-1 (a) and RbSTAT5-2 in heart cells after *in vitro* immune challenge with rRbIL-10. The fold change of mRNA expression at each time point was compared with the un-treated (UT) control at corresponding time points and, represented as relative fold changes. The results are reported as mean \pm standard deviation (SD) of triplicates, and results were statistically compared relative to the un-treated control (UT) using t-test. Data with statistically difference at $P < 0.05$ are indicated by asterisks.

7.3. Discussion

The JAK/STAT signaling pathway is one of the major signaling pathways, transduce the signals from cell membrane to the nucleus and there by initiate the transcription of functional genes. The STAT5 paralog which is typically existed as two isoforms (STAT5a and STAT5b) are well documented in mammals. Herein, we reported molecular insights and functional aspects of two isoforms of STAT5 paralogs isolated from rock bream. Sequence analysis revealed that both RbSTAT5 members were shared similar structural features as other STAT members. In comparison of RbSTAT5 isoforms with other counterparts, the conservation of sequence was comparatively very high. In addition, the functional residues resided mostly in SH2 domain, and a tyrosine residue which is phosphorylated during activation was well conserved. Moreover, we have compared the 3D structural topology of RbSTAT5-1 and RbSTAT5-2 with mouse STAT5a model and revealed the high structural resemblance. The comparative structural studies clearly indicate that both RbSTAT5-1 and RbSTAT5-2 identified in this study could be presented similar functional characteristics as mammals.

The evolutionary insights were analyzed by phylogenetic study and genomic structural comparison. According to the phylogenetic tree which was constructed based on the NJ method, mammal STAT5 group was clearly clustered into two different clades indicating two different evolutionary paths for mammalian STAT5a and STAT5b. Interestingly, teleostean STAT5 also have clustered into two distinct groups implying the existence of two types of STAT5 isoforms. Fascinatingly, two STAT5 members identified in this study were also clustered in each branch. However, teleostean and mammalian groups were seemed to be evolved separately. Previously, it has been reported that the presence of two isoforms of STAT5 members in mammals might have been generated due to the gene duplication during evolution (Copeland et al., 1995). In a similar manner, we can suggest that the presence of two closely related STAT5 orthologs in fish lineage might be evolved with the effect of gene duplication. Further, we have compared the genomic organization of STAT5 members among different species and evaluated the structural correlation. However, no considerable difference was observed between teleostean and mammals genomic structures. But, genomic organization of mammal STAT5a and STAT5b were found to be noticeably different at fifteenth exon in the CDS region. The size of the fifteenth exon in CDS of mammalian STAT5a was 156 bp, while in STAT5b was 171 bp. Hence, genomic structures of STAT5 from large number of fish species are required to be analyzed to understand the proper evolutionary relationship.

Numbers of TFBSs were predicted in the promoter proximal region of RbSTAT5-1 gene, and most of them were known to be crucial for the immune functions. It has been reported that most of the transcription factors such as NF-1 (Xu et al., 2005), NF- κ B (Oeckinghaus and Ghosh, 2009), AP-1 (Foletta et al., 1998), C/EBP (Wedel and Ziegler-Heitbrock, 1995; Lekstrom-Himes and Xanthopoulos, 1998), GATA1 (Ferreira et al., 2005), Oct-1 (Kemler and Schaffner, 1990; Tantin et al., 2005), and ICSBP (Horiuchi et al., 2012) are crucial for the various immune/stress related functions. Previous study in human STAT5a and STAT5b, have reported the existence of putative TFBSs such as TFII-1, TFII-D, GATA, CACA, SP1, CCAAT, NF- κ B and CREB in their promoter regions. In addition, they have demonstrated the biological effect of SP1 on the transcription of STAT5a and STAT5b (Crispi et al., 2004). Studies analyzing promoter region of STAT5 gene are still under investigation level. Consequently, further studies are required to be conducted to explore the elements that can mediate the transcription of RbSTAT5 genes.

The evaluation of expression level of RbSTAT5s in different tissues of healthy fish will be supportive to understand the biological importance of those genes under normal physiological conditions. In mammals, various functional aspects of STAT5 have been reported. STAT5 is a key factor for the proliferation and differentiation of normal mammary epithelial cells (Hennighausen et al., 1997; Watson, 2001). The mammalian STAT5a and STAT5b were found to be critical regulator for the mast cell development and survival (Shelburne et al., 2003), and macrophage differentiation (Lokuta et al., 1998). However, the studies about teleostean STAT5 members and their functional aspects were limitedly reported. STAT5 expression in different tissues was reported in pufferfish and showed the more or less similar pattern (Sung et al., 2003). Meanwhile, mandarin fish STAT5 transcription was reported to be high in intestine, spleen and kidney tissues, while showing highest expression liver (Guo et al., 2009). In the present study, transcription of both RbSTAT5-1 and RbSTAT5-2 was highly detected in blood, liver and heat tissues. The occurrence of highest level of RbSTAT5s mRNA in blood cells indicating that the main role of RbSTAT5s might be occurred in blood. As observed in mammalian models, RbSTAT5s might also be involved in macrophage differentiation.

To understand the immunological responses of RbSTAT5s against invading microbial pathogens, we injected the two bacterial species including *E. tarda* and *S. iniae*, and RBIV those were known to be serious pathogens for rock bream, and analyzed the transcriptional modulation. In addition, LPS a common bacterial component and poly I:C which is commercially available double stranded RNA viral mimic also injected to the fish. According to the results, the expression of both RbSTAT5-1 and RbSTAT5-2 seemed to be wave pattern. Significant up-regulations as well as down-regulations were observed during the experimental time. Previous study in mandarin fish demonstrated the significant down-regulations of STAT5 transcription upon poly I:C stimulation (Guo et al., 2009). In addition, no studies reported to show the possible immune modulations of teleostean STAT5 orthologs even though some fish described about the genomic structural features. However, the results of the present study hypothesize the potential immune regulation roles of RbSTAT5-1 and RbSTAT5-2 in response to the bacterial and viral pathogens.

Further, studies were carried out to understand the involvement of RbSTAT5s on wound healing process following tissue injury. Results depicted the significant changes of RbSTAT5s

transcription in liver tissue and blood cells. As identified in tissue specific expressional studies, RbSTAT5s transcripts in blood cells might be play a crucial role in various biological functions. Significantly down-regulated expression of RbSTAT5s in blood cells which was detected after injury may indicate the rapid translation of RbSTAT5s mRNA into protein to show the essential function. Previous study on mammalian intestinal injury reported the vital role of STAT5 on intestinal stem cell proliferation and regeneration (Gilbert et al., 2015). However, more studies are needed to carry out to understand the real wound healing mechanism and involvement of RbSTAT5s.

7.4. Conclusion

In this study, we have identified and characterized two cDNA sequences of *STAT5* ortholog from rock bream. Both RbSTAT5 orthologs shared the similar characteristic domain architecture and structural topology with mammalian equivalents indicating its functional similarity. The phylogenetic tree and the detail analysis of *RbSTAT5s* genomic structure provided the important information about the molecular evolution of STAT5 family members. The transcripts of *RbSTAT5s* were mainly expressed in adult blood cells, liver and heart tissues indicating their functional specificity in different tissues and key role in blood. Significant up-regulations of *RbSTAT5s* transcripts upon pathogenic and PAMPs stimulation speculated the immediate immune defensive action in response to the pathogenic attack. In addition, transcriptional changes following injury implied their essential role in wound healing process. These findings may help for further understanding of various functional aspects and evolution of teleostean JAK/STAT signaling pathway.

CHAPTER 8

Structural insights and transcriptional modulation of signal transducer and activator of transcription 6 (STAT6) from rock bream, *Oplegnathus fasciatus*

Abstract

Signal transducer and activator of transcription 6 (STAT6) is one of the crucial transcription factors in janus kinase (JAK)/STAT signaling pathway first isolated from interleukin-4 (IL-4) treated human monocytic Thp-1 cells. In the current study, a homolog of STAT6 was identified from rock bream transcriptome database (RbSTAT6). Bioinformatics analysis of RbSTAT6 revealed its structural conservation as other STAT6 counterparts. Mainly, six different domain regions including N-terminal domain, coiled coil domain, DNA binding domain, linker domain, Src homology 2 (SH2) domain and transactivation domain (TAD), and some residues important for function were conserved well. However, in comparison of RbSTAT6 with other counterparts revealed that STAT6 orthologs from higher vertebrate shared relatively low percent of identity. Phylogenetic studies presented the separate evolutionary path for teleosteans and non-teleostean vertebrates. Quantitative real time PCR (qPCR) analysis revealed the universal expression of *RbSTAT6* in different tissues, while showing higher expression in blood cells and liver tissue. Transcriptional changes of *RbSTAT6* mRNA were detected in blood and liver tissues following challenges with bacteria (*E. tarda* and *S. iniae*), rock bream irido virus (RBIV) and immune stimulants (LPS and Poly I:C). Significant changes of RbSTAT6 transcription was observed after tissue injury. In addition, transcriptional modulations were observed in rock bream heart cells after rock bream IL-10 (rRbIL-10) stimulation. Taken together the results of current study provide great evidences for the potential host immune responses and wound healing capability of rock bream STAT6.

8.1. Introduction

Signal transducers and activators of transcription (STATs) are a family of transcription factors that exist in a latent state in cytoplasm; they are activated in response to various extracellular polypeptide ligands such as cytokines, growth factors, and hormones. Activated STAT proteins accumulate in the nucleus to drive transcription (Ihle and Kerr, 1995; Schindler et al., 1995; Watanabe and Arai, 1996). In mammals, there are seven STAT proteins with different functions (Darnell, 1997).

The STAT6 protein was first isolated from IL-4-treated human monocytic Thp-1 cells, and its encoding gene was cloned by PCR amplification (Hou et al., 1994). In addition, screening a database of expressed sequence tags led to the identification of murine STAT6 (Quelle et al., 1995). IL-4 is produced by activated T cells, thymocytes, basophils, and mast cells, and it is an effective cytokine which regulates growth and differentiation in a variety of cells (Paul, 1991). In hematopoietic cells, IL-4 induces the development of Th2 cells in T helper cells and immunoglobulin (Ig) isotype switching in B cells (Coffman et al., 1993; Seder and Paul, 1994). Many transcriptional responses mediated by IL-4 depend on activation of STAT6. The significant role of STAT6 in IL-4-mediated biological responses was further confirmed in STAT6-deficient mice, which showed defects in functions mediated by IL-4, including Th2 development, induction of CD23 and major histocompatibility complex class II expression, and immunoglobulin class switching to IgE (Takeda et al., 1996). STAT6 is also activated by IL-13, and its cognate receptor shares a component of IL-4R with the IL-4 receptor (Lin et al., 1995).

The STAT6 protein, like other STAT proteins, is organized into several highly conserved functional domains, including an N-terminal domain, a coiled-coil domain, a DNA-binding domain, a linker domain, an SH2 domain, and a transactivation domain. The specific roles of individual domains in STAT6 activation are well established. Upon IL-4 binding, the α chain of the IL-4 R complex is tyrosine-phosphorylated by JAK kinases, creating docking sites for STAT6 (Hou et al., 1994; Kammer et al., 1996; Ryan et al., 1996). Through an interaction of the SH2 domain with phosphorylated tyrosine motifs of IL-4Ra, STAT6 is recruited to the IL-4 receptor complex and phosphorylated at tyrosine residue 641 by JAK 2 kinase (Schindler et al., 1995). Then phosphorylated STAT6 monomers undergo homodimerization via a reciprocal interaction involving the SH2 domain and are translocated to the nucleus, where they can bind to specific

DNA elements. STAT6-binding sites were identified in the promoter region of several IL-4-inducible genes, including the Fc receptor for IgE (CD23), major histocompatibility complex (MHC) class II, and Ig germline promoters (Rothman et al., 1991; Kotanides and Reich, 1993; Lundgren et al., 1994). The transactivation domain of STAT6 located in the C-terminus of the protein was characterized as a non-acidic module. Within this domain, many proline, serine, threonine, leucine, and glutamine residues are found. This unique feature was not observed in the transactivation domain of other STATs (Mikita et al., 1996; Lu et al., 1997).

Up to now very limited studies have been reported on the teleostean STAT6. A study characterized a STAT6 ortholog from pufferfish and showed its functional association of IL-4 (Sung et al., 2010). Mitra and coworkers reported the structural insights of zebrafish STAT6 along with two other transcription factors such as t-bet and foxp3, and demonstrated the transcriptional responses upon phytohaemagglutinin, lipopolysaccharide or Poly I:C stimulation (Mitra et al., 2010).

In this study, our main objectives were to determine the structural characteristics and diverse functions of STAT6 ortholog identified from commercial crucial rock bream, *Oplegnathus fasciatus*. We identified a cDNA contig containing full length coding sequence (CDS) from rock bream. For the functional aspects, transcriptional profiles were analyzed after live bacteria (*Edwardsiella tarda* and *Streptococcus iniae*), rock bream irido virus (RBIV) and two pathogen associated molecular patterns (PAMPs; LPS and Poly I:C) to understand the immune role of STAT6. In addition, transcription profile was analyzed after tissue injury. Apart from that rock bream IL-10 (RbIL-10) was used to challenge the rock bream heart cells to evaluate the functional response of STAT6.

Table 8.1. Primers used in this study

Primer	Purpose	Sequence, 5'-3'
<i>RbSTAT6-F</i>	qPCR amplification, BAC screening	TTTCCAGCTGCTGAAGGAGTGTGT
<i>RbSTAT6-R</i>	qPCR amplification, BAC screening	TGCAGAGGGTTGAGGTTGTCATCA
<i>Rb β-actin F</i>	qPCR internal reference	TCATCACCATCGGCAATGAGAGGT
<i>Rb β-actin R</i>	qPCR internal reference	TGATGCTGTTGTAGGTGGTCTCGT
<i>RbIL-10/pMAL-F</i>	Clone into pMAL-c5x	(GA) ₃ gaattcAGTCCCATGTGCAACAACCACTG - EcoRI
<i>RbIL-10/pMAL-R</i>	Clone into pMAL-c5x	(GA) ₃ aaagcttTCAATTAGAGGCCACTTGTTTTCGGAC - HindIII

Restriction sites in the cloning primers are shown with small case letters and indicated at the end of each primer sequence.

8.2. Results

8.2.1. cDNA sequence characterization of RbSTAT6

The full-length cDNA of RbSTAT6 was 4683 bp, (**Fig. 8.1**), and contained an open reading frame (ORF) of 2313 bp that encodes 771 amino acids (aa). The 5'-untranslated region (UTR) and 3'-UTR were 544 and 1826 bp, respectively. The calculated molecular mass and the isoelectric point of the RbSTAT6 protein were 87.9 kDa and 5.81, respectively. Two polyadenylation signals (AATAAA) and five RNA instability motifs (ATTTA) were identified in the 3'-UTR of RbSTAT6. Conserved domain analysis indicated the presence of characteristic domains including N-terminal domain, coiled-coil domain, DNA binding domain, linker domain, SH2 domain and TAD domain in the RbSTAT6 amino acid sequence.

GGCTCGAGACCGCTGCCCTGCCCTGGTGTATTCCTTACAATAAAAAACAGACACCCGATAATCAAATGTAAGCAGGAGCAGACAGGAGCA 100
CACTGGACACCGCTGGAGCGAACTGCAATTTAATACGTGTAAGACACTAAACCGCGCTCTGGCGTCCGCTGGAGCTTCAATGTGTGTAAC 200
TTGACCGTGGAGCGAGAAATAAAGCCGCTCTCCGCTTAGTGGCACGTCGCTGTAACAGGGAAGTGACCTAACCTACTTCTACGTGTGTAAGATT 300
CCCTGTTCCCTGTTAGGGCTGCTCCGGCTCAAGATTGATTTCTCTCCGCTCAAACGACGTAATTTGTCAGCTTTTGAAGGGCCGACGTGGCGTTAA 400
ATTGGGTGATGGAGCGAGAAATGTTGAGTGGATATTCAGCACTTATGAGACAGAGGAGGAGGAGGAGCGACCGACCCAGCGCTTATTTCAAATGTTG 500
TGAAACCTATAATTAAGTGAAGCTGTTGATGCCCTGCTTGACCA**ATGG**CCCAAGTGGATGCACATGTCCAGATGATACAGCTGCTGTGTGTAAGAACTGT 600
M A Q W M H M S Q M I Q C L S D E T V
CAACAGCCTTATCCACCAGCCGCTCCCCATTGAAGTCAGACACTTTTACGTGAATGGATTGAGAACCAAGGATGGGACGACTTGTGTGTAAGAAAG 700
N S L Y P P A A F P I E V R H F L A E W I E N Q G W D D F V L E K 52
GTGGAGCAGGAGGACCCAGCTCCGCTCTGTTGGACAGACCTCAGCATGCTGCAATCAATTCAGCAGAACCCCAACGCTGTGTGACAGGATGAAGC 800
V E Q E S Q A R A L L D Q T I S M L Q S I A Q Q N A N V V D R M K 85
TGATCGAGTACAGGAAACATGACCAATGTTTCAGCAGACGCTCTGCAATTTGATGATGTCAGGGACATCCTCAGGAAAGGAGAGGCTGTGCTCG 900
L M Q I S R N M T M F Q Q Q P L Q F V V M V R D I L R K E R A L L G 119
CACGTCCGCTCAGATACAAACCCACACAGTACCAAGTACCCGAGTAGAGATTCCTGTTCCCAATGCGAGATGTAGACCACTGCTGTCTGAAG 1000
T S A Q I Q N P P Q Y Q Q Y P S R E S S F L N M Q D V D H L V L K 152
GTGTGGAGTCCAGATATCCGACAAAAGTACACAGCTCCAAAGAGGCTCAACTGGGAGGCGAGAATATGAGGGCTTACAAGGGCCGATCCAAAC 1100
V L E V Q D I R Q K I H Q L Q E E L N W E R Q N Y E G L Q G P I Q 185
AGAAGCGAGCTGATCCCAAAGTCAAGAACTCAGAACTCAGAAACACATCCAGCACTGGAGTCAATGTGAAAGCAATGGCCACGAGCGTTTCA 1200
Q N G L D P T K S E I Q K L Q N H I Q Q L E Y N V K A M A T K R F Q 219
CCTGCTGAAGGAGTGTGTGACTGTCTGGACAGTCCAGACCCGACTGATCAGCAGTGAAGCGTGGAGGTGGAGGACAGCAAGGCCCGCATCGA 1300
L L K E C V D C L D Q C Q T R L I S R L K A W R W E Q H K A A I G 252
CATCCCTTGTGACAACTCAACCTCTGACAGCTGTGTGACAGCTCTTGGGTGAACCGAAGCTGAGACAGGAATGATGCTGATAGCGGAC 1400
H P F D D N L N P L Q T W C E Q L L G V N G K L R Q E L M L I G E 285
CGATCCGAGCTCCAGGAAAGCTGGGCACTTCTGCAAGTCTGATGAAAGCTCTGATGAGTGAACAAGCGCCCTCAGCTGATTAAGACTCA 1500
P I P E L Q E R L G Q L L Q V L I Q S S L V V D K Q P P Q V I K T Q 319
GTCAAAGTTCCTCACTGTCGATACCTGCTGGGGGAAAGTACCTCCCGGAAAGCTGTGGTGTGAAAGCGCAATATTAACGAGCTCAGAGCC 1600
S K F S T T V R Y L L G E K V A P G K P V V L K A Q I I N E L Q A 352
AGGAAGCTGGCAGTGTACAGTGTATAATGCTGGGAACTGATCAACACAGCCATCTAGAACAACAACCGCCAGCAAGAGCAGATGTGCCAFT 1700
R N L G S V P G D N V G E L I N N T A I L E H N T A S K S T C A T 385
TCAGGAATGTCCATAAAAGATCAAGAGGCGAGACAGAAAGGGCTGAATCTGTGACAGAGGAGAAATTTGCTCTCTGTCTGACAGAGATCAC 1800
F R N M S I K K I K R A D R K G S E S V T E E K F A L L F S T E I T 419
CATCACAGCTGTGACACTCCCTACAGATACAGATGATCTCACTGCGCGTGTGTGATGTCATGTCATGAAAGTCAAGACAAACCGCTGCGCCACATC 1900
I T G C D T P Y R I Q M I S L P V V V I V H G S Q D N N A L A T I 452
ATATGGGACTGTCTTTCTGAAGCAGACAGGATGCCGTGCTGTGTCGGGCGCTGCCCTGGAGGATGATGTACAGCACTCTCAACAGTAATTA 2000
I W D C A F S E A D R M P F V P E R V P W R M M Y S T L N S K F 485
CTGCTGAGTCCGGAGCGACCAACTGCGACCACTACAAACAGCACTTCTGGCCAGAGATATTGACAAAGCGCCTTGGCCGAGGATCCAGAA 2100
T A E V G T Q H N L D H Y N Q H F L A Q K I F D K P D F A D D F S N 519
CATGATGTTCTCGGCCAGTTTAATAAGAGGTTCTCCCGGTGACCGTTCACCTCTGGCAGTGGTTGAGGAGTGTGAGGCTGACCAAGAG 2200
M M V S W A Q F N K E V L P G R P F T F W Q W F E G V M E L T K K 552
CACTGAGAGCTTGGAGCGAAGGCGTGTATTTGGTTTCATGGGAAAGCAGCATCTACATTAATTTCAAGCAGCGCCCAACCGGAGCTTCTTCC 2300
H L K T Y W S E G L I F G F I G K Q H L H L I L K D R P N G T F L 585
TTCCCTTAAAGCCTGATGAGCGCATCACCATCCATATGCTGCTCTGAGAAATGGGGACAGAAATCCAGAACATCCAGCCCTTCAACCA 2400
L R F S D S E I G G I T I A Y V S A S E N G G Q K I Q N I Q P F T K 619
GAGAGATCTGAGATCCGACGCTTGTGACCGCATCCGACATACACACACTGATTCCTGAAATTTCTAAACATGAAGTTTCAAAAAA 2500
R D L E I R S L G D R I R D I G H I T H L Y P E F P K H E V F K K 652
TTCTACTGGAGCTCAAGCGTCACTATCCGAGTTACATCCCGTGTCTCCATACCAAAGTGGCAGGAGCTGGCAGACGACACCCAGCTC 2600
F Y S E P Q A S P I G Y I P V S L H T K V G T E A G T A T P P A 685
CCAATATGGCACCAACCTATGCTGAAAGCCTCACAGCAATGTTGGCTCCCGTGCATCAATTCAGCAGCCATTCAGCCCGAAGGTGCTACAC 2700
P N M A P P P I A E S P H S N V G F P V H Q F Q P P S P Q E S I T 719
TCAAGCATAATGGAAAGTGCACCCGCTTCGGTGGAGTTCAGTCCGAACTCCCTGTTGCTTCCCTGAACACATTCCTCAGGTAACAATATGGATCA 2800
Q D I M E S A P A S V E F S P N P P V V F P E H I P A G N N M D L 752
GATTTAGACTTTCAGATTTAATCATGAGATTCCTTTTCGAGACTTCCATGAT**TAG**GAAAGATTTCCATCAAAGCTGCTTTTGGATGAAAGCCG 2900
D L D F A D F N H A D S L F E T L H D * 771
ACATCGATGAGACCGGACCACTGCTGCTGACCTTCAATGAAACAGTGCATGTTGTTGGAGGCTTTCCTTCTACCTTTCATCAACACC 3000
CTACAGCTTCACTACTATTGAGTAAAACTTGCAGAAAGAGCAAAATGGATTTCTTGGAGCTCAACCATTTGAGCTGGTGTACAGGAGCAGG 3100
AATCACTTCAAGGACAAAGTAAACTGAAACAGAAAGTGCCTGCAAGCTGCTGCGCCATCCTGTTGGGGAACCTTTTCTCTCTCTCTCT 3200
TTGCTCATCTGGTGGTAAGTTTGTGATGTT**ATT77A**TTTCCCTGCTGCTTATACCACTGCATGC**ATT77A**GGAAAAAAGTGAAGTGAAGTGAATGATCA 3300
GTAAGTAAATAGCTGCTTTTCAACAACGACAAAGCTGCAGAAAGCAGAAAGTGCAGTGCATGGAACAATAATGAAATGATGTTGCCCATCAG 3400
TGACAGTCACTATGTTGAGATATGTTGCTCTTGTGCTGTTGCTGATGTTGTTAGTCAATGATGAGCAGAAAGATTTGAATGATATATCCCTAT 3500
GTGATAACCTTCTGATTTGAAGCTGGCTAAGTCTCAGCTATAGCATGTTATATATCTCAGTCTCAGAGTAATGCAATATGATGATGATAACT 3600
TCATACTCAGCATGGTCAATCGATGTTGTAAGTCAAGTCTGCTGATAGTGAAGTAAAGATATAAAAGGAAACAATAAGCTTTTCCATCAC 3700
TGTGAAATGGAACTATACCACTTGTGATGATGCTTACAATGGCGGAGAGTCAAGAAATGATGATGATGAGTGGTGAATGCTTATATGTTGCTACTTAA 3800
AGACTCAATGTTGTTGTTTCTGTTAT 3900
CCTTTTCTCAAGTTTGTATCAAGTCTACTAAAGGAGCATGATGTTACTGGTTACATGGTTTGTATTTTTTATTTTCT**ATT77A**AGTCCATAATGC 4000
ACAAAAACAACAGCAGCTTGTCTGCAAGTGTGATGCTGTTACAGTCTTGGAGTGAACAACCTGATAAAAAATAGTGAAGTAAATGATCAACGGT 4100
ACATCCAAACCACTTCTCTTATTTCAAGATGTTGATTTCAAAATAGATGCTGTTTTCATGTAACCTAAATTAATATATGTTGGAGTCTCATAAA 4200
CGTGAATGCTCC**ATT77A**ATGTTTGTGTTAAGTCTGTGTTGAAAGATTAAAAAGCTGTT**AAATAA**AGTCCAAACCAATATGAAAGGTAAG 4300
AAGTAAATGTTGCAATTA**ATT77A**AAATATTACAGAGTAAAGAAATATATATCTGACAGGGAGTGCAGTATCTTGTCTTGTGGAGCTCAAAATC 4400
GAATTTGTTGATTTTGAAGCTTTTATGCTGATGTAAGTGTAAACCGATCTCCCAATAAACTGGTTTATGAGAAAGCTTTGACACTACCTAC 4500
ATCAGCTTAAATGTTGATGATGATAATAAAGGAT 4600
TGACTTTTGAATAAATCACTTGGAGGCTACACTCAATCCATGTAATCTTCAACTGTGAC**AAATAA**ATCAATTTTCT 4683

Fig. 8.1. Nucleotide and deduced amino acid sequence of RbSTAT6. RNA instability motifs (ATTTA) are marked with italics bolded letters. Polyadenylation signals (AATAAA) are shown by bolded letters.

8.2.2. Amino acid sequence comparison and tertiary structure of RbSTAT6

BLAST analysis and pairwise sequence analysis showed that RbSTAT6 shared high sequence identity (85.9%) and similarity (88.3%) with a STAT6 ortholog from mandarinfish (*Siniperca chuatsi*). In addition, RbSTAT6 exhibited 36 - 38% identity and 55 - 59% similarity to that of previously characterized STAT6 orthologs from higher vertebrates at amino acid level (**Fig. 8.2**). The CDD in NCBI revealed that several amino acid residues important for phosphotyrosine (Lys⁵⁶⁹, Arg⁵⁸⁷, Asn⁶¹³ and Gln⁶¹⁵) and hydrophobic binding pockets (Ile⁶¹⁴ and Arg⁶³⁰). Further the completely conserved tyrosine (Y⁶⁶⁵) residue which is phosphorylated during activation was also identified at the TA domain region (**Fig. 8.2**). The homology model of RbSTAT6 was generated by SWISS-MODEL, using mouse STAT5a as a template, since there is no crystal structure of STAT6 available. Results revealed that the structural topology of RbSTAT6 was more or less similar with the mammalian counterpart (**Fig. 8.3**).

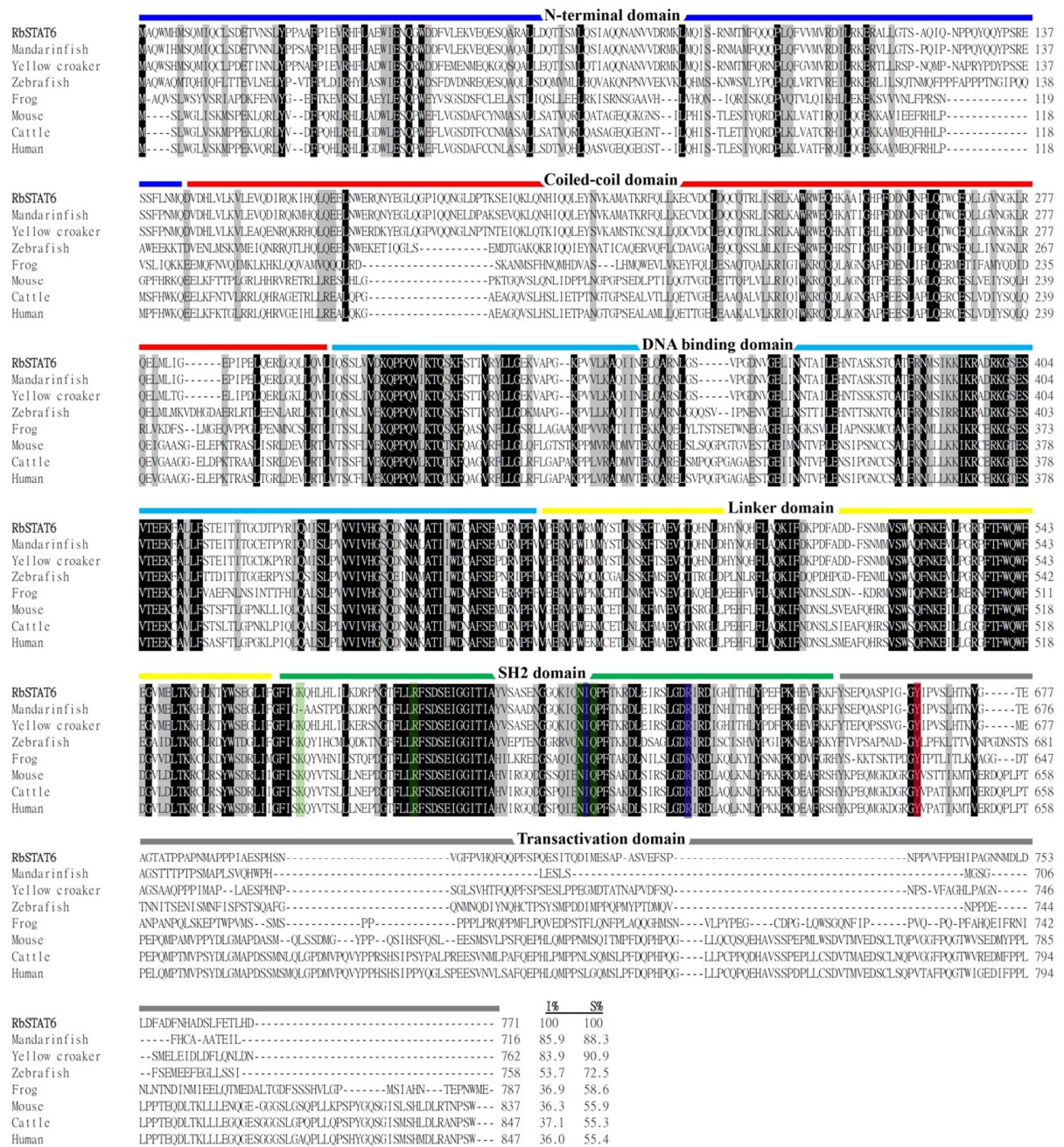


Fig. 8.2. Multiple sequence alignment and pairwise comparison of RbSTAT6 with other STAT6 members. Residues in phosphotyrosine binding pocket and hydrophobic binding pocket are marked with green and purple color, respectively. Completely identical and similar residues among all species are shaded with black color and gray color, respectively. Conserved Tyr residue phosphorylation site is showed in red color box. Percent of identity (I%) and similarity (S%) of RbSTAT6 with other species are shown at the end of each sequences.

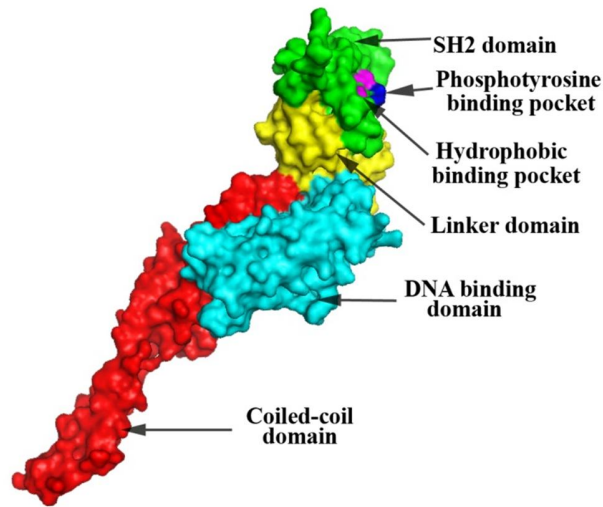


Fig. 8.3. Surface representation of RbSTAT6 3D homology model. The domain regions were highlighted with different surface colors and residues important for the phosphotyrosine binding pocket and hydrophobic binding pocket are marked with pink and blue color, respectively. The images were generated from SWISS-MODEL and visualized by PyMOL molecular graphic software version 1.3.

8.2.3. Phylogenetic analysis

To understand the evolutionary position of RbSTAT6 with respect to the other fish species and vertebrate counterparts, molecular phylogenetic tree was constructed based on the NJ method. STAT ortholog from drosophila was used as an out group. Results revealed that RbSTAT6 was closely clustered with mandarin fish as expected within the fish clade. As other STAT members, fish and other vertebrates have evolved distinctly. In addition, STAT6 members in fish group also clustered into two distinct groups (**Fig. 8.4**).

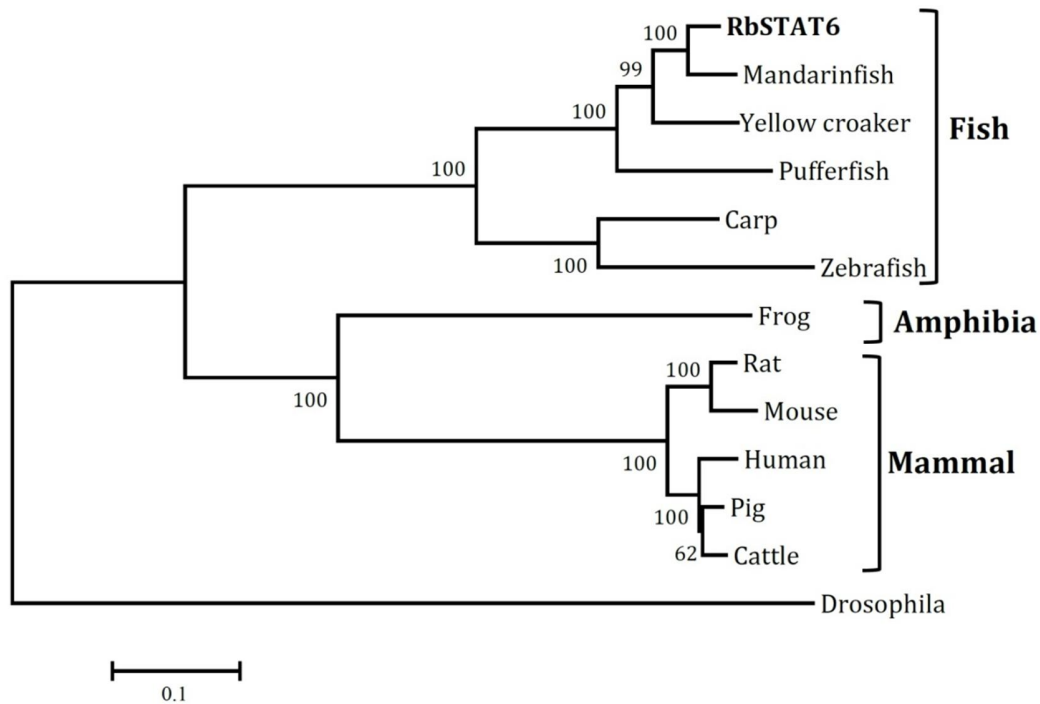


Fig. 8.4. Phylogeny of RbSTAT6. The rooted phylogenetic tree was constructed using NJ method based on the ClustalW alignment of core sequences of STAT6 family members from various taxonomical origins. The numbers at the each nodes are represented the bootstrap confidence values (%) according to the 5000 bootstrap replications.

8.2.4. Expression profiles of RbSTAT6 mRNA

The expression profile of *RbSTAT6* transcripts was assessed by SYBR Green qPCR and dissociation curve was analyzed for all the assays. The results revealed that the dissociation curve had a single peak for both *RbSTAT6* and β -actin suggesting that the amplification was target specific.

8.2.4.1. Expression profile in different tissues of healthy fish

Under normal physiological conditions, RbSTAT6 was highly expressed in blood cells followed by liver, heart and gill tissues. Muscle, skin and intestine showed lower expression of RbSTAT6, while presenting moderate expression in other tissues (**Fig. 8.5**).

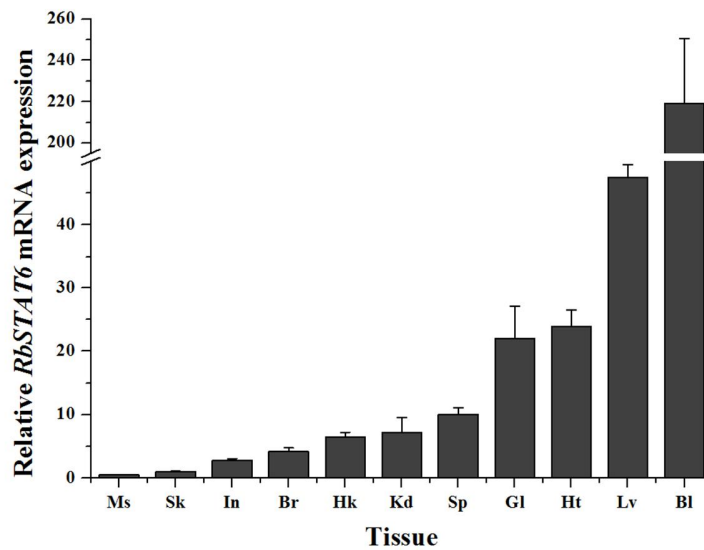


Fig. 8.5. Tissue-specific expression of rock bream STAT6 transcripts in healthy fish. Eleven different tissues including muscle (Ms), skin (Sk), head kidney (Hk), kidney (Kd), brain (Br), gill (GI), intestine (In), spleen (Sp), liver (Lv), heart (Ht) and blood cells (BI) were used. The results are reported as mean \pm standard deviation (SD) of triplicates.

8.2.4.2. Expression profile after *in vivo* immune challenge

The expression profiles of RbSTAT6 obtained by qPCR analysis after pathogenic and PAMPs stimulations showed the significant changes. Upon poly I:C challenge, remarkably higher expression (8.96-fold) was observed at 12 h post injection (p.i.) in blood cells, while showing less expression at 24 h. In addition, significant down-regulations were also detected at 3 h and 48 h p.i. (Fig. 8.6a). In the case of liver tissue, significantly up-regulated expression were detected at 3 h and 48 h p.i. of poly I:C, while depicting down-regulation at 12 h p.i. (Fig. 8.6b). RBIV challenge was caused to induce the expression of RbSTAT6 at 12 h and 24 h in blood cells, while showing suppressed expression at 3 h and 48 h p.i. In contrast elevated expression was observed at 3 h p.i. of RBIV in liver tissues. After LPS stimulation, significantly higher expression was observed at 12 - 24 h p.i. in blood cells, and 3 h, 6 h and 48 h in liver tissues. Upon bacterial challenge, similar expression patterns were observed for both Gram-negative *E. tarda* and Gram-positive *S. iniae* infections in blood cells, and higher expressions were detected at 12 - 24 h. Whereas the expression of RbSTAT6 mRNA in liver tissue, up-regulated expression was detected at 6 h p.i. of *E. tarda*, while showing elevated expressions at 3 h, 6 h and 48 h p.i. of *S. iniae*.

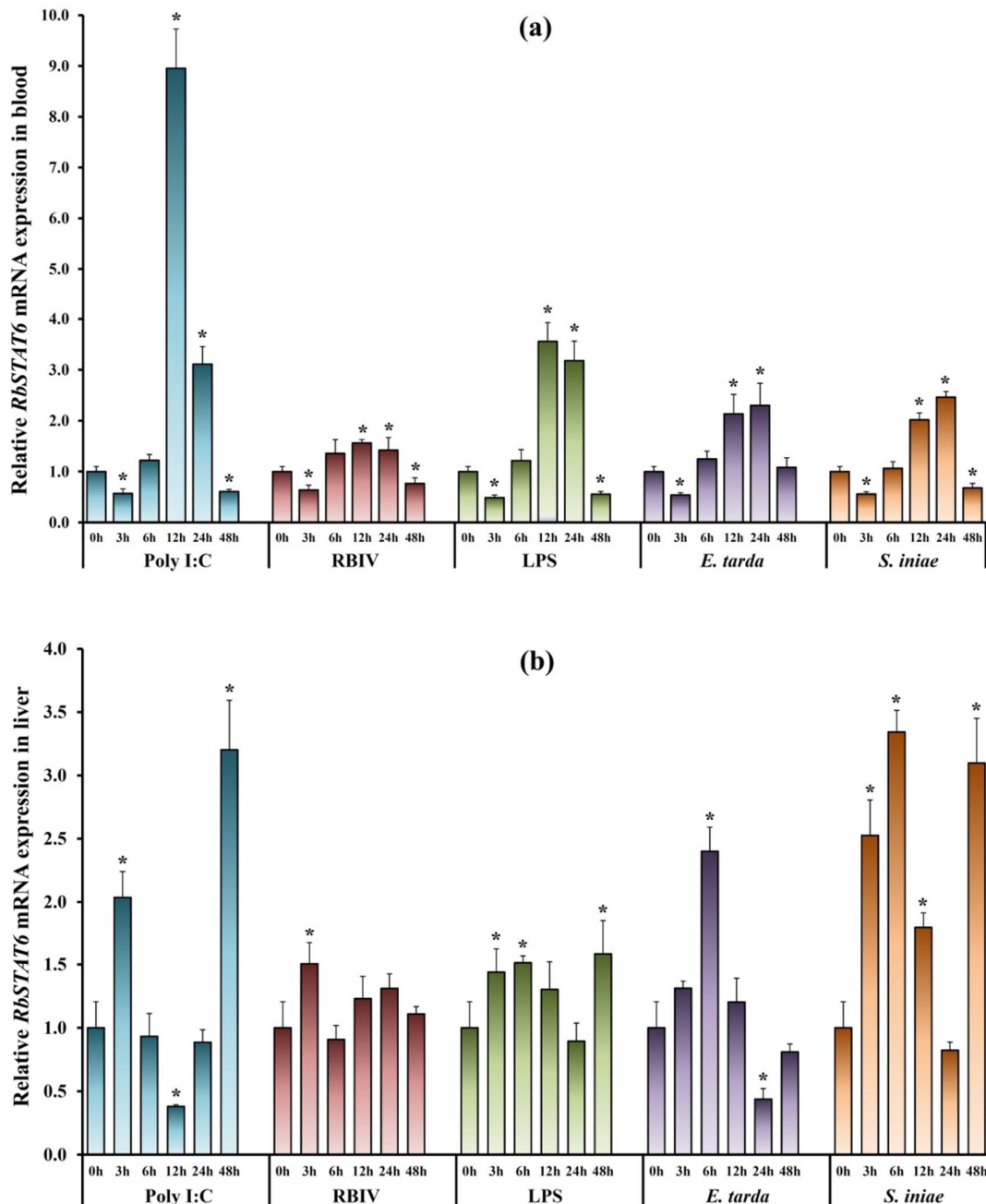


Fig. 8.6. The expressional patterns of RbSTAT6 in blood cells (a) liver (b) after *in vivo* immune challenges. The rock bream β -actin was used as an internal reference gene to calculate the relative mRNA expression. The fold change of mRNA expression at each time point was compared with the PBS-injected control at corresponding time points and, represented as relative fold changes. The results are reported as mean \pm standard deviation (SD) of triplicates, and results were statistically compared relative to the un-injected control (0 h) using t-test. Data with statistically difference at $P < 0.05$ are indicated by asterisks.

8.2.4.3. Expression profile after tissue injury

Transcription level of RbSTAT6 was checked by qPCR analysis in blood and liver tissue to examine the role of RbSTAT6 on wound healing process. Results revealed that blood tissues showed more responses towards tissue injury exhibiting strong down-regulations during experimental periods except at 24 h. However, the transcription profile of RbSTAT6 in liver tissue displayed mild down-regulation only at 12 h post injury (**Fig. 8.7**).

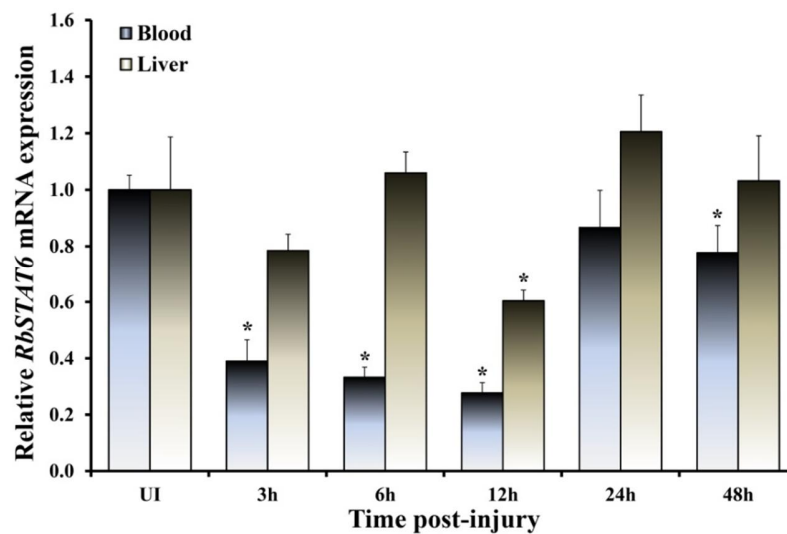


Fig. 8.7. The expressional patterns of RbSTAT6 in blood cells and liver tissue after injury. The fold change of mRNA expression at each time point was compared with the un-injured control (UI) and, represented as relative fold changes. The results are reported as mean \pm standard deviation (SD) of triplicates, and results were statistically compared relative to the un-injured control (UI) using t-test. Data with statistically difference at $P < 0.05$ are indicated by asterisks.

8.2.4.4. Expression profile after rRbIL-10 challenge

Level of transcription of RbSTAT6 was assessed by qPCR after rRbIL-10 stimulation in rock bream heart cells. Results depicted the significant elevations at 6 – 24 h post treatment. The highest expression of RbSTAT6 transcripts was detected at 12 h. In addition, significantly down-regulated expressions were also observed at 3 h and 48 h post stimulation (**Fig. 8.8**).

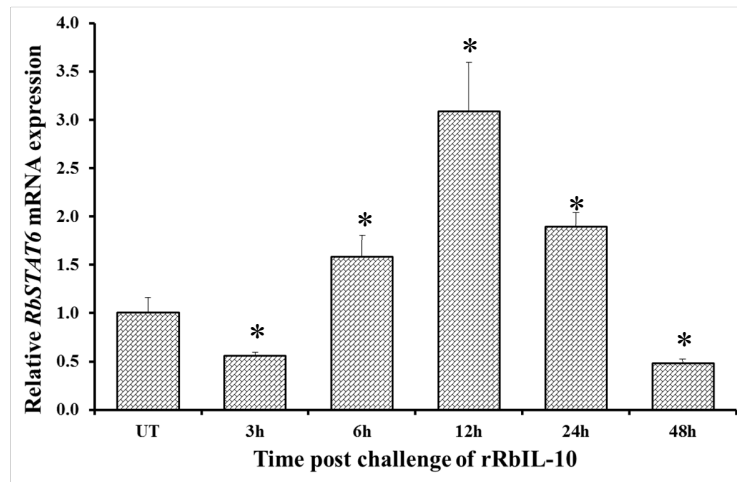


Fig. 8.8. The expressional patterns of RbSTAT6 in heart cells after in vitro immune challenge with rRbIL-10. The fold change of mRNA expression at each time point was compared with the un-treated (UT) control at corresponding time points and, represented as relative fold changes. The results are reported as mean \pm standard deviation (SD) of triplicates, and results were statistically compared relative to the un-treated control (UT) using t-test. Data with statistically difference at $P < 0.05$ are indicated by asterisks.

8.3. Discussion

The research on STAT6 gene characterization is comparatively low even in mammals. Herein we reported the molecular characteristics and functional aspect of STAT6 ortholog identified from rock bream. Based on the *in silico* analysis results evaluated using NCBI and other web based tools, RbSTAT6 indeed a member of STAT6 member. Comparatively other STAT members, RbSTAT6 seems to be moderately conserved from fish to mammals. But, within the fish group it was highly conserved. According to the sequence comparison results, some regions particularly TA domain region of the aa sequence of RbSTAT6 was not conserved well. However, most of the functional residues located in the SH2 domain were conserved among other species. In addition tyrosine residue which is phosphorylated upon activation was completely conserved in all species analyzed. Moreover, we have constructed the 3D structure of RbSTAT6 protein to understand the conservation of structural topology using mouse STAT5a model as a template. Results depicted the similar structural features as other STAT paralogs and indicate the functional conservation from fish to mammals.

For the phylogeny of STAT6, rooted tree was constructed based on the clustalW alignment with thirteen STAT6 orthologs. It was clearly demonstrated that the distinct evolution between fish and other vertebrates. Within the fish group, two separated sister clades were identified and indicate the different evolutionary path among fish group as well. Previous study in zebrafish, also reported the similar kind of separation between fish and other vertebrates (Mitra et al., 2010). However, to understand the real evolutionary paths among species, STAT6 orthologs are required to be identified from large number of species those belong to various taxonomical origins.

The level of mRNA expression under normal physiological condition indicates the biological roles in different tissues. In the present results, the level of RbSTAT6 mRNA was highly detected in blood cells followed by liver tissue. This may suggest that the main role of RbSTAT6 sowed in blood. Previous study in mandarin fish demonstrated that the expression of STAT6 was higher in spleen and gill tissues (Guo et al., 2009). Meanwhile another study in pufferfish showed the expression of STAT6 highly in intestine, liver, testis and heart tissues (Sung et al., 2010). However, the expression level of STAT6 was not reported in those studies. Therefore, more analysis are required to be conducted to understand the real functional role of STAT6 under normal conditions.

To further understand the role of RbSTAT6 under pathological conditions, we have injected two bacterial, viral and two commercially available PAMPs, and measured the level of transcription at different time points. Based on the results the higher expressions were mostly observed at middle phase of experiment in blood cell and liver tissues. The overall pattern was seemed like wave by increasing and decreasing of expression, while significant suppressions also detected in some time points. These results indicate that RbSTAT6 showed immediate responses by converting mRNA into protein. Down-regulated expressions might be caused due to these biological conversions. A group of researchers reported that the expression of zebrafish STAT6 was downregulated at 4 h after LPS and poly I:C stimulation in head kidney and spleen tissues (Mitra et al., 2010). Guo C.J and coworkers demonstrated the significant down-regulations as well as up-regulations of mandarin fish STAT6 mRNA expression upon poly I:C stimulation in MFF-1 cells (Guo et al., 2009). The expression pattern of mandarin fish STAT6 was more or less similar with the current results as shown as a wave pattern. However, no studies regarding

expression patterns upon bacterial infections reported yet. According to the current results, we can suggest that RbSTAT6 may play a vital role in bacterial and viral infections.

Wound healing is an essential biological role in the living organisms in order to replace the damaged cells or tissues. These biological processes are known to be mediated by vast array of elements including cytokines (Filkor et al., 2015), stem cells, growth factors (Pikula et al., 2015) and many signaling molecules (Xu and Yu, 2011; Portou et al., 2015). A study in mice showed that the important role of STAT6 in hepatic ischemia/reperfusion injury (Shen et al., 2003). Another study reported the potential role of STAT4 and STAT6 in pancreatitis-associated lung injury (Simovic et al., 2007). Yoshidome *et al* (Yoshidome et al., 1999) showed the role of STAT6 in inhibition of liver injury induced by ischemia/reperfusion via IL-13 activation. In addition, contribution of STAT6 signaling on modification of gene expression underlying vascular smooth muscle cell activation in the context of acute vascular proliferative diseases has been reported (Baetta et al., 2000). As a preliminary study, we have injured the fish and analyzed the expression of RbSTAT6 at different time points in blood and liver tissue. Results depicted the significant down-regulations of *RbSTAT6* expression remarkably in blood cells. The results of the current study and previous evidences might support to imply the possible role of RbSTAT6 in wound healing mechanism.

The interleukins are one of the leading cytokines involved in activating the various signaling pathways, one of which JAK/STAT signaling cascade is activated via complex of interleukin receptors. Many STAT members response to the interleukins and transduce the signal into the nucleus to initiate the respective genes to show the functional responses. IL-10 one of the leading cytokines, promote the activation of various STATs (Riley et al., 1999; Mosser and Zhang, 2008; Cui et al., 2011). However, the expressions of *STAT6* associated with IL-10 are very limited even in the mammals. In this study, the expression of *RbSTAT6* was measured upon rRbIL-10 stimulation in rock bream heart cells and revealed the significant modulation. Thus, based on the results of current study we can suggest that rock bream IL-10 might be involved in modulation of *RbSTAT6* transcription.

8.4. Conclusion

Herein, we reported the molecular insights and functional aspects of teleostean STAT6 ortholog from rock bream. *In silico* analysis of RbSTAT6 revealed that it is conserved among vertebrates but not like other STAT orthologs. In comparison of teleostean STAT6 with other higher vertebrates indicate the low percentage of identity (< 40%) and similarity (< 60%). Molecular phylogenetic study revealed the distinct evolution among fish and other vertebrates as other STAT paralogs. The highest expression of *RbSTAT6* mRNA in blood cells of healthy fish implied its major tissue of function. Transcriptional changes were observed upon bacterial, viral and PAMPs challenges, as well as after tissue injury. In addition, rock bream IL-10 was caused to modulate the expression of RbSTAT6 mRNA. By taking all the results we can suggest that RbSTAT6 may play essential immune roles against invading pathogens and tissue injury.

9. Concluding remarks

The present study provides the existence and evolutionary conservation of all STAT members in teleost JAK/STAT signaling pathway. Here, we have identified and characterized all STAT members including two isoforms of STAT1 (RbSTAT1 and RbSTAT1L), STAT2, STAT3, STAT4, two isoforms of STAT5 (RbSTAT5-1 and RbSTAT5-2) and STAT6 from one of the commercially crucial teleosts, rock bream (*Oplegnathus fasciatus*). Bioinformatic analysis revealed the structural conservation of all STAT genes throughout the vertebrate origins, while presenting features for RbSTAT1L as a novel STAT family member. Genomic structure organization and phylogenetic analysis demonstrated the distinct evolution of STATs between teleosts and other higher vertebrates.

Transcriptional analysis demonstrated that all the RbSTAT members except *RbSTAT4* were highly expressed in blood cells indicating their major role in blood. Whereas, *RbSTAT4* transcripts were highly expressed in gill tissue under normal physiological condition. Upon immune stimulation, significantly ($P < 0.05$) triggered transcriptions were detected for all STAT members highlighting their innate immune responses against invading viral and bacterial pathogens. Transcriptional modulations of *RbSTATs* were examined in time course manner in response to the tissue injury suggesting their involvement in wound healing process. In addition, transcriptional elevations of all *RbSTAT* members except *RbSTAT5-1* and *RbSTAT5-2* were examined in response to the rock bream IL-10 stimulation in *in vitro* experiment, indicating the activation of JAK/STAT signaling pathway by IL-10 through all RbSTATs except RbSTAT5-1 and RbSTAT5-2. Antiviral potential of RbSTAT1, RbSTAT1L and RbSTAT2 observed in heart cells in the presence of RBIV suggested their possible role in activation of antiviral machineries.

In brief, the current study provides structural and functional features of all the STAT members which are the crucial cytosolic elements of the JAK/STAT signaling cascade. These structural and functional insights of STAT members investigated in this study will provide a strong foundation to establish the teleost JAK/STAT signaling pathway.

10. References

- Aaronson, D.S. and Horvath, C.M., 2002. A road map for those who don't know JAK-STAT. *Science* 296, 1653-5.
- Agaisse, H., Petersen, U.M., Boutros, M., Mathey-Prevot, B. and Perrimon, N., 2003. Signaling role of hemocytes in *Drosophila* JAK/STAT-dependent response to septic injury. *Dev Cell* 5, 441-50.
- Aggarwal, B.B., Sethi, G., Ahn, K.S., Sandur, S.K., Pandey, M.K., Kunnumakkara, A.B., Sung, B. and Ichikawa, H., 2006. Targeting signal-transducer-and-activator-of-transcription-3 for prevention and therapy of cancer: modern target but ancient solution. *Ann N Y Acad Sci* 1091, 151-69.
- Ahsan, H., Aziz, M.H. and Ahmad, N., 2005. Ultraviolet B exposure activates Stat3 signaling via phosphorylation at tyrosine705 in skin of SKH1 hairless mouse: a target for the management of skin cancer? *Biochem Biophys Res Commun* 333, 241-6.
- Akira, S., Nishio, Y., Inoue, M., Wang, X.J., Wei, S., Matsusaka, T., Yoshida, K., Sudo, T., Naruto, M. and Kishimoto, T., 1994. Molecular cloning of APRF, a novel IFN-stimulated gene factor 3 p91-related transcription factor involved in the gp130-mediated signaling pathway. *Cell* 77, 63-71.
- Alonzi, T., Maritano, D., Gorgoni, B., Rizzuto, G., Libert, C. and Poli, V., 2001. Essential role of STAT3 in the control of the acute-phase response as revealed by inducible gene inactivation [correction of activation] in the liver. *Mol Cell Biol* 21, 1621-32.
- Ashour, J., Morrison, J., Laurent-Rolle, M., Belicha-Villanueva, A., Plumlee, C.R., Bernal-Rubio, D., Williams, K.L., Harris, E., Fernandez-Sesma, A., Schindler, C. and Garcia-Sastre, A., 2010. Mouse STAT2 restricts early dengue virus replication. *Cell Host Microbe* 8, 410-21.
- Bacon, C.M., Petricoin, E.F., 3rd, Ortaldo, J.R., Rees, R.C., Lamer, A.C., Johnston, J.A. and O'Shea, J.J., 1995. Interleukin 12 induces tyrosine phosphorylation and activation of STAT4 in human lymphocytes. *Proc Natl Acad Sci U S A* 92, 7307-11.
- Baetta, R., Soma, M., De-Fraja, C., Comparato, C., Teruzzi, C., Magrassi, L. and Cattaneo, E., 2000. Upregulation and activation of Stat6 precede vascular smooth muscle cell proliferation in carotid artery injury model. *Arterioscler Thromb Vasc Biol* 20, 931-9.
- Barillas-Mury, C., Han, Y.S., Seeley, D. and Kafatos, F.C., 1999. *Anopheles gambiae* Ag-STAT, a new insect member of the STAT family, is activated in response to bacterial infection. *EMBO J* 18, 959-67.
- Barton, G.M. and Medzhitov, R., 2002. Control of adaptive immune responses by Toll-like receptors. *Curr Opin Immunol* 14, 380-3.

- Bathige, S.D., Umasuthan, N., Whang, I., Lim, B.S., Won, S.H. and Lee, J., 2014. Antibacterial activity and immune responses of a molluscan macrophage expressed gene-1 from disk abalone, *Haliotis discus discus*. *Fish Shellfish Immunol* 39, 263-72.
- Becker, S., Groner, B. and Muller, C.W., 1998. Three-dimensional structure of the Stat3beta homodimer bound to DNA. *Nature* 394, 145-51.
- Bhattacharya, S., Eckner, R., Grossman, S., Oldread, E., Arany, Z., D'Andrea, A. and Livingston, D.M., 1996. Cooperation of Stat2 and p300/CBP in signalling induced by interferon-alpha. *Nature* 383, 344-7.
- Blaszczyk, K., Olejnik, A., Nowicka, H., Ozgyin, L., Chen, Y.L., Chmielewski, S., Kostyrko, K., Wesoly, J., Balint, B.L., Lee, C.K. and Bluysen, H.A., 2015. STAT2/IRF9 directs a prolonged ISGF3-like transcriptional response and antiviral activity in the absence of STAT1. *Biochem J* 466, 511-24.
- Bowden, T.J., Cook, P. and Rombout, J.H., 2005. Development and function of the thymus in teleosts. *Fish Shellfish Immunol* 19, 413-27.
- Bowman, T., Garcia, R., Turkson, J. and Jove, R., 2000. STATs in oncogenesis. *Oncogene* 19, 2474-88.
- Bradford, M.M., 1976. A rapid and sensitive method for the quantitation of microgram quantities of protein utilizing the principle of protein-dye binding. *Anal Biochem* 72, 248-54.
- Bromberg, J. and Darnell, J.E., Jr., 2000. The role of STATs in transcriptional control and their impact on cellular function. *Oncogene* 19, 2468-73.
- Bustin, S.A., Benes, V., Garson, J.A., Hellems, J., Huggett, J., Kubista, M., Mueller, R., Nolan, T., Pfaffl, M.W., Shipley, G.L., Vandesompele, J. and Wittwer, C.T., 2009. The MIQE guidelines: minimum information for publication of quantitative real-time PCR experiments. *Clin Chem* 55, 611-22.
- Carballo, M., Conde, M., El Bekay, R., Martin-Nieto, J., Camacho, M.J., Monteseirin, J., Conde, J., Bedoya, F.J. and Sobrino, F., 1999. Oxidative stress triggers STAT3 tyrosine phosphorylation and nuclear translocation in human lymphocytes. *J Biol Chem* 274, 17580-6.
- Chen, L.S., Wei, P.C., Liu, T., Kao, C.H., Pai, L.M. and Lee, C.K., 2009. STAT2 hypomorphic mutant mice display impaired dendritic cell development and antiviral response. *J Biomed Sci* 16, 22.
- Chen, W.Y., Ho, K.C., Leu, J.H., Liu, K.F., Wang, H.C., Kou, G.H. and Lo, C.F., 2008. WSSV infection activates STAT in shrimp. *Dev Comp Immunol* 32, 1142-50.
- Chen, X., Vinkemeier, U., Zhao, Y., Jeruzalmi, D., Darnell, J.E., Jr. and Kuriyan, J., 1998. Crystal structure of a tyrosine phosphorylated STAT-1 dimer bound to DNA. *Cell* 93, 827-39.

- Cho, S.S., Bacon, C.M., Sudarshan, C., Rees, R.C., Finbloom, D., Pine, R. and O'Shea, J.J., 1996. Activation of STAT4 by IL-12 and IFN-alpha: evidence for the involvement of ligand-induced tyrosine and serine phosphorylation. *J Immunol* 157, 4781-9.
- Coffman, R.L., Leberman, D.A. and Rothman, P., 1993. Mechanism and regulation of immunoglobulin isotype switching. *Adv Immunol* 54, 229-70.
- Collet, B., Bain, N., Prevost, S., Besinque, G., McBeath, A., Snow, M. and Collins, C., 2008. Isolation of an Atlantic salmon (*Salmo salar*) signal transducer and activator of transcription STAT1 gene: kinetics of expression upon ISAV or IPNV infection. *Fish Shellfish Immunol* 25, 861-7.
- Collet, B., Ganne, G., Bird, S. and Collins, C.M., 2009. Isolation and expression profile of a gene encoding for the Signal Transducer and Activator of Transcription STAT2 in Atlantic salmon (*Salmo salar*). *Dev Comp Immunol* 33, 821-9.
- Crispi, S., Sanzari, E., Monfregola, J., De Felice, N., Fimiani, G., Ambrosio, R., D'Urso, M. and Ursini, M.V., 2004. Characterization of the human STAT5A and STAT5B promoters: evidence of a positive and negative mechanism of transcriptional regulation. *FEBS Lett* 562, 27-34.
- Cui, W., Liu, Y., Weinstein, J.S., Craft, J. and Kaech, S.M., 2011. An interleukin-21-interleukin-10-STAT3 pathway is critical for functional maturation of memory CD8⁺ T cells. *Immunity* 35, 792-805.
- Darnell, J.E., Jr., 1997. STATs and gene regulation. *Science* 277, 1630-5.
- Darnell, J.E., Jr., Kerr, I.M. and Stark, G.R., 1994. Jak-STAT pathways and transcriptional activation in response to IFNs and other extracellular signaling proteins. *Science* 264, 1415-21.
- Dauer, D.J., Ferraro, B., Song, L., Yu, B., Mora, L., Buettner, R., Enkemann, S., Jove, R. and Haura, E.B., 2005. Stat3 regulates genes common to both wound healing and cancer. *Oncogene* 24, 3397-408.
- Demoulin, J.B., Uyttenhove, C., Van Roost, E., DeLestre, B., Donckers, D., Van Snick, J. and Renauld, J.C., 1996. A single tyrosine of the interleukin-9 (IL-9) receptor is required for STAT activation, antiapoptotic activity, and growth regulation by IL-9. *Mol Cell Biol* 16, 4710-6.
- Di Domenico, F., Casalena, G., Sultana, R., Cai, J., Pierce, W.M., Perluigi, M., Cini, C., Baracca, A., Solaini, G., Lenaz, G., Jia, J., Dziennis, S., Murphy, S.J., Alkayed, N.J. and Butterfield, D.A., 2010. Involvement of Stat3 in mouse brain development and sexual dimorphism: a proteomics approach. *Brain Res* 1362, 1-12.
- Do, J.W., Moon, C.H., Kim, H.J., Ko, M.S., Kim, S.B., Son, J.H., Kim, J.S., An, E.J., Kim, M.K., Lee, S.K., Han, M.S., Cha, S.J., Park, M.S., Park, M.A., Kim, Y.C., Kim, J.W. and Park,

- J.W., 2004. Complete genomic DNA sequence of rock bream iridovirus. *Virology* 325, 351-63.
- Dostert, C., Jouanguy, E., Irving, P., Troxler, L., Galiana-Arnoux, D., Hetru, C., Hoffmann, J.A. and Imler, J.L., 2005. The Jak-STAT signaling pathway is required but not sufficient for the antiviral response of drosophila. *Nat Immunol* 6, 946-53.
- Durali, D., de Goer de Herve, M.G., Giron-Michel, J., Azzarone, B., Delfraissy, J.F. and Taoufik, Y., 2003. In human B cells, IL-12 triggers a cascade of molecular events similar to Th1 commitment. *Blood* 102, 4084-9.
- Durbin, J.E., Hackenmiller, R., Simon, M.C. and Levy, D.E., 1996. Targeted disruption of the mouse Stat1 gene results in compromised innate immunity to viral disease. *Cell* 84, 443-50.
- Dziennis, S. and Alkayed, N.J., 2008. Role of signal transducer and activator of transcription 3 in neuronal survival and regeneration. *Rev Neurosci* 19, 341-61.
- Elliott, J., Lynch, O.T., Suessmuth, Y., Qian, P., Boyd, C.R., Burrows, J.F., Buick, R., Stevenson, N.J., Touzelet, O., Gadina, M., Power, U.F. and Johnston, J.A., 2007. Respiratory syncytial virus NS1 protein degrades STAT2 by using the Elongin-Cullin E3 ligase. *J Virol* 81, 3428-36.
- Eshleman, E.M. and Lenz, L.L., 2014. Type I interferons in bacterial infections: taming of myeloid cells and possible implications for autoimmunity. *Front Immunol* 5, 431.
- Ferreira, R., Ohneda, K., Yamamoto, M. and Philipsen, S., 2005. GATA1 function, a paradigm for transcription factors in hematopoiesis. *Mol Cell Biol* 25, 1215-27.
- Filkor, K., Nemeth, T., Nagy, I., Kondorosi, E., Urban, E., Kemeny, L. and Szolnoky, G., 2015. The expression of inflammatory cytokines, TAM tyrosine kinase receptors and their ligands is upregulated in venous leg ulcer patients: a novel insight into chronic wound immunity. *Int Wound J*.
- Foletta, V.C., Segal, D.H. and Cohen, D.R., 1998. Transcriptional regulation in the immune system: all roads lead to AP-1. *J Leukoc Biol* 63, 139-52.
- Frucht, D.M., Aringer, M., Galon, J., Danning, C., Brown, M., Fan, S., Centola, M., Wu, C.Y., Yamada, N., El Gabalawy, H. and O'Shea, J.J., 2000. Stat4 is expressed in activated peripheral blood monocytes, dendritic cells, and macrophages at sites of Th1-mediated inflammation. *J Immunol* 164, 4659-64.
- Fujii, H., Watanabe, S., Yamane, D., Ueda, N., Iha, K., Taniguchi, S., Kato, K., Tohya, Y., Kyuwa, S., Yoshikawa, Y. and Akashi, H., 2010. Functional analysis of *Rousettus aegyptiacus* "signal transducer and activator of transcription 1" (STAT1). *Dev Comp Immunol* 34, 598-602.

- Fukao, T., Frucht, D.M., Yap, G., Gadina, M., O'Shea, J.J. and Koyasu, S., 2001. Inducible expression of Stat4 in dendritic cells and macrophages and its critical role in innate and adaptive immune responses. *J Immunol* 166, 4446-55.
- Gao, B., 2005. Cytokines, STATs and liver disease. *Cell Mol Immunol* 2, 92-100.
- Gao, H., Guo, R.F., Speyer, C.L., Reuben, J., Neff, T.A., Hoesel, L.M., Riedemann, N.C., McClintock, S.D., Sarma, J.V., Van Rooijen, N., Zetoune, F.S. and Ward, P.A., 2004. Stat3 activation in acute lung injury. *J Immunol* 172, 7703-12.
- Gatsios, P., Terstegen, L., Schliess, F., Haussinger, D., Kerr, I.M., Heinrich, P.C. and Graeve, L., 1998. Activation of the Janus kinase/signal transducer and activator of transcription pathway by osmotic shock. *J Biol Chem* 273, 22962-8.
- Gilbert, S., Nivarthi, H., Mayhew, C.N., Lo, Y.H., Noah, T.K., Vallance, J., Rulicke, T., Muller, M., Jegga, A.G., Tang, W., Zhang, D., Helmuth, M., Shroyer, N., Moriggl, R. and Han, X., 2015. Activated STAT5 confers resistance to intestinal injury by increasing intestinal stem cell proliferation and regeneration. *Stem Cell Reports* 4, 209-25.
- Gotoh, B., Takeuchi, K., Komatsu, T. and Yokoo, J., 2003. The STAT2 activation process is a crucial target of Sendai virus C protein for the blockade of alpha interferon signaling. *J Virol* 77, 3360-70.
- Gronowski, A.M., Zhong, Z., Wen, Z., Thomas, M.J., Darnell, J.E., Jr. and Rotwein, P., 1995. In vivo growth hormone treatment rapidly stimulates the tyrosine phosphorylation and activation of Stat3. *Mol Endocrinol* 9, 171-7.
- Guo, C.J., Zhang, Y.F., Yang, L.S., Yang, X.B., Wu, Y.Y., Liu, D., Chen, W.J., Weng, S.P., Yu, X.Q. and He, J.G., 2009. The JAK and STAT family members of the mandarin fish *Siniperca chuatsi*: molecular cloning, tissues distribution and immunobiological activity. *Fish Shellfish Immunol* 27, 349-59.
- Guo, T., Leng, X.J., Wu, X.F., Li, J.L., Gao, J.Z., Li, X.Q., Gan, T. and Wei, J., 2013. Cloning, molecular characterization, and expression analysis of the signal transducer and activator of transcription 3 (STAT3) gene from grass carp (*Ctenopharyngodon idellus*). *Fish Shellfish Immunol* 35, 1624-34.
- Hahn, B., Trifilo, M.J., Zuniga, E.I. and Oldstone, M.B., 2005. Viruses evade the immune system through type I interferon-mediated STAT2-dependent, but STAT1-independent, signaling. *Immunity* 22, 247-57.
- Hambleton, S., Goodbourn, S., Young, D.F., Dickinson, P., Mohamad, S.M., Valappil, M., McGovern, N., Cant, A.J., Hackett, S.J., Ghazal, P., Morgan, N.V. and Randall, R.E., 2013. STAT2 deficiency and susceptibility to viral illness in humans. *Proc Natl Acad Sci U S A* 110, 3053-8.
- Hansson, G.K., Libby, P., Schönbeck, U. and Yan, Z.-Q., 2002. Innate and Adaptive Immunity in the Pathogenesis of Atherosclerosis. *Circulation Research* 91, 281-291.

- Harrison, D.A., 2012. The Jak/STAT pathway. *Cold Spring Harb Perspect Biol* 4.
- Hennighausen, L., Robinson, G.W., Wagner, K.U. and Liu, W., 1997. Prolactin signaling in mammary gland development. *J Biol Chem* 272, 7567-9.
- Hirano, T., Ishihara, K. and Hibi, M., 2000. Roles of STAT3 in mediating the cell growth, differentiation and survival signals relayed through the IL-6 family of cytokine receptors. *Oncogene* 19, 2548-56.
- Horiuchi, M., Wakayama, K., Itoh, A., Kawai, K., Pleasure, D., Ozato, K. and Itoh, T., 2012. Interferon regulatory factor 8/interferon consensus sequence binding protein is a critical transcription factor for the physiological phenotype of microglia. *J Neuroinflammation* 9, 227.
- Hou, J., Schindler, U., Henzel, W.J., Ho, T.C., Brasseur, M. and McKnight, S.L., 1994. An interleukin-4-induced transcription factor: IL-4 Stat. *Science* 265, 1701-6.
- Huang, M., Qian, F., Hu, Y., Ang, C., Li, Z. and Wen, Z., 2002. Chromatin-remodelling factor BRG1 selectively activates a subset of interferon-alpha-inducible genes. *Nat Cell Biol* 4, 774-81.
- Huang, W., Zhou, W., Saberwal, G., Konieczna, I., Horvath, E., Katsoulidis, E., Plataniias, L.C. and Eklund, E.A., 2010. Interferon consensus sequence binding protein (ICSBP) decreases beta-catenin activity in myeloid cells by repressing GAS2 transcription. *Mol Cell Biol* 30, 4575-94.
- Huang, X., Huang, Y., Yang, Y., Wei, S. and Qin, Q., 2014. Involvement of fish signal transducer and activator of transcription 3 (STAT3) in SGIV replication and virus induced paraptosis. *Fish Shellfish Immunol* 41, 308-16.
- Huang, Y., Huang, X., Yang, Y., Wang, W., Yu, Y. and Qin, Q., 2015. Involvement of fish signal transducer and activator of transcription 3 (STAT3) in nodavirus infection induced cell death. *Fish Shellfish Immunol* 43, 241-8.
- Ihle, J.N., 1996. STATs: signal transducers and activators of transcription. *Cell* 84, 331-4.
- Ihle, J.N. and Kerr, I.M., 1995. Jaks and Stats in signaling by the cytokine receptor superfamily. *Trends Genet* 11, 69-74.
- Improta, T., Schindler, C., Horvath, C.M., Kerr, I.M., Stark, G.R. and Darnell, J.E., Jr., 1994. Transcription factor ISGF-3 formation requires phosphorylated Stat91 protein, but Stat113 protein is phosphorylated independently of Stat91 protein. *Proc Natl Acad Sci U S A* 91, 4776-80.
- Jacobson, N.G., Szabo, S.J., Weber-Nordt, R.M., Zhong, Z., Schreiber, R.D., Darnell, J.E., Jr. and Murphy, K.M., 1995. Interleukin 12 signaling in T helper type 1 (Th1) cells involves tyrosine phosphorylation of signal transducer and activator of transcription (Stat)3 and Stat4. *J Exp Med* 181, 1755-62.

- Jung, S.J. and Oh, M.J., 2000. Iridovirus-like infection associated with high mortalities of striped beakperch, *Oplegnathus fasciatus* (Temminck et Schlegel), in southern coastal areas of the Korean peninsula. *Journal of Fish Diseases* 23, 223-226.
- Kadeppagari, R.K., Sanchez, R.L. and Foster, T.P., 2012. HSV-2 inhibits type-I interferon signaling via multiple complementary and compensatory STAT2-associated mechanisms. *Virus Res* 167, 273-84.
- Kaestner, K.H., 2000. The hepatocyte nuclear factor 3 (HNF3 or FOXA) family in metabolism. *Trends Endocrinol Metab* 11, 281-5.
- Kammer, W., Lischke, A., Moriggl, R., Groner, B., Ziemiecki, A., Gurniak, C.B., Berg, L.J. and Friedrich, K., 1996. Homodimerization of interleukin-4 receptor alpha chain can induce intracellular signaling. *J Biol Chem* 271, 23634-7.
- Kasthuri, S.R., Wan, Q., Umasuthan, N., Bathige, S.D., Lim, B.S., Jung, H.B., Lee, J. and Whang, I., 2013. Genomic characterization, expression analysis, and antimicrobial function of a glyrichin homologue from rock bream, *Oplegnathus fasciatus*. *Fish Shellfish Immunol* 35, 1406-15.
- Kato, K., Nomoto, M., Izumi, H., Ise, T., Nakano, S., Niho, Y. and Kohno, K., 2000. Structure and functional analysis of the human STAT3 gene promoter: alteration of chromatin structure as a possible mechanism for the upregulation in cisplatin-resistant cells. *Biochim Biophys Acta* 1493, 91-100.
- Kemler, I. and Schaffner, W., 1990. Octamer transcription factors and the cell type-specificity of immunoglobulin gene expression. *FASEB J* 4, 1444-9.
- Khorooshi, R., Babcock, A.A. and Owens, T., 2008. NF-kappaB-driven STAT2 and CCL2 expression in astrocytes in response to brain injury. *J Immunol* 181, 7284-91.
- Kim, H.J., Kwon, Y.M., Kim, Y.I., Lee, I.H., Jin, B.R., Han, Y.S., Cheon, H.M., Kang, Y.J. and Seo, S.J., 2011. Molecular cloning and characterization of the STAT gene in *Hyphantria cunea* haemocytes. *Insect Mol Biol* 20, 723-32.
- Kim, H.S. and Lee, M.S., 2005. Essential role of STAT1 in caspase-independent cell death of activated macrophages through the p38 mitogen-activated protein kinase/STAT1/reactive oxygen species pathway. *Mol Cell Biol* 25, 6821-33.
- Kim, J.Y., Lee, S.H., Song, E.H., Park, Y.M., Lim, J.Y., Kim, D.J., Choi, K.H., Park, S.I., Gao, B. and Kim, W.H., 2009. A critical role of STAT1 in streptozotocin-induced diabetic liver injury in mice: controlled by ATF3. *Cell Signal* 21, 1758-67.
- Kisseleva, T., Bhattacharya, S., Braunstein, J. and Schindler, C.W., 2002. Signaling through the JAK/STAT pathway, recent advances and future challenges. *Gene* 285, 1-24.
- Kotanides, H. and Reich, N.C., 1993. Requirement of tyrosine phosphorylation for rapid activation of a DNA binding factor by IL-4. *Science* 262, 1265-7.

- Lau, J.F., Nusinzon, I., Burakov, D., Freedman, L.P. and Horvath, C.M., 2003. Role of metazoan mediator proteins in interferon-responsive transcription. *Mol Cell Biol* 23, 620-8.
- Lau, J.F., Parisien, J.P. and Horvath, C.M., 2000. Interferon regulatory factor subcellular localization is determined by a bipartite nuclear localization signal in the DNA-binding domain and interaction with cytoplasmic retention factors. *Proc Natl Acad Sci U S A* 97, 7278-83.
- Lee, J.W., Kang, H.S., Lee, J.Y., Lee, E.J., Rhim, H., Yoon, J.H., Seo, S.R. and Chung, K.C., 2012. The transcription factor STAT2 enhances proteasomal degradation of RCAN1 through the ubiquitin E3 ligase FBW7. *Biochem Biophys Res Commun* 420, 404-10.
- Lekstrom-Himes, J. and Xanthopoulos, K.G., 1998. Biological role of the CCAAT/enhancer-binding protein family of transcription factors. *J Biol Chem* 273, 28545-8.
- Levy, D.E. and Lee, C.K., 2002. What does Stat3 do? *J Clin Invest* 109, 1143-8.
- Lewis, R.S. and Ward, A.C., 2004. Conservation, duplication and divergence of the zebrafish *stat5* genes. *Gene* 338, 65-74.
- Li, H., Sun, Z.P., Li, Q. and Jiang, Y.L., 2011. [Characterization of an iridovirus detected in rock bream (*Oplegnathus fasciatus*; Temminck and Schlegel)]. *Bing Du Xue Bao* 27, 158-64.
- Li, X., Leung, S., Kerr, I.M. and Stark, G.R., 1997. Functional subdomains of STAT2 required for preassociation with the alpha interferon receptor and for signaling. *Mol Cell Biol* 17, 2048-56.
- Lin, C.C., Chou, C.M., Hsu, Y.L., Lien, J.C., Wang, Y.M., Chen, S.T., Tsai, S.C., Hsiao, P.W. and Huang, C.J., 2004. Characterization of two mosquito STATs, AaSTAT and CtSTAT. Differential regulation of tyrosine phosphorylation and DNA binding activity by lipopolysaccharide treatment and by Japanese encephalitis virus infection. *J Biol Chem* 279, 3308-17.
- Lin, J.X., Migone, T.S., Tsang, M., Friedmann, M., Weatherbee, J.A., Zhou, L., Yamauchi, A., Bloom, E.T., Mietz, J., John, S. and et al., 1995. The role of shared receptor motifs and common Stat proteins in the generation of cytokine pleiotropy and redundancy by IL-2, IL-4, IL-7, IL-13, and IL-15. *Immunity* 2, 331-9.
- Liu, B.S., Stoop, J.N., Huizinga, T.W. and Toes, R.E., 2013. IL-21 enhances the activity of the TLR-MyD88-STAT3 pathway but not the classical TLR-MyD88-NF-kappaB pathway in human B cells to boost antibody production. *J Immunol* 191, 4086-94.
- Lokuta, M.A., McDowell, M.A. and Paulnock, D.M., 1998. Cutting Edge: Identification of an Additional Isoform of STAT5 Expressed in Immature Macrophages. *The Journal of Immunology* 161, 1594-1597.
- Lu, B., Reichel, M., Fisher, D.A., Smith, J.F. and Rothman, P., 1997. Identification of a STAT6 domain required for IL-4-induced activation of transcription. *J Immunol* 159, 1255-64.

- Lu, J., Yi, L., Zhao, J., Yu, J., Chen, Y., Lin, M.C., Kung, H.F. and He, M.L., 2012. Enterovirus 71 disrupts interferon signaling by reducing the level of interferon receptor 1. *J Virol* 86, 3767-76.
- Lundgren, M., Larsson, C., Femino, A., Xu, M., Stavnezer, J. and Severinson, E., 1994. Activation of the Ig germ-line gamma 1 promoter. Involvement of C/enhancer-binding protein transcription factors and their possible interaction with an NF-IL-4 site. *J Immunol* 153, 2983-95.
- Luu, K., Greenhill, C.J., Majoros, A., Decker, T., Jenkins, B.J. and Mansell, A., 2014. STAT1 plays a role in TLR signal transduction and inflammatory responses. *Immunol Cell Biol* 92, 761-9.
- Magnadottir, B., 2006. Innate immunity of fish (overview). *Fish Shellfish Immunol* 20, 137-51.
- Magnadottir, B., 2010. Immunological control of fish diseases. *Mar Biotechnol (NY)* 12, 361-79.
- Marrero, M.B., 2005. Introduction to JAK/STAT signaling and the vasculature. *Vascul Pharmacol* 43, 307-9.
- McCartney, E.M., Helbig, K.J., Narayana, S.K., Eyre, N.S., Aloia, A.L. and Beard, M.R., 2013. Signal transducer and activator of transcription 3 is a proviral host factor for hepatitis C virus. *Hepatology* 58, 1558-68.
- Medzhitov, R., 2001. Toll-like receptors and innate immunity. *Nat Rev Immunol* 1, 135-45.
- Meraz, M.A., White, J.M., Sheehan, K.C., Bach, E.A., Rodig, S.J., Dighe, A.S., Kaplan, D.H., Riley, J.K., Greenlund, A.C., Campbell, D., Carver-Moore, K., DuBois, R.N., Clark, R., Aguet, M. and Schreiber, R.D., 1996. Targeted disruption of the Stat1 gene in mice reveals unexpected physiologic specificity in the JAK-STAT signaling pathway. *Cell* 84, 431-42.
- Mikita, T., Campbell, D., Wu, P., Williamson, K. and Schindler, U., 1996. Requirements for interleukin-4-induced gene expression and functional characterization of Stat6. *Mol Cell Biol* 16, 5811-20.
- Mitchell, T.J. and John, S., 2005. Signal transducer and activator of transcription (STAT) signalling and T-cell lymphomas. *Immunology* 114, 301-12.
- Mitra, S., Alnabulsi, A., Secombes, C.J. and Bird, S., 2010. Identification and characterization of the transcription factors involved in T-cell development, t-bet, stat6 and foxp3, within the zebrafish, *Danio rerio*. *FEBS J* 277, 128-47.
- Mohanty, B.R. and Sahoo, P.K., 2007. Edwardsiellosis in fish: a brief review. *J Biosci* 32, 1331-44.
- Monroe, K.M., McWhirter, S.M. and Vance, R.E., 2010. Induction of type I interferons by bacteria. *Cell Microbiol* 12, 881-90.

- Mosser, D.M. and Zhang, X., 2008. Interleukin-10: new perspectives on an old cytokine. *Immunol Rev* 226, 205-18.
- Mowen, K.A., Tang, J., Zhu, W., Schurter, B.T., Shuai, K., Herschman, H.R. and David, M., 2001. Arginine methylation of STAT1 modulates IFN α /beta-induced transcription. *Cell* 104, 731-41.
- Murphy, K.M., Ouyang, W., Farrar, J.D., Yang, J., Ranganath, S., Asnagli, H., Afkarian, M. and Murphy, T.L., 2000. Signaling and transcription in T helper development. *Annu Rev Immunol* 18, 451-94.
- Murray, P.J., 2007. The JAK-STAT signaling pathway: input and output integration. *J Immunol* 178, 2623-9.
- Neculai, D., Neculai, A.M., Verrier, S., Straub, K., Klumpp, K., Pfitzner, E. and Becker, S., 2005. Structure of the unphosphorylated STAT5a dimer. *J Biol Chem* 280, 40782-7.
- Nerlov, C., 2007. The C/EBP family of transcription factors: a paradigm for interaction between gene expression and proliferation control. *Trends Cell Biol* 17, 318-24.
- Nguyen, K.B., Watford, W.T., Salomon, R., Hofmann, S.R., Pien, G.C., Morinobu, A., Gadina, M., O'Shea, J.J. and Biron, C.A., 2002a. Critical role for STAT4 activation by type 1 interferons in the interferon-gamma response to viral infection. *Science* 297, 2063-6.
- Nguyen, V.P., Saleh, A.Z., Arch, A.E., Yan, H., Piazza, F., Kim, J. and Krolewski, J.J., 2002b. Stat2 binding to the interferon-alpha receptor 2 subunit is not required for interferon-alpha signaling. *J Biol Chem* 277, 9713-21.
- O'Shea, J.J., Gadina, M. and Schreiber, R.D., 2002. Cytokine signaling in 2002: new surprises in the Jak/Stat pathway. *Cell* 109 Suppl, S121-31.
- O'Shea, J.J. and Plenge, R., 2012. JAK and STAT signaling molecules in immunoregulation and immune-mediated disease. *Immunity* 36, 542-50.
- Oates, A.C., Wollberg, P., Pratt, S.J., Paw, B.H., Johnson, S.L., Ho, R.K., Postlethwait, J.H., Zon, L.I. and Wilks, A.F., 1999. Zebrafish stat3 is expressed in restricted tissues during embryogenesis and stat1 rescues cytokine signaling in a STAT1-deficient human cell line. *Dev Dyn* 215, 352-70.
- Oeckinghaus, A. and Ghosh, S., 2009. The NF-kappaB family of transcription factors and its regulation. *Cold Spring Harb Perspect Biol* 1, a000034.
- Okemoto, K., Wagner, B., Meisen, H., Haseley, A., Kaur, B. and Chiocca, E.A., 2013. STAT3 activation promotes oncolytic HSV1 replication in glioma cells. *PLoS One* 8, e71932.
- Osuka, K., Watanabe, Y., Usuda, N., Atsuzawa, K., Yasuda, M., Aoshima, C., Wakabayashi, T. and Takayasu, M., 2011. Activation of STAT1 in neurons following spinal cord injury in mice. *Neurochem Res* 36, 2236-43.

- Park, E.M., Kang, J.H., Seo, J.S., Kim, G., Chung, J. and Choi, T.J., 2008. Molecular cloning and expression analysis of the STAT1 gene from olive flounder, *Paralichthys olivaceus*. *BMC Immunol* 9, 31.
- Park, S.B., Aoki, T. and Jung, T.S., 2012. Pathogenesis of and strategies for preventing *Edwardsiella tarda* infection in fish. *Vet Res* 43, 67.
- Park, S.I., 2009. Disease Control in Korean Aquaculture. *Fish Pathology* 44, 19-23.
- Paul, W.E., 1991. Interleukin-4: a prototypic immunoregulatory lymphokine. *Blood* 77, 1859-70.
- Perry, A.K., Chen, G., Zheng, D., Tang, H. and Cheng, G., 2005. The host type I interferon response to viral and bacterial infections. *Cell Res* 15, 407-22.
- Perry, S.T., Buck, M.D., Lada, S.M., Schindler, C. and Shresta, S., 2011. STAT2 mediates innate immunity to Dengue virus in the absence of STAT1 via the type I interferon receptor. *PLoS Pathog* 7, e1001297.
- Pikula, M., Langa, P., Kosikowska, P. and Trzonkowski, P., 2015. Stem cells and growth factors in wound healing. *Postepy Hig Med Dosw (Online)* 69, 874-85.
- Platanias, L.C., 2005. Mechanisms of type-I- and type-II-interferon-mediated signalling. *Nat Rev Immunol* 5, 375-86.
- Portou, M.J., Baker, D., Abraham, D. and Tsui, J., 2015. The innate immune system, toll-like receptors and dermal wound healing: A review. *Vascul Pharmacol* 71, 31-6.
- Quelle, F.W., Shimoda, K., Thierfelder, W., Fischer, C., Kim, A., Ruben, S.M., Cleveland, J.L., Pierce, J.H., Keegan, A.D., Nelms, K. and et al., 1995. Cloning of murine Stat6 and human Stat6, Stat proteins that are tyrosine phosphorylated in responses to IL-4 and IL-3 but are not required for mitogenesis. *Mol Cell Biol* 15, 3336-43.
- Radaeva, S., Sun, R., Pan, H.N., Hong, F. and Gao, B., 2004. Interleukin 22 (IL-22) plays a protective role in T cell-mediated murine hepatitis: IL-22 is a survival factor for hepatocytes via STAT3 activation. *Hepatology* 39, 1332-42.
- Ramana, C.V., Chatterjee-Kishore, M., Nguyen, H. and Stark, G.R., 2000. Complex roles of Stat1 in regulating gene expression. *Oncogene* 19, 2619-27.
- Rawlings, J.S., Rosler, K.M. and Harrison, D.A., 2004. The JAK/STAT signaling pathway. *J Cell Sci* 117, 1281-3.
- Reitsma, J.M. and Terhune, S.S., 2013. Inhibition of cellular STAT3 synergizes with the cytomegalovirus kinase inhibitor maribavir to disrupt infection. *Antiviral Res* 100, 321-7.
- Richard, A.J. and Stephens, J.M., 2014. The role of JAK-STAT signaling in adipose tissue function. *Biochim Biophys Acta* 1842, 431-9.

- Riley, J.K., Takeda, K., Akira, S. and Schreiber, R.D., 1999. Interleukin-10 receptor signaling through the JAK-STAT pathway. Requirement for two distinct receptor-derived signals for anti-inflammatory action. *J Biol Chem* 274, 16513-21.
- Rothman, P., Li, S.C., Gorham, B., Glimcher, L., Alt, F. and Boothby, M., 1991. Identification of a conserved lipopolysaccharide-plus-interleukin-4-responsive element located at the promoter of germ line epsilon transcripts. *Mol Cell Biol* 11, 5551-61.
- Ryan, J.J., McReynolds, L.J., Keegan, A., Wang, L.H., Garfein, E., Rothman, P., Nelms, K. and Paul, W.E., 1996. Growth and gene expression are predominantly controlled by distinct regions of the human IL-4 receptor. *Immunity* 4, 123-32.
- Santos, C.I. and Costa-Pereira, A.P., 2011. Signal transducers and activators of transcription—from cytokine signalling to cancer biology. *Biochim Biophys Acta* 1816, 38-49.
- Schindler, U., Wu, P., Rothe, M., Brasseur, M. and McKnight, S.L., 1995. Components of a Stat recognition code: evidence for two layers of molecular selectivity. *Immunity* 2, 689-97.
- Seder, R.A. and Paul, W.E., 1994. Acquisition of lymphokine-producing phenotype by CD4+ T cells. *Annu Rev Immunol* 12, 635-73.
- Serfling, E., Berberich-Siebelt, F., Chuvpilo, S., Jankevics, E., Klein-Hessling, S., Twardzik, T. and Avots, A., 2000. The role of NF-AT transcription factors in T cell activation and differentiation. *Biochim Biophys Acta* 1498, 1-18.
- Shelburne, C.P., McCoy, M.E., Piekorz, R., Sexl, V., Roh, K.H., Jacobs-Helber, S.M., Gillespie, S.R., Bailey, D.P., Mirmonsef, P., Mann, M.N., Kashyap, M., Wright, H.V., Chong, H.J., Bouton, L.A., Barnstein, B., Ramirez, C.D., Bunting, K.D., Sawyer, S., Lantz, C.S. and Ryan, J.J., 2003. Stat5 expression is critical for mast cell development and survival. *Blood* 102, 1290-7.
- Shen, X., Hong, F., Nguyen, V.A. and Gao, B., 2000. IL-10 attenuates IFN-alpha-activated STAT1 in the liver: involvement of SOCS2 and SOCS3. *FEBS Lett* 480, 132-6.
- Shen, X.D., Ke, B., Zhai, Y., Gao, F., Anselmo, D., Lassman, C.R., Busuttill, R.W. and Kupiec-Weglinski, J.W., 2003. Stat4 and Stat6 signaling in hepatic ischemia/reperfusion injury in mice: HO-1 dependence of Stat4 disruption-mediated cytoprotection. *Hepatology* 37, 296-303.
- Shi, J., Zhang, Y.B., Liu, T.K., Sun, F. and Gui, J.F., 2012. Subcellular localization and functional characterization of a fish IRF9 from crucian carp *Carassius auratus*. *Fish Shellfish Immunol* 33, 258-66.
- Shinohara, H., Yamasaki, S., Maeda, S., Saito, T. and Kurosaki, T., 2009. Regulation of NF-kappaB-dependent T cell activation and development by MEKK3. *Int Immunol* 21, 393-401.

- Shuai, K., 1999. The STAT family of proteins in cytokine signaling. *Prog Biophys Mol Biol* 71, 405-22.
- Simovic, M.O., Ballard, B.R., Gray, K.D. and Stain, S.C., 2007. The STAT4 and STAT6 pathways in pancreatitis-associated lung injury. *J Surg Res* 137, 10-5.
- Skjesol, A., Hansen, T., Shi, C.Y., Thim, H.L. and Jorgensen, J.B., 2010. Structural and functional studies of STAT1 from Atlantic salmon (*Salmo salar*). *BMC Immunol* 11, 17.
- Sobhkhez, M., Skjesol, A., Thomassen, E., Tollersrud, L.G., Iliev, D.B., Sun, B., Robertsen, B. and Jorgensen, J.B., 2014. Structural and functional characterization of salmon STAT1, STAT2 and IRF9 homologs sheds light on interferon signaling in teleosts. *FEBS Open Bio* 4, 858-71.
- Sotillos, S., Diaz-Meco, M.T., Moscat, J. and Castelli-Gair Hombria, J., 2008. Polarized subcellular localization of Jak/STAT components is required for efficient signaling. *Curr Biol* 18, 624-9.
- Sow, F.B., Alvarez, G.R., Gross, R.P., Satoskar, A.R., Schlesinger, L.S., Zwilling, B.S. and Lafuse, W.P., 2009. Role of STAT1, NF-kappaB, and C/EBPbeta in the macrophage transcriptional regulation of hepcidin by mycobacterial infection and IFN-gamma. *J Leukoc Biol* 86, 1247-58.
- Stadelmann, W.K., Digenis, A.G. and Tobin, G.R., 1998. Physiology and healing dynamics of chronic cutaneous wounds. *Am J Surg* 176, 26S-38S.
- Stark, G.R. and Darnell, J.E., Jr., 2012. The JAK-STAT pathway at twenty. *Immunity* 36, 503-14.
- Steen, H.C. and Gamero, A.M., 2013. STAT2 phosphorylation and signaling. *JAKSTAT* 2, e25790.
- Stein, C., Caccamo, M., Laird, G. and Leptin, M., 2007. Conservation and divergence of gene families encoding components of innate immune response systems in zebrafish. *Genome Biol* 8, R251.
- Stephanou, A., 2004. Role of STAT-1 and STAT-3 in ischaemia/reperfusion injury. *J Cell Mol Med* 8, 519-25.
- Stout, B.A., Bates, M.E., Liu, L.Y., Farrington, N.N. and Bertics, P.J., 2004. IL-5 and granulocyte-macrophage colony-stimulating factor activate STAT3 and STAT5 and promote Pim-1 and cyclin D3 protein expression in human eosinophils. *J Immunol* 173, 6409-17.
- Strehlow, I. and Schindler, C., 1998. Amino-terminal signal transducer and activator of transcription (STAT) domains regulate nuclear translocation and STAT deactivation. *J Biol Chem* 273, 28049-56.

- Sun, Y., Liu, C.S. and Sun, L., 2011. A multivalent killed whole-cell vaccine induces effective protection against *Edwardsiella tarda* and *Vibrio anguillarum*. *Fish Shellfish Immunol* 31, 595-9.
- Sung, P.S., Cheon, H., Cho, C.H., Hong, S.H., Park do, Y., Seo, H.I., Park, S.H., Yoon, S.K., Stark, G.R. and Shin, E.C., 2015. Roles of unphosphorylated ISGF3 in HCV infection and interferon responsiveness. *Proc Natl Acad Sci U S A* 112, 10443-8.
- Sung, S.C., Cheng, C.H., Chou, C.M., Chu, C.Y., Chen, G.D., Hwang, P.P., Huang, F.L. and Huang, C.J., 2010. Expression and characterization of a constitutively active STAT6 from Tetraodon. *Fish Shellfish Immunol* 28, 819-28.
- Sung, S.C., Fan, T.J., Chou, C.M., Leu, J.H., Hsu, Y.L., Chen, S.T., Hsieh, Y.C. and Huang, C.J., 2003. Genomic structure, expression and characterization of a STAT5 homologue from pufferfish (*Tetraodon fluviatilis*). *Eur J Biochem* 270, 239-52.
- Takagi, Y., Harada, J., Chiarugi, A. and Moskowitz, M.A., 2002. STAT1 is activated in neurons after ischemia and contributes to ischemic brain injury. *J Cereb Blood Flow Metab* 22, 1311-8.
- Takeda, K. and Akira, S., 2000. STAT family of transcription factors in cytokine-mediated biological responses. *Cytokine Growth Factor Rev* 11, 199-207.
- Takeda, K., Kaisho, T., Yoshida, N., Takeda, J., Kishimoto, T. and Akira, S., 1998. Stat3 activation is responsible for IL-6-dependent T cell proliferation through preventing apoptosis: generation and characterization of T cell-specific Stat3-deficient mice. *J Immunol* 161, 4652-60.
- Takeda, K., Noguchi, K., Shi, W., Tanaka, T., Matsumoto, M., Yoshida, N., Kishimoto, T. and Akira, S., 1997. Targeted disruption of the mouse Stat3 gene leads to early embryonic lethality. *Proc Natl Acad Sci U S A* 94, 3801-4.
- Takeda, K., Tanaka, T., Shi, W., Matsumoto, M., Minami, M., Kashiwamura, S., Nakanishi, K., Yoshida, N., Kishimoto, T. and Akira, S., 1996. Essential role of Stat6 in IL-4 signalling. *Nature* 380, 627-30.
- Tan, N.Y. and Khachigian, L.M., 2009. Sp1 phosphorylation and its regulation of gene transcription. *Mol Cell Biol* 29, 2483-8.
- Tanabe, Y., Nishibori, T., Su, L., Arduini, R.M., Baker, D.P. and David, M., 2005. Cutting edge: role of STAT1, STAT3, and STAT5 in IFN-alpha beta responses in T lymphocytes. *J Immunol* 174, 609-13.
- Tantin, D., Schild-Poulter, C., Wang, V., Hache, R.J. and Sharp, P.A., 2005. The octamer binding transcription factor Oct-1 is a stress sensor. *Cancer Res* 65, 10750-8.

- Teglund, S., McKay, C., Schuetz, E., van Deursen, J.M., Stravopodis, D., Wang, D., Brown, M., Bodner, S., Grosveld, G. and Ihle, J.N., 1998. Stat5a and Stat5b proteins have essential and nonessential, or redundant, roles in cytokine responses. *Cell* 93, 841-50.
- Thieu, V.T., Yu, Q., Chang, H.C., Yeh, N., Nguyen, E.T., Sehra, S. and Kaplan, M.H., 2008. Signal transducer and activator of transcription 4 is required for the transcription factor T-bet to promote T helper 1 cell-fate determination. *Immunity* 29, 679-90.
- Tort, L., Balasch, J.C. and Mackenzie, S., 2003. Fish immune system. A crossroads between innate and adaptive responses. *Immunología* 22, 277-286.
- Trilling, M., Le, V.T., Rashidi-Alavijeh, J., Katschinski, B., Scheller, J., Rose-John, S., Androsiac, G.E., Jonjic, S., Poli, V., Pfeffer, K. and Hengel, H., 2014. "Activated" STAT proteins: a paradoxical consequence of inhibited JAK-STAT signaling in cytomegalovirus-infected cells. *J Immunol* 192, 447-58.
- Tso, C.H., Hung, Y.F., Tan, S.P. and Lu, M.W., 2013. Identification of the STAT1 gene and the characterisation of its immune response to immunostimulants, including nervous necrosis virus (NNV) infection, in Malabar grouper (*Epinephelus malabaricus*). *Fish Shellfish Immunol* 35, 1339-48.
- Urso, K., Alfranca, A., Martinez-Martinez, S., Escolano, A., Ortega, I., Rodriguez, A. and Redondo, J.M., 2011. NFATc3 regulates the transcription of genes involved in T-cell activation and angiogenesis. *Blood* 118, 795-803.
- Vaisse, C., Halaas, J.L., Horvath, C.M., Darnell, J.E., Jr., Stoffel, M. and Friedman, J.M., 1996. Leptin activation of Stat3 in the hypothalamus of wild-type and ob/ob mice but not db/db mice. *Nat Genet* 14, 95-7.
- Varinou, L., Ramsauer, K., Karaghiosoff, M., Kolbe, T., Pfeffer, K., Muller, M. and Decker, T., 2003. Phosphorylation of the Stat1 transactivation domain is required for full-fledged IFN-gamma-dependent innate immunity. *Immunity* 19, 793-802.
- Vinkemeier, U., Moarefi, I., Darnell, J.E., Jr. and Kuriyan, J., 1998. Structure of the amino-terminal protein interaction domain of STAT-4. *Science* 279, 1048-52.
- Wan, Q., Wicramaarachchi, W.D., Whang, I., Lim, B.S., Oh, M.J., Jung, S.J., Kim, H.C., Yeo, S.Y. and Lee, J., 2012. Molecular cloning and functional characterization of two duplicated two-cysteine containing type I interferon genes in rock bream *Oplegnathus fasciatus*. *Fish Shellfish Immunol* 33, 886-98.
- Wang, H., Lafdil, F., Kong, X. and Gao, B., 2011a. Signal transducer and activator of transcription 3 in liver diseases: a novel therapeutic target. *Int J Biol Sci* 7, 536-50.
- Wang, K., Wang, C., Xiao, F., Wang, H. and Wu, Z., 2008. JAK2/STAT2/STAT3 are required for myogenic differentiation. *J Biol Chem* 283, 34029-36.

- Wang, K.S., Frank, D.A. and Ritz, J., 2000. Interleukin-2 enhances the response of natural killer cells to interleukin-12 through up-regulation of the interleukin-12 receptor and STAT4. *Blood* 95, 3183-90.
- Wang, N., Wang, X.L., Yang, C.G. and Chen, S.L., 2013. Molecular cloning, subcellular location and expression profile of signal transducer and activator of transcription 2 (STAT2) from turbot, *Scophthalmus maximus*. *Fish Shellfish Immunol* 35, 1200-8.
- Wang, N., Yang, C.G., Sun, Z.Z., Wang, X.L. and Chen, S.L., 2011c. Signal transducer and activator of transcription 3 (STAT3) homologue in turbot (*Scophthalmus maximus*): molecular characterization and expression analysis. *Fish Shellfish Immunol* 30, 255-62.
- Watanabe, S. and Arai, K., 1996. Roles of the JAK-STAT system in signal transduction via cytokine receptors. *Curr Opin Genet Dev* 6, 587-96.
- Watford, W.T., Hissong, B.D., Bream, J.H., Kanno, Y., Muul, L. and O'Shea, J.J., 2004. Signaling by IL-12 and IL-23 and the immunoregulatory roles of STAT4. *Immunol Rev* 202, 139-56.
- Watson, C.J., 2001. Stat transcription factors in mammary gland development and tumorigenesis. *J Mammary Gland Biol Neoplasia* 6, 115-27.
- Wedel, A. and Ziegler-Heitbrock, H.W., 1995. The C/EBP family of transcription factors. *Immunobiology* 193, 171-85.
- Wehinger, J., Gouilleux, F., Groner, B., Finke, J., Mertelsmann, R. and Weber-Nordt, R.M., 1996. IL-10 induces DNA binding activity of three STAT proteins (Stat1, Stat3, and Stat5) and their distinct combinatorial assembly in the promoters of selected genes. *FEBS Lett* 394, 365-70.
- Wen, A.Y., Sakamoto, K.M. and Miller, L.S., 2010. The role of the transcription factor CREB in immune function. *J Immunol* 185, 6413-9.
- Wurster, A.L., Tanaka, T. and Grusby, M.J., 2000. The biology of Stat4 and Stat6. *Oncogene* 19, 2577-84.
- Xu, H., Uno, J.K., Inouye, M., Collins, J.F. and Ghishan, F.K., 2005. NF1 transcriptional factor(s) is required for basal promoter activation of the human intestinal NaPi-IIb cotransporter gene. *Am J Physiol Gastrointest Liver Physiol* 288, G175-81.
- Xu, K. and Yu, F.S., 2011. Impaired epithelial wound healing and EGFR signaling pathways in the corneas of diabetic rats. *Invest Ophthalmol Vis Sci* 52, 3301-8.
- Xu, X., Sun, Y.L. and Hoey, T., 1996. Cooperative DNA binding and sequence-selective recognition conferred by the STAT amino-terminal domain. *Science* 273, 794-7.
- Yamamoto, K., Quelle, F.W., Thierfelder, W.E., Kreider, B.L., Gilbert, D.J., Jenkins, N.A., Copeland, N.G., Silvennoinen, O. and Ihle, J.N., 1994. Stat4, a novel gamma interferon

- activation site-binding protein expressed in early myeloid differentiation. *Mol Cell Biol* 14, 4342-9.
- Yamashita, S., Miyagi, C., Carmany-Rampey, A., Shimizu, T., Fujii, R., Schier, A.F. and Hirano, T., 2002. Stat3 Controls Cell Movements during Zebrafish Gastrulation. *Dev Cell* 2, 363-75.
- Yang, C., Bolotin, E., Jiang, T., Sladek, F.M. and Martinez, E., 2007a. Prevalence of the initiator over the TATA box in human and yeast genes and identification of DNA motifs enriched in human TATA-less core promoters. *Gene* 389, 52-65.
- Yang, X.O., Panopoulos, A.D., Nurieva, R., Chang, S.H., Wang, D., Watowich, S.S. and Dong, C., 2007b. STAT3 regulates cytokine-mediated generation of inflammatory helper T cells. *J Biol Chem* 282, 9358-63.
- Yoshida, T., Hanada, T., Tokuhisa, T., Kosai, K., Sata, M., Kohara, M. and Yoshimura, A., 2002. Activation of STAT3 by the hepatitis C virus core protein leads to cellular transformation. *J Exp Med* 196, 641-53.
- Yoshidome, H., Kato, A., Miyazaki, M., Edwards, M.J. and Lentsch, A.B., 1999. IL-13 activates STAT6 and inhibits liver injury induced by ischemia/reperfusion. *Am J Pathol* 155, 1059-64.
- Yu, F.F., Zhang, Y.B., Liu, T.K., Liu, Y., Sun, F., Jiang, J. and Gui, J.F., 2010. Fish virus-induced interferon exerts antiviral function through Stat1 pathway. *Mol Immunol* 47, 2330-41.
- Zhang, Y. and Gui, J., 2004. Molecular characterization and IFN signal pathway analysis of *Carassius auratus* CaSTAT1 identified from the cultured cells in response to virus infection. *Dev Comp Immunol* 28, 211-27.
- Zhong, Z., Wen, Z. and Darnell, J.E., Jr., 1994a. Stat3 and Stat4: members of the family of signal transducers and activators of transcription. *Proc Natl Acad Sci U S A* 91, 4806-10.
- Zhong, Z., Wen, Z. and Darnell, J.E., Jr., 1994c. Stat3: a STAT family member activated by tyrosine phosphorylation in response to epidermal growth factor and interleukin-6. *Science* 264, 95-8.
- Zou, J., Carrington, A., Collet, B., Dijkstra, J.M., Yoshiura, Y., Bols, N. and Secombes, C., 2005. Identification and bioactivities of IFN-gamma in rainbow trout *Oncorhynchus mykiss*: the first Th1-type cytokine characterized functionally in fish. *J Immunol* 175, 2484-94.